ÇUKUROVA UNIVERSITY
INSTITUE OF NATURAL AND APPLIED SCIENCES

PhD THESIS

Aslı ABDULVAHİTOĞLU

PERFORMANCE AND EXHAUST EMISSION CHARACTERISTICS OF A CI ENGINE FUELED WITH SYNTHESIZED FUEL BLENDS

DEPARTMENT OF MECHANICAL ENGINEERING

ADANA, 2009

ÇUKUROVA UNIVERSITY
INSTITUE OF NATURAL AND APPLIED SCIENCES

PERFORMANCE AND EXHAUST EMISSION CHARACTERISTICS OF A CI ENGINE FUELED WITH SYNTHESIZED FUEL BLENDS

Aslı ABDULVAHİTOĞLU

PhD THESIS

DEPARTMENT OF MECHANICAL ENGINEERING

We certify this thesis is satisfactory for the award of PhD degree at the date 14/12/2009.

Signature:.....
Prof.Dr. Kadir AYDIN
Supervisor

Signature:.....
Prof.Dr. Burhan ARIKAN
Member of Examining Commitee

Signature:.....
Prof.Dr. Ertuğrul BALTACIOĞLU
Member of Examining Commitee

Signature:.....
Assoc.Prof.Dr. Hüseyin AKILLI
Member of Examining Commitee

Signature:.....
Assist.Prof.Dr. Alper YILMAZ
Member of Examining Commitee

Certified that this thesis conforms to the formal standarts of the Institute. **Code No :**

Prof. Dr. İlhami YEĞİNGİL
Director
Institute of Natural and
Applied Science

This work is supported by the Çukurova University Academic Research Projects Unit.
Proje No: MMF2007D15

Note: Without giving the references of the original writings, tables, figures and photographs used in this thesis are protected with the copyright of their owners by the law 5846 of Turkish Republic.

ABSTRACT

PhD THESIS

PERFORMANCE AND EXHAUST EMISSION CHARACTERISTICS OF A CI ENGINE FUELED WITH SYNTHESIZED FUEL BLENDS

Aslı ABDULVAHİTOĞLU

DEPARTMENT OF MECHANICAL ENGINEERING
INSTITUTE OF NATURAL AND APPLIED SCIENCES
UNIVERSITY OF ÇUKUROVA

Supervisor : Prof.Dr. Kadir AYDIN
Year : 2009, Pages:221
Jury : Prof.Dr. Kadir AYDIN
Prof.Dr. Burhan ARIKAN
Prof.Dr. Ertuğrul BALTACIOĞLU
Assoc.Prof.Dr. Hüseyin AKILLI
Assist.Prof.Dr. Alper YILMAZ

In this study; new fuel blends were developed by using biofuels which would be used in today's modern diesel vehicles without any modification and any problem. In order to improve the worst properties of biodiesel compared to diesel fuel, different hydrocarbons were used as fuel additives. 45 different fuel blends were prepared with 10% to 50% rapeseed biodiesel, 35% to 85% low sulphur diesel fuel and 5% to 15% different hydrocarbons (n-hexane, n-heptane and xylene) additive.

The fuel properties of blends (such as density, heat of combustion, Cetane number and viscosity) were measured and compared with diesel fuel. It was found that, the fuel properties of 5% to 10% alkenes blends were too close to the standard limit for diesel fuel and these blends could be used directly in diesel engines. Although the performance results indicated that there was a decrease in maximum torque 0.57% and increase in specific fuel consumption 1.04% the suitable blend was M50RSB40HX10 with an increased power rating 15.31%.

KeyWords: Diesel Engine, Biodiesel, Fuel Blend, Performance, Emissions

ÖZ

DOKTORA TEZİ

SENTEZLENMİŞ YAKIT KARIŞIMLARI İLE ÇALIŞAN BİR DİZEL MOTORUN PERFORMANS VE EMİSYON KARAKTERİSTİKLERİ

Aslı ABDULVAHİTOĞLU

ÇUKUROVA ÜNİVERSİTESİ
FEN BİLİMLERİ ENSTİTÜSÜ
MAKİNE MÜHENDİSLİĞİ ANABİLİM DALI

Supervisor : Prof.Dr. Kadir AYDIN
Year : 2009, Pages:221
Jury : Prof.Dr. Kadir AYDIN
Prof.Dr. Burhan ARIKAN
Prof.Dr. Ertuğrul BALTACIOĞLU
Doç.Dr. Hüseyin AKILLI
Yrd.Doç.Dr. Alper YILMAZ

Bu çalışmada; biyoyakıtlar kullanılarak günümüz dizel motorlu araçlarda herhangi bir değişiklik yapılmadan sorunsuz olarak kullanılabilecek yeni yakıt karışımları geliştirilmiş, biyodizelin motorine göre kötü olan yoğunluk ve viskozite özelliklerini iyileştirmek amacıyla da farklı hidrokarbon maddeleri katkı olarak kullanılmıştır. %10 ile %50 oran aralığında değişen miktarlardaki kanola biyodizeli, %45 ile %85 aralığında değişen miktarlardaki düşük kükürtlü motorin ve %5 oranında hafif hidrokarbon katkı maddeleri (n-hegzan, n-heptan ve ksilen) kullanılarak 15 adet yakıt karışımı hazırlanmıştır.

Karışımların yakıt özellikleri (yoğunluk, ısıl değer, Setan sayısı ve viskozite gibi) ölçülerek motorinin özellikleri ile karşılaştırılmış olup, elde edilen %5 ve %10 alkenli karışımların yakıt özelliklerinin motorinin standart değerlerine yakın olduğu ve dizel motorlarda doğrudan yakıt olarak kullanılabilecekleri görülmüştür. Motor performans testlerinin sonucunda her ne kadar maksimum torkda %0.57 ve özgül yakıt tüketiminde %1.04 lük bir artış gözlense bile D50RSB40HX10 gücü %15.31 artırarak en uygun sonucu vermiştir.

Anahtar Kelimeler: Dizel Motor, Biyodizel, Yakıt Karışımı, Performans, Emisyonlar

ACKNOWLEDGEMENT

On the completion of this dissertation I would like to express my appreciation to all those who have contributed in one way or another.

I gratefully thank Prof. Dr. Kadir Aydın for his supervision in every stages of this dissertation. He directed my research with perfect timing. In addition, I am obliged to him for his effort in correcting the English text.

I have been working as a student in Fuel Analysis Laboratory of Çukurova University, Automotive Engineering Laboratories for a long time. I would like to thank all the team members for their continuous support during my long dissertation period. I should also thank technician Cevdet Yıldırım without his help it was impossible to complete this dissertation.

I would like to thank my mother Semiha and my father Murat for their kind support in every stage of my life.

Finally, I wish to thank to my husband Adnan for his constant patience and support, my little son Murat for his pure love which made it possible for me to concentrate fully on the work for this dissertation.

TABLE OF CONTENTS Pages

ABSTRACT …….. I

ÖZ…….....II

ACKNOWLEDGEMENT…….....III

TABLE of CONTENTS……....IV

LIST of TABLES……...…….…….VIII

LIST of FIGURES…….……....XI

SYMBOLS…….……...……...XVIII

1. INTRODUCTION……1

2. LITERATURE REVIEW……...12

3. COMBUSTION IN DIESEL ENGINE.....…….24

3.1. Operation of Four-Stroke Engines…….25

3.1.1. Combustion……30

3.1.1.1. Ignition Delay……31

3.1.1.2. Fuel Ignition Quality …….31

3.1.1.3. Factors Affecting Ignition Delay……...32

4. BIODIESEL PRODUCTION AND QUALITY…….33

4.1. Production and Usage of Biodiesel……34

4.1.1. Triglycerids as Diesel Fuels……...34

4.1.1.1 Chemical Structure of Fatty Acid……...36

4.2 The Production of Biodiesel……36

4.2.1. Dilution……..38

4.2.2. Microemulsion……...38

4.2.3. Pyrolysis (Thermal Cracking) ……...38

4.2.4. Transesterification (Alcoholysis) ……..40

4.2.4.1. Catalytic Transesterification……..43

4.2.4.1.(1.) Alkali-Catalyzed Transesterification…..……44

4.2.4.1.(2.) Acid Catalyzed Transesterification……46

4.2.4.1.(3.) Enzyme Catalyzed Transesterification…….…..47

4.2.4.1.(4.) Non-Catalytic Supercritical Methanol Transesterification…….....……47

4.3. Process Variables……49

4.3.1. Reaction Temperature……49

4.3.2. Ratio of Alcohol to Oil……..49

4.3.3. Catalyst Type and Concentration…….....50

4.3.4. Mixing Intensity…….....50

4.3.5. Purity of Reactants……51

4.4. Advantages of Biodiesel…….....51

4.5. Disadvantages of Biodiesel……....52

4.6. Evaluation of Types of Biodiesel……...53

4.6.1. Evaluation of Biodiesel Quality…….55

4.6.1.1. Flash Point…….55

4.6.1.2. Viscosity……....56

4.6.1.3. Sulphated Ash ……..57

4.6.1.4. Sulphur……..57

4.6.1.5. Copper Strip Corrosion…….....58

4.6.1.6. Cetane Number……..58

4.6.1.7. Carbon Residue……..59

4.6.1.8. Phosphorus Content……...59

4.6.1.9. Density……...59

4.6.1.10 Cold Filter Plugging Point……60

4.7. Emission Types……...61

4.7.1. NO_x……61

4.7.2. PM ……...61

4.7.3. HC ……62

4.7.4.CO……...63

4.7.5.CO_2 …..…….....63

5. MATERIALS and METHODS ……64

5.1. Biodiesel Production.……64

5.2. Mixture Preparation.…….....69

5.3. Fuel Quality Measurement Methods……72

5.3.1. Density Measurement……72

5.3.2. Viscosity Measurement……..73

5.3.3. Heat Capacity Measurement……..74

5.3.4. Cetane Number Measurement……74

5.3.5. Cold Flow Measurement……75

5.3.6. Flash Point……76

5.4. Experimental Setup……..77

5.4.1. Engine……77
5.5. Measurements…….....79
5.5.1. Exhaust Emission Tests…….79
5.6. Formulas Necessary for Calculations ……80
6. FUEL QUALITY EXPERIMENTS……...82
6.1. Density……84
6.2. Viscosity……...86
6.3. Heating Capacity……..88
6.4. Cetane Number…….....91
6.5. Pour Point…….....93
6.6. Flash Point…….……..95
7. ENGINE PERFORMANCE AND EMISSION RESULTS…….....……98
7.1. Torque vs Speed…….....98
7.2. Power vs Speed…….……111
7.3. Specific Fuel Consumption vs Speed …….....126
7.4. CO Emission…….....138
7.5. NO_x Emission…….152
7.6. CO_2 Emission…….....164
8. CONCLUSIONS AND RECOMMENDATIONS.....178
REFERENCES …….....182
CURRICULUM VITAE…….....188
APPENDIXES……..189

LIST of TABLES

Pages

Table 1.1. The EU's Biodiesel Production by Country (1000 ton)…….....6

Table 1.2. Present and planned biomass energy production in Turkey (K tone)…....7

Table 1.3. Comparison Chart for Diesel and Biodiesel……....9

Table 4.1. Fatty acid composition of vegetable oils……...35

Table 4.2. Properties of vegetable oil…….....35

Table 4.3. Chemical structure of common fatty acids……..…….....36

Table 4.4. Physical Properties of Chemicals Related to Transesterification…….....42

Table 4.5. Melting Points of Fatty Acids, Methyl Esters and Mono-, Di-, and Triglyceridea…….....42

Table 4.6 Comparison of the yields in alkaline-catalyzed, acid-catalyzed and supercritical methanol…….....48

Table 4.7. Generally applicable requirements and test methods TS EN 14214…....54

Table 5.1. Reactants specifications……....65

Table 5.2. Fuel blends with Hexane…….....70

Table 5.3. Fuel blends with Heptane…….....71

Table 5.4. Fuel blends with Xylene……....71

Table 5.5. Property chart of used substances…….....72

Table 6.6. Properties of engine used in the experiments…….....78

Table 5.7. Dynometer Technical specification…….....78

Table 6.1. Fuel Quality Results of Eurodiesel (D) and Rapeseed Biodiesel (RSB)..82

Table 6.2. Fuel Quality Results of n-Hexane Blends…….....82

Table 6.3. Fuel Quality Results of n-Heptane Blends…….....83

Table 6.4. Fuel Quality Results of Xylene Blends…….83

Table 7.1. Performance and Emission Results for Fuel Coded D100 ….....…….190

Table 7.2. Performance and Emission Results for Fuel Coded RSB100.....…….191

Table 7.3. Performance and Emission Results for Fuel Coded D85RSB10HX5....192

Table 7.4. Performance and Emission Results for Fuel Coded D75RSB20HX5....193

Table 7.5. Performance and Emission Results for Fuel Coded D65RSB30HX5....194

Table 7.6. Performance and Emission Results for Fuel Coded D55RSB40HX5....195

Table 7.7. Performance and Emission Results for Fuel Coded D45RSB50HX5…196

Table 7.8. Performance and Emission Results for Fuel Coded D80RSB10HX10..197

Table 7.9. Performance and Emission Results for Fuel Coded D75RSB20HX10..198

Table 7.10. Performance and Emission Results for Fuel Coded D65RSB30HX10.....199

Table 7.11. Performance and Emission Results for Fuel Coded D55RSB40HX10….....200

Table 7.12. Performance and Emission Results for Fuel Coded D45RSB50HX10.....201

Table 7.13. Performance and Emission Results for Fuel Coded D75RSB10HX15.....202

Table 7.14. Performance and Emission Results for Fuel Coded D65RSB20HX15.....203

Table 7.15. Performance and Emission Results for Fuel Coded D55RSB30HX15.....204

Table 7.16. Performance and Emission Results for Fuel Coded D45RSB40HX15.....205

Table 7.17. Performance and Emission Results for Fuel Coded D35RSB50HX15.....206

Table 7.18. Performance and Emission Results for Fuel Coded D85RSB10HP5.....207

Table 7.19. Performance and Emission Results for Fuel Coded D75RSB20HP5.....208

Table 7.20. Performance and Emission Results for Fuel Coded D65RSB30HP5.....209

Table 7.21. Performance and Emission Results for Fuel Coded D55RSB40HP5.....210

Table 7.22. Performance and Emission Results for Fuel Coded D45RSB50HP5.....211

Table 7.23. Performance and Emission Results for Fuel Coded D80RSB10HP10.....212

Table 7.24. Performance and Emission Results for Fuel Coded D75RSB20HP10.....213

Table 7.25. Performance and Emission Results for Fuel Coded D65RSB30HP10.....214

Table 7.26. Performance and Emission Results for Fuel Coded D55RSB40HP10.....215

Table 7.27. Performance and Emission Results for Fuel Coded D45RSB50HP10 216

Table 7.28. Performance and Emission Results for Fuel Coded D75RSB10HP15….....217

Table 7.29. Performance and Emission Results for Fuel Coded D65RSB20HP15….....218

Table 7.30. Performance and Emission Results for Fuel Coded D55RSB30HP15….....219

Table 7.31. Performance and Emission Results for Fuel Coded D45RSB40HP15….....220

Table 7.32. Performance and Emission Results for Fuel Coded D35RSB50HP15.....221

LIST of FIGURES

Pages

Figure 1.1. World Marketed Energy Consumption by Region, 2004-2030.....1

Figure 1.2. World Marketed Energy Use by Fuel Type, 1980-2030.....2

Figure 1.3 World Marketed Energy Use by Fuel Type, 1980-2030.....3

Figure 1.4. Schematic of biodiesel production path.....8

Figure 3.1. Basic Components of a Reciprocating Engine.....25

Figure 3.2. Four stroke diesel operation 26

Figure 3.3. Pressure-Volume Diagram for 4-Stroke Naturally-Aspirated Engines...27

Figure 3.4. Pressure-Crank Angle Diagram for a four- stroke Diesel Engine.....28

Figure 3.5. Combustion steps in DI diesel engine.....31

Figure 4.1. Biodiesel processing flow diagram.....37

Figure 4.2. The mechanism of thermal decomposition of triglycerids.....39

Figure 4.3. General equation of transesterification.....40

Figure 4.4. General equation of the triglyceride with methanol.....41

Figure 4.5. The transesterification reactions of vegetable oil with alcohol to esters and glycerol.....43

Figure 4.6. Catalytic bio-diesel production diagram.....44

Figure 4.7. Mechanism of base catalyzed transesterification.....45

Figure 4.8. Mechanism of acid catalyzed transesterification.....46

Figure 4.9. Summary of U.S. Enviromental Protection Agency evaluation of biodiesel effects on pollutant emissions for heavy –duty engines 62

Figure 5.1. Stainless Steel Biodiesel Reactor 64

Figure 5.2. Stainless Steel Biodiesel Reactor Schema 65

Figure 5.3. Maturation containers 66

Figure 5.4. Suction pump 66

Figure 5.5. Separation of glycerin from RME 67

Figure 5.6. First washing of RME 67

Figure 5.7. Last washing of RME 68

Figure 5.8. The RME before drying 68

Figure 5.9. The Rapeseed Biodiesel 69

Figure 5.10. Kyoto Electronics DA-130 Portable Densimeter..... 73

Figure 5.11. Saybolt Universal Viscosimeter 73

Figure 5.12. IKA-Werke C2000 Calorimeter 74

Figure 5.13 Zeltex ZX440 75

Figure 5.14. Tanaka MPC-102L.....76

Figure 5.15. Tanaka APM-7 76

Figure 5.16. Engine test bed 77

Figure 5.17. The test panel.....79

Figure 5.18. Testo 354 Exhaust Gas Analyzer 80

Figure 6.1 Density measurements results of n-hexane blends.....84

Figure 6.2 Density measurements results of n-heptane blends.....85

Figure 6.3 Density measurements results of xylene blends 85

Figure 6.4. Viscosity measurements results of n-hexane blends.....87

Figure 6.5. Viscosity measurements results of n-heptane blends.....87

Figure 6.6. Viscosity measurements results of xylene blends.....88

Figure 6.7. Lower Heating Value measurements results of n-hexane blends..... 89

Figure 6.8. Lower Heating Value measurements results of n-heptane blends.....90

Figure 6.9. Lower Heating Value measurements results of xylene blends.....90

Figure 6.10. Cetane Number measurements results of n-hexane blends.....91

Figure 6.11. Cetane Number measurements results of n-heptane blends.....92

Figure 6.12. Cetane Number measurements results of xylene blends.....92

Figure 6.13. Pour Point measurements results of n-hexane blends 93

Figure 6.14. Pour Point measurements results of n-heptane blends.....94

Figure 6.15. Pour Point measurements results of xylene blends 94

Figure 6.16. Flash Point measurements results of n-hexane blends.....96

Figure 6.17. Flash Point measurements results of n-heptane blends.....96

Figure 6.18. Flash Point measurements results of xylene blends.....97

Figure 7.1. Torque-Speed Graphic of 85%Diesel, 10%RSB and 5%Alkanes.....99

Figure 7.2. Torque-Speed Graphic of 75%Diesel, 20%RSB and 5%Alkanes 99

Figure 7.3. Torque-Speed Graphic of 65%Diesel, 30%RSB and 5%Alkanes 100

Figure 7.4. Torque-Speed Graphic of 55%Diesel, 40%RSB and 5%Alkanes.....101

Figure 7.5. Torque-Speed Graphic of 45%Diesel, 50%RSB and 5%Alkanes 102

Figure 7.6. Torque-Speed Graphic of 80%Diesel, 10%RSB and 10%Alkanes.....103

Figure 7.7. Torque-Speed Graphic of 70%Diesel, 20%RSB and 10%Alkanes.....104

Figure 7.8. Torque-Speed Graphic of 60%Diesel, 30%RSB and 10%Alkanes.....105

Figure 7.9. Torque-Speed Graphic of 50%Diesel, 40%RSB and 10%Alkanes.....105

Figure 7.10. Torque-Speed Graphic of 40%Diesel, 50%RSB and 10%Alkanes.....106

Figure 7.11. Torque-Speed Graphic of 75%Diesel, 10%RSB and 15%Alkanes.....107

Figure 7.12. Torque-Speed Graphic of 65%Diesel, 20%RSB and 15%Alkanes.....108

Figure 7.13. Torque-Speed Graphic of 55%Diesel, 30%RSB and 15%Alkanes.....109

Figure 7.14. Torque-Speed Graphic of 45%Diesel, 40%RSB and 15%Alkanes.....110

Figure 7.15. Torque-Speed Graphic of 35%Diesel, 50%RSB and 15% Alkanes...110

Figure 7.16. Power-Speed Graphic of 85%Diesel, 10%RSB and 5%Alkanes.....111

Figure 7.17. Power-Speed Graphic of 75%Diesel, 20%RSB and 5%Alkanes.....112

Figure 7.18. Power-Speed Graphic of 65%Diesel, 30%RSB and 5%Alkanes.....113

Figure 7.19. Power-Speed Graphic of 55%Diesel, 40%RSB and 5%Alkanes.....114

Figure 7.20. Power-Speed Graphic of 45%Diesel, 50%RSB and 5%Alkanes.....115

Figure 7.21. Power-Speed Graphic of 80%Diesel, 10%RSB and 10%Alkanes.....116

Figure 7.22. Power-Speed Graphic of 70%Diesel, 20%RSB and 10%Alkanes.....117

Figure 7.23. Power-Speed Graphic of 60%Diesel, 30%RSB and 10%Alkanes.....118

Figure 7.24. Torque-Speed Graphic of 50%Diesel, 40%RSB and 10%Alkanes.....119

Figure 7.25. Power-Speed Graphic of 40%Diesel, 50%RSB and 10%Alkanes.....120

Figure 7.26. Power-Speed Graphic of 75%Diesel, 10%RSB and 15%Alkanes.....121

Figure 7.27. Power-Speed Graphic of 65%Diesel, 20%RSB and 15%Alkanes.....122

Figure 7.28. Power-Speed Graphic of 55%Diesel, 30%RSB and 15%Alkanes.....123

Figure 7.29. Power-Speed Graphic of 45%Diesel, 40%RSB and 15%Alkanes.....124

Figure 7.30. Power-Speed Graphic of 35%Diesel, 50%RSB and 15%Alkanes.....125

Figure 7.31. Specific Fuel Consumption-Speed Graphic of 85%Diesel, 10%RSB and 5%Alkanes.....126

Figure 7.32. Specific Fuel Consumption-Speed Graphic of 75%Diesel, 20%RSB and 5%Alkanes.....127

Figure 7.33. Specific Fuel Consumption-Speed Graphic of 65%Diesel, 30%RSB and 5%Alkanes.....128

Figure 7.34. Specific Fuel Consumption-Speed Graphic of 55%Diesel, 40%RSB and 5%Alkanes.....129

Figure 7.35. Specific Fuel Consumption-Speed Graphic of 45%Diesel, 50%RSB and 5%Alkanes.....130

Figure 7.36. Specific Fuel Consumption-Speed Graphic of 80%Diesel, 10%RSB and 10%Alkanes.....130

Figure 7.37. Specific Fuel Consumption-Speed Graphic of 70%Diesel, 20%RSB and 10%Alkanes.....131

Figure 7.38. Specific Fuel Consumption-Speed Graphic of 60%Diesel, 30%RSB and 10%Alkanes.....132

Figure 7.39. Specific Fuel Consumption-Speed Graphic of 50%Diesel, 40%RSB and 5%Alkanes.....133

Figure 7.40. Specific Fuel Consumption-Speed Graphic of 40%Diesel, 50%RSB and 10%Alkanes.....134

Figure 7.41. Specific Fuel Consumption-Speed Graphic of 75%Diesel, 10%RSB and 15%Alkanes.....135

Figure 7.42. Specific Fuel Consumption-Speed Graphic of 65%Diesel, 20%RSB and 15%Alkanes..... 135

Figure 7.43. Specific Fuel Consumption-Speed Graphic of 55%Diesel, 40%RSB and 15%Alkanes.....136

Figure 7.44. Specific Fuel Consumption-Speed Graphic of 45%Diesel, 40%RSB and 15%Alkanes.....137

Figure 7.45. Specific Fuel Consumption-Speed Graphic of 35%Diesel, 50%RSB and 15%Alkanes.....138

Figure 7.46. CO-Speed Graphic of 85%Diesel, 10%RSB and 5%Alkanes 139

Figure 7.47. CO-Speed Graphic of 75%Diesel, 20%RSB and 5%Alkanes.....140

Figure 7.48. CO-Speed Graphic of 65%Diesel, 30%RSB and 5%Alkanes.....141

Figure 7.49. CO-Speed Graphic of 55%Diesel, 40%RSB and 5%Alkanes.....142

Figure 7.50. CO-Speed Graphic of 45%Diesel, 10%RSB and 5%Alkanes.....142

Figure 7.51. CO-Speed Graphic of 80%Diesel, 10%RSB and 10%Alkanes.....143

Figure 7.52. CO-Speed Graphic of 70%Diesel, 20%RSB and 10%Alkanes.....144

Figure 7.53. CO-Speed Graphic of 60%Diesel, 30%RSB and 10%Alkanes.....145

Figure 7.54. CO-Speed Graphic of 50%Diesel, 40%RSB and 10%Alkanes.....146

Figure 7.55. CO-Speed Graphic of 40%Diesel, 50%RSB and 10%Alkanes.....147

Figure 7.56. CO-Speed Graphic of 75%Diesel, 10%RSB and 15%Alkanes.....148

Figure 7.57. CO-Speed Graphic of 65%Diesel, 20%RSB and 15%Alkanes.....148

Figure 7.58. CO-Speed Graphic of 55%Diesel, 30%RSB and 15%Alkanes.....149

Figure 7.59. CO-Speed Graphic of 45%Diesel, 40%RSB and 15%Alkanes.....150

Figure 7.60. CO-Speed Graphic of 35%Diesel, 50%RSB and 15%Alkanes.....151

Figure 7.61. NO_x-Speed Graphic of 85%Diesel, 10%RSB and 5%Alkanes.....152

Figure 7.62. NO_x-Speed Graphic of 75%Diesel, 20%RSB and 5%Alkanes.....153

Figure 7.63. NO_x-Speed Graphic of 65%Diesel, 30%RSB and 5%Alkanes.....154

Figure 7.64. NO_x -Speed Graphic of 55%Diesel, 40%RSB and 5%Alkanes.....155

Figure 7.65. NO_x-Speed Graphic of 45%Diesel, 50%RSB and 5%Alkanes.....155

Figure 7.66. NO_x-Speed Graphic of 80%Diesel, 10%RSB and 10%Alkanes.....156

Figure 7.67. NO_x-Speed Graphic of 70%Diesel, 20%RSB and 10%Alkanes.....157

Figure 7.68. NO_x-Speed Graphic of 60%Diesel, 30%RSB and 10%Alkanes.....158

Figure 7.69. NO_x-Speed Graphic of 50%Diesel, 40%RSB and 10%Alkanes.....159

Figure 7.70. NO_x-Speed Graphic of 40%Diesel, 50%RSB and 10%Alkanes.....160

Figure 7.71. NO_x-Speed Graphic of 75%Diesel, 10%RSB and 15%Alkanes.....160

Figure 7.72. NO_x-Speed Graphic of 65%Diesel, 20%RSB and 15%Alkanes.....161

Figure 7.73. NO_x-Speed Graphic of 55%Diesel, 30%RSB and 15%Alkanes.....162

Figure 7.74. NO_x-Speed Graphic of 45%Diesel, 40%RSB and 15%Alkanes.....163

Figure 7.75. NO_x-Speed Graphic of 35%Diesel, 50%RSB and 15%Alkanes.....164

Figure 7.76. CO_2-Speed Graphic of 85%Diesel, 10%RSB and 5%Alkanes.....165

Figure 7.77. CO_2-Speed Graphic of 75%Diesel, 20%RSB and 5%Alkanes.....165

Figure 7.78. CO_2-Speed Graphic of 65%Diesel, 30%RSB and 5%Alkanes.....166

Figure 7.79. CO_2-Speed Graphic of 55%Diesel, 40%RSB and 5%Alkanes.....167

Figure 7.80. CO_2-Speed Graphic of 45%Diesel, 50%RSB and 5%Alkanes.....168

Figure 7.81. CO_2-Speed Graphic of 80%Diesel, 10%RSB and 10%Alkanes.....169

Figure 7.82. CO_2-Speed Graphic of 70%Diesel, 20%RSB and 10%Alkanes.....170

Figure 7.83. CO_2-Speed Graphic of 60%Diesel, 30%RSB and 10%Alkanes.....170

Figure 7.84. CO_2-Speed Graphic of 50%Diesel, 40%RSB and 10%Alkanes.....171

Figure 7.85. CO_2-Speed Graphic of 40%Diesel, 50%RSB and 10%Alkanes.....172

Figure 7.86. CO_2-Speed Graphic of 75%Diesel, 10%RSB and 15%Alkanes.....173

Figure 7.87. CO_2-Speed Graphic of 65%Diesel, 20%RSB and 15% Alkanes.....174

Figure 7.88. CO_2-Speed Graphic of 55%Diesel, 30%RSB and 15% Alkanes.....174

Figure 7.89. CO_2-Speed Graphic of 45%Diesel, 40%RSB and 15% Alkanes.....175

Figure 7.90. CO_2-Speed Graphic of 35%Diesel, 50% RSB and 15% Alkanes.....176

SYMBOLS

BDC : Bottom Dead Center

BDC : Bottom Dead Center

CFPP : Cold Filter Plugging Point

CI : Compression Ignition

CO : Carbon Monoxide

CO_2 : Carbon Dioxide

CP : Cloud Point

DI : Direct Injection

EGR : Exhaust Gas Recirculation

EVC : Exhaust Valve Closing

EVO : Exhaust Valve Open

HC : Hydrocarbons

HP : Heptane

HX : Hexane

ID : Ignition Delay

IVC : Intake Valve Closing

IVO : Intake Valve Open

KOH : Potassium Hydroxide

N_2O : Nitrous Oxide

NaOH : Sodium Hydroxide

NO : Nitric Oxide

NO_2 : Nitrogen Dioxide

NO_3 : Nitrates

NO_x : Nitrogen Oxides

PM : Particulate Matter

PP : Pour Point

ppm : Parts Per Million

RME : Rapeseed Metal Ester

rpm : Revolution Per Minute

RSB : Rapeseed Biodiesel

SFC : Specific Fuel Consumption

TDC : Top Dead Center

TDC : Top Dead Center

VOC : Volatile Organic Compounds

Wt : Weight

XL : Xylene

1. INTRODUCTION

The world's energy demand has been steadily increasing since the beginning of industrialization in the 19th Century. Growth rates were particularly strong in western industrialized countries during the economic boom that followed the Second World War.

The 20th Century saw the rise of liquid fuels based on petroleum (petrol, diesel, kerosene, etc.). These fuels are especially important in the transportation sector. Their high energy content and ease of storage in tanks are to their advantage.

Depending on the definitions and methods of calculation used, fossil fuels, i.e., coal, oil and gas, account for 80 to 90% of global primary energy supply. Nuclear energy, hydropower and mostly in developing countries non-commercial biomass fuels are further sources of energy worth of note. In most regions, oil is the most important source of energy.

Total world energy use rises from 471 Peta Joule in 2004 to 590 Peta Joule in 2015 and then to 740 Peta Joule in 2030 (Figure 1.1). Global energy demand grows despite the relatively high world oil and natural gas prices.

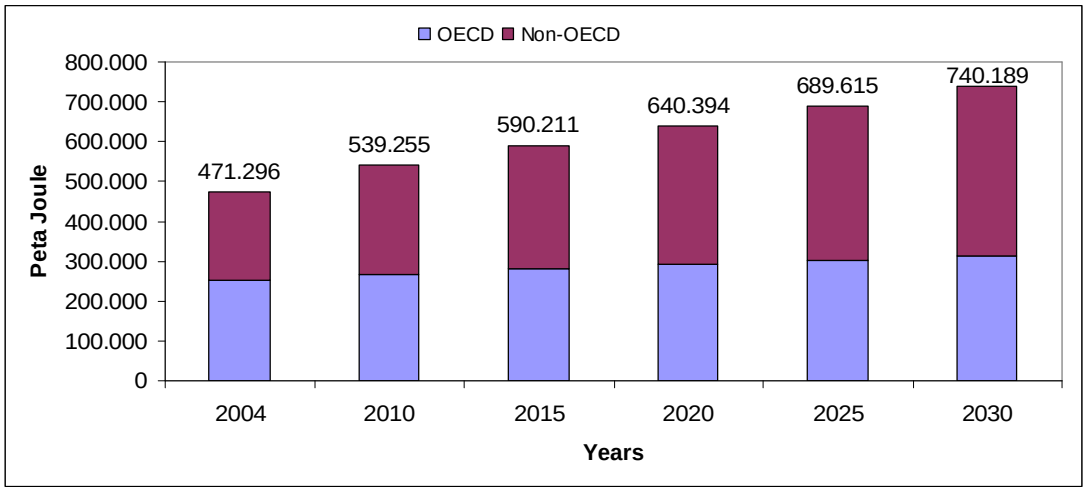


Figure 1.1. World Marketed Energy Consumption by Region, 2004-2030 (International Energy Outlook, 2007)

The world consumption of marketed energy from all sources assumed to be increased over the 2004 to 2030 projection period (Figure 1.2). Fossil fuels (petroleum and other liquid fuels, natural gas, and coal) are expected to continue supplying much of the energy used worldwide (International Energy Outlook, 2007).

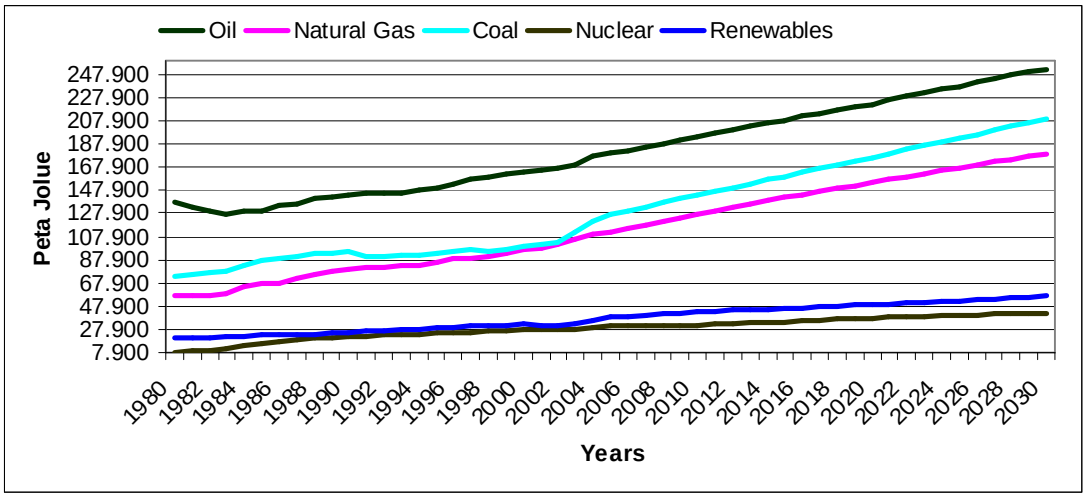


Figure 1.2. World Marketed Energy Use by Fuel Type, 1980-2030 (International Energy Outlook, 2007)

In most regions of the world, the role of liquid fuels outside the transportation sector continues to erode. Liquids remain the most important fuels for transportation, because there are few alternatives that can compete widely with petroleum-based liquid fuels (International Energy Outlook, 2007).

Unconventional resources (including biofuels, coal-to-liquids, and gas-to-liquids) from both OPEC and non-OPEC sources are expected to become increasingly competitive. Fossil fuels continue to supply much of the increment in marketed energy use worldwide throughout the projections. Liquids (primarily, oil and other petroleum products) are expected to continue to provide the largest share of world energy consumption over the projection period, but their share falls from 38% in 2004 to 34% in 2030 (Figure 1.3), largely because rising world oil prices dampen the demand for liquids after 2015 (International Energy Outlook, 2007).

Humankind's rising demand for energy can basically be covered by two sources: the natural resources in the Earth's crust that can be used to produce energy

(fossil fuels, uranium and thorium) and the "renewable" sources of energy that regenerate themselves endlessly. Fossil fuels are exhaustible natural resources. They will not be able to continue playing a lead role in the world's energy supply and infinitum.

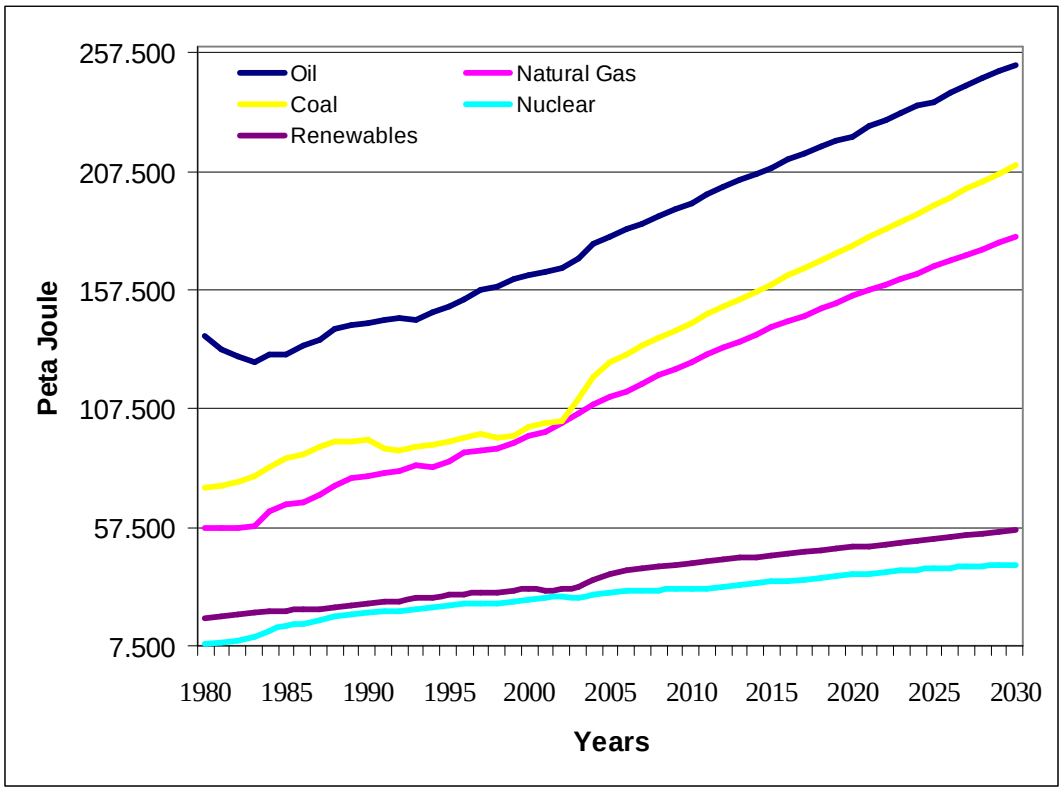


Figure 1.3. World Marketed Energy Use by Fuel Type, 1980-2030 (International Energy Outlook, 2007)

Biofuels are being investigated as potential substitutes for current high pollutant fuels obtained from the conventional sources. In the past, fuels were generally selected on the basis of lowest cost relating to the requirements of the engine, and no attention was given to the possible effects of their use on the environment. Recent concerns over the environment, increasing liquid fuel prices and scarcity of supply in the last decade have promoted interest in the development of alternative sources of liquid energy (Nwafor, 2004).

The use of vegetable oils as a diesel fuel is a concept nearly as old as the diesel engine (Knothe and Dunn, 2005). Rudolph Diesel, the inventor of the engine

that bears his name, experimented with fuels ranging from powdered coal to peanut oil (Radich, 2008).

Transesterification of a vegetable oil was conducted as early as 1853, by scientists E. Duffy and J. Patrick, many years before the first diesel engine became functional. Rudolf Diesel's prime model, a single 3 m. iron cylinder with a flywheel at its base, ran on its own power for the first time in Augsburg, Germany on 10^{th} of August, 1893. In remembrance of this event, 10^{th} of August has been declared International Biodiesel Day. Diesel later demonstrated his engine and received the "Grand Prix" (highest prize) at the World Fair in Paris, France in 1900. This engine stood as an example of Diesel's vision because it was powered by peanut oil—a biofuel, though not strictly biodiesel, since it was not transesterified. He believed that the utilization of a biomass fuel was the real future of his engine. In a 1912 speech, Rudolf Diesel said "the use of vegetable oils for engine fuels may seem insignificant today, but such oils may become, in the course of time, as important as petroleum and the coal-tar products of the present time" (Guo, 2007).

During the 1920s diesel engine manufacturers altered their engines to utilize the lower viscosity of the fossil fuel (petrodiesel) rather than vegetable oil, a biomass fuel. The petroleum industries were able to make inroads in fuel markets because their fuel was much cheaper to produce than the biomass alternatives. The result was, for many years, a near elimination of the biomass fuel production infrastructure. Only recently have environmental impact concerns and a decreasing cost differential made biomass fuels such as biodiesel a growing alternative (Anonymous, 2008a).

The revival of biodiesel production started with farm co-operatives in the 1980s in Austria, but in 1991 the first industrial-scale plant opened in Aschach, also in Austria, with a capacity in excess of 10,000 million per year. Throughout the 1990s, plants were opened in many European countries, including the Czech Republic, France, Germany and Sweden. At the same time, nations in other parts of world also saw local production of biodiesel starting up and by 1998, the Austrian Biofuels institute identified 21 countries with commercial biodiesel projects. In the 1990s, France launched the local production of biodiesel fuel (known locally as diester) obtained by the transesterification of rapeseed oil. It is mixed to the

proportion of 5% into regular diesel fuel, and to the proportion of 30% into the diesel fuel used by some captive fleets (public transportation). Renault, Peugeot, and other manufacturers have certified truck engines for use with up to this partial biodiesel. Experiments with 50% biodiesel are underway (Anonymous, 2008a).

The global bio-diesel industry is among the fastest-growing markets the chemical industry has ever seen. Bio-diesel production is highest in the EU, where more bio-diesel is produced than ethanol, but total production of both fuels is fairly small compared to production of bio-ethanol in Brazil and the United States. Two factors have contributed to the EU's becoming the world leader in bio-diesel production. One is the reform of the Common Agricultural Policy (CAP), a supranational and domestically oriented farm policy for EU member countries, adopted in 1992 and implemented in 1993–1994. The 1992 reform addressed agricultural surpluses through supply control in the form of a mandatory, paid, ''set-aside" program. The second factor is high fuel taxes, which have enabled indirect subsidies for bio-fuel production through partial or full exemption of the fuel excise tax. Taxes normally constitute 50% or more of the retail price of diesel in EU member states. In February 1994, the European Parliament adopted a 90% tax exemption for bio-diesel. The EU is the world leader in the production and consumption of bio-diesel. According to the European Bio-diesel Board's 2007 figures, the EU produced 4.98 million tons of bio-diesel in 2006, up from 3.18 million tons in 2005. The EU accounted for 77% of global bio-diesel production in 2006. Bio-diesel accounted for nearly 80% of EU bio-fuel production. The EU is expected to continue to be the main market and producer of bio-diesel, followed by the United States and Brazil. The EC Bio-fuels Directive of 2003 required a voluntary market share of 5.75% bio-fuels for each member state by 2010. Other countries (including Netherlands, India, China, Thailand and New Zealand) and individual states in the United States and Canada have since established mandatory bio-fuels targets and yet others have removed excise taxes. Such policies should see additional capacity for bio-ethanol and bio-diesel production developed. Bio-diesel output in Germany – where the biggest in the EU industry was hit by taxes last year – jumped to 2.66 million tons in 2006 from 1.67 million tons in 2005. Looking at

world bio-diesel production, 42% of the world total in 2006 was accounted for by Germany, where market conditions were highly favorable. Other countries with significant bio-diesel markets in 2006 included France, the United States, Italy and the United Kingdom.

Table 1.1. The EU's Biodiesel Production by Country (1000 ton) (Balat and Balat, 2008)

Country	2004	2005	2006
Germany	1035	1669	2662
France	348	492	743
Italy	320	396	447
UK	9	51	192
Austria	57	85	123
Poland	0	100	116
Czech Rep.	60	133	107
Spain	13	73	99
Portugal	0	1	91
Slovakia	15	78	82
Denmark	70	71	80
Others	6	35	148
Total EU	1933	3184	4890

The United States was the world's second-largest producer of bio-diesel, behind the EU. The United States bio-diesel production remained very small and flat until the United States Department of Agriculture (USDA) created the Bioenergy Program in Fiscal Year (FY) 2000 that encouraged bio-diesel production through cash payments to producers. Mostly as a result of this program, bio-diesel production reached from 3300 tons in 1999 to 836,000 tons in 2006. By 2010, the United States is expected to become the largest single bio-diesel market, accounting for roughly 18% of world bio-diesel consumption. Experts predict that, in the best case scenario, in the next 20 years bio-diesel could take care of 25% of the United States diesel needs (Balat and Balat , 2008)

Turkey is an energy importing country; more than half of the energy requirement has been supplied by imports. Oil has the biggest share in total primary energy consumption. Due to the diversification efforts of energy sources, use of

natural gas that was newly introduced into Turkish economy, has been growing rapidly.

Renewable energy supply in Turkey is dominated by hydropower and biomass, but environmental and scarcity-of-supply concerns have led to a decline in biomass use, mainly for residential heating. Total renewable energy supply declined from 1990 to 2004, due to a decrease in biomass supply. As a result, the composition of renewable energy supply has changed and wind power is beginning to claim market share. As a contributor of air pollution and deforestation, the share of biomass in the renewable energy share is expected to decrease with the expansion of other renewable energy sources

Turkey spent a total of US$ 120 million (2005 prices and exchange rates) on government energy research and development between 1980 and 2005. In this period, 15.6% of its total energy research and development (R&D) budget (US$17.4 million) was allocated to renewable energy. Government R&D expenditures for renewables followed the general trend in overall energy R&D expenditures, rising in the late 1980s and then falling in the early 1990s. Public funding increased substantially in 1997.

Table 1.2. Present and planned biomass energy production in Turkey (K tone) (Balat and Balat, 2008)

Years	Classic Biomass	Modern Biomass	Total
2005	6494	766	7260
2010	5754	1660	7414
2015	4790	2530	7320
2020	4000	3520	7520
2025	3345	4465	7810
2030	3310	4895	8205
Total	34658	17853	52511

Biodiesel is a light to dark yellow liquid. It is practically immiscible with water, has a high boiling point and low vapor pressure. Typical methyl ester biodiesel has a flash point of ~ 150 ^{o}C, making it rather non-flammable. Biodiesel has a density of ~ 0.85 kg/lt, less than that of water. Biodiesel uncontaminated with

starting material can be regarded as non-toxic. Biodiesel has a viscosity similar to petrodiesel, the industry term for diesel produced from petroleum. It can be used as an additive in formulations of diesel to increase the lubricity of pure Ultra-Low Sulfur Petrodiesel fuel (Anonymous, 2008b).

Biodiesel can be produced using a variety of esterification technologies. The oils and fats are filtered and preprocessed to remove water and contaminants. If free fatty acids are present, they can be removed or transformed into biodiesel using special pretreatment technologies. The pretreated oils and fats are then mixed with an alcohol (usually methanol) and a catalyst (usually sodium hydroxide). The oil molecules (triglycerides) are broken apart and reformed into methyl esters and glycerin, which are then separated from each other and purified (Anonymous, 2008c).The schematic of biodiesel production path (figure 1.4) is given below (Anonymous, 2008d)

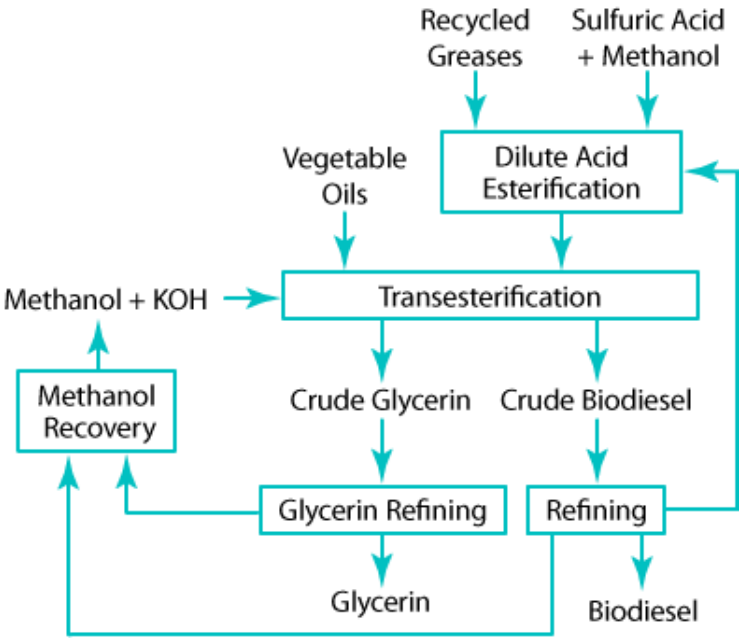


Figure 1.4. Schematic of biodiesel production path (Anonymous, 2008d)

Table 1.3. Comparison Chart for Diesel and Biodiesel (Anonymous, 2008e)

	No. 2 Diesel	Biodiesel
Chemical Structure	C_8 to C_{25}	Methyl esters of C_{12} to C_{22} fatty acids
Cetane Number	40-55	48-65
Pump Octane Number	N/A	N/A
Main Fuel Source	Crude Oil	Fats and oils from sources such as soy beans, waste cooking oil, animal fats, and rapeseed
Energy Content (Lower Heating Value)	35.8 MJ/lt	33.3 MJ/lt for B100
Energy Content (Higher Heating Value)	38.3 MJ/lt	35.7 MJ/lt for B100
Energy Comparison (percent of gasoline energy)	111%	B100 has 103% the energy of gasoline or 93% of diesel. B20 has 109% of gasoline or 99% of diesel
Physical State	Liquid	Liquid
Types of Vehicles Available Today	All size classes subcompact and larger	Most diesel vehicles can use biodiesel blends up to 20%
Environmental Impacts of Burning Fuel	Diesel is highly flammable, but vehicles have been engineered to reduce risks. Diesel is not biodegradable, so spills pollute soil and water.	Reduces hydrocarbons, toxic compounds, CO, particulate matter, and global warming gases. Has uncertain impact on NOx.
Energy Security Impacts	Manufactured using oil, of which nearly is 2/3 imported.	Biodiesel is domestically produced, renewable, and has an energy ratio of 3.2 units biodiesel per 1 unit of fossil energy input.
Maintenance Issues		Hoses and seals may be affected with higher-percent blends, lubricity is improved over that of conventional diesel fuel.
Safety Issues	Diesel is a relatively safe fuel since people have learned to use it safely. Diesel is not biodegradable though, so a spill could pollute soil and water.	B100 is non-toxic and biodegradable. Furthermore, it doesn't ignite as easily as diesel fuel.

Biodiesel can be used in its pure form (B100) or blended with petroleum diesel. Common blends include B2 (2% biodiesel), B5 and B20 (Anonymous, 2008f).

Inorder to investigate the fuel quality results of the blends which were prepared from diisopropylether, 13 different blends were prepared with 5% to 10% diisopropylether, 5% to 40% rapeseed biodiesel and also 5% to 90% diesel fuel. The fuel properties and engine performance values of these fuel blends were measured. Test results showed that, the fuel properties and engine performance values were close to the standard limits for diesel fuel, the viscocity and cold flow properties of biodiesel were improved and these blends could be used directly in diesel engines (Tüccar et al, 2009).

High viscosity and cold flow properties are the biggest problems of biodiesel. In order to improve these specifications, diesel or alcohol is added in biodiesel. Although solvents, which are produced from flue gas of ISDEMIR, are not legally allowed to mix with fuels, they are mixed with and sold in fuel sector because these solvents are cheap and easy to buy.

The aim of the thesis was using three types of solvents as additives for improving the viscosity and cold flow properties of biodiesel.

Thence in this study, eurodiesel was blended with various types of substances including rapeseed biodiesel, n-hexane, n-heptane and xylene. After preparing blends, engine performance and exhaust emission tests were performed. The results were compared with each other and eurodiesel fuel. Both fuel quality and engine test results were given in order to find not only the perfect blending percentage according to fuel quality standards but also its effect on engine performance and emission characteristics.

Previous studies about biodiesel production from vegetable oil, effects of blends on engine performance and exhaust emissions were briefly explained in chapter two.

Diesel combustion is briefly explained in chapter three.

In chapter four; biodiesel production methods and fuel quality specifications have been briefly summarized.

In chapter five; biodiesel production, preparation of blends and experimental setup is explained.

In chapter six; fuel quality results are compared to the fuel standards.

In chapter seven; engine performance tests and exhaust emission results of blends were compared to each other.

Conclusion and recommendations for further work were outlined in the final chapter.

2. PREVIOUS WORKS

Makareviciene and Janulis (2003), noted that exhaust emission tests were conducted on rapeseed oil methyl ester (RME), rapeseed oil ethyl ester (REE) and fossil diesel fuel as well as on their mixtures. Results showed that when considering emissions of nitrogen oxides (NO*x*), carbon monoxide (CO) and smoke density, rapeseed oil ethyl ester had less negative effect on the environment in comparison with that of rapeseed oil methyl ester. When fuelled with rapeseed oil ethyl ester, the emissions of NO_x showed an increase of 8.3% over those of fossil diesel fuel. When operated on 25–50% bioester mixed with fossil diesel fuel, NO_x emissions marginally decreased. When fuelled with pure rapeseed oil ethyl ester, HC emissions decreased by 53%, CO emissions by 7.2% and smoke density 72.6% when compared with emissions when fossil diesel fuel was used. Carbon dioxide (CO_2) emissions, which cause greenhouse effect, decreased by 782.87 g/kWh when rapeseed oil ethyl ester was used and by 782.26 g/kWh when rapeseed oil methyl ester was used instead of fossil diesel fuel. Rapeseed oil ethyl ester was more rapidly biodegradable in aqua environment when compared with rapeseed oil methyl ester and especially with fossil diesel fuel. During a standard 21 day period, 97.7% of rapeseed oil methyl ester, 98% of rapeseed oil ethyl ester and only 61.3% of fossil diesel fuel were biologically decomposed.

Nwafor (2004), stated that the purpose of the research was to evaluate the potential of rapeseed methyl ester (RME) as a liquid fuel for diesel engines in relation to meeting emission requirements. The test results showed that RME and its blends with diesel fuel emitted high CO_2 compared to test results on diesel fuel. A very significant reduction in emissions of hydrocarbon (HC) were recorded when running on RME and the blends. HC emissions were noted to increase with increased amount of diesel fuel in the blend. The fuel economy was a little worse when running on RME due to its low energy content. There were no marked difference noted for the exhaust temperatures of the blends, RME and diesel fuel at high speed operation. However,

the diesel fuel operation produced high exhaust temperatures at low engine speed. Lubricating oil analysis showed reduction in viscosity indicating oil dilution.

Chiu et al (2004) informed that the cold flow properties of biodiesel (B100) and 80% (B80) to 90% biodiesel in kerosene were evaluated with pour point depressants, toward the objective of identifying approaches to transport and mix biodiesel with diesel in cold climates. Four cold flow improver additives were tested at 0.1–2% in B80, B90, and B100 blends. Two additives significantly decreased the pour points of soybean biodiesel blends, but all the four additives had little effect on cloud points. A mixture of 0.2% additive, 79.8% biodiesel, and 20% kerosene reduced the pour point of B100 by 27 ºC .

Rakopoulos et al (2006), stated that an extended experimental study is conducted to evaluate and compare the use of various Diesel fuel supplements at blend ratios of 10/90 and 20/80, in a standard, fully instrumented, four stroke, direct injection (DI), Ricardo/Cussons 'Hydra' Diesel engine. A high variety of vegetable oils or bio-diesels of various origins are tested as supplements, i.e. cottonseed oil, soybean oil, sunflower oil and their corresponding methyl esters, as well as rapeseed oil methyl ester, palm oil methyl ester, corn oil and olive kernel oil. The series of tests are conducted using each of the above fuel blends, with the engine working at a speed of 2000 rpm and at a medium and high load. In each test, volumetric fuel consumption, exhaust smokiness and exhaust regulated gas emissions such as nitrogen oxides (NO_x), carbon monoxide (CO) and total unburned hydrocarbons (HC) are measured. From the first measurement, specific fuel consumption and brake thermal efficiency are computed. The differences in the measured performance and exhaust emission parameters from the baseline operation of the engine, i.e. when working with neat Diesel fuel, are determined and compared. This comparison is extended between the use of the vegetable oil blends and the bio-diesel blends. Theoretical aspects of Diesel engine combustion, combined with the widely differing physical and chemical properties of these Diesel fuel supplements against the normal Diesel fuel, are used to aid the correct interpretation of the observed engine behavior.

Agarwal et al (2006), stated that vegetable oils produced from numerous oil seed crops (edible and non-edible), e.g., rapeseed oil, linseed oil, rice bran oil, soybean oil were resulted less carbon monoxide (CO), unburned hydrocarbon (HC), and particulate emissions compared to mineral diesel fuel but higher NO_x emissions. Exhaust gas recirculation (EGR) is effective to reduce NO_x from diesel engines because it lowers the flame temperature and the oxygen concentration in the combustion chamber. However, EGR results in higher particulate matter (PM) emissions. Thus, the drawback of higher NO_x emissions while using biodiesel may be overcome by employing EGR. The objective of current research work is to investigate the usage of biodiesel and EGR simultaneously in order to reduce the emissions of all regulated pollutants from diesel engines. A two-cylinder, air-cooled, constant speed direct injection diesel engine used for experiments. HCs, NO_x, CO, and opacity of the exhaust gas measured to estimate the emissions. Various engine performance parameters such as thermal efficiency, brake specific fuel consumption (BSFC), and brake specific energy consumption (BSEC), etc. calculated from the acquired data. Application of EGR with biodiesel blends resulted in reductions NO_x emissions without any significant penalty in PM emissions or BSEC.

Labeckas and Slavinskas (2006) informed that the comparative bench testing results of a four stroke, four cylinder, direct injection, unmodified, naturally aspirated Diesel engine when operating on neat RME and its 5%, 10%, 20% and 35% blends with Diesel fuel were presented. The purpose of this research is to examine the effects of RME inclusion in Diesel fuel on the brake specific fuel consumption (BSFC) of a high-speed Diesel engine, its brake thermal efficiency, emission composition changes and smoke opacity of the exhausts. The brake specific fuel consumption at maximum torque (273.5 g/kW h) and rated power (281 g/kW h) for RME is higher by 18.7% and 23.2% relative to Diesel fuel. It is difficult to determine the RME concentration in Diesel fuel that could be recognized as equally good for all loads and speeds. The maximum brake thermal efficiency varies from 0.356 to 0.398 for RME and from 0.373 to 0.383 for Diesel fuel. The highest fuel energy content based upon economy (9.36–9.61 MJ/kW h) is achieved during operation on blend B10, whereas the lowest

ones belong to B35 and neat RME. The maximum NOx emissions increase proportionally with the mass percent of oxygen in the biofuel and engine speed, reaching the highest values at the speed of 2000 min^{-1}, the highest being 2132 ppm value for the B35 blend and 2107 ppm for RME. The carbon monoxide, CO, emissions and visible smoke emerging from the biodiesel over all load and speed ranges are lower by up to 51.6% and 13.5% to 60.3%, respectively. The carbon dioxide, CO_2, emissions along with the fuel consumption and gas temperature, are slightly higher for the B20 and B35 blends and neat RME. The emissions of unburned hydrocarbons, HC, for all biofuels are low, ranging at 5–21 ppm levels.

Nabi et al (2006), stated that combustion and exhaust emissions with neat diesel fuel and diesel–biodiesel blends have been investigated. In the investigation, firstly biodiesel from non-edible neem oil has been produced by esterification. The experiment has been conducted with neat diesel fuel and diesel–biodiesel blends in a four stroke naturally aspirated (NA) direct injection (DI) diesel engine. Compared with conventional diesel fuel, diesel–biodiesel blends showed lower carbon monoxide (CO), and smoke emissions but higher oxides of nitrogen (NO_x) emission. However, compared with the diesel fuel, NO_x emission with diesel–biodiesel blends was slightly reduced when EGR was applied.

Crookes (2006), stated that an experimental programme examining performance and emissions from spark- and compression-ignition engines, running on a variety of bio-fuels, including simulated bio-gas and commercial seed oil was presented. Both engines were single-cylinder laboratory-type engines of comparable power output having variable speed and load capability, the spark-ignition engine additionally having variable compression ratio. For bio-gas, containing carbon dioxide, emissions of oxides of nitrogen were reduced relative to natural gas, while unburnt hydrocarbons were increased. Brake power and specific fuel consumption changed little and carbon monoxide was predominantly affected by air-fuel ratio. Equivalent effects were demonstrated with nitrogen replacing carbon dioxide in the simulated bio-gas and similar trends were evident as compression ratio was increased. Seed-oil bio-fuel gave similar performance to diesel fuel without major disadvantages,

other than increased specific fuel consumption. Tests with cetane and rape-seed methyl ester bio-diesel are also presented for comparison. Specific fuel consumption was about the same and specific NOx emissions were lower with bio-fuel than results from the spark-ignition engine tests running on biogas.

Tsolakis et al (2007), stated that the combustion of RME as pure fuel or blended with diesel in an unmodified engine results in advanced combustion, reduced ignition delay and increased heat release rate in the initial uncontrolled premixed combustion phase. The increased in-cylinder pressure and temperature lead to increased NO_x emissions while the more advanced combustion assists in the reduction of smoke compared to pure diesel combustion. The lower calorific value of RME results in increased fuel consumption but the engine thermal efficiency is not affected significantly. When similar percentages (% by volume) of exhaust gas recirculation (EGR) are used in the cases of diesel and RME, NO_x emissions are reduced to similar values, but the smoke emissions are significantly lower in the case of RME. The retardation of the injection timing in the case of pure RME and 50/50 (by volume) blend with diesel results in further reduction of NO_x at a cost of small increases of smoke and fuel consumption.

Keskin et al (2007) informed that production of tall oil biodiesel and usability as alternative fuel for diesel engine were studied. Tall oil is a by-product in the pulp manufacturing by craft or sulphate pulping process. Fatty acids and resinic acids were distilled from crude tall oil by fractional distillation. Tall oil methyl ester (biodiesel) was produced from tall oil fatty acids. Blend of 90% tall oil biodiesel and 10% diesel fuel for test fuel was evaluated. It was tested between 1800 and 3200 rpm at full load-different engine speeds in a single cylinder direct injection diesel engine. According to diesel fuel value, torque and power output of the engine with blend fuel decreased by 2.99% and 2.94%. Average increasing of the blend fuel's specific fuel consumption value was 7.63%. Using of tall oil biodiesel decreased emissions of CO (up to 35.44%) and smoke (up to 13.27%), emissions of NO_x increased by 13,29% .

Canoira et al (2007), informed that Biodiesel has been produced by transesterification of waste frying oil with methanol catalysed by sodium methoxide.

The unsaturated fatty acid methyl esters of the biodiesel produced have been nitrated by two alternative nitration methods, showing an incorporation of nitrogen between 3.43 and 5.10 wt.%, in the chemical form of nitro, nitrate and acetoxy functional groups. A detailed gas chromatography–mass spectrometry analysis has been carried out on the nitrated biodiesel samples in order to identify the nitration products of this complex mixture. The nitrated biodiesel has been added to a base diesel fuel in a 1000 mg L-1 concentration resulting in an increase of the cetane number of the fuel by more than five points, from 54.7 to 60.5.

Kleinova et al (2007), stated that cold flow properties of neat esters of branched chain alcohols with fatty acids and blends of these esters with fossil diesel fuel were studied. According to determined CFPP values, the influence of alcohol branching on the fuel filterability is negligible. Fossil fuel blending with fatty esters of branched alcohols up to 10% vol. does not substantially change the cold flow properties of fossil fuel. The low-temperature properties of fossil diesel and fatty acid methyl/ethyl ester (FAME/FAEE) blends with low ester content (up to 10% vol.), prepared mainly from oils/fats with higher share of saturated fatty acids namely palm oil, tallow and lard were also measured. The obtained results show that studied esters do not change low temperature properties of fossil fuel in the blends with the low esters content of 3–5 % vol., although their own CFPP is over the value permissible by the standard EN 14 214. However, current standard EN 590 specifies to meet all parameters of the standard EN 14 214 also for FAME assigned for blended fuels entirely. The proposal to repeal the CFPP limit for esters assigned for blending is fully justified, without any negative effects on fuel quality.

Dzida and Prusakiewicz (2008), stated that three commercial fuels were studied: biodiesel (based mainly of the fatty acids methyl esters of rapeseed oil), diesel oil Ekodiesel Ultra (standard petroleum diesel oil with sulphur content less than 10 mg/kg), and ON BIO 10 (blend of 20% vol. of biodiesel with 80% vol. of standard petroleum diesel oil with sulphur content less than 10 mg/kg). The speeds of sound were measured within the temperatures from 293 to 318 K and at pressures from 0.1 to 101 MPa. The densities and heat capacities were measured under atmospheric

pressure in the temperature range from 273 to 363 K and 283 to 359 K, respectively. Using the experimental results, the physicochemical properties such as: density, isentropic bulk modulus, heat capacity, and isobaric thermal expansion were calculated in the same temperature and pressure range as the speed of sound was measured. The results obtained show that although the bulk modulus of ON BIO 10 is higher than that of diesel oil Ekodiesel Ultra over the whole pressure range, the difference is rather small and can be compensated by temperature. Isobaric thermal expansivity of biodiesel decreases with pressure slightly less than that of the diesel oil Ekodiesel Ultra. It is approximately independent of temperature and composition of the fuel at pressures 40 ± 5 MPa.

Issariyakul et al (2008), objected that used cooking oil (UCO) was mixed with canola oil at various ratios in order to make use of used cooking oil for production of biodiesel and also lower the cost of biodiesel production. Methyl and ethyl esters were prepared by means of KOH-catalyzed transesterification from the mixtures of both the oils. Water content, acid value and viscosity of most esters met ASTM standard except for ethyl esters prepared from used cooking oil. Canola oil content of at least 60% in the used cooking oil/canola oil feedstock is required in order to produce ethyl ester satisfying ASTM specifications. Although ethanolysis was proved to be more challenging, ethyl esters showed reduced crystallization temperature (−45.0 to −54.4 °C) as compared to methyl esters (−35.3 to −43.0 °C). A somewhat better low-temperature property of ester was observed at higher used cooking oil to canola oil ratio in spite of similar fatty acid compositions of both oils

Alptekin and Canakci (2008), noted that commercially available two different diesel fuels were blended with the biodiesels produced from six different vegetable oils (sunflower, canola, soybean, cottonseed, corn oils and waste palm oil). The blends (B2, B5, B10, B20, B50 and B75) were prepared on a volume basis. The key fuel properties such as density and viscosities of the blends were measured by following ASTM test methods. Generalized equations for predicting the density and viscosities for the blends were given and a mixing equation, originally proposed by Arrhenius and described by Grunberg and Nissan, was used to predict the viscosities

of the blends. For all blends, it was found that there is an excellent agreement between the measured and estimated values of the density and viscosities. According to the results, the density and viscosities of the blends increased with the increase of biodiesel concentration in the fuel blend.

Cao et al (2008), noted that high-purity fatty acid methyl ester (FAME) was produced from different lipids, such as soybean oil, canola oil, a hydrogenated palm oil/palm oil blend, yellow grease, and brown grease, combined with methanol using a continuous membrane reactor. The membrane reactor combines reaction and separation in a single unit, provides continuous mixing of raw materials, and maintains a high molar ratio of methanol to lipid in the reaction loop while maintaining two phases during the reaction. It was demonstrated that the membrane reactor can be operated using a very broad range of feedstocks at highly similar operating conditions to produce FAME. The total glycerine and free glycerine contents of the FAME produced were below the ASTM D6751 standard after a single reaction step. Under essentially the same reaction conditions, a conventional batch reaction was not able to achieve the same degree of FAME purity. The effect of the fatty acid composition of the lipid feedstocks on the FAME purity was also shown. It was demonstrated that, due to the fatty acid composition, FAME from virgin soybean oil and virgin canola oil was produced in the membrane reactor within ASTM specifications even without a water washing step.

Bhale et al (2008), reminded that the cold flow properties of 100% biodiesel fuel obtained from Madhuca indica was investigated. In this paper, the cold flow properties of biodiesel were evaluated with and without pour point depressants towards the objectives of identifying the pumping and injecting of these biodiesel in CI engines under cold climates. Effect of ethanol, kerosene and commercial additive on cold flow behavior of this biodiesel was studied. A considerable reduction in pour point has been noticed by using these cold flow improvers. The performance and emission with ethanol blended Mahua biodiesel fuel and ethanol–diesel blended Mahua biodiesel fuel have also been studied. A considerable reduction in emission was obtained. Ethanol blended biodiesel is totally a renewable, viable alternative fuel

for improved cold flow behavior and better emission characteristics without affecting the engine performance.

Keskin et al (2008), stated that usability of cotton oil soapstock biodiesel–diesel fuel blends as an alternative fuel for diesel engines were studied. Biodiesel was produced by reacting cotton oil soapstock with methyl alcohol at determined optimum condition. The cotton oil biodiesel–diesel fuel blends were tested in a single cylinder direct injection diesel engine. Engine performances and smoke value were measured at full load condition. Torque and power output of the engine with cotton oil soapstock biodiesel–diesel fuel blends decreased by 5.8% and 6.2%, respectively. Specific fuel consumption of engine with cotton oil soapstock–diesel fuel blends increased up to 10.5%. At maximum torque speeds, smoke level of engine with blend fuels decreased up to 46.6%, depending on the amount of biodiesel. These results were compared with diesel fuel values.

Zheng et al (2008), noted that engine performance and emission comparisons were made between the use of soy, Canola and yellow grease derived B100 biodiesel fuels and an ultra-low sulphur diesel fuel in the high load engine operating conditions. Compared to the diesel fuel engine-out emissions of nitrogen oxides (NO_x), a high-cetane number (CN) biodiesel fuel produced comparable NO_x while the biodiesel with a CN similar to the diesel fuel produced relatively higher NO_x at a fixed start of injection. The soot, carbon monoxide and un-burnt hydrocarbon emissions were generally lower for the biodiesel-fuelled engine. Exhaust gas recirculation (EGR) was then extensively applied to initiate low temperature combustion (LTC) mode at medium and low load conditions. An intake throttling valve was implemented to increase the differential pressure between the intake and exhaust in order to increase and enhance the EGR. Simultaneous reduction of NO_x and soot was achieved when the ignition delay was prolonged by more than 50% from the case with 0% EGR at low load conditions. Furthermore, a preliminary ignition delay correlation under the influence of EGR at steady-state conditions was developed. The correlation considered the fuel CN and oxygen concentrations in the intake air and fuel. The

research intends to achieve simultaneous reductions of NO_x and soot emissions in modern production diesel engines when biodiesel is applied.

Albuquerque et al (2009), stated that the objective of the study was to evaluate the properties of biodiesel oils obtained from different biomass sources (castor, soybean, cotton, and canola) and their binary blends prepared in concentration ranges between 20 and 80% vol. Each sample was analyzed for viscosity, specific gravity and iodine index. The proper formulation to meet the European specifications for biodiesel (DIN – 14214) using those sources of biomass was presented and discussed. It was observed that the biodiesel obtained from castor oil presents problems for specific gravity and viscosity specification within the European limits. Blends of castor biodiesel oil with the other biodiesel oils can improve these properties in order to comply with the European specification. As for the soybean biodiesel oil, the iodine index can be improved by blending with the other biodiesel oils that were studied. The different behaviors observed for these oleaginous sources can be related to their chemical nature (hydroxyl and unsaturated groups for castor oil, and unsaturated double bonds for soybean oil).

Ozsezen et al (2009), informed that the performance and combustion characteristics of a direct injection (DI) diesel engine fueled with biodiesels such as waste (frying) palm oil methyl ester (WPOME) and canola oil methyl ester (COME) were discussed. In order to determine the performance and combustion characteristics, the experiments were conducted at the constant engine speed mode (1500 rpm) under the full load condition of the engine. The results indicated that when the test engine was fueled with WPOME or COME, the engine performance slightly weakened; the combustion characteristics slightly changed when compared to petroleum based diesel fuel (PBDF). The biodiesels caused reductions in carbon monoxide (CO), unburned hydrocarbon (HC) emissions and smoke opacity, but they caused to increases in nitrogen oxides (NO_x) emissions.

Soltic et al (2009), informed that the effects of mineral diesel fuel, gas-to-liquid fuel, rapeseed methyl ester, neat soybean and neat rapeseed oil on injection, combustion, efficiency and pollutant emissions have been studied on a compression

ignition heavy duty engine operated near full load and equipped with a combined exhaust gas aftertreatment system (oxidation catalyst, particle filter, selective catalytic NO_x reduction). In a first step, the engine calibration was kept constant for all fuels which led to differences in engine torque for the different fuels. In a second step, the injection duration was modified so that all fuels led to the same engine torque. In a third step, the engine was recalibrated in order to keep the NO_x emissions at an equal level for all fuels (injection pressure, injection timing, EGR rate). The experiments show that the critical NO_x emissions were higher (even behind the exhaust gas aftertreatment systems) for oxygenated fuels in case of the engine not being recalibrated for the fuel. GTL and the oxygenated fuels show lower emissions for some pollutants and higher efficiency after recalibration to equal NO_x levels.

Wu et al (2009), stated that the performance of five methyl esters with different sources was studied: cottonseed methyl ester (CME), soybean methyl ester (SME), rapeseed methyl ester (RME), palm oil methyl ester (PME) and waste cooking oil methyl ester (WME). Total particulate matter (PM), dry soot (DS), non-soot fraction (NSF), nitrogen oxide (NO_x), unburned hydrocarbon (HC), and carbon monoxide (CO) were investigated on a Cummins ISBe6 Euro III diesel engine and compared with a baseline diesel fuel. Results show that using different methyl esters results in large PM reductions ranging from 53% to 69%, which include the DS reduction ranging from 79% to 83%. Both oxygen content and viscosity could influence the DS emission. Higher oxygen content leads to less DS at high load while lower viscosity results in less DS at low load. NSF decreases consistently as cetane number increases except for PME. The cetane number could be responsible for the large NSF difference between different methyl esters.

Alptekin and Canakci (2009), stated that characterizing of the fuel properties of diesel fuels, alternative fuels and their blends can assist the researchers who work on alternative fuels for diesel engines. Therefore, in this study, methyl esters were produced from five edible vegetable oils (sunflower, soybean, canola, corn and cottonseed) and blended with two different diesel fuels at 2%, 5%, 10%, 20%, 50% and 75% on a volume basis to characterize the key fuel properties of the blends such

as density, viscosity, pour point, distillation temperatures and flash point. The results showed that the fuel properties of the blends were very close to those of diesel fuels at low concentrations upto 20% of methyl esters.

3. COMBUSTION IN DIESEL ENGINES

Autoignition characterizes diesel engine combustion. Combustible fuel is injected toward the end of the compression cycle into the hot, compressed cylinder charge, mixed with it, and ignited. During the ignition lag (between injection and the start of autoignition), a series of complex physical and chemical subprocesses occur such as spray formation, vaporization, mixing, and chain branching (initial chemical reactions) without any notable conversion of energy (Anonymous, 2008g).

Ignition depends on the starting conditions of mixture formation:

- The pressure and temperature of the charge
- The temperature, viscosity, vaporization characteristics, and ignitability of the fuel
- The pressure, time, and characteristic of injection, as well as the nozzle geometry that determines the spray formation (size, distribution, and pulse of the droplets)
- Charge movement
- Charge composition, i.e., the oxygen component and the changes in the specific thermal capacity from the EGR, etc.
- The combustion chamber geometry

Autoignition starts locally in the areas with completely evaporated fuel mixed with sufficient atmospheric oxygen. During this phase, injection typically continues, and combustion and mixture preparation occur simultaneously.

In internal combustion engines, the working fluid is the combustible mixture of air and fuel. This fluid is responsible for releasing heat energy that is stored in the fuel and producing useful work. Worthwhile goals common to the design and development of all heat engines include: maximizing work (power output), minimizing energy consumption, and reducing pollutants that may be formed in the process of producing work. Figure 3.1 shows the main components of a reciprocating engine.

Diesel engines achieve their high performance and excellent fuel economy by compressing air to high pressures then injecting a small amount of fuel into this highly

compressed air. The charge of air and fuel in these engines is described as heterogeneous meaning that the fuel remains separate from the air for a finite time in the combustion chamber. Heat generated due to the compression of air in the cylinder causes the small amount of highly atomized injected fuel to evaporate. Mixing with the hot surrounding air in the combustion chamber, the evaporated fuel reaches its auto-ignition temperature and burns thus releasing the energy that is stored in that fuel. The auto-ignition temperature of fuel depends on its chemistry. Combustion in compression-ignited engines occurs at many points where the A/F ratio and temperature can sustain this process.

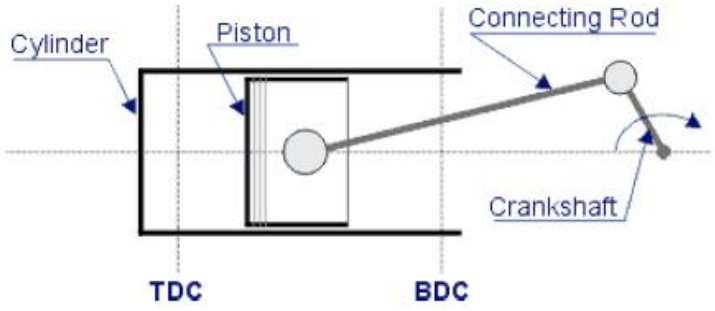


Figure 3.1. Basic Components of a Reciprocating Engine (Anonymous, 2008g)

3.1. Operation of Four-Stroke Engines

It takes four strokes to complete the combustion cycle in four-stroke engines. Figure 3.2 is a schematic representation of the four-stroke combustion cycle as applied to a diesel engine.

In the first stroke, the intake stroke, the piston moves from its position at top-dead-center (TDC) toward the bottom-dead-center (BDC). During most of the intake stroke, filtered air is inducted into the cylinder.

In the second stroke, air that was inducted into the cylinder is compressed by the piston moving back to TDC from its starting position at BDC. This second stroke is known as the compression stroke where air in that cylinder heats up to a temperature usually above the auto-ignition temperature of the fuel which is injected

into the cylinder near TDC. As the fuel burns, heat energy is released raising the pressure inside a greatly reduced volume near TDC. This energy release produces pressure that is applied to the top surface of the piston thus pushing it back toward its BDC.

The last of the four strokes is the exhaust stroke where combustion by-products are exhausted into the exhaust system for evacuation into the atmosphere. In general, today's four-stroke diesel engines are equipped with devices that enhance air charging and allow injecting additional fuel in amounts proportional to the additional air inducted to improve specific power output. This stroke is known as the expansion stroke since it is through that expansion that power (pressure) was imparted to the piston and caused it to move to BDC. The expansion stroke is also known as the power stroke for obvious reasons. It is also referred to by some as the work stroke since the expanding gases were producing work by applying their pressure to the top of piston (Anonymous, 2008g).

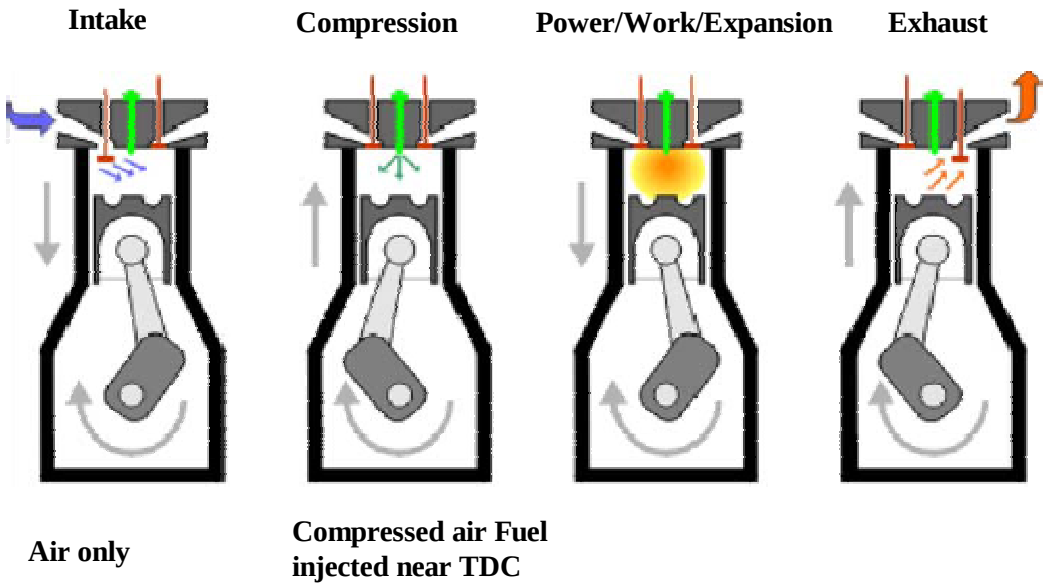


Figure 3.2. Four stroke diesel operation (Anonymous, 2008h)

Changes in pressure, volume, temperature, and mixture composition occur during the four strokes. The pressure-volume diagram is often used to describe

changes in pressure and volume in the cylinder during a complete cycle. Figure 3.3 illustrates pressure and volume changes for a naturally-aspirated diesel engine. In Figure 3.3, intake and exhaust valve events are marked by points 1 through 4, where Point No. 1 is the point at which intake valve opens, Point No. 2 is intake valve closing, Point No. 3 is exhaust valve opening, and Point No. 4 is exhaust valve closing. It is important to note that both intake and exhaust valves remain open during the time between Points 1 and 4 as well as its equivalent crank angle duration. This period is referred to as valve overlap and plays an important role in engine performance and its emission characteristics. The intake valve closing occurs a few degrees beyond BDC to improve cylinder filling and therefore, the volumetric efficiency of the engine. Effective and rapid compression of the working fluid (air) begins after intake valve closing as the piston travels from BDC to TDC (Anonymous, 2008g).

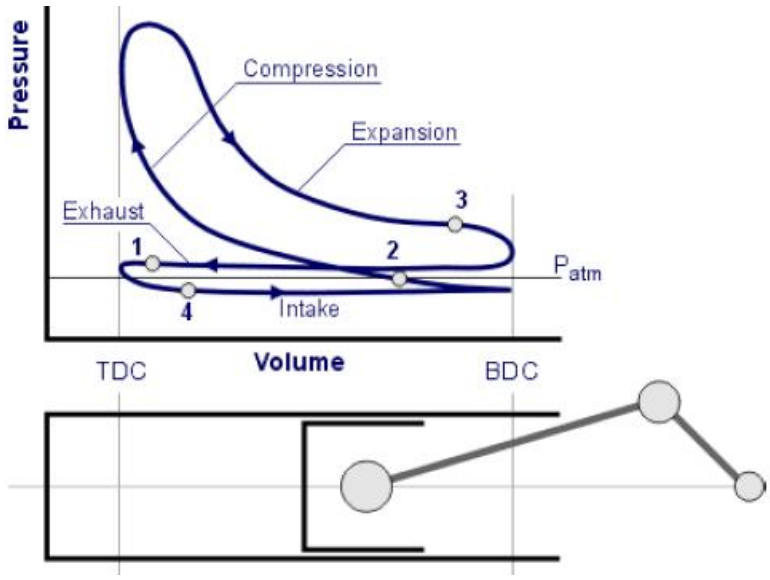


Figure 3.3. Pressure-Volume Diagram for Four-Stroke Naturally-Aspirated Engines (Anonymous, 2008g)

In naturally aspirated engines, pressure inside the cylinder during the intake stroke is below atmospheric pressure. Restrictions through the air intake filter, air inlet piping, intake manifold, intake port, and intake valve contribute to pressure loss

and help reduce cylinder pressure to below atmospheric. Shortly following combustion, the expansion stroke begins and is marked by a number of chemical reactions and heat transfer processes while the piston travels from TDC to BDC. At Point No. 3, the exhaust valve opens thus allowing some of the combustion products to go through a blowdown process as a result of the pressure differential between the cylinder and the exhaust system. The remainder of the exhaust gases is expelled from the cylinder by virtue of the piston motion from BDC to TDC during the exhaust stroke (Anonymous, 2008g).

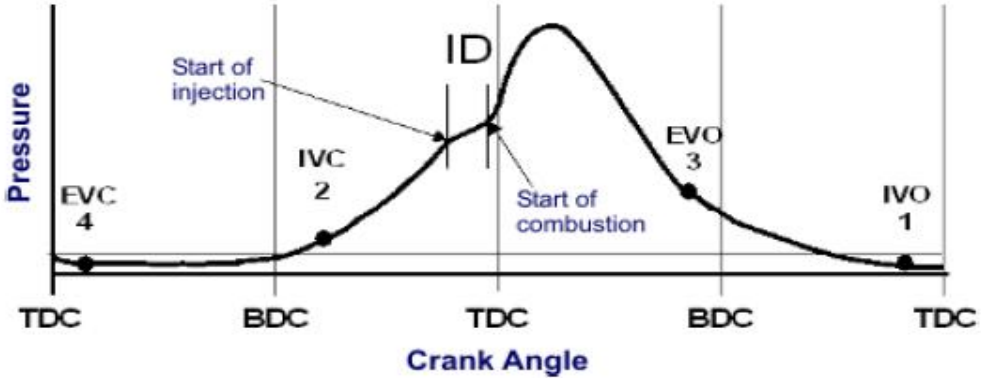


Figure 3.4. Pressure-Crank Angle Diagram for a four- stroke Diesel Engine ID – ignition delay; EVC – exhaust valve closing; IVC – intake valve closing; TDC – top dead center; BDC – bottom dead center; EVO – exhaust valve open; IVO – intake valve open (Anonymous, 2008g)

In addition to the details outlined in the description of the pressure-volume diagram, the pressure-crank angle diagram (Figure 3.4) highlights the point at which fuel is injection (I) as well as ignition delay. During this delay fuel injected into the cylinder evaporates using heat from the working fluid that had been compressed. Following the start of combustion, the rate of pressure rise increases dramatically and the combustion pressure peaks a few crank angle degrees past TDC. Factors controlling the rate of pressure rise include: the ignition delay, fuel quality, and the rate of injection. In many designs, the engine noise, vibration, and harshness characteristics is often tied to the rate of pressure rise in the cylinder.

Together with the rise in cylinder pressure, cylinder temperature also increases and reaches its peak. The maximum combustion temperature depends on several factors including: fuel rate, fuel injection timing, fuel quality especially its calorific value and cetane number, initial cylinder pressure at intake valve closing, and charge temperature. So far intake and exhaust valve motion has been treated generally in relation to the specifics of the pressure-volume or pressure-crank angle diagrams. Earlier, valve overlap was cited as a parameter having major influence on engine performance and its emission characteristics.

A more detailed look into the opening and closing of these two valves reveals more insight into their effect on volumetric efficiency and total charge composition. Starting with the exhaust valve, its opening takes place at a point near the end of the power stroke. The timing of EVO should not be too early lest useful work is lost, yet it is beneficial to effect the valve opening while cylinder pressure is at a level capable of clearing exhaust products through the exhaust valve area during the blow down time.

To ensure complete clearing of the exhaust gases through the exhaust valve opening it is usually kept open e few degrees past TDC. It is worth noting that both valves do not reach their fully open position instantaneously, but have a finite length of time during which they move from a fully closed to fully open position. To make the best use of both valves they must be in their fully open position at the time when they are exposed to the maximum pressure differential causing the working fluid to flow across them.

To ensure this aspect of the cylinder filling and emptying processes, the intake and exhaust valves are usually opened before the start of the intake and exhaust strokes, respectively. They are also held open a few degrees past their respective strokes for the same purpose. As the exhaust valve is opened exhaust gases are expelled by their own kinetic energy, thus reducing the work required by the piston during the exhaust stroke to expel the remaining exhaust gases. Ensuring the expulsion of all exhaust products from the cylinder facilitates the induction of a fresh and generous charge to sustain combustion of the tiny quantity fuel injected into the

cylinder. The intake valve opens towards the end of the exhaust stroke while exhaust gases are exiting through the exhaust valve at high velocity. Their high exit velocity creates a pressure drop in the cylinder that helps draw the fresh charge and maximizes induction. If the intake valve opening is too early, some of the exhaust products may actually flow back through its opening into the intake port and then on to the intake manifold. This portion will be inducted once again into the cylinder during the intake stroke and contaminates the fresh charge with exhaust. The proper function of both valves may require timing their opening and closing in a way that may interfere with the piston position. In such cases two solutions may be used: valve recess in the cylinder head as or valve cutouts in the piston crown. Therefore, it is extremely important to carefully design the timing of intake and exhaust valve opening, closing, lift, flow area as well as intake and exhaust valve overlap (Anonymous, 2008g).

3.1.1. Combustion

The combustion process proceeds by the following stages:

Ignition delay (ab)-fuel is injected directly into the cylinder towards the end of the compression stroke. The liquid fuel atomizes into small drops and penetrates into the combustion chamber. The fuel vaporizes and mixes with the high-temperature high-pressure air.

Premixed combustion phase (bc)–combustion of the fuel which has mixed with the air to within the flammability limits (air at high-temperature and high-pressure) during the ignition delay period occurs rapidly in a few crank angles.

Mixing controlled combustion phase (cd)–after premixed gas consumed, the burning rate is controlled by the rate at which mixture becomes available for burning. The rate of burning is controlled in this phase primarily by the fuel-air mixing process.

Late combustion phase (de)–heat release may proceed at a lower rate well into the expansion stroke (no additional fuel injected during this phase).

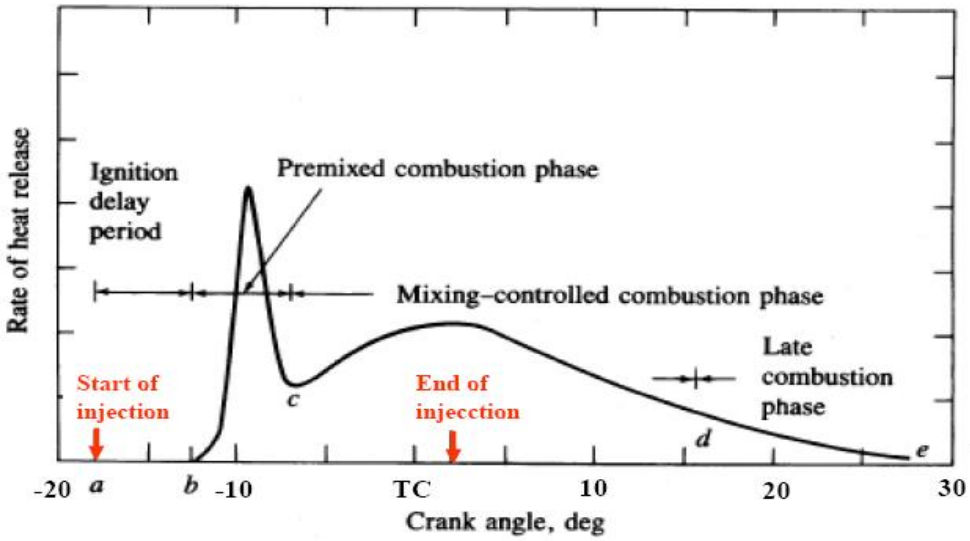


Figure 3.5. Combustion steps in DI diesel engine (Anonymous, 2008h)

3.1.1.1. Ignition Delay

Ignition delay is defined as the time (or crank angle interval) from when the fuel injection starts to the onset of combustion. Both physical and chemical processes must take place before a significant fraction of the chemical energy of the injected liquid is released. *Physical processes* are fuel spray atomization, evaporation and mixing of fuel vapour with cylinder air. Good atomization requires high fuel-injection pressure, small injector hole diam., optimum fuel viscosity, high cylinder pressure (large divergence angle). Rate of vaporization of the fuel droplets depends on droplet diameter, velocity, fuel volatility, pressure and temperature of the air. *Chemical processes* similar to that described for autoignition Phenomenon in premixed fuel-air, only more complex since heterogeneous reactions (reactions occurring on the liquid fuel drop surface) also occur (Anonymous, 2008h)

3.1.1.2. Fuel Ignition Quality

The ignition characteristics of the fuel affect the ignition delay. The ignition quality of a fuel is defined by its cetane number CN. For *low* cetane fuels the ignition delay is long and most of the fuel is injected before autoignition and rapidly burns,

under extreme cases this produces an audible knocking sound referred to as “diesel knock”.

For *high* cetane fuels the ignition delay is short and very little fuel is injected before autoignition, the heat release rate is controlled by the rate of fuel injection and fuel-air mixing –smoother engine operation (Anonymous, 2008h).

3.1.1.3. Factors Affecting Ignition Delay

Injection timing–At normal engine conditions the minimum delay occurs with the start of injection at about 10-15 BTC. The increase in the delay time with earlier or later injection timing occurs because of the air temperature and pressure during the delay period.

Injection quantity–For a CI engine the air is not throttled so the load is varied by changing the amount of fuel injected. Increasing the load (bmep) increases the residual gas and wall temperature which results in a higher charge temperature at injection which translates to a decrease in the ignition delay.

Intake air temperature and pressure–an increase in ether will result in a decrease in the ignition delay, an increase in the compression ratio has the same effect (Anonymous, 2008h).

4. BIODIESEL PRODUCTION AND QUALITY

Biodiesel is a fuel for diesel engines that consists of the mono-alkyl esters of fatty acids from vegetable oils and animal fats. It can be used either pure, or in blends with petroleum-based diesel fuel. It does not require that engines or fueling infrastructure be modified although checking elastomers for compatibility is recommended when pure biodiesel (B100) is used. Biodiesel allows diesel engines to produce lower exhaust emissions of smoke, particulate, carbon monoxide, and unburned hydrocarbons. Oxides of nitrogen may increase slightly under some operating conditions but the difference for biodiesel blends up to 20% is difficult to measure (Van Gerpen, 2007).

Biodiesel provides a major new market for excess supplies of vegetable oil and animal fats. The reduction in these excess supplies should improve prices for commodity oilseeds such as soybeans and canola. It could also encourage the development of greater diversity in crop production as oilseeds with greater oil yield per acre become economically viable.

Biodiesel can also displace a portion of the petroleum used for transportation and, because it is biologically-based, may reduce the impact of global warming. However, its impact on these issues should not be exaggerated. Current world production of vegetable oils and animal fats and competition for these oils and fats from food uses will limit biodiesel’s contribution to less than 5% of petroleum diesel fuel for the foreseeable future.

Biodiesel provides an improvement in diesel fuel lubricity, even when used in blends as low as 1 to 2%. This benefit is increasingly important as low-lubricity desulfurized diesel fuels are required. Recent work suggests that the actual lubricity benefit may be associated with contaminants in the biodiesel, such as free fatty acids and monoglycerides, rather than the combination of high petroleum prices and government incentives has caused a surge in interest in biodiesel. Production capacity is increasing rapidly (Van Gerpen, 2007).

4.1. Production and Usage of Biodiesel

Biodiesel is a natural, renewable resource. It is a cleaner-burning diesel replacement fuel made from natural, renewable sources such as new and used vegetable oils and animal fats. Just like petroleum diesel, biodiesel operates in compression-ignition engines or Diesel engines. Biodiesel has physical properties very similar to conventional diesel (Bozbaş, 2008).

4.1.1. Triglycerids as Diesel Fuels

Triglycerids also known as fats and oils are a special class of esters that consist of three long-chain fatty (carboxylic) acids attached to a backbone of glycerol(1, 2, 3-propanetriol). The acid fractions of triglycerides can vary in chain length and degree of saturation. Fats, which are solid or semi-solid at room temperature, have a high percentage of saturated acids, whereas oils, which are liquid at room temperature, have a high percentage of unsaturated acids. Plant-derived triglycerides are typically oils containing unsaturated fatty acids, including oleic, linoleic, and linolenic acids (Brown, 2003).

The usability of vegetable oils, such as palm, soya bean, sunflower, peanut and olive oils as alternative fuels for diesel engines were dates back almost nine decades. Due to the rapid decline in crude oil reserves, the use of vegetable oils as diesel fuels is again promoted in many countries. Depending upon climate and soil conditions, different nations are looking into different vegetable oils for diesel fuels. For example, soya bean oil in the United States, rapeseed and sunflower oils in Europe, palm oil in Southeast Asia (mainly Malaysia and Indonesia), and coconut oil in The Philippines are being considered as substitutes for diesel fuels (Srivastava and Prasad, 2000).

Table 4.1. Fatty acid composition of vegetable oils[a] (Srivastava and Prasad, 2000).

Vegetable oil	Fatty acid composition, wt.%									
	14:0	16:0	18:0	20:0	22:0	24:0	18:1	22:1	18:2	18:3
Corn	0	12	2	Tr	0	0	25	0	6	Tr
Cottonseed	0	28	1	0	0	0	13	0	58	0
Crambe	0	2	1	2	1	1	19	59	9	7
Linseed	0	5	2	0	0	0	20	0	18	55
Peanut	0	11	2	1	2	1	48	0	32	1
Rapeseed	0	3	1	0	0	0	64	0	22	8
Safflower	0	9	2	0	0	0	12	0	78	0
H.O.Safflower	Tr	5	2	Tr	0	0	79	0	13	0
Sesame	0	13	4	0	0	0	53	0	30	0
Soya bean	0	12	3	0	0	0	23	0	55	6
Sunflower	0	6	3	0	0	0	17	0	74	0

[a]Tr=traces

Table 4.2. Properties of vegetable oil (Murugesan et al, 2008)

Vegetable oil	Kinematic viscosity at 38ºC (mm^2/s)	Cetane no.	Heating value (Mj/kg)	Cloud Point (ºC)	Pour Point (ºC)	Flash Point (ºC)	Density (kg/l)
Corn	34,9	37,6	39,5	-1,1	-40,0	277	0,9095
Cottonseed	33,5	41,8	39,5	1,7	-15,0	234	0,9148
Crambe	53,6	44,6	40,5	10,0	-12,2	274	0,9048
Linseed	27,2	34,6	39,3	1,7	-15,0	241	0,9236
Peanut	39,6	41,8	39,8	12,8	-6,7	271	0,9026
Rapeseed	37,0	37,6	39,7	-3,9	-31,7	246	0,9115
Safflower	31,3	41,3	39,5	18,3	-6,7	260	0,9144
Sesame	35,5	40,2	39,3	-3,9	-9,4	260	0,9133
Soya bean	32,6	37,9	39,6	-3,9	-12,2	254	0,9138
Sunflower	33,9	37,1	39,6	7,2	-15,0	274	0,9161
Palm	39,6	42,0	-	31,0	-	267	0,918
Babassu	30,3	38,0	-	20,0	-	150	0,9460
Diesel	3,06	50	43,8	-	-16	76	0,855

4.1.1.1. Chemical Structure of Fatty Acid

Fats and oils are compounds containing three fatty acids each chemically connected to oxygen on a glycerine molecule, called triglycerides. Free fatty acids are those structures that are no longer connected to the glycerine. They are a degradation product and a measure of the quality of the fat. A high quality fat has a low FFA level (Mendez, 2006)

Table 4.3. Chemical structure of common fatty acids (Murugesan, 2008).

Name of fatty acid	Chemical name of fatty acids	Structure (xx:y)	Chemical formula
Lauric	Dodecanoic	12:0	$C_{12}H_{24}O_2$
Myristic	Tetradecanoic	14:0	$C_{14}H_{28}O_2$
Palmitic	Hexadecanoic	16:0	$C_{16}H_{32}O_2$
Stearic	Octadecanoic	18:0	$C_{18}H_{36}O_2$
Arachidic	Eicosanoic	20:0	$C_{20}H_{40}O_2$
Behenic	Docosanoic	22:0	$C_{24}H_{44}O_2$
Lignoceric	Tetracosanoic	24:0	$C_{24}H_{48}O_2$
Oleic	Cis-9-Octadecanoic	18:1	$C_{18}H_{34}O_2$
Linoleic	Cis-9, cis-12-Octadecadienoic	18:2	$C_{18}H_{32}O_2$
Linolenic	Cis-9, cis-12 cis-15-Octadecadienoic	18:3	$C_{18}H_{30}O_2$
Erucle	Cis-13-Docosenoic	22:1	$C_{32}H_{42}O_2$

xx indicates the number of carbon,
y the number of double bonds in the fatty acid chain.

4.2. The Production of Biodiesel

A variety of biolipids can be used to produce biodiesel. These are

- virgin vegetable oil feedstock; rapeseed and soybean oils are most commonly used, though other crops such as mustard, palm oil, sunflower, hemp and even algae show promise;
- waste vegetable oil;
- animal fats including tallow, lard and yellow grease and
- non-edible oils such as Jatropha, neem oil, castor oil, tall oil, etc. (Demirbaş, 2007)

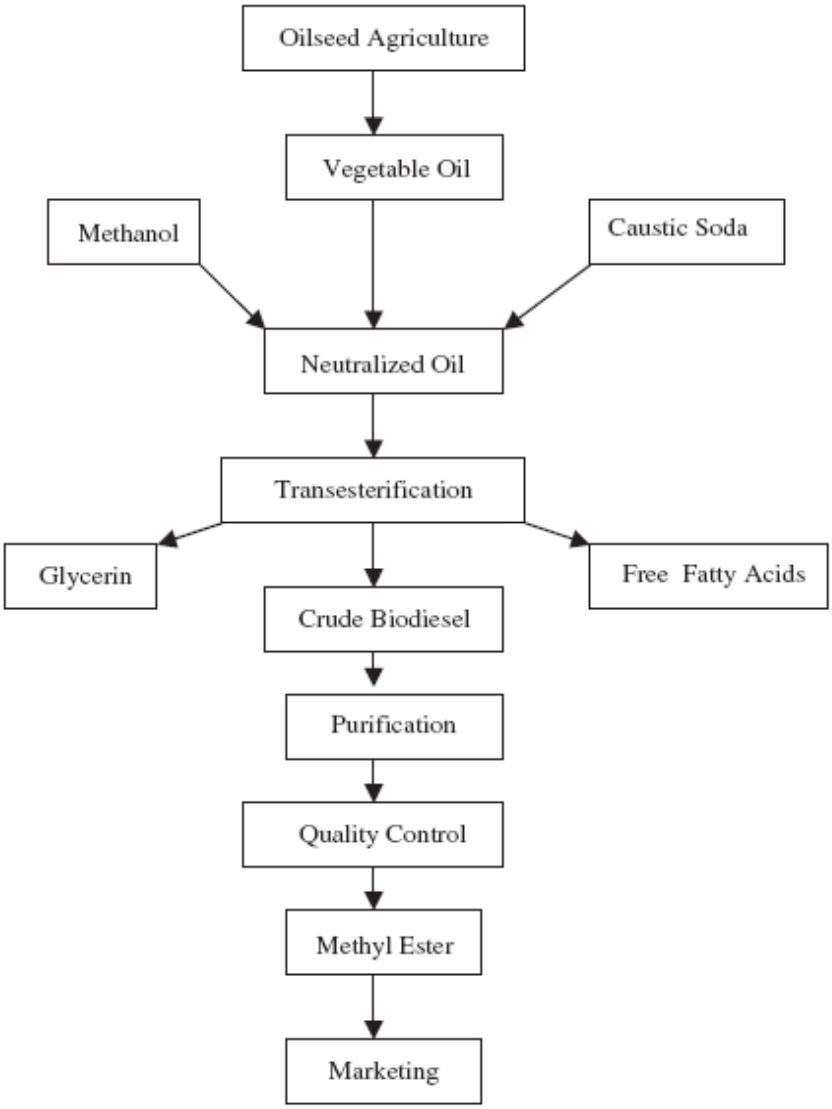


Figure 4.1. Biodiesel processing flow diagram (Demirbaş, 2007)

Considerable efforts have been made to develop vegetable oil derivatives that approximate the properties and performance of the hydrocarbon-based diesel fuels. The problems with substituting triglycerides for diesel fuels are mostly associated with their high viscosities, low volatilities and polyunsaturated character. These can be changed in at least four ways:

- dilution;
- microemulsification;
- pyrolysis;
- transesterification (Srivastava and Prasad, 2000).

4.2.1. Dilution

Dilution of vegetable oils can be accomplished with such materials as diesel fuels, a solvent or ethanol (Srivastava and Prasad, 2000). Dilution is an additional possible solution to the viscosity problem of vegetable oils. Viscosity of vegetable oil can be lowered by blending with pure ethanol (Balat and Balat, 2008).

4.2.2. Microemulsion

Microemulsions are defined as transparent, thermodynamically stable colloidal dispersions in which the diameter of the dispersed-phase particles is less than one fourth the wavelength of visible light. Microemulsion-based fuels are sometimes also termed ‘‘hybrid fuels”, although blends of conventional diesel fuel with vegetable oils have also been called hybrid fuels.

Microemulsions are isotropic, clear, or translucent thermodynamically stable dispersions of oil, water, surfactant, and often a small amphiphilic molecule, called co-surfactant. The droplet diameters in microemulsions range from 100 to 1000 Å. A microemulsion can be made of vegetable oils with an ester and dispersant (cosolvent), or of vegetable oils, an alcohol and a surfactant, with or without diesel fuels.

Microemulsions because of their alcohol content have lower volumetric heating values than diesel fuels, but the alcohols have high latent heat of vaporization and tend to cool the combustion chamber, which would reduce nozzle coking. A microemulsion of methanol with vegetable oils can perform nearly as well as diesel fuels (Srivastava and Prasad, 2000).

4.2.3. Pyrolysis (Thermal Cracking)

Pyrolysis refers to a chemical change caused by the application of thermal energy in the presence of air or nitrogen sparge. Many investigators have studied the pyrolysis of triglycerides to obtain products suitable for diesel engines. These studies include the effect of temperature on the type of products obtained, the use of

catalysts, largely metallic salts, to obtain parafins and olefins similar to those present in hydrocarbon-based diesel fuels, the characterization of the thermal decomposition products.

Thermal decomposition of triglycerides produces the compounds of classes including alkanes, alkenes, alkadienes, aromatics and carboxylic acids. Different types of vegetable oils produce large differences in the composition of the thermally decomposed oil. Figure 4.2 outlines a schematic that accounts for the formation of alkanes, alkenes, alkadienes, aromatics and carboxylic acids from pyrolysis of triglycerides. Mechanisms for the thermal decomposition of triglycerides are likely to be complex because of many structures and multiplicity of possible reactions of mixed triglycerides.

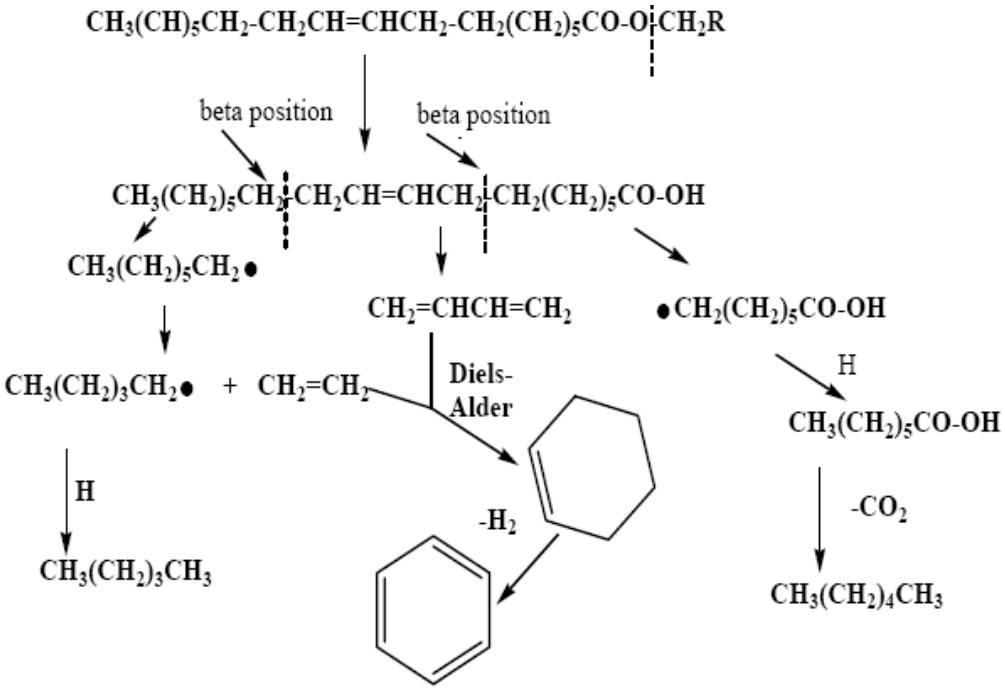


Figure 4.2. The mechanism of thermal decomposition of triglycerids (Adebanjo A., 2005)

Generally, thermal decomposition of these structures proceeds through either a free-radical or carbonium ion mechanism. Formation of homologous series of alkanes and alkenes is accountable from the generation of the RCOO radical from the

triglyceride cleavage and subsequent loss of carbon dioxide. The R radical, upon disproportionation and ethylene elimination, gives the odd-numbered carbon alkanes and alkenes. The presence of unsaturation enhances cleavage at a position a, b to the unsaturation. Thermal positional isomerization and subsequent cleavage could account for the higher amounts of C_5 to C_{10} alkanes obtained from safflower compared with soya bean oil. The formation of aromatics is supported by a Diels-Alder addition of ethylene to a conjugated diene formed in the pyrolysis reaction. Carboxylic acids formed during the pyrolysis of vegetable oils probably result from cleavage of the glyceride moiety (Srivastava and Prasad, 2000).

4.2.4. Transesterification (Alcoholysis)

Transesterification, also called alcoholysis, is the displacement of alcohol from an ester by another alcohol in a process similar to hydrolysis, except than an alcohol is used instead of water. This process has been widely used to reduce the viscosity of triglycerides (Meher et al, 2006).

The transesterification reaction is represented by the general equation:

$$\underset{\text{Ester}}{\text{RCOOR'}} + \underset{\text{Alcohol}}{\text{R''OH}} \overset{\text{Catalyst}}{\rightleftharpoons} \underset{\text{Ester}}{\text{RCOOR''}} + \underset{\text{Alcohol}}{\text{R'OH}}$$

Figure 4.3. General equation of transesterification (Meher et al, 2006)

Transesterification of triglycerides produce fatty acid alkyl esters and glycerol. The glycerol layer settles down at the bottom of the reaction vessel. Diglycerides and monoglycerides are the intermediates in this process (Meher et al, 2006).

The step wise reactions are reversible and a little excess of alcohol is used to shift the equilibrium towards the formation of esters. In presence of excess alcohol, the foreword reaction is pseudo-first order and the reverse reaction is found to be second order. It was also observed that transesterification is faster when catalyzed by alkali (Meher et al, 2006).

Transesterification can be catalyzed by Brownsted acids, preferably by sulfonic and sulfuric acids. These catalysts give very high yields in alkyl esters but these reactions are slow, requiring typically temperature above 100 ºC and more than 3 h to complete the conversion (Meher et al, 2006).

If methanol is used in the above reaction, it is termed Methanolysis (Srivastava and Prasad, 2000). The reaction of triglyceride with methanol is represented by the general equation:

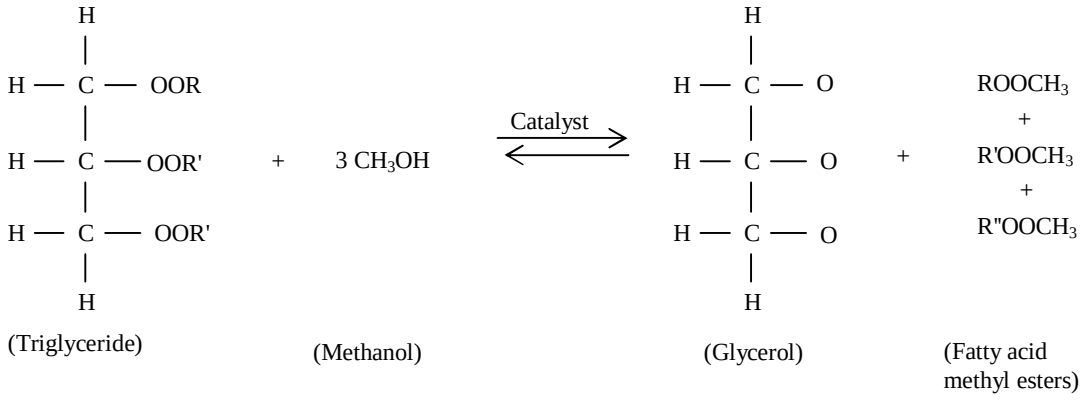


Figure 4.4. General equation of the triglyceride with methanol (Srivastava and Prasad, 2000)

The physical properties of the primary chemical products of transesterification are summarized in Tables 4.4 and 4.5. The boiling points and melting points of the fatty acids, methyl esters, mono-, di- and triglycerides increase as the number of carbon atoms in the carbon chain increase, but decrease with increases in the number of double bonds. The melting points increase in the order of tri-, di- and monoglycerides due to the polarity of the molecules and hydrogen bonding (Ma and Hanna, 1999).

Transesterification consists of a number of consecutive, reversible reactions. The triglyceride is converted stepwise to diglyceride, monoglyceride and finally glycerol (Figure 4.5). A mole of ester is liberated at each step. The reactions are reversible, although the equilibrium lies towards the production of fatty acid esters and glycerol. The reaction mechanism for alkali-catalyzed transesterification was formulated as three steps. The first step is an attack on the carbonyl carbon atom of

the triglyceride molecule by the anion of the alcohol (methoxide ion) to form a tetrahedral intermediate. In the second step, the tetrahedral intermediate reacts with an alcohol (methanol) to regenerate the anion of the alcohol (methoxide ion). In the last step, rearrangement of the tetrahedral intermediate results in the formation of a fatty acid ester and a diglyceride. When NaOH, KOH, K_2CO_3 or other similar catalysts were mixed with alcohol, the actual catalyst, alkoxide group is formed. A small amount of water, generated in the reaction, may cause soap formation during transesterification.

Table 4.4. Physical Properties of Chemicals Related to Transesterification (Ma and Hanna, 1999)

Name	Specific gravity, g/ml (ºC)	Melting point (ºC)	Boiling point (ºC)	Solubility (>10%)
Methly Myristate	0.875 (75)	18.8	-	-
Methyl Palmitate	0.825 (75)	30.6	196.0	Acids, benzene, EtOH, Et_2O
Methyl Streate	0.850	38.0	215.0	Et_2O, chloroform
Methyl Olcate	0.875	-19.8	190.0	EtOH, Et_2O
Methanol	0.792	-97.0	64.7	H_2O, ether, EtOH
Ethanol	0.789	-112.0	78.4	$H_2O(\infty)$, ether(∞)
Glycerol	1.260	17.9	290.0	EtOH, H_2O

Table 4.5. Melting Points of Fatty Acids, Methyl Esters and Mono-, Di-, and Triglyceridea[a] (Ma and Hanna, 1999)

Fatty acid		Melting point (ºC)				
Name	Carbons	Acid	Methyl	1-Monoglyceride	1,3-Diglyceride	Triglyceride
Myristic	14	54,4	18,8	70,5	66,8	57,0
Palmitic	16	62,9	30,6	77,0	76,3	63,5
Stearic	18	69,6	39,1	81,5	79,4	73,1
Oleic	18:1	16,3	-19,8	35,2	21,5	5,5
Linoleic	18:2	-6,5	-35,0	12,3	-2,6	-13,1

[a] Melting point of highest melting most stable polymorphic form.

Generally, the reaction temperature near the boiling point of the alcohol is recommended. Nevertheless, the reaction may be carried out at room temperature. The reactions take place at low temperatures (65ºC) and at modest pressures (2 atm,

1 atm = 101.325 kPa). Biodiesel is further purified by washing and evaporation to remove any remaining methanol. The oil (87%), alcohol (9%), and catalyst (1%) are the inputs in the production of biodiesel (86%), the main output. Pre-treatment is not required if the reaction is carried out under high pressure (9000 kPa) and high temperature (240 ºC), where simultaneous esterification and transesterification take place with maximum yield obtained at temperatures ranging from 60 to 80 ºC at a molar ratio of 6:1. The alcohols employed in the transesterification are generally short chain alcohols such as methanol, ethanol, propanol, and butanol (Balat and Balat, 2008).

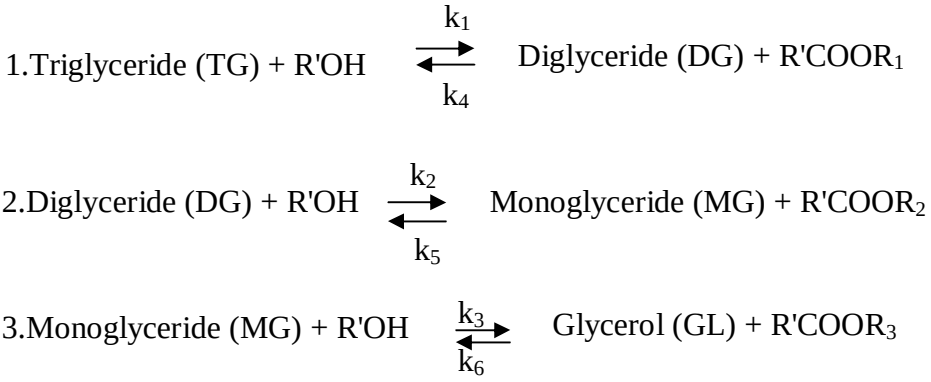


Figure 4.5. The transesterification reactions of vegetable oil with alcohol to esters and glycerol (Ma and Hanna 1999)

4.2.4.1. Catalytic Transesterification

Catalysts used for the transesterification of triglycerides are classified as alkali, acid, enzyme or heterogeneous catalysts, among which alkali catalysts like sodium hydroxide, sodium methoxide, potassium hydroxide, potassium methoxide are more effective. Sulfuric acid, hydrochloric acid and sulfonic acid are usually preferred as acid catalysts. The heterogeneous catalysts include enzymes, titanium-silicates, alkaline-earth metal compounds, anion exchange resins and guanadines heterogenized on organic polymers. The catalytic transesterification of vegetable oils with methanol is an important industrial method used in biodiesel synthesis. Also known as methanolysis, this reaction is well studied and established using acids or alkalis, such as sulfuric acid or sodium hydroxide as catalysts. However, these

catalytic systems are less active or completely inactive for long chain alcohols. Usually, industries use sodium or potassium hydroxide or sodium or potassium methoxide as catalyst, since they are relatively cheap and quite active for this reaction. Figure 4.6 shows the catalytic biodiesel production diagram (Balat and Balat, 2008).

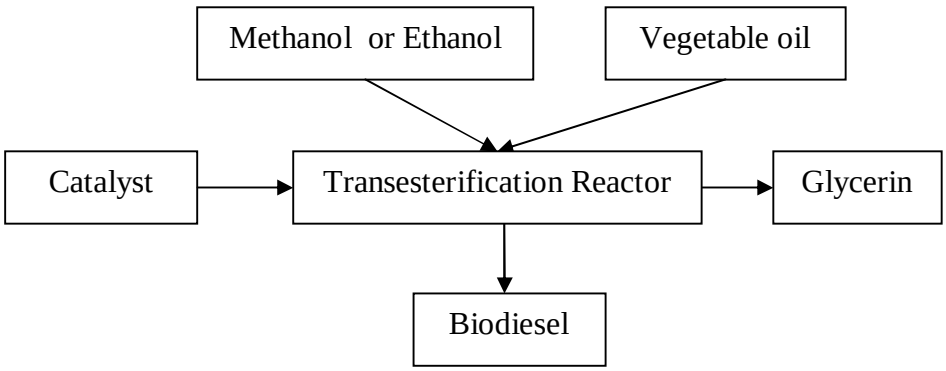


Figure 4.6. Catalytic biodiesel production diagram

4.2.4.1.(1). Alkali-Catalyzed Transesterification

The transesterification process is catalyzed by alkaline metal alkoxides, and hydroxides, as well as sodium or potassium carbonates. The alkaline catalysts show high performance for obtaining vegetable oils with high quality, but a question often arises; that is, the oils contain significant amounts of free fatty acids which cannot be converted into biodiesels but to a lot of soap. These free fatty acids react with the alkaline catalyst to produce soaps that inhibit the separation of the biodiesel, glycerin, and wash water. Triglycerides are readily transesterified batch wise in the presence of alkaline catalyst at atmospheric pressure and at a temperature of approximately 60–70 ºC with an excess of methanol. It often takes at least several hours to ensure the alkali (NaOH or KOH) catalytic transesterification reaction is complete. Moreover, removal of these catalysts is technically difficult and brings extra cost to the final product.

Alkaline metal alkoxides (as CH_3ONa for the methanolysis) are the most active catalysts, since they give very high yields (>98%) in short reaction times (30

min) even if they are applied at low molar concentrations (0.5 mol%). Alkaline metal hydroxides (KOH and NaOH) are cheaper than metal alkoxides, but less active. Nevertheless, they are a good alternative since they can give the same high conversions of vegetable oils just by increasing the catalyst concentration to 1 or 2 mol % (Balat and Balat, 2006).

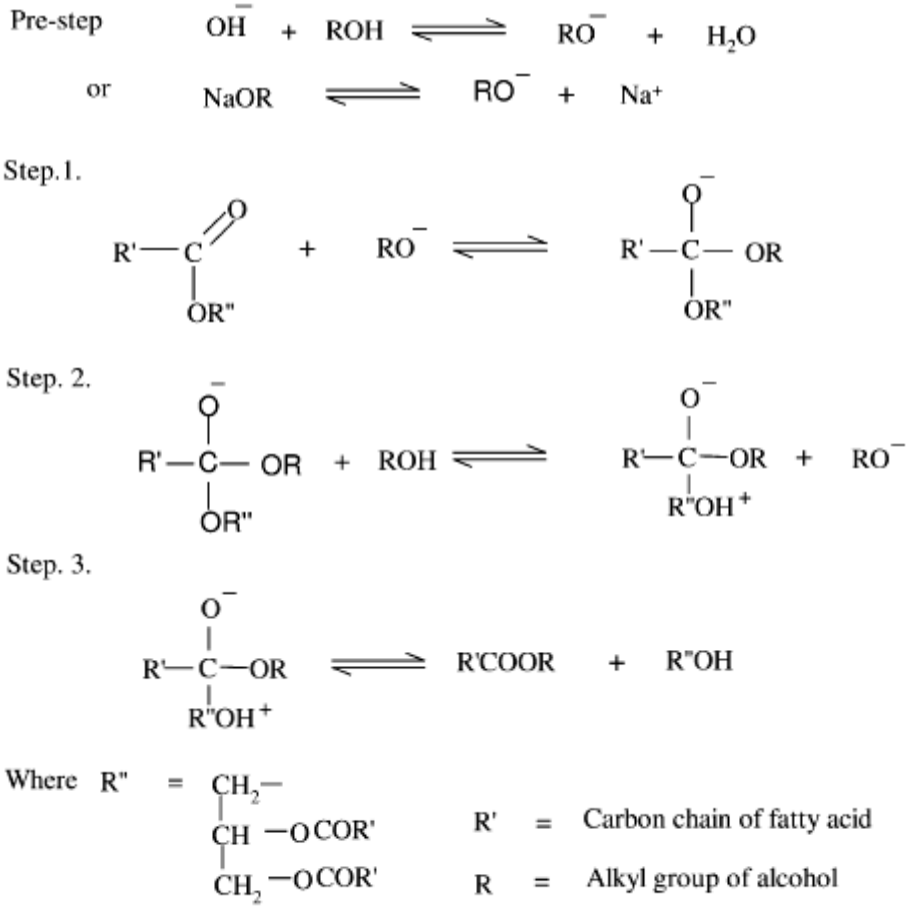


Figure 4.7. Mechanism of base catalyzed transesterification (Meher et al, 2006)

The mechanism of alkali-catalyzed transesterification is described in Figure 4.7. The first step involves the attack of the alkoxide ion to the carbonyl carbon of the triglyceride molecule, which results in the formation of a tetrahedral intermediate. The reaction of this intermediate with an alcohol produces the alkoxide ion in the second step. In the last step the rearrangement of the tetrahedral intermediate gives rise to an ester and a diglyceride (Meher et al, 2006).

4.2.4.1.(2). Acid Catalyzed Transesterification

The transesterification process is catalyzed by sulfuric, hydrochloric, and organic sulfonic acids. In general, acid catalyzed reactions are performed at high alcohol-to-oil molar ratios, low-to-moderate temperatures and pressures, and high acid catalyst concentrations. Acid-catalyzed reactions require the use of high alcohol-to-oil molar ratios in order to obtain good product yields in practical reaction times. However, ester yields do not proportionally increase with molar ratio. Despite its insensitivity to free fatty acids in the feedstock, acid-catalyzed transesterification has been largely ignored mainly because of its relatively slower reaction rate (Balat and Balat, 2008).

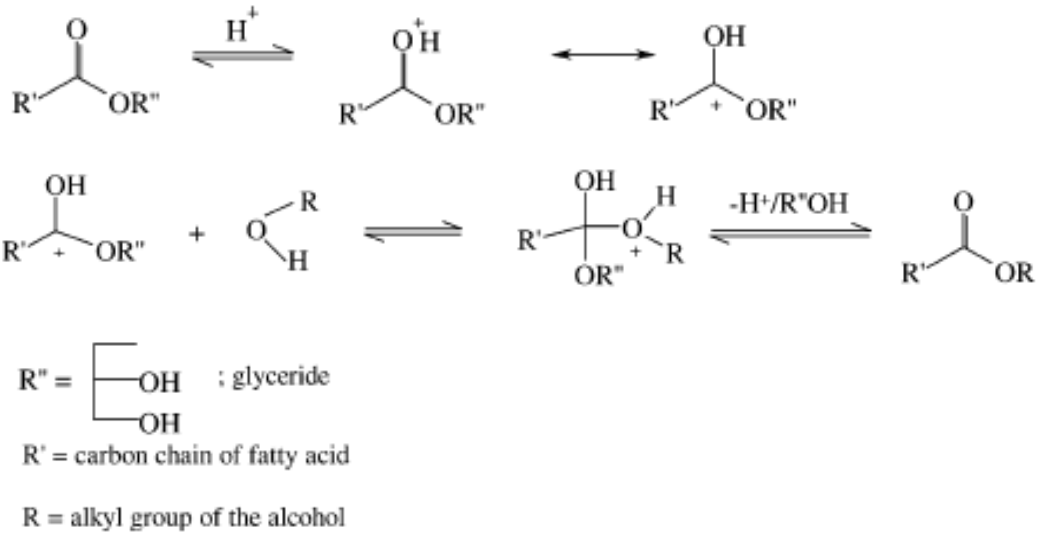


Figure 4.8. Mechanism of acid catalyzed transesterification (Meher et al, 2006)

The mechanism of acid catalyzed transesterification of vegetable oil (for a monoglyceride) is shown in Figure. 4.8. However, it can be extended to di- and tri-glycerides. The protonation of carbonyl group of the ester leads to the carbocation, which after a nucleophilic attack of the alcohol produces a tetrahedral intermediate. This intermediate eliminates glycerol to form a new ester and to regenerate the catalyst (Meher et al, 2006).

4.2.4.1.(3). Enzyme Catalyzed Transesterification

The transesterification process is catalyzed by lipases such as Candida Antarctica, Candida rugasa, Pseudomonas cepacia, immobilized lipase (Lipozyme RMIM), Pseudomonas sp., and Rhizomucor miehei.

As for the enzyme-catalyzed system, it requires a much longer reaction time than the other two systems. Both extracellular and intracellular lipases are also able to effectively catalyze the transesterification of triglycerides in either aqueous or non-aqueous systems, enzymatic transesterification methods can overcome the problems mentioned above. The advantages of lipase-catalyzed transesterification, compared to the chemically-catalyzed reaction, are emphasized. The main problem of the lipase-catalyzed process is the high cost of the lipases used as catalyst. The enzyme reactions are highly specific and chemically clean. Because the alcohol can be inhibitory to the enzyme, a typical strategy is to feed the alcohol into the reactor in three steps of 1:1 mole ratio each. The reactions are very slow, with a three step sequence requiring from 4 to 40 h, or more. The reaction conditions are modest, from 35 to 45 ºC (Balat and Balat, 2008).

4.2.4.1.(4). Non-Catalytic Supercritical Methanol Transesterification

The transesterfication of triglycerides by supercritical methanol (SCM), ethanol, propanol and butanol has proved to be the most promising process. The non-catalyst options are designed to overcome the reaction initiation lag time caused by the extremely low solubility of the alcohol in the TG phase. One approach that is nearing commercialization is the use of a co-solvent, tetrahydrofuran (THF), to solubilize the methanol. The result is a fast reaction, on the order of 5–10 min, and no catalyst residues in either the ester or the glycerol phase. The THF co-solvent is chosen, in part, because it has a boiling point very close to that of methanol. This system requires a rather low operating temperature, 30 ºC. Another non-catalytic approach is the use of a high (42:1) alcohol to oil ratio. Under supercritical conditions (350–400 ºC and >80 atm). The reaction is complete in about 4 min (Balat and Balat 2008).

Reaction by supercritical methanol has some advantages:

- glycerides and free fatty acids are reacted with equivalent rates,
- the homogeneous phase eliminates diffusive problems,
- the process tolerates great percentages of water in the feedstock catalytic process require the periodical renoval of water in the feedstock or in intermediate stage to prevent catalyst deactivation,
- the catalyst renoval step is eliminated, and
- if high methanol:oil ratios are used, total conversion of the oil can be achieved in a few minutes.

Some disadvantages of the one-stage supercritical method are clear:

- it operates at very high pressures (25–40 MPa),
- the high temperatures bring along proportionally high heating and cooling costs,
- high methanol:oil ratios (usually set at 42) involve high costs for the evaporation of the unreacted methanol,
- the process as posed to date does not explain how to reduce free glycerol to less than 0.02% as established in the ASTM D6584 or other equivalent international standards (Balat and Balat, 2008).

Table 4.6. Comparison of the yields in alkaline-catalyzed, acid-catalyzed and supercritical methanol (Balat and Balat, 2008)

Raw Material	***Free fatty acid content (wt%)***	***Water content (wt%)***	***Yields of methyl esters(wt%)***		
			Alkaline catalyzed	***Acid catalyzed***	***Supercritical methanol***
Rapeseed oil	2.0	0.02	97.0	98.4	98.5
Palm oil	5.3	2.1	94.4	97.8	98.9
Frying oil	5.6	0.2	94.1	97.8	96.9
Waste palm oil	>20.0	>61.0	-	-	95.8

4.3. Process Variables

The most important variables that influence transesterification reaction time and conversion are (Srivastava and Prasad, 2000)

- reaction temperature;
- ratio of alcohol to oil;
- catalyst type and concentration;
- mixing intensity;
- purity of reactants.

4.3.1. Reaction Temperature

The rate of reaction is strongly influenced by the reaction temperature. However, given enough time, the reaction will proceed to near completion even at room temperature. Generally, the reaction is conducted close to the boiling point of methanol (60 to 70ºC) at atmospheric pressure. These mild reaction conditions, however, require the removal of free fatty acids from the oil by refining or pre-esterification. Therefore, the degummed and deacidified feedstock is used at these conditions. The pretreatment is not required if the reaction is carried out under high pressure (9000 kPa) and high temperature (240ºC). Under these conditions, simultaneous esterification and transesterification take place. The maximum yield of esters occurs at temperatures ranging from 60 to 80ºC at a molar ratio (alcohol to oil) of 6:1. Further increase in temperature is reported to have a negative effect on the conversion (Srivastava and Prasad, 2000).

4.3.2. Ratio of Alcohol to Oil

Another important variable affecting the yield of ester is the molar ratio of alcohol to vegetable oil. The stoichiometry of the transesterification reaction requires 3 mol of alcohol per mole of triglyceride to yield 3 mol of fatty esters and 1 mol of glycerol. To shift the transesterification reaction to the right, it is necessary to use either a large excess of alcohol or to remove one of the products from the reaction

mixture. The second option is preferred wherever feasible, since in this way, the reaction can be driven to completion. When 100% excess methanol is used, the reaction rate is at its highest. A molar ratio of 6:1 is normally used in industrial processes to obtain methyl ester yields higher than 98% by weight (Srivastava and Prasad, 2000).

4.3.3. Catalyst Type and Concentration

Catalysts used for the transesterification of triglycerides are classified as alkali, acid, enzyme or heterogeneous catalysts, among which alkali catalysts like sodium hydroxide, sodium methoxide, potassium hydroxide, potassium methoxide are more effective. If the oil has high free fatty acid content and more water, acid catalyzed transesterification is suitable. The acids could be sulfuric acid, phosphoric acid, hydrochloric acid or organic sulfonic acid (Meher et al, 2006).

Alkali metal alkoxides are the most effective transesterification catalyst compared to the acidic catalyst. Sodium alkoxides are among the most efficient catalysts used for this purpose, although KOH and NaOH can also be used. Transmethylations occur approximately 4000 times faster in the presence of an alkaline catalyst than those catalysed by the same amount of acidic catalyst. Partly for this reason and partly because alkaline catalysts are less corrosive to industrial equipment than acidic catalysts, most commercial transesterifications are conducted with alkaline catalysts. The alkaline catalyst concentration in the range of 0.5 to 1% by weight yields 94 to 99% conversion of vegetable oil into esters. Further, increase in catalyst concentration does not increase the conversion and it adds to extra costs because it is necessary to remove it from the reaction medium at the end (Srivastava and Prasad, 2000).

4.3.4. Mixing Intensity

In the transesterification reaction, the reactants initially form a two-phase liquid system. The reaction is diffusion-controlled and poor diffusion between the phases results in a slow rate. As methyl esters are formed, they act as a mutual

solvent for the reactants and a single-phase system is formed. The mixing effect is most significant during the slow rate region of the reaction. As the single phase is established, mixing becomes insignificant. The understanding of the mixing effects on the kinetics of the transesterification process is a valuable tool in the process scale-up and design (Srivastava and Prasad, 2000).

4.3.5. Purity of Reactants

Impurities present in the oil also affect conversion levels. Under the same conditions, 67 to 84% conversion into esters using crude vegetable oils can be obtained, compared with 94 to 97% when using refined oils. The free fatty acids in the original oils interfere with the catalyst. However, under conditions of high temperature and pressure this problem can be overcome (Srivastava and Prasad, 2000).

4.4. Advantages of Biodiesel

Biodiesel is an ecological fuel which has the following characteristics:

- It is obtained from renewable raw materials. Biodiesel can be produced from vegetal, animal and recycled oils. Among vegetables, although there are more than three hundred types of oil, the most common one in biodiesel production is soybean, rape, sunflower and palm. The recycled oils come from the collection of sectors such as restaurants, nourishing, domestic kitchens, etc.
- During its combustion it costs smaller amount of CO_2 than the one absorbed on their growth, so that the final balance of CO_2 emissions is positive. In fact, it is considered as a CO_2 neutral emissary. Therefore, the combustion of biodiesel does not contribute to the greenhouse effect; it is neutral and it aids to fulfil the protocol of Kyoto. This is extremely important. In detail, according to the European Environment Agency, BAFF, changes (%) in EU greenhouse gas emissions by sector (1990-99) has increased around 20% in the transport sector, so by using biodiesel this value could be decreased.

- Do contain neither benzene nor other carcinogenic aromatic substances, such as aromatic hydrocarbons.
- It is easily biodegradable, and in case of spill and/or accident, it do not put in danger neither the ground nor underground waters. Biodiesel is biodegradable in approximately 21 days. The absence of a chemical and synthetic compound makes it innocuous with our environment.
- Is not dangerous merchandise, the flash point is over 110º C. Biodiesel flash point is over 110ºC, for that reason it is not classified like dangerous merchandise, which helps on safe storage and safe manipulation (Mendez, 2006).

A number of technical advantages of biodiesel fuel:

- It prolongs engine life and reduces the need for maintenance (biodiesel has better lubricating qualities than fossil diesel),
- It is safer to handle, being less toxic, more biodegradable, and having a higher flash point,
- It reduces some exhaust emissions (although it may, in some circumstances, raise others) (Bozbaş, 2008).

4.5. Disadvantages of Biodiesel

The technical disadvantages of biodiesel/fossil diesel blends

- fuel freezing in cold weather,
- reduced energy density,
- degradation of fuel under storage for prolonged periods (Bozbaş, 2008).

One additional problem is encountered when blends are first introduced into equipment that has a long history of pure hydrocarbon usage. Hydrocarbon fuels typically form a layer of deposits on the inside of tanks, hoses, etc. Biodiesel blends loosen these deposits, causing them to block fuel filters. However, this is a minor problem, easily remedied by proper filter maintenance during the period following introduction of the biodiesel blend (Bozbaş, 2008). At low temperatures, it can begin to solidify and to form crystals that can obstruct the conducts of the fuel. Due to its

solvent properties, it can soften and degrade certain materials, such as natural rubber and polyurethane foam (Mendez, 2006).

Therefore, sometimes it can be necessary to change some hoses and detents of the engine, especially in old vehicles. Since the 1990's, almost all vehicle manufacturers, specially the German ones, have replaced these conduits by others made of plastic or derived materials, that cannot be dissolved by pure biodiesel. Therefore, in order to use pure biodiesel in a secure way, in cars older than ten years, the rubber conduits must be replaced by plastic ones.

Production costs still can be higher than the cost of diesel itself. It all basically depends on the oil source which has been used.

Biodiesel performance per litre is about 10% less in terms of energy than the performance of petroleum diesel fuel. That is because 41.92 MJ/Kg diesel is compared to 37.55 MJ/Kg biodiesel energy content (Mendez, 2006).

4.6. Evaluation of Types of Biodiesel

The quality of biodiesel depends on two main factors. One is the type of oil used as a raw material, which can be refined oil, dry or neutral; and the other one is the degree of correct production. Due to this, the importance of having a standard regulation which fulfils the international basic quality parameters comes out as a real need. So this biofuel must guarantee a good performance on petrol engines.

There are already very tight quality standards. The most well known are CEN 14214 for the EU, and ASTM standard for the US. The most important one is the ASTM PS 121/1999 "Provisional Specification for Biodiesel Fuel (B 100) Blend Stock for Distillate Fuels" for the US; ASTM D 6751:2002 "Standard Specification for Biodiesel Fuel (B-100) Blend Stock for Distillate Fuels" for the US; and the pr ENN 14214/May 2001 "Automotive fuels - Fatty acid methyl esters (FAME) for diesel engines - Requirements and test methods" for the EU countries.

Table 4.7. Generally applicable requirements and test methods (TS EN 14214/ 2003)

Property	**Unit**	**Limits**		
		Minimum	**Maximum**	**Test method [a]**
Ester content [a]	% (m/m)	96,5 [b]		EN 14103
Density at 15°C [c]	Kg/m^3	860	900	EN ISO 3675 EN ISO 12185
Viscosity at 40 °C [d]	mm^2/s	3,50	5,00	EN ISO 3104
Flash Point	°C	120	-	prEN ISO 3679 [e]
Sulphur content	Mg/kg	-	10,0	prEN ISO 20846 prEN ISO 20884
Carbon residue (on 10% distillation residue) [f]	% (m/m)	-	0,3	EN ISO 10370
Cetane number [g]		51		EN ISO 5165
Sulfated ash content	% (m/m)	-	0,02	ISO 3987
Water content	mg/kg	-	500	EN ISO 12937
Total contamination [h]	mg/kg	-	24	EN 12662
Copper strip corrosion (3 h at 50 °C)	rating	class 1		EN ISO 2160
Oxidation stability, 110 °C	hours	6,0	-	EN 14112
Acid value	mg KOH/g		0,5	EN 14104
Iodine value	gr iodine/100 gr		120	EN 14111
Linolenic acid methyl ester	% (m/m)		12,0	EN 14103
Polyunsaturated (>=4 douyble bonds) methyl esters [i]	% (m/m)		1	
Methanol content	% (m/m)		0,20	EN 14110
Monoglyceride content	% (m/m)		0,80	EN 14105
Diglyceride content	% (m/m)		0,20	EN 14105
Triglycerid content [j]	% (m/m)		0,20	EN 14105
Free glycerol [j]	% (m/m)		0,02	EN 14105 EN 14106
Total glycerol	% (m/m)		0,25	EN 14105
Group I metals (Na+K) [k] Group II metals (Ca+Mg) [l]	mg/kg mg/kg		5,0 5,0	EN 14108 EN 14109 prEN 14538
Phosphorus content	mg/kg		10,0	EN 14107

a ,b See standart for more detail

c Density may be measured by EN ISO 3675 over a range of temperatures from 20 °C to 60 °C. Temperature correction shall be made according to the formula given in Annex C.

d If CFPP is -20 oC or lower, the viscosity measured at -200oC shall not exceed 48 mm2/s. In this case, EN ISO 3104 is applicable without the precision data owing to non-Newtonian behaviour in a two-phase system.

e See standart for more detail

f ASTMD 1160 shall be used to obtain the 10% distillation residue.

g ,h See standart for more detail

i Suitable test method to be developed

j ,k ,l See standart for more detail

4.6.1. Evaluation of Biodiesel Quality

The critical items to attend for the determination of biodiesel quality are:

• *Complete reaction to the mono alkyl esters.*

This quality assurance is based on the conversion of the fat or oil to mono alkyl esters measured through measurement of the total.

• *The elimination of free glycerine.*

This quality assurance is based on the measurement of glycerine, which includes all mono-, di-, and triglycerides as well as free glycerine.

• *The elimination of residual catalyst.*

This quality assurance is based on the removal of the catalyst measured through the measurement of the ash content.

• *The elimination of reactant alcohol.*

This quality assurance is based on the removal of the alcohol and it is ensured through measurement of the flash point.

• *The absence of free fatty acids.*

This quality assurance is based on the absence of fatty acids measured through measurement of the acid number.

4.6.1.1 Flash Point

The flash point is the temperature at which fuel vapors can be ignited by externally supplied ignition. It is important for determining the fire hazard and the subsequent safety measures in the storage and distribution systems. In the danger classification for this purpose, diesel fuel is rated AIII- that is less hazardous and must, therefore, have a flash point over 55ºC. When producing diesel fuel, the flash point also restricts the use of highly volatile components (Van Basshuysen and Schäfer, 2004).

The flashing point parameter is used to limit the level of un-reacted alcohol remaining in the finished fuel. The flashing point also has an important connection with the legal requirements and safety precautions involved in fuel handling and

storage. It is normally specified to meet insurance and fire regulations. The flashing point specification for biodiesel is intended to be 100°C minimum. Typical values are over 160°C (Mendez, 2006).

4.6.1.2. Viscosity

The viscosity or inner friction of diesel fuel generally increases with the density. It must be prevented from falling below the set minimum value to ensure that there is sufficient lubrication between the sliding parts of the fuel injection system. If it is too high, the droplet size rises at the provided injection pressure. This results in poorer mixture formation and, hence, energy exploitation, lower performance, and higher soot emissions. The viscosity initially increases quickly as the temperature rises and then gradually decreases at a slower rate (Van Basshuysen and Schäfer, 2004).

Viscosity is the most important property of biodiesel since it affects the operation of the fuel injection equipment, particularly at low temperatures when the increase in viscosity affects the fluidity of the fuel. Biodiesel has a viscosity close to that of diesel fuels. The higher viscosity range of biodiesel helps to reduce barrel/plunger leakage and increase injector efficiency in engines. Viscosity measurements have been made over the temperature range 20–100 ºC for blends of different biodiesel with No. 2 diesel fuel. The viscosity of the distillate was 10.2 mm^2/s at 38 ºC, which is higher than the ASTM specification for No. 2 Diesel fuel (1.9–4.1 mm^2/s) but considerably below that of soybean oil (32.6 mm^2/s) .

This is especially important on engines. For some engines, it may be advantageous to specify a minimum viscosity because of power loss due to injection pump and injector leakage, and also because sulphur emissions. Maximum allowable viscosity, on the other hand, is limited by considerations involved in engine design and size, and the characteristics of the injection system. The upper limit for the viscosity of biodiesel is 5.0 mm^2/s at 40 °C and the minimum is 3.5 mm^2/s at 40 °C (Mendez, 2006).

4.6.1.3. Sulphated Ash

Sulphated ash is the "... residue remaining after a (fuel) sample has been carbonized, and the residue subsequently treated with sulfuric acid and heated to a constant weight." This test monitors the mineral ash residual when a fuel is burned. For biodiesel, this test is an important indicator of the quantity of residual metals in the fuel that came from the catalyst used in the esterification process (Van Gerpen, 2004).

Ash-forming materials may be present in biodiesel in three forms: abrasive solids, un-removed catalysts, and soluble metallic soaps. Abrasive solids and un-removed catalysts can contribute to injector, fuel pump, and engine deposits. These unwanted materials can also lead to premature piston and ring wear. Soluble metallic soaps have little effect on wear but may contribute to filter plugging and engine deposits (Mendez, 2006).

4.6.1.4. Sulphur

One important value which is worthy to be considered is the sulphur contents, mainly because it is a basic characteristic in diesel engines, and also because of its negative effect in the environment by measures of acid rain. Thus, in the US and in Europe, legislation tries to take the diesel oil sulphur content, at levels close to zero. Meanwhile no sulphur emissions are produced with the use of biodiesel. Therefore, of particular concern are the requirements to reduce the sulphur contents of diesel fuel. Ultra-low sulphur diesel has less than 50 ppm sulphur and new diesel regulations in most IEA countries will bring this level to less than 10 ppm by 2010.

Reducing the sulphur contents also reduces fuel lubricity. That is reason of oil companies must add to diesel some chemical and synthetic additives to mitigate that anomaly. Blending biodiesel can help, since it does not contain sulphur and helps improve lubricity. For example, in France all diesels sold have been added with Biodiesel to 2%, due to the fact that biodiesel is a good lubricant. On the other hand, blending only small quantities of biodiesel with conventional diesel does not bring the average sulphur contents down appreciatively. To reduce 350 ppm sulphur diesel

down to 50 ppm, for example, requires a blend of more than 85% biodiesel. At current biodiesel production costs, refiners will likely prefer to cut the sulphur content of conventional diesel at the refinery.

Sulphur is being extremely controlled by international standards in order to reduce the greenhouse effect and for other environmental reasons. Therefore, sulphur fuel can also affect the performance of the emissions control systems. On the other hand, the effect of sulphur content on engine wear and deposits appears to vary considerably in importance and depends largely on operating conditions. B100 is essentially sulphur free, although some biodiesel produced from used cooking oils has been shown to have as much as 30 ppm sulphur (Mendez,2006).

4.6.1.5. Copper Strip Corrosion

The copper strip corrosion test indicates potential compatibility problems with fuel system components made of copper alloys such as brass and bronze. The limit specified is the same as that for petroleum diesel fuel (Anonymous, 2008i)

For B 100, the most likely source of a test failure would be excessive free fatty acids, which are determined in accordance with an additional specification (Van Gerpen, 2004).

4.6.1.6. Cetane Number

Cetane number is a measure of the fuel's ignition and combustion quality characteristics (Anonymous, 2008i). The Cetane number measures how easily ignition occurs and the smoothness of combustion. Higher the cetane number results better its ignition properties. Cetane number affects a number of engine performance parameters like combustion, stability, drivability, white smoke, noise and emissions of CO and HC. Biodiesel has higher Cetane number than conventional diesel fuel, which results in higher combustion efficiency (Mendez, 2006)

To a point, a high number indicates good ignition, easy starting, starting at a low temperature, low ignition pressures, and smooth operation with lower knocking

traits. In the EU a minimum of 49 Cetane is normally required, so low-sulphur diesel is sometimes dismissed under this value.

The Cetane number requirements depend on engine design, size, nature of speed and load variations, and on starting and atmospheric conditions. It is important to subscribe that substantiating data to support the calculation of Cetane index with biodiesel or biodiesel blends does not exist (Mendez, 2006).

4.6.1.7. Carbon Residue

The carbon residue is a measure of how much residual carbon remains after combustion. The test basically involves heating the fuel to a high temperature in the absence of oxygen. Most of the fuel will vaporize and be driven off, but a portion may decompose and pyrolyze to hard carbonaceous deposits. This is particularly important in diesel engines because of the possibility of carbon residues clogging the fuel injectors (Grepen, 2004).

4.6.1.8. Phosphorus Content

Phosphorus has been shown to damage the ability of after treatment systems to reduce exhaust emissions as intended. The influence of phosphorus is cumulative; therefore, very low levels of contamination over the significant amount of fuel consumed by an engine may lead to unexpected deterioration of the aftertreatment system (Anonymous, 2008i).

4.6.1.9. Density

Density is an essential parameter. As the density increases, the energy content increases per unit volume. Given an unchanging injected quantity of fuel, the energy supplied to the engine increases with the density, which increases engine performance. However, the exhaust emissions and, especially, the particles increase under a full load due to the richer mixture. On the other hand, the volumetric fuel consumption increases as density decreases (Van Basshuysen and Schäfer, 2004).

Density is another important property of biodiesel. It is the weight of a unit volume of fluid. Specific gravity is the ratio of the density of a liquid to the density of water. Specific gravity of biodiesels ranges between 0.87 and 0.89. Fuel injection equipment operates on a volume metering system, hence a higher density for biodiesel results in the delivery of a slightly greater mass of fuel.

The density of biodiesel meeting the specifications EN14214 falls between 0.86 and 0.90 g/m^3, with typical values falling between 0.88 and 0.89. Since biodiesel density falls between 0.86 and 0.90, a separate specification is not needed. The density of raw oils and fats is similar to biodiesel; therefore, the use of density as an expedient check of fuel quality may not be as useful for biodiesel as it is for petrodiesel (Mendez, 2006).

4.6.1.10. Cold Filter Plugging Point

Cold Filter Plugging Point (CFPP) of a fuel reflects its cold weather performance. At low operating temperature fuel may thicken and might not flow properly affecting the performance of fuel lines, fuel pumps and injectors. CFPP defines the fuels limit of filterability, having a better correlation than cloud point for biodiesel as well as petrodiesel. Normally either pour point or CFFP are specified. Pour point is the lowest temperature at which the oil specimen can still be moved. French and Italian biodiesel specifications specify pour point where as others specify CFPP.

Two important parameters for low temperature applications of a fuel are Cloud Point (CP) and Pour Point (PP). The CP is the temperature at which wax first becomes visible when the fuel is cooled. The PP is the temperature at which the amount of wax out of solution is sufficient to gel the fuel, thus it is the lowest temperature at which the fuel can flow. Biodiesel has higher CP and PP compared to conventional diesel. The esters have CP and PP that are 15–25 ºC higher than those of diesel fuels (Mendez, 2006).

4.7. Emission Types

The scope of the emissions impact analysis covers five types of emissions: NO_x (nitrogen oxides), PM (particulate matter), HC (hydrocarbons), CO (carbon monoxide), and CO_2 (carbon dioxide). While CO_2 is not a hazardous air toxin, it is considered a greenhouse gas emission causing global warming and, in some cases, may be capable of generating emissions credits (Strong et al, 2004).

4.7.1. NO_x

Nitrogen oxides (NO_x) is the generic term for a group of highly reactive gases containing nitrogen and oxygen in varying amounts, including nitric oxide (NO), nitrous oxide (N_2O), nitrates (NO_3 –), and nitrogen dioxide (NO_2). NO_x and volatile organic compounds, in the presence of hot, stagnant air and sunlight, convert to ozone. NO_x are classified as hazardous airborne toxins because of their deleterious health and environmental effects. The U.S. Environmental Protection Agency (EPA) has noted that NO_x is a major cause of ground- level ozone (a.k.a. smog), acid rain, respiratory disease (emphysema and bronchitis), water quality determination, and global warming (Strong et al, 2004).

4.7.2. PM

Particulate matter (PM) is a generic term used for a type of airborne pollution which consists of varying mixtures, complexity and sizes of particles. PM is problematic because it compounds respiratory problems, such as asthma and cardiopulmonary disease. The American Lung Association reports that high concentrations and/or specific types of particles have been found to present a serious danger to human health.

There are two types of regulated PM: PM2.5 and PM10. PM2.5 is a particulate matter of 2.5 micrometers or less in diameter and PM10 is a particulate matter of 10 micrometers or less in diameter. Both PM2.5 and PM10 are by products of internal combustion engines. There are two major differences between PM2.5 and

PM10. First, the size contributes to greater health risks because larger particles can be inhaled and accumulated in the respiratory system. Secondly, in contrast to PM2.5, PM10 easily reacts with chemicals such as SO_2, NOx, and volatile organic compounds (VOCs). All of these chemical reactions can result in smog (Strong et al, 2004).

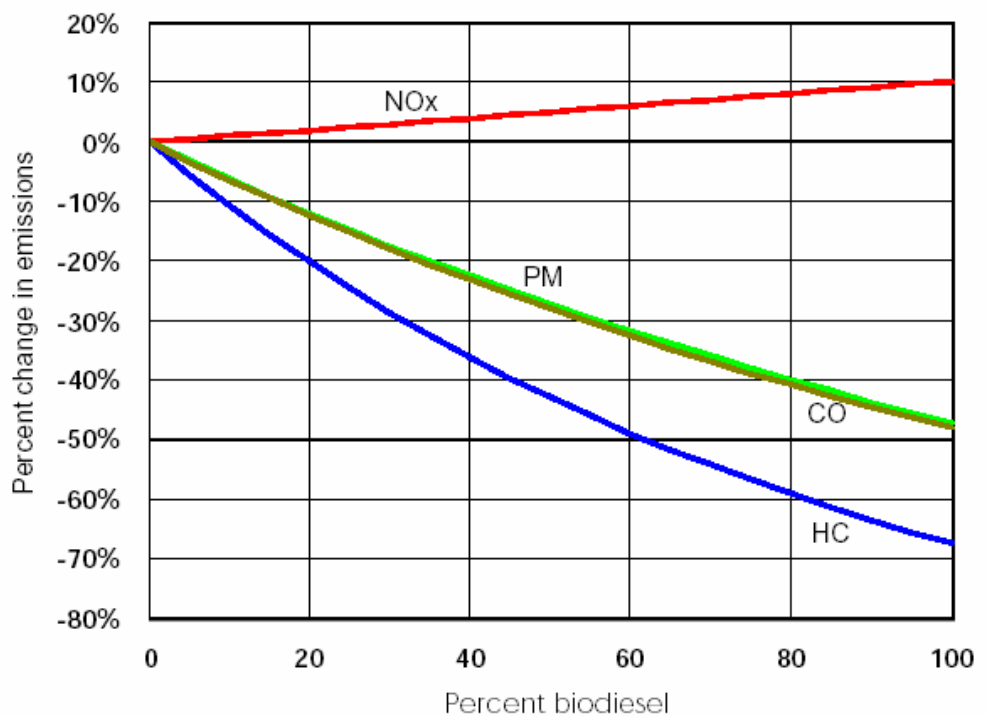


Figure 4.9. Summary of U.S. Enviromental Protection Agency evaluation of biodiesel effects on pollutant emissions for heavy –duty engines (Strong et al, 2004).

4.7.3. HC

The Agency for Toxic Substances and Disease Registry reports that hydrocarbons (HC) “enter the air mostly as releases from volcanoes, forest fires, burning coal, and automobile exhaust”. A 1999 EPA study estimates that on-road vehicle sources were responsible for 29 percent of the total emission of HC.

Mobile sources release two types of regulated HC measured as speciated hydrocarbons (C_1-C_{22}) and a subset of known or suspected carcinogenic compounds

titled polycyclic aromatic hydrocarbons (PAH). A presentation given to the National Biodiesel Board entitled “Biodiesel Tier I Health Effects” presented a correlation between the emission rate of C_1 to C_{12} and the potential reduction of ozone and also stated that HC are carcinogen. The Department of Health and Human Services reiterated this health concern, specifying that some PAHs are known to cause cancer.

4.7.4. CO

Carbon monoxide (CO) is produced from incomplete combustion whenever any carbon fuel, such as gas, oil, kerosene, wood, or charcoal is burned. Unlike many gases, CO has no odor, color, or taste, and it does not cause skin irritation. According to the Centers for Disease Control and Prevention¸ red blood cells can attach themselves to CO at a quicker rate than oxygen. If there is a large quantity of CO in the air, the red blood cell may replace oxygen with CO, leading to possible tissue damage, carbon monoxide poisoning or death. As CO levels increase and remain above 70 parts per million (ppm), symptoms may become more noticeable (headache, fatigue, nausea). As CO levels increase above 150 to 200 ppm, disorientation, unconsciousness, and death are possible (Strong et al, 2004).

4.7.5. CO_2

Carbon dioxide is a naturally occurring gas that is linked to global warming. It is also released into the atmosphere by human activity, such as when solid waste, fossil fuels (oil, natural gas, and coal), and wood and wood products are burned. Carbon dioxide by itself is not considered to be a toxin. However, any impacts on global climate could cause health problems (Strong et al, 2004).

5. MATERIALS AND METODS

This study was carried out at the Çukurova University Mechanical Engineering Department Automotive Engineering Laboratories. The objective of this study was the investigation of the effect of biodiesel blend level on density, viscosity, heat capacity, cold flow, cetane number, and the performance characteristics of the blends.

5.1. Biodiesel Production

In this study, the rapeseed oil was provided by Çukobirlik Oil Factory. In order to produce biodiesel from rapeseed oil, the biodiesel production unit, which was constructed in the Çukurova University Mechanical Engineering Department Automotive Engineering Laboratories, was used. A digital control unit was used for controlling the heater and the stirring speed of the motor. A stainless steel reactor (figure 5.1) with a max capacity of 50 lt was used for transesterification process.



Figure 5.1. Stainless Steel Biodiesel Reactor

The dimensions and the parts of the Biodiesel reactor were given in Figure 5.2.

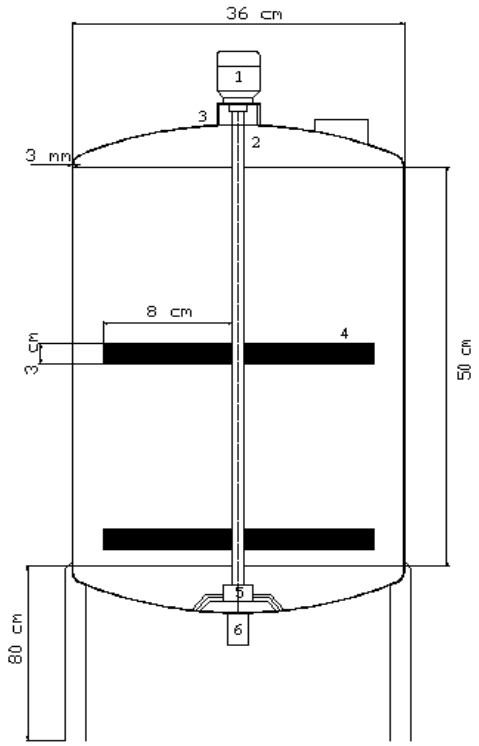


Figure 5.2. Stainless Steel Biodiesel Reactor Schema 1: Electric Motor 2: Shaft, 3: Cover 4: Blades, 5: Bearing system, 6 Bottom Vane

Specifications of chemical substances that are used in the reaction are tabulated in table 5.1.

Table 5.1. Reactants specifications

Firm	Tekkim	Carlo Erba Reagenti
Code	TK.120320.1000	480507[c]
Name	Methanol	Sodium hydroxide anhydrous pellets
CAS Number	67-56-1	1310-73-2
Linear Formula	CH_3OH	NaOH
Purity	%99.5	>%97

In order to keep the catalyst from humidity and carbon dioxide which was in the atmosphere; a rapid measurement was done to determine the weight of the catalyst. Rapeseed Oil/Methanol molar rate is 6:1. The used catalyst was NaOH with 0.4%. 25 liter of rapeseed oil was filled in the reactor and heated up to 50°C. The methoxide (the mixture of methanol and sodium hydroxide) send to the reactor. And heater was set to 65°C. The reaction took 2 hours. The mixture was send to the maturation containers (figure 5.3) by pump (figure 5.4). Solution let to cool down for 8 hours. The RME was stayed the upper side of the maturation container and glycerin at the down side (figure 5.5).



Figure 5.3. Maturation containers



Figure 5.4. Suction pump



Figure 5.5. Separation of glycerin from RME

The washing step is washing the rapeseed methyl ester with water. This process was repeated 3 times. Water and all the other substances precipitated at the bottom (figure 5.6).



Figure 5.6. First washing of RME



Figure 5.7. Last washing of RME

After the washing step, vacuum type drying was done. The RME (figure 5.8) send to the reactor and heated up to 85 °C at a vacuum pressure of 100 mmHg. The drying process was done for 1 hour respectively.



Figure 5.8. The RME before drying

After the drying process RME let to be cool down. In order to neglect the possibility of impurities the RME drained from paper filter. This production process was repeated for 3 times and each party collected in the same vessel to get a homogenous biodiesel. The quality of biodiesel (figure 5.9) was tested in the Automotive Engineering Laboratories.



Figure 5.9. The Rapeseed Biodiesel

5.2. Mixture Preparation

Samples were made by mixing eurodiesel, biodiesel which was produced from rapeseed and three different substance. These substances were n-hexane, n-heptane and xylene.

n-Hexane is an alkane hydrocarbon with the chemical formula $CH_3(CH_2)_4CH_3$ or C_6H_{14}. The "hex" prefix refers to its six carbons, while the "ane" ending indicates that its carbons are connected by single bonds. Hexane isomers are largely unreactive, and are frequently used as an inert solvent in organic reactions because they are very non-polar (Anonymous, 2009a).

***n*-Heptane** is the straight-chain alkane with the chemical formula $H_3C(CH_2)_5CH_3$ or C_7H_{16}. It is the zero point of the octane rating scale (the 100 point is iso-octane). Heptane (and its many isomers) is widely applied in laboratories as a totally non-polar solvent. *n*-Heptane is the zero point of the octane rating scale. It is

undesirable in petrol, because it burns explosively, causing engine knocking, as opposed to branched-chain octane isomers, which burn more slowly and give better performance. It was chosen as the zero point of the scale because of the availability of very high purity *n*-heptane, unmixed with other isomers of heptane or other alkanes (Anonymous, 2009b).

Xylene refers to a mixture of three aromatic hydrocarbon isomers which is used as a solvent in the printing, rubber, and leather industries. Xylene is a clear, colorless, sweet-smelling liquid that is very flammable. Like other solvents, xylene is also used as an inhalant drug for its intoxicating properties (Anonymous, 2009c).

In the tables below are the blends and their rates indicated for the experiments.

Table 5.2. Fuel blends with Hexane

D= Eurodiesel RSB= Rapeseed Biodiesel HX=n-Hexane D85RSB10HX5=%85 Diesel+%10 Rapeseed Biodiesel+%5 n-Hexane						
Blends Code	Eurodiesel		Rapeseed Biodiesel		n-Hexane	
	%	Amount (cc)	%	Amount (cc)	%	Amount (cc)
D100	100%	3000	0	0	0	0
RSB100	0	0	100%	3000	0	0
D85RSB10HX5	85%	2550	10%	300	5%	150
D75RSB20HX5	75%	2250	20%	600	5%	150
D65RSB30HX5	65%	1950	30%	900	5%	150
D55RSB40HX5	55%	1650	40%	1200	5%	150
D45RSB50HX5	45%	1350	50%	1500	5%	150
D80RSB10HX10	80%	2400	10%	300	10%	300
D70RSB20HX10	70%	2100	20%	600	10%	300
D60RSB30HX10	60%	1800	30%	900	10%	300
D50RSB40HX10	50%	1500	40%	1200	10%	300
D40RSB50HX10	40%	1200	50%	1500	10%	300
D75RSB10HX15	75%	2250	10%	300	15%	450
D65RSB20HX15	65%	1950	20%	600	15%	450
D55RSB30HX15	55%	1650	30%	900	15%	450
D45RSB40HX15	45%	1350	40%	1200	15%	450
D35RSB50HX15	35%	1050	50%	1500	15%	450

Table 5.3. Fuel blends with Heptane

D= Eurodiesel RSB= Rapeseed Biodiesel HP=n-Heptane D85RSB10HP5=%85 Diesel+%10 Rapeseed Biodiesel+%5 n-Heptane						
Blends	Eurodiesel		Rapeseed Biodiesel		n-Heptane	
Code	%	Amount (cc)	%	Amount (cc)	%	Amount (cc)
D85RSB10HP5	85%	2550	10%	300	5%	150
D75RSB20HP5	75%	2250	20%	600	5%	150
D65RSB30HP5	65%	1950	30%	900	5%	150
D55RSB40HP5	55%	1650	40%	1200	5%	150
D45RSB50HP5	45%	1350	50%	1500	5%	150
D80RSB10HP10	80%	2400	10%	300	10%	300
D70RSB20HP10	70%	2100	20%	600	10%	300
D60RSB30HP10	60%	1800	30%	900	10%	300
D50RSB40HP10	50%	1500	40%	1200	10%	300
D40RSB50HP10	40%	1200	50%	1500	10%	300
D75RSB10HP15	75%	2250	10%	300	15%	450
D65RSB20HP15	65%	1950	20%	600	15%	450
D55RSB30HP15	55%	1650	30%	900	15%	450
D45RSB40HP15	45%	1350	40%	1200	15%	450
D35RSB50HP15	35%	1050	50%	1500	15%	450

Table 5.4. Fuel blends with Xylene

D= Eurodiesel RSB= Rapeseed Biodiesel XL=Xylene D85RSB10XL5=%85 Diesel+%10 Rapeseed Biodiesel+%5 Xylene						
Blends	Eurodiesel		Rapeseed Biodiesel		Xylene	
Code	%	Amount (cc)	%	Amount (cc)	%	Amount (cc)
D85RSB10XL5	85%	2550	10%	300	5%	150
D75RSB20XL5	75%	2250	20%	600	5%	150
D65RSB30XL5	65%	1950	30%	900	5%	150
D55RSB40XL5	55%	1650	40%	1200	5%	150
D45RSB50XL5	45%	1350	50%	1500	5%	150
D80RSB10XL10	80%	2400	10%	300	10%	300
D70RSB20XL10	70%	2100	20%	600	10%	300
D60RSB30XL10	60%	1800	30%	900	10%	300
D50RSB40XL10	50%	1500	40%	1200	10%	300
D40RSB50XL10	40%	1200	50%	1500	10%	300
D75RSB10XL15	75%	2250	10%	300	15%	450
D65RSB20XL15	65%	1950	20%	600	15%	450
D55RSB30XL15	55%	1650	30%	900	15%	450
D45RSB40XL15	45%	1350	40%	1200	15%	450
D35RSB50XL15	35%	1050	50%	1500	15%	450

The property chart of the used substances are stated below. The values were taken from products their quality certificate.

Table 5.5. Property chart of used substances

Firm	Riedel-de Haën	Riedel-de Haën	CarloErbaReagenti
Code	15677[a]	16446[b]	446903[c]
Name	n-heptane	xylene	n-hexane
CAS Number:	142-82-5	1330-20-7	110-54-3
Linear Formula:	$CH_3(CH_2)_5CH_3$	$C_6H_4(CH_3)_2$	$CH_3(CH_2)_4CH_3$
Mol. Weight:	100.20	106.17	86
EC Number:	205-563-8	215-535-7	203-777-6
vapor pressure	83 mmHg at 37.7 C	18 mmHg at 37.7 C	160 hPa at 20 C
grade	≥99%	Min 96%	Min 95%
bp	98 °C(lit.)	137-140 °C(lit.)	69 °C
mp	−91 °C(lit.)		-95 °C
density	0.684 g/mL at 25 C(lit.)	0.86 g/mL at 25 C(lit.)	0.66 g/mL at 20 C
Flash Point(C)	-4 °C	25 °C	-26 °C

[a] (Anonymous, 2008j) [b] (Anonymous, 2008k) [c] (Anonymous, 2008l)

5.3. Fuel Quality Measurement Methods

The fuel quality measurements of the blends were done according to European petrodiesel standard EN 590. The testing equipments and their measuring methods were briefly explained below.

5.3.1. Density Measurement

The density measurement was done using Kyoto Electronics DA-130 type densimeter (figure 5.10). This densimeter uses the resonant frequency method to measure the densities. With the densimeter we can also measure the specific weight, API gravity, % Brix, volume and mass alcohol rates. The measurement interval of the device is 0 to 2 g/cm^3 and 0 to 40 ºC. The device has a sensitivity of ±0.001 g/cm^3, and a stability of 0.0001 g/cm^3. The device is measuring according to the standards of TS 6311, ASTM D 4052-96 (Abdulvahitoğlu et al, 2008).



Figure 5.10. Kyoto Electronics DA-130 portable densimeter

5.3.2. Viscosity Measurement:

The viscosities of the blends, biodiesel and petrodiesel are measured with Saybolt Universal Viscosimeter (figure 5.11) produced from Ubbelohde tube with ASTM D88 standards. The measurement results were recorded in seconds. Then using a conversion table the results were converted from SSU (Saybolt Universal Second) to centistokes (cst) unit. The measurements were done at 40 ºC according to the TS EN 14214 standard (Abdulvahitoğlu et al, 2008).



Figure 5.11. Saybolt Universal Viscosimeter

5.3.3. Heat Capacity Measurement:

The heat capacities of liquid fuels can be measured automatically with IKA-Werke C2000 calorimeter (figure 5.12). The working temperatures are between +15 ºC to +35 ºC. The combustion is done with a cotton wire instead of a tungsten wire. The results are measured in cal/gr units. The device can measure according to the TS 1740**,** ASTM 240 D, ISO 1928, DIN 51900, BSI standards (Abdulvahitoğlu et al, 2008).



Figure 5.12. IKA-Werke C2000 Calorimeter

5.3.4. Cetane Number Measurement

The Cetane number and indexes were measured by Zeltex ZX440 (figure 5.13) type device, which works under the close infrared spectrometer (NIR) principal. With the help of this principal the Cetane number measurement experiment became very fast and cheap with only 3% error compared to the time consuming expensive motor tests (Abdulvahitoğlu et al, 2008).



Figure 5.13 Zeltex ZX440

5.3.5. Cold Flow Measurement:

Tanaka MPC-102 (figure 5.14) has been designed for automatic determination of Pour Point (PP) and Cloud Point (CP). PP measurement is made utilizing a new ASTM test method, namely "Air Pressure Method" (ASTM D6749 on "Standard Test Method for Pour Point of Petroleum Products (Automatic Air Pressure Method 1)), which yields eventually no bias against the conventional test method, repeatability/reproducibility of $1^{o}C/2^{o}C$ and 2-3 times faster determinations. The device can measure according to the ASTM D6749/D97, ISO 3016 (PP), ASTM D2500, ISO 3015 (CP). Measuring range is $+51^{o}C$ to $-40^{o}C$ with tap water of $20^{o}C$ and $+51^{o}C$ to $-65^{o}C$ with cooling liquid of $-35^{o}C$. Amount of applied air pressure for PP detection, to accommodate different sample types: L(low) for diesel fuels, H(high) for lube oils, VH(very high) and UH (ultra high) for residual fuels and similar samples. Testing intervals: $1.0^{o}C$, $2.5^{o}C$, or $3.0^{o}C$



Figure 5.14. Tanaka MPC-102L

5.3.6. Flash Point

Automated Pensky-Martens Closed Cup Flash Point Tester, model APM-7. It is conforming the standards, ISO 2719, ASTM D93, IP 34, etc. Measurıng range is from ambient temperature to 370 ^{o}C . This instruments tests according to ASTM D93 (ISO 2719, IP 34) A+B, Special (Fast Search), Simulated TAG modes.



Figure 5.15. Tanaka APM-7

5.4. Experimental Setup

The experimental setup contains a four cylinder diesel engine (Mitsubishi Canter 4D32-2A), a hydraulic dynamometer, testing panel and exhaust gas analyzer unit.

5.4.1. Engine

In the experiments, Mitsubishi Canter 4D32-2A model (figure 5.16) four stroke diesel engine with four cylinders which has a maximum torque 255 Nm at 1800 rpm has been used. Note that the maximum torque value and maximum brake power values that obtained in the test engine could be change depending upon the fuel that used in engine. The engine specifications are given in Table 5.6.



Figure 5.16. Engine test bed

Table 5.6. Properties of engine used in the experiments (Anonymous 2009d)

4 Stroke Diesel Engine – Model 4d 32-2A	
Configuration	In line 4
Type	Direct injection diesel with glow plug
Swept Volume	3567 cm^3
Bore	104 mm
Stroke	105 mm
Oil Cooler	Water cooled
Maximum Torque	255 Nm at 1800 rpm
Maximum Brake Power	80 kW at 3500 rpm
Recom. Max. Speed	3600 rpm

Dynamometer is a device to measure the torque with using viscosity and inertia of fluid. Inside a disk, there are fins on two sides. When we deliver water to inside of this, the fixed one (outer fins) is forced by the rotating fins (connected to motors shaft). The force acting on the outer disk is measured at a point and the scale is calibrated to show the multiplication of force and distance. We can read directly the torque from the torque indicator located on test rig.

Table 5.7. Dynamometer Technical specification

Torque Range	0–1700 Nm ± 1
Speed range	0- 7500 rpm
Body weight	45 kgf
Total weight	110 kgf
Body diameter	350 mm
Torque arm length	350 mm

The speed sensor used to detect prime mover speed is the magnetic pickup (MPU). When a magnetic material (usually a gear tooth driven by the prime mover) passes through the magnetic field at the end of the magnetic pickup, a voltage is developed. The frequency of this voltage is translated by the speed control into a signal which accurately depicts the speed of the prime mover. S Tipi Load Cell is used to measure the torque of dynamometer Stainless steel IP66 which has a sensitivity of

1/3000. Dynamometer control unit was used for receiving and collecting all the data that was measured by the system including engine speed torque power fuel consumption and calculating power and specific fuel consumption.



Figure 5.17. The test panel

5.5. Measurements

During experiments speed, torque, power, fuel consumption and specific fuel consumption were measured and calculated by engine test equipment (figure 5.17). In order to measure air consumption a multislope manometer (P7025) and laminar flow meter (P7201) was used. Exhaust emission test were taken by Testo 354 model exhaust emission analyzer.

5.5.1. Exhaust Emission Tests

As it is mentioned before, in the experiments a four stroke with one cylinder diesel engine has been used. A Testo 354 model exhaust emission test analyzer

(figure 5.18) was used. The probe connected to the exhaust system. The data which were collected from analyzer send to computer and saved digitally.



Figure 5.18. Testo 354 Exhaust Gas Analyzer

5.6. Formulas Necessary for Calculations

$$P_B(real) = \frac{2p.N.T}{60} \quad (\text{W}) \tag{5.1}$$

Air Consumption Rate Calculation

$$Ao = \frac{p.D_o^{\,2}}{4} (\text{mm}^2) \tag{5.2}$$

$$b = \frac{D_o}{D} \tag{5.3}$$

$$m_a = C_d \cdot \frac{A_o}{\sqrt{1-b^4}} \cdot \sqrt{\frac{2 \cdot \Delta P}{r_a}} \tag{5.4}$$

Where C_d= 0.605

D_o= Orifice diameter (80 mm)

D = Diameter (160 mm)

ρ_a = density of air

V_s = swept volume (3567cm^3)

n = 2 for four-stroke engines

Air-Fuel Ratio Calculation

$$AFR = \frac{m_a}{m_f} \tag{5.5}$$

Specific Fuel Consumption Calculation

$$Sfc = \frac{m_f.10^3}{P_B} \quad \text{(g/kWh)} \quad (P_B \text{ is taken as real power output}) \tag{5.6}$$

Brake Mean Effective Pressure Calculation

$$bmep = \frac{P_B.n_R}{V_s.N} = \frac{(2.p.N.T)(2)}{V_s.N} = \frac{12,6T}{V_s}(kPa) \tag{5.7}$$

Brake Thermal Efficiency Calculation

$$h_b = \frac{P_B.3600}{m_f.H}$$

(5.8)

Volumetric Efficiency Calculation

$$h_v = \frac{m_a.n}{60.N.r_a.V_s}$$

(5.9)

6. FUEL QUALITY EXPERIMENTS

This study was carried out at the Çukurova University Mechanical Engineering Department of Automotive Engineering Laboratories. Density, viscosity, heating capacity, cetane number, pour point and flash point were the characteristics that tested according the standards. Fuel quality testing results were tabulated below. Table 6.1 includes European Petrodiesel Standard EN 590 and Biodiesel Standard TS EN 14212.

Table 6.1. Fuel Quality Results of Eurodiesel (D) and Rapeseed Biodiesel (RSB)

	Density (kg/m^3)	**Calorific Value (kJ/kg)**	**Cetane Number**	**Pour Point (^oC)**	**Viscosity (cSt)**	**Flash Point (^oC)**
EN590	**820-845**	**-**	**Min 51**	**-**	**2.0-4.5**	**Min 55**
D100	828	45646.15	60.554	-14	2.43947	70.50
EN14214	**860-900**	**-**	**Min 51**	**-**	**3.5-5.0**	**Min 120**
RSB100	878	39430.24	53.459	-9	5.09688	155.67

Table 6.2. Fuel Quality Results of n-Hexane Blends

Sample Code	**Density (kg/m^3)**	**Calorific Value (kJ/kg)**	**Cetane Number**	**Pour Point (^oC)**	**Viscosity (cSt)**	**Flash Point (^oC)**
D85RSB10HX5	824	44783.87	58.498	-15	3.17500	74.28
D75RSB20HX5	830	44172.75	57.447	-15	3.22813	82.88
D65RSB30HX5	833	43477.9	56.273	-14	3.37813	91.48
D55RSB40HX5	839	42603.07	54.637	-13	3.82100	100.08
D45RSB50HX5	843	42234.72	54.150	-12	3.90933	108.68
D80RSB10HX10	820	44603.88	64.366	-19	2.33079	69.45
D70RSB20HX10	822	43883.93	63.030	-16	2.38421	78.05
D60RSB30HX10	826	43297.92	61.544	-16	2.70219	86.65
D50RSB40HX10	830	42778.88	60.601	-15	3.27594	95.25
D40RSB50HX10	833	42050.55	58.737	-14	3.75667	103.85
D75RSB10HX15	808	44181.12	66.276	-20	2.30605	64.63
D65RSB20HX15	814	43971.83	64.788	-19	2.35711	73.23
D55RSB30HX15	818	43251.87	63.521	-18	2.50567	81.83
D45RSB40HX15	822	42582.14	62.236	-17	2.83031	90.43
D35RSB50HX15	828	41858	61.104	-15	3.00625	99.03

Table 6.3. Fuel Quality Results of n-Heptane Blends

Sample Code	Density (kg/m^3)	Calorific Value (kJ/kg)	Cetane Number	Pour Point (^oC)	Viscosity (cSt)	Flash Point (^oC)
D85RSB10HP5	826	44264.84	61.595	-15	3.48844	75.40
D75RSB20HP5	830	44047.17	60.022	-14	3.60100	84.00
D65RSB30HP5	835	42887.71	59.119	-13	3.60900	92.50
D55RSB40HP5	841	42678.42	58.142	-12	3.70767	100.99
D45RSB50HP5	847	42138.45	56.698	-11	3.81900	109.50
D80RSB10HP10	819	44779.69	63.429	-17	2.55219	71.90
D70RSB20HP10	824	43900.67	62.855	-16	2.71781	80.38
D60RSB30HP10	829	43511.39	61.277	-15	3.48438	88.90
D50RSB40HP10	833	42510.98	59.545	-14	3.61100	97.40
D40RSB50HP10	838	42167.75	58.769	-13	3.89567	105.88
D75RSB10HP15	810	44490.87	64.826	-18	2.42368	68.29
D65RSB20HP15	815	43708.12	64.222	-18	2.73656	76.80
D55RSB30HP15	819	43486.28	63.087	-17	2.82406	85.30
D45RSB40HP15	824	42657.49	62.590	-16	2.92188	93.80
D35RSB50HP15	828	42092.4	60.113	-15	3.33844	102.40

Table 6.4. Fuel Quality Results of Xylene Blends

Sample Code	Density (kg/m^3)	Calorific Value (kJ/kg)	Cetane Number	Pour Point (^oC)	Viscosity (cSt)	Flash Point (^oC)
D85RSB10XL5	836	44294.14	55.499	-15	2.48947	76.70
D75RSB20XL5	838	43557.43	54.732	-14	3.28969	85.30
D65RSB30XL5	845	43050.95	53.356	-13	3.60667	92.50
D55RSB40XL5	848	42494.24	51.822	-12	3.63433	102.30
D45RSB50XL5	855	42067.29	51.193	-11	3.88767	110.80
D80RSB10XL10	835	44218.79	50.694	-15	2.46658	73.20
D70RSB20XL10	842	43482.09	50.247	-15	3.21031	81.58
D60RSB30XL10	845	42958.87	49.481	-14	3.34063	90.30
D50RSB40XL10	852	42456.57	48.488	-13	3.48031	99.40
D40RSB50XL10	857	41841.26	47.723	-12	3.73100	107.28
D75RSB10XL15	836	43670.45	47.723	-16	2.36053	72.19
D65RSB20XL15	842	43553.25	46.749	-16	2.95719	80.71
D55RSB30XL15	848	42628.19	45.423	-15	3.19469	89.23
D45RSB40XL15	854	42360.3	44.842	-14	3.41969	97.70
D35RSB50XL15	859	41611.04	44.397	-14	3.65333	106.30

6.1. Density

The density of petrodiesel fuel is lower than that of a biodiesel, which is 820-845 kg/m^3 in the European Petrodiesel Standard EN 590. Due to the lower densities of n-hexane, n-heptane and xylene in accordance with the Rapeseed Biodiesel (RSB) and Eurodiesel (D) were caused to lower the density of the blends. On the other hand, any increase in the percentage of the RSB caused an increase in the blend density (figure 6.1, 6.2, 6.3). The reason for this increase was higher value of RSB density, which were 878 kg/m^3 respectively. However, the blends, which were prepared with xylene, had much more higher densities according to the n-hexane and n-heptane blends with the same percentages of RSB. Hence D75RSB10HX15, D65RSB20HX15, D55RSB30HX15, D80RSB10HP10, D75RSB10HP15, D65RSB20HP15, D55RSB30HP15 had lower densities; D45RSB50HP5, D55RSB40XL5, D50RSB40XL10, D40RSB50XL10, D55RSB30XL15, D45RSB40XL15 D35RSB50XL15 had higher densities than the standard EN 590.

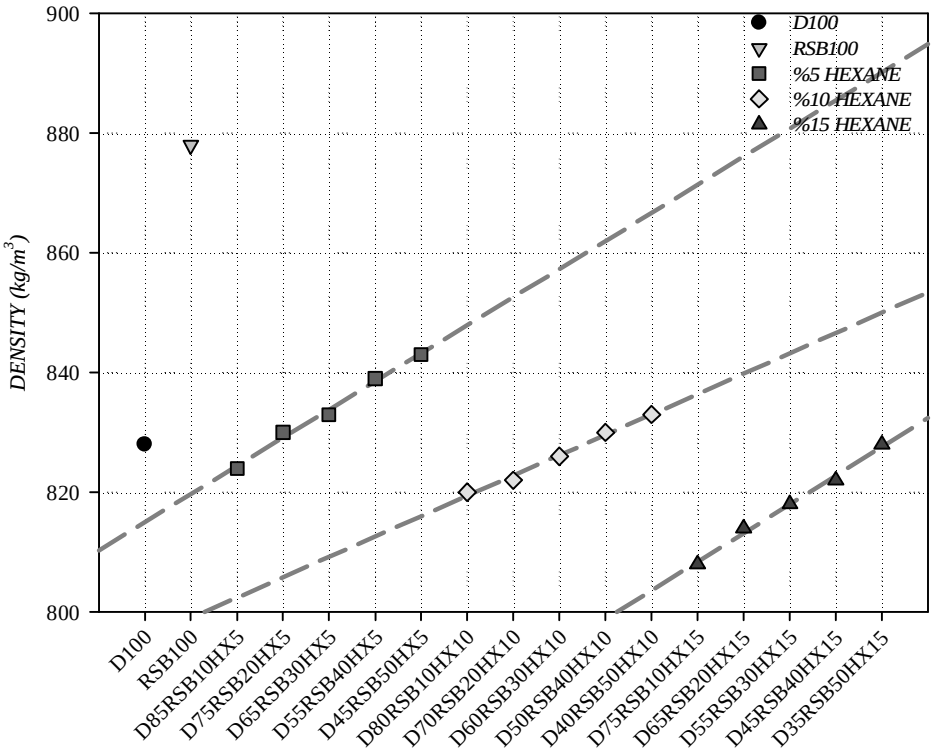


Figure 6.1. Density measurements results of n-hexane blends

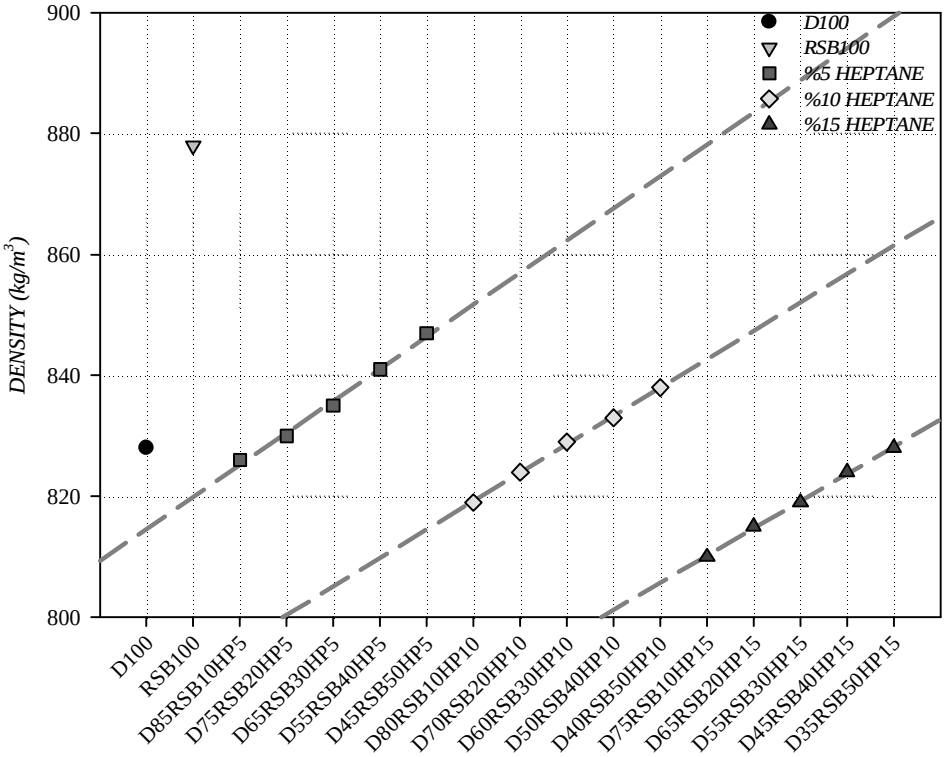


Figure 6.2. Density measurements results of n-heptane blends

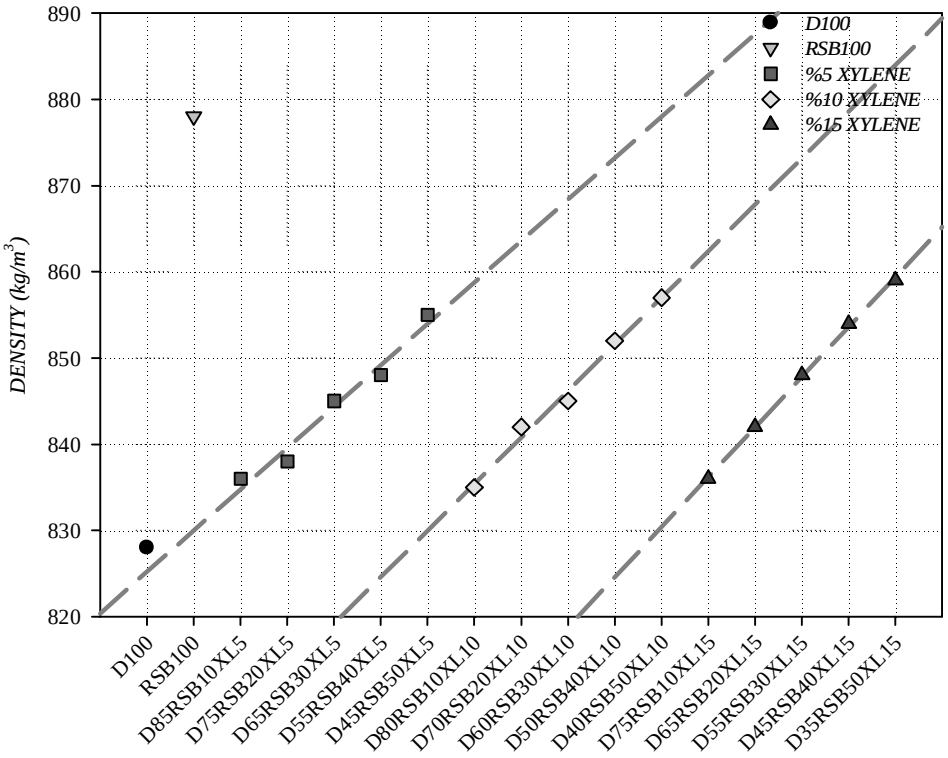


Figure 6.3. Density measurements results of xylene blends

6.2. Viscosity

Viscosity, which is a measure of resistance to flow of a liquid due to internal friction of one part of a fluid moving over another, affects the atomization of a fuel upon injection into the combustion chamber and thereby, the formation of the engine deposits (DOE/GO-102006-2358, 2006).

The higher value of the viscosity results the greater the tendency of the fuel to cause such problems. The viscosity of petrodiesel fuel is lower than that of a biodiesel, which is 2.0-4.5 mm^2/s in the European petrodiesel standard EN 590. If fuel viscosity is high, the injection pump will be unable to supply sufficient fuel to fill the pumping chamber. The effect will be a loss in power. If fuel viscosity extremely excessive, there will be a degradation of the spray in cylinder causing poor atomization, contamination of the lubricating oil, and the production of black smoke (Gerpen, 2004).

Due to the lower viscosities of n-hexane, n-heptane and xylene in accordance with the Rapeseed Biodiesel (RSB) were caused to lower the viscosities of the blends. On the other hand, any increase in the percent of the RSB caused an increase in the blend viscosity (figure 6.4, 6.5, 6.6). The reason for this increase was higher value of RSB viscosity, which was nearly 5.097 cst. However, the blends that were prepared from xylene had much more higher viscosities according to the n-hexane and n-heptane blends with the same percentages of RSB. Although all of the viscosity results were acceptable according to the standards, the best results were taken in the blends of n-hexane.

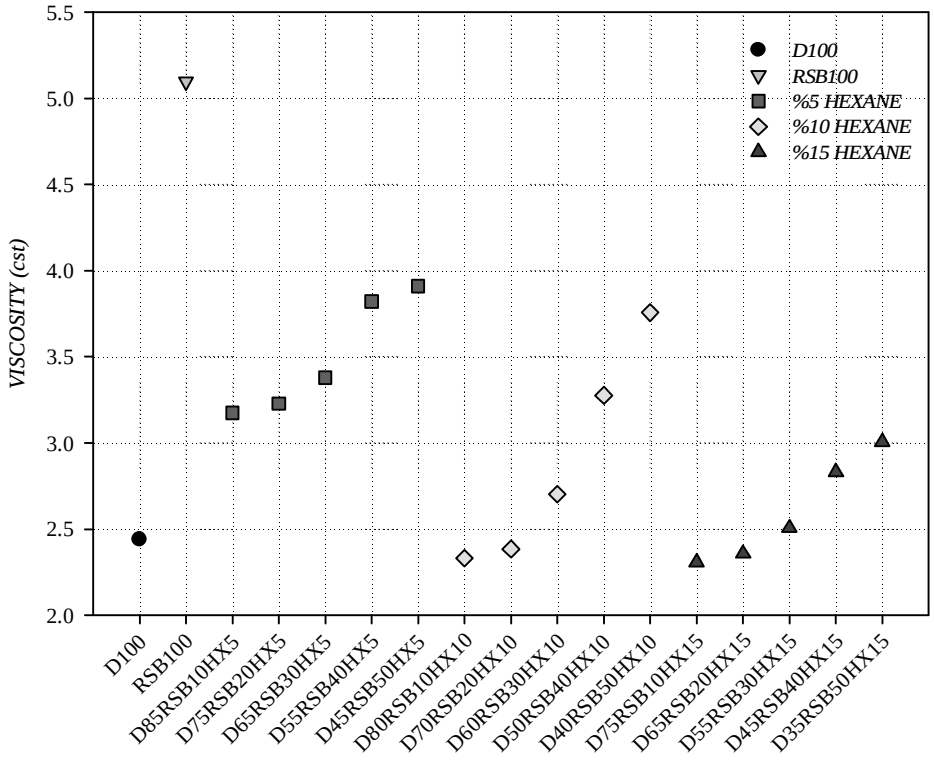


Figure 6.4. Viscosity measurements results of n-hexane blends

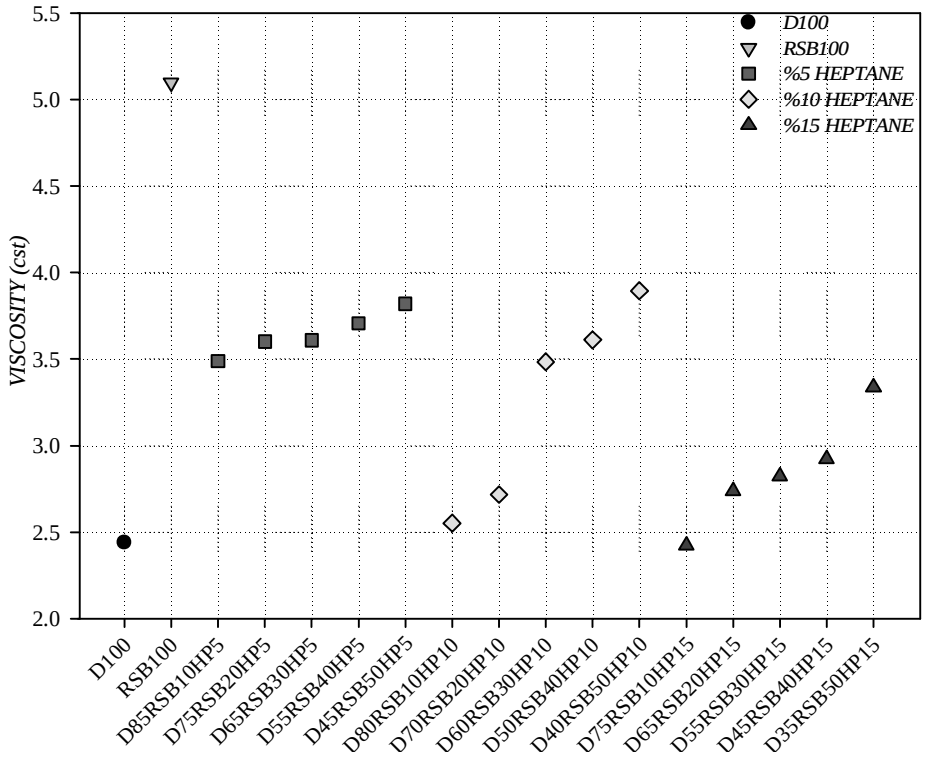


Figure 6.5. Viscosity measurements results of n-heptane blends

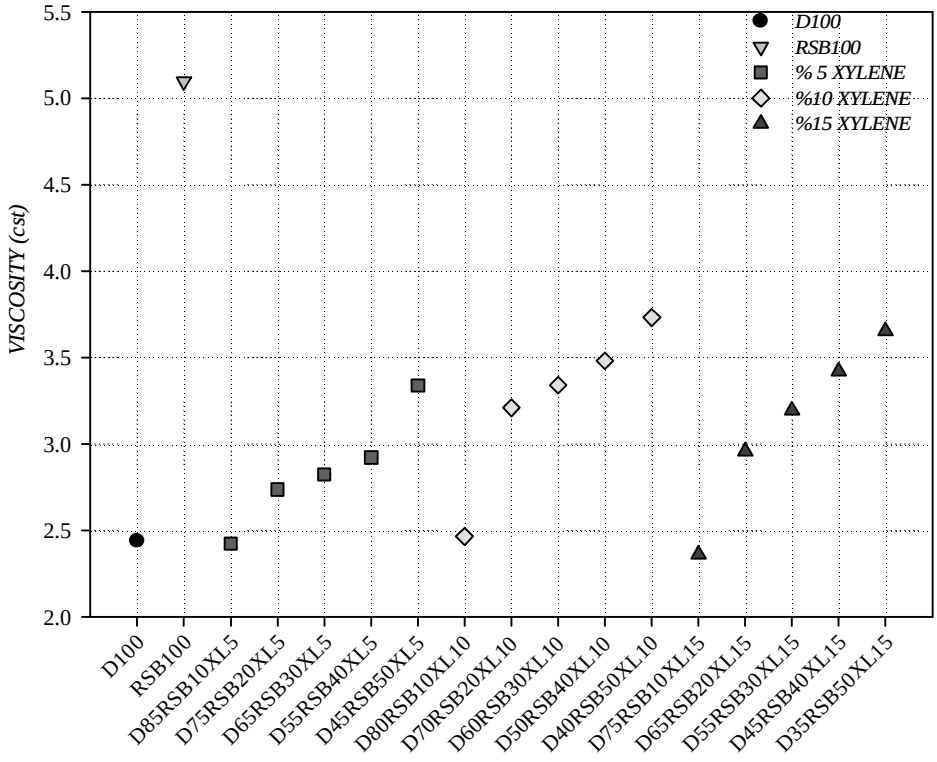


Figure 6.6. Viscosity measurements results of xylene blends

6.3 Heating Capacity

The actual benefit of the lower heating value for diesel fuel will vary depending on the refinery in which it was produced, the time of year, and the source of the petroleum feedstock because all of these variables affect the composition of the fuel. Diesel fuels with high percentages of aromatics tend to have high energy contents per liter even though the aromatics have low heating values per kilogram. Their high density more than compensates for their lower energy content on a weight basis. This is of a special importance for diesel engines because fuel is metered to the engine volumetrically. A fuel with lower energy content per liter will cause the engine to produce less peak power. At part load conditions, the engine operator will still be able to meet the demand for power but a greater volume of fuel injection timing when the fuel flow rate increases and this can cause an increase in the NO_x emissions (Gerpen, 2004).

Although Eurodiesel (D) has higher value of heating capacity, the blends have lower values of LHV (lower heating value) due to the lower heating capacity values of n-hexane, n-heptane, xylene and RSB. Therefore, any increase in the percent of the RSB caused a decrease in the blend's heating capacity (figure 6.7, 6.8, 6.9). The reason for this decrease was lower value of RSB heating capacity. However, the blends which were prepared from xylene had much more lower heating capacity with the same percentages of RSB. Although all of the heating capacity results were acceptable according to the standards, the best results were taken in the blends of n-hexane.

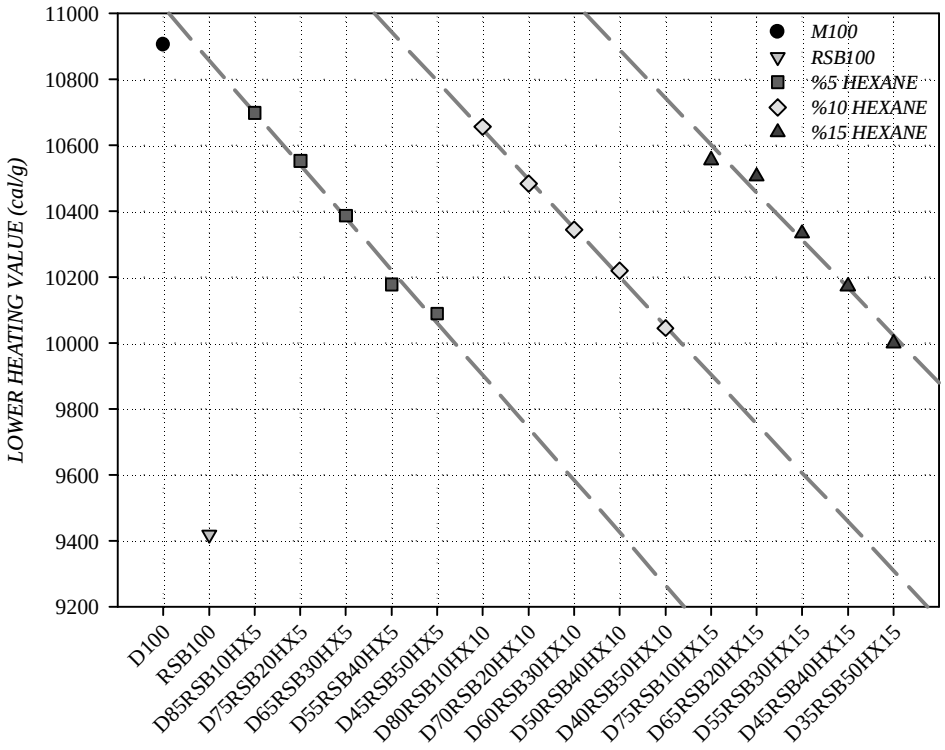


Figure 6.7. Lower Heating Value measurements results of n-hexane blends

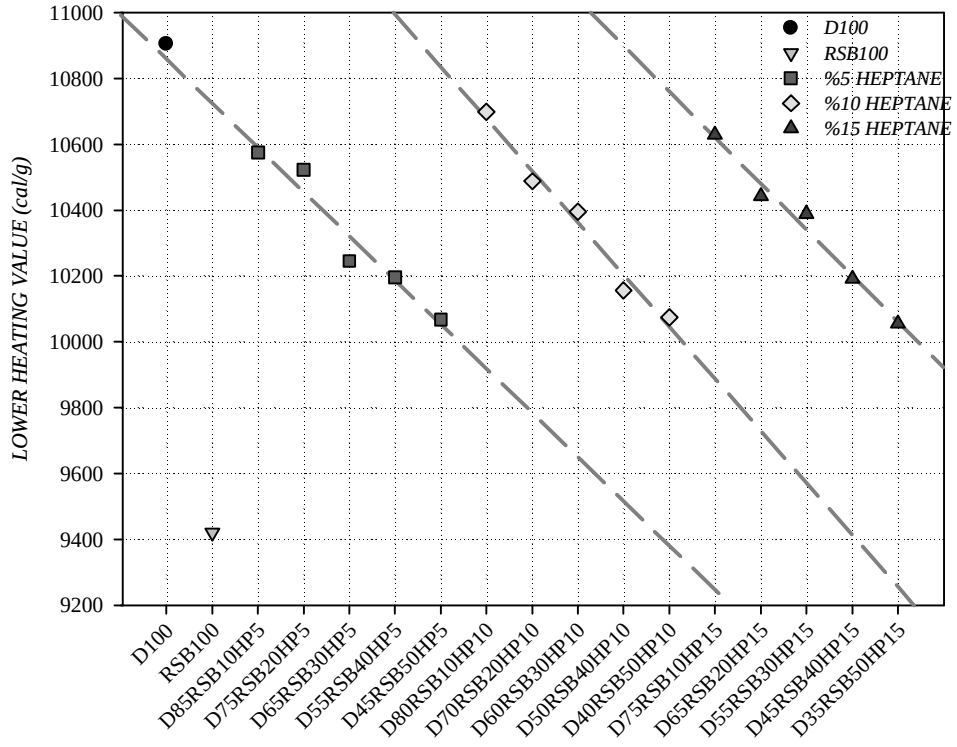


Figure 6.8. Lower Heating Value measurements results of n-heptane blends

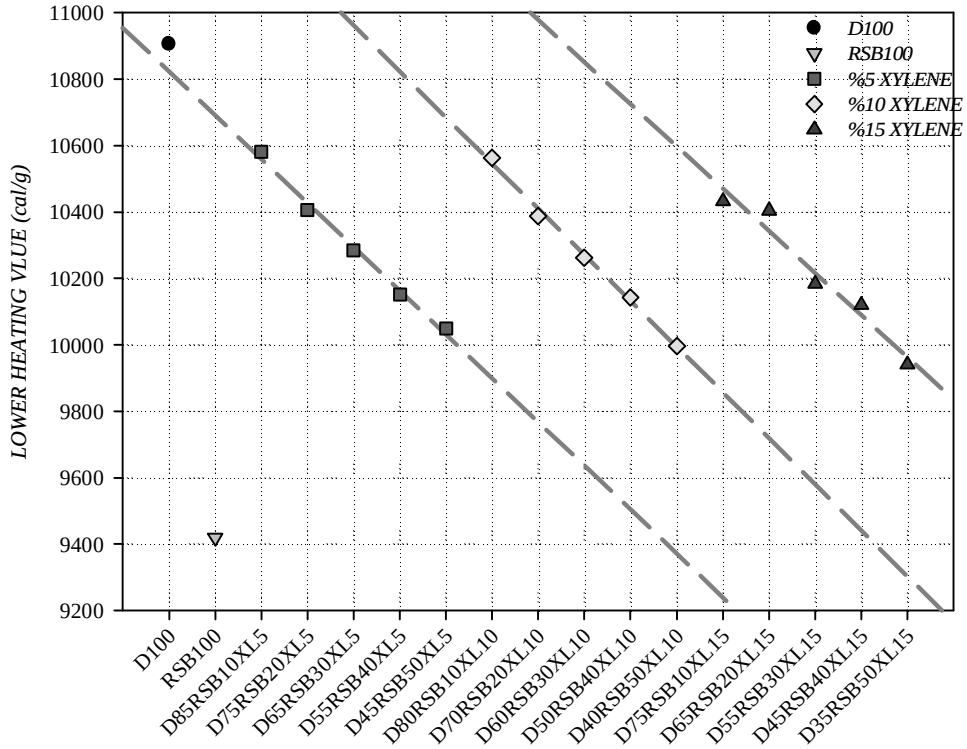


Figure 6.9. Lower Heating Value measurements results of xylene blends

6.4. Cetane Number

An adequate Cetane number is required for good engine performance. Higher Cetane numbers help ensure good cold start properties and minimize the formation of white smoke. The cetane index (ASTM D976) is not an accurate predictor of Cetane number for biodiesel or biodiesel blends since it is based on a calculation using specific gravity and distillation curve, both of which are different for biodiesel than for petrodiesel. Although the RSB which was used in the blends had lower cetane number nearly 15 % than Eurodiesel (D) an increased was obtained by n-hexane and n-heptane blends. On the other hand, when the xylene mixed to the blends the Cetane number slightly decreased. An increase in the percentage of xylene caused decrease in the Cetane number. Being an aromatic xylene had higher Octane rating than Cetane rating therefore blending with diesel and Rapeseed biodiesel caused a decrease in the Cetane number of the blends. Xylene was not suitable for using in diesel engines.

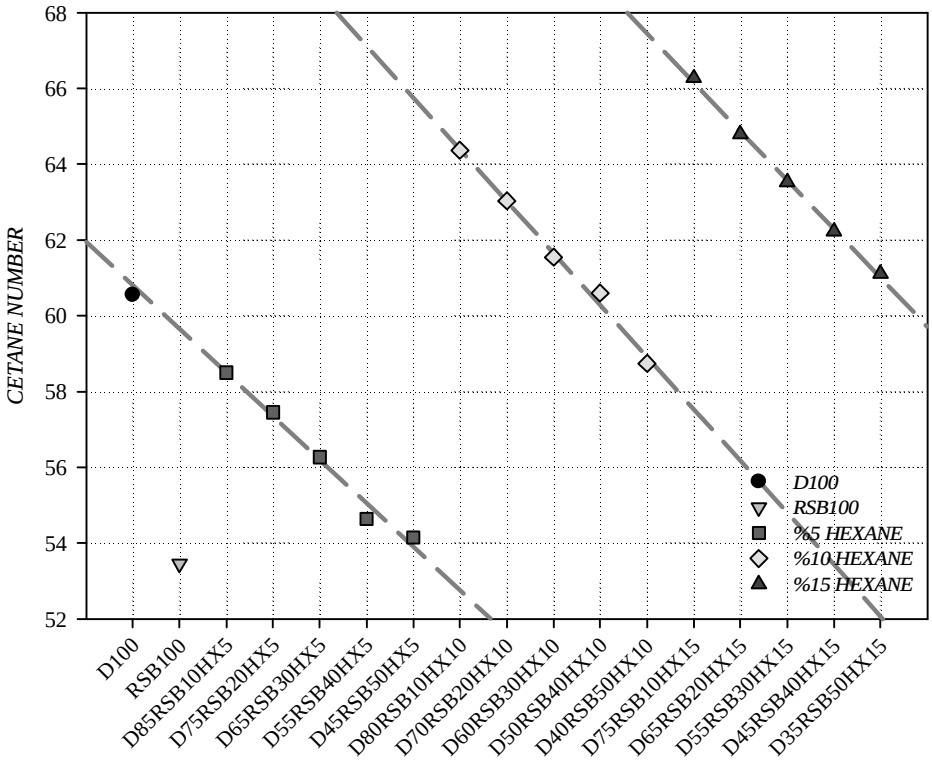


Figure 6.10. Cetane Number measurements results of n-hexane blends

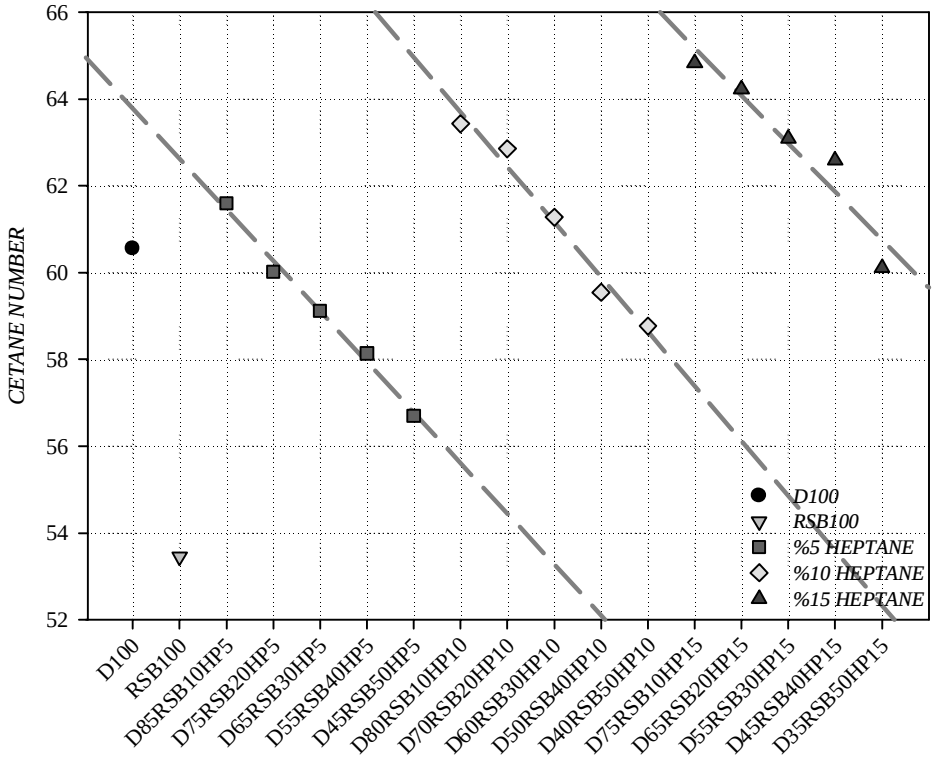


Figure 6.11. Cetane Number measurements results of n-heptane blends

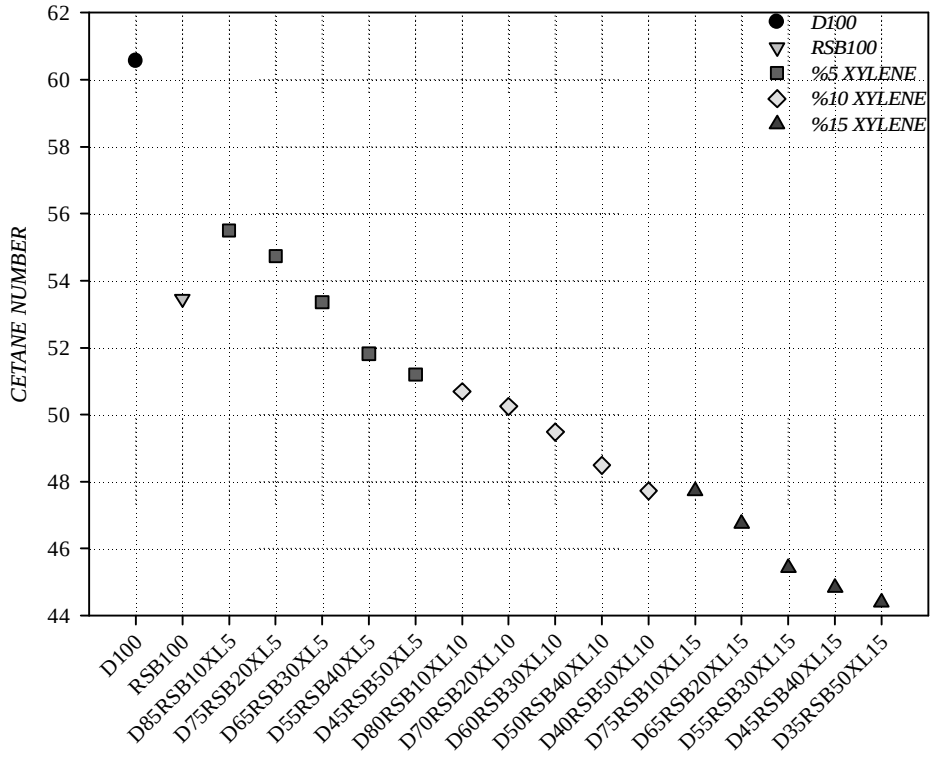


Figure 6.12. Cetane Number measurements results of xylene blends

6.5. Pour Point (PP)

The temperature at which the fuel contains so many agglomerated crystals it is essentially a gel and will no longer flow. This measurement is of little practical value to users, since the fuel has clogged the filter long before reaching its pour point (DOE/GO-102006-2358, 2006). As it was plotted in the figure 6.13, 6.14 and 6.15 blending decreased the PP of mixtures. Due to the testing interval which was 1ºC PP results of the blends coded D85RSB10HX5 - D75RSB20HX5, D70RSB20HX10 - D60RSB30HX10, D75RSB10HP15 - D65RSB20HP15, D80RSB10XL10 - D70RSB20XL10, D75RSB10XL15 - D65RSB20XL15 and also D45RSB40XL15 - D35RSB50XL15 gave the same results. Although it seemed blending gave good results, the best results were taken from %15 hexane blends.

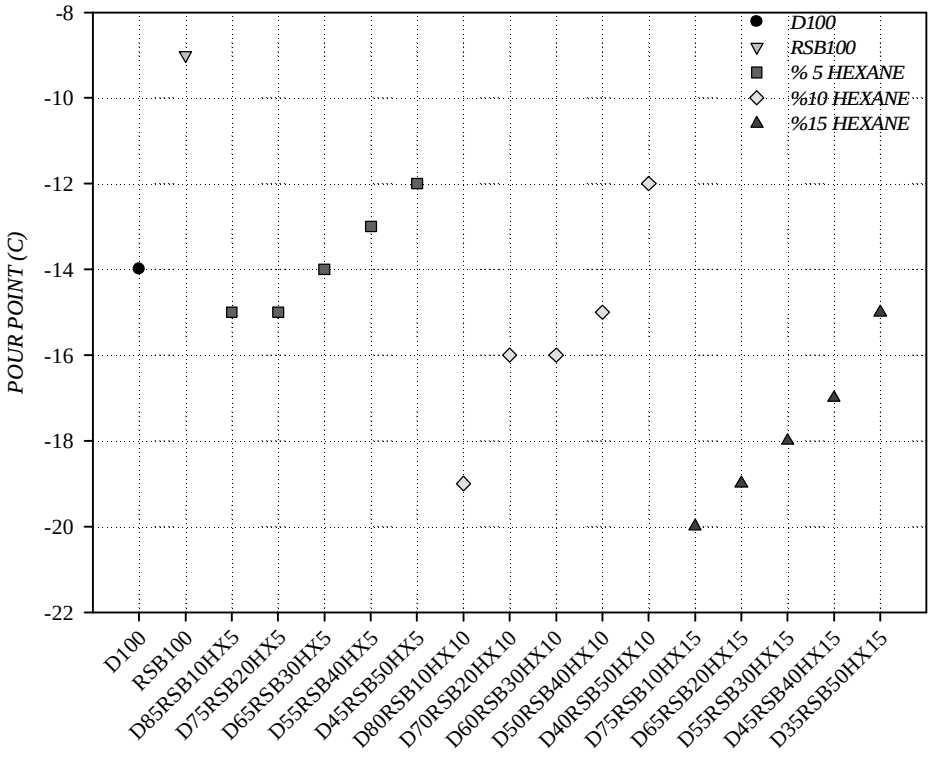


Figure 6.13. Pour Point measurements results of n-hexane blends

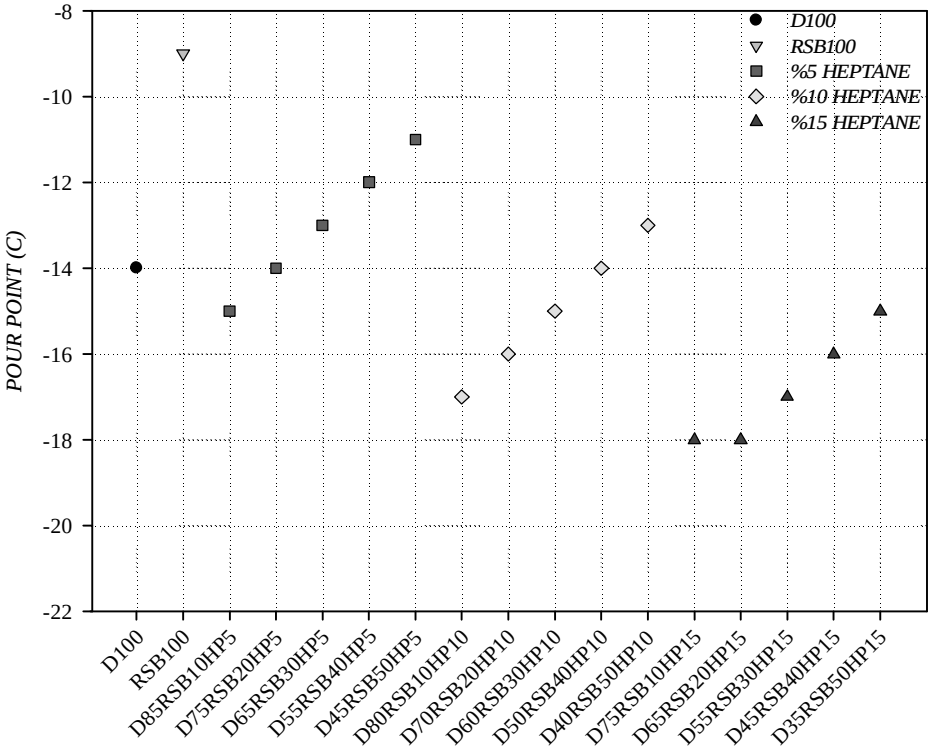


Figure 6.14. Pour Point measurements results of n-heptane blends

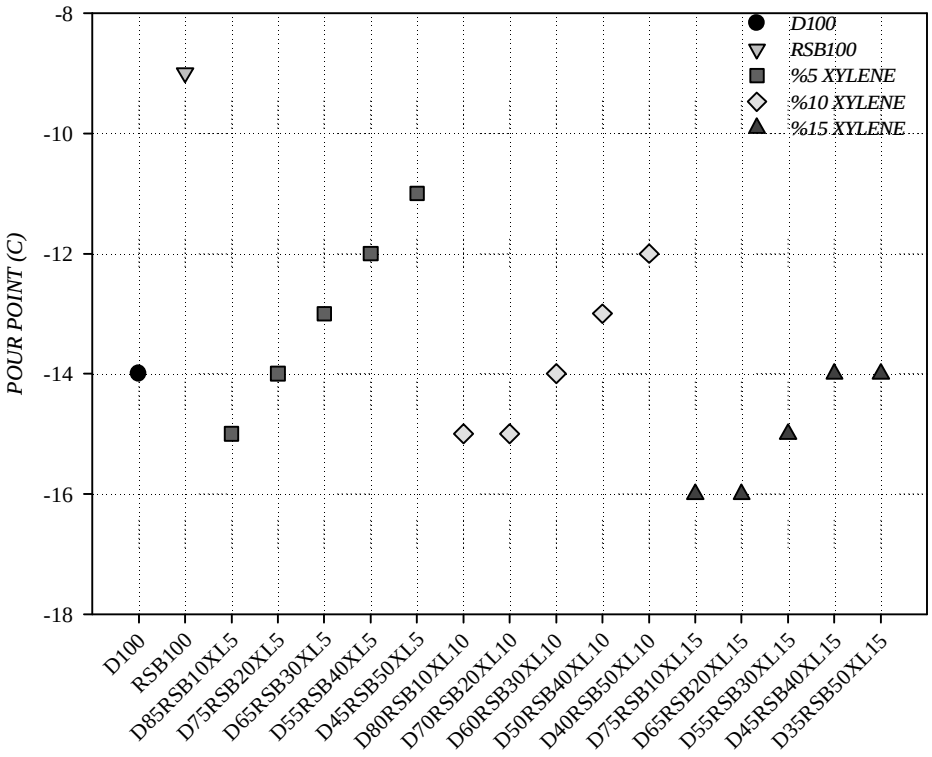


Figure 6.15. Pour Point measurements results of xylene blends

6.6. Flash Point

Flash point is related not only with ignition characteristic but also fuel's vapour pressure. According to EN 590 for diesel fuel a minimum flash point of 55 ^{O}C is required for fire safety. B100's flash point is typically much higher than diesel fuel's (minimum 120 ^{O}C according to TS EN 14214) to ensure that the manufacturer has removed excess methanol used in the manufacturing process. Residual methanol in the fuel is a safety issue because even very small amounts reduce the flash point. Residual methanol, which can be found in biodiesel with low, out-of-specification flash point, can also affect fuel pumps, seals and elastomers, and can result in poor combustion properties.

The substances, which were used in the blends, were highly volatile so during the experiments n-hexane, n-heptane and xylene were vaporized rapidly by the increasing of temperature. This vapor flashed then ended with rapid and wrong results of experiments. Because of this the flash points of Eurodiesel (D) and RSB were measured, the flash points of the substances were taken from the certificates of them and the flash points of the blends were theoretically calculated by using volumetric percentages. The results showed that storage and transporting of blends were safe. As the percentage of RSB increased flash point increased too. On the other hand xylene blends had higher flash points. The ranging of the flash points were xylene blends>n-heptane blends>n-hexane blends (fig. 6.16, 6.17, 6.18).

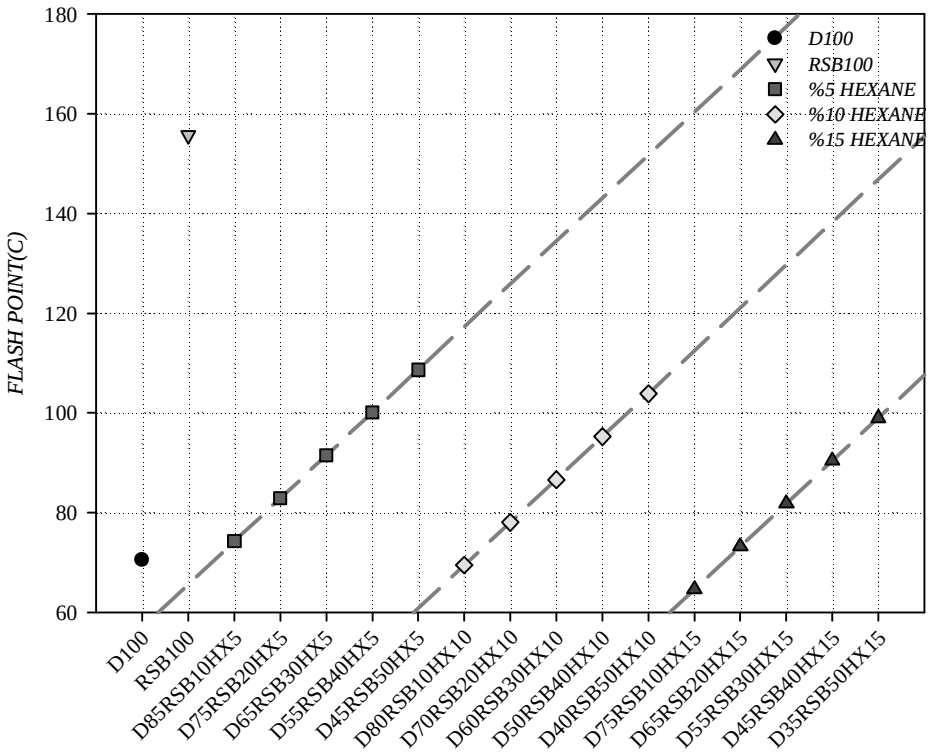


Figure 6.16. Flash Point measurements results of n-hexane blends

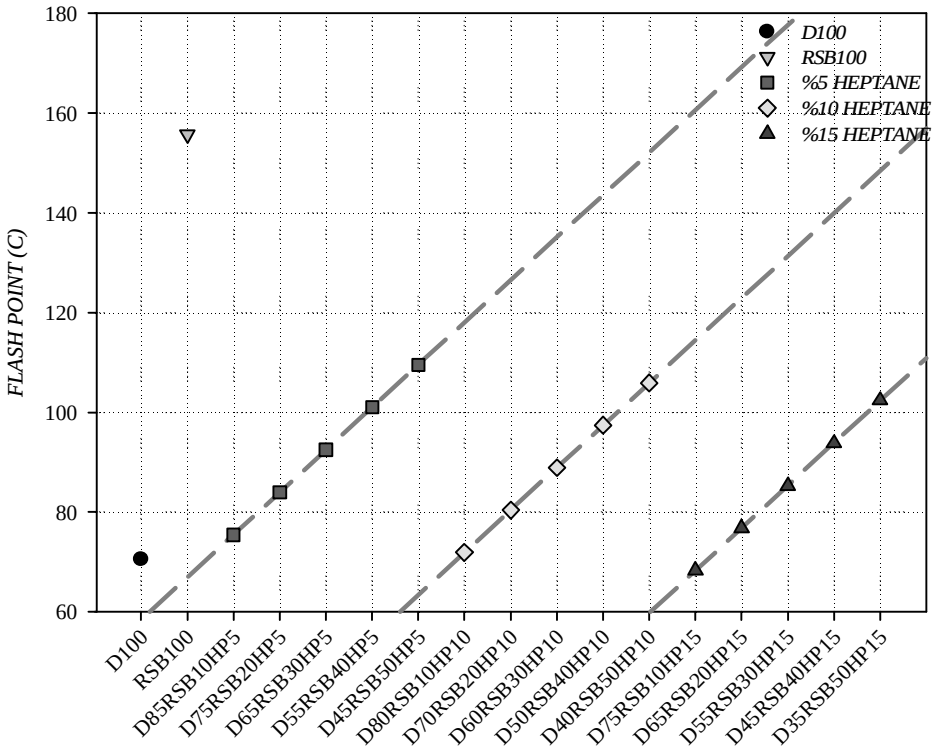


Figure 6.17. Flash Point measurements results of n-heptane blends

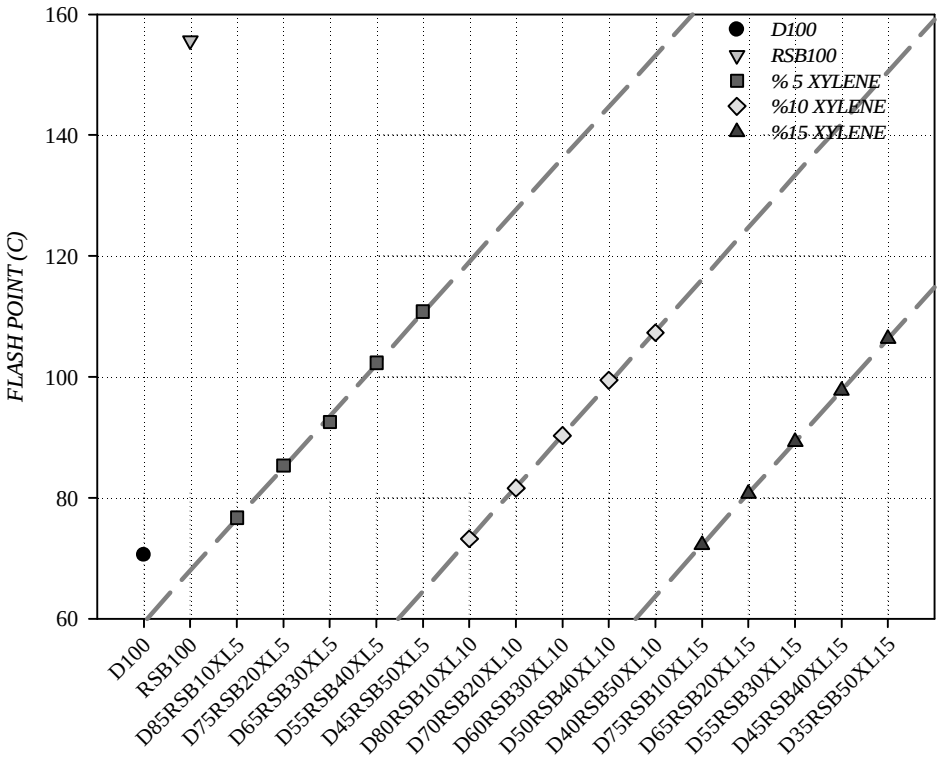


Figure 6.18. Flash Point measurements results of xylene blends

7. PERFORMANCE AND EMISSION RESULTS

This study was carried out at the Çukurova University Mechanical Engineering Department Automotive Engineering Laboratories. In this study torque, power, specific fuel consumption, volumetric efficiency, brake mean effective pressures were investigated as engine performance. Besides CO, CO_2, NO, NO_2 and NOx were the emissions that are recorded**.** Below sections include torque, power, specific fuel consumptions, CO, CO_2 and NO_x emission results were discussed in the below sections. The appendixes the recorded results were tabulated.

7.1. Torque versus Speed

The performance test measurements showed that the blends had tendency to increase torque values according to Eurodiesel (D100). The reason for this increase is the improvement of the quality of fuel by adding Alkenes to the mixture of biodiesel – Eurodiesel blends. Being saturated hydrocarbons alkenes have tendency to ignite. Having more hydrogen atoms caused higher heating capacity. Cetane numbers of alkenes are high (n-heptane is accepted as 100 Cetane) because of these specifications the blends combustion efficiency were increased.

The results were tabulated for pure diesel D100 in table 7.1, for pure rapeseed biodiesel RSB100 table 7.2, for the blend coded D85RSB10HX5 in table 7.3, and for the blend coded D85RSB10HP5 in table 7.18. The gained values, which were suitable for the engine torque characteristic curve, were shown in the torque versus speed graphic (Figure 7.1). The measured maximum torque values were for the sample coded D100 264.695 Nm at 1756 rpm, for the sample coded RSB100 265.588 Nm at 1754 rpm, for the sample coded D85RSB10HX5 265.474 Nm at 1614 rpm, and for the sample coded D85RSB10HP5 269.988 Nm at 1853 rpm respectively. The highest torque values were recorded from the blend D85RSB10HP5. After 1650 rpm the highest torque values were measured from D85RSB10HX5.

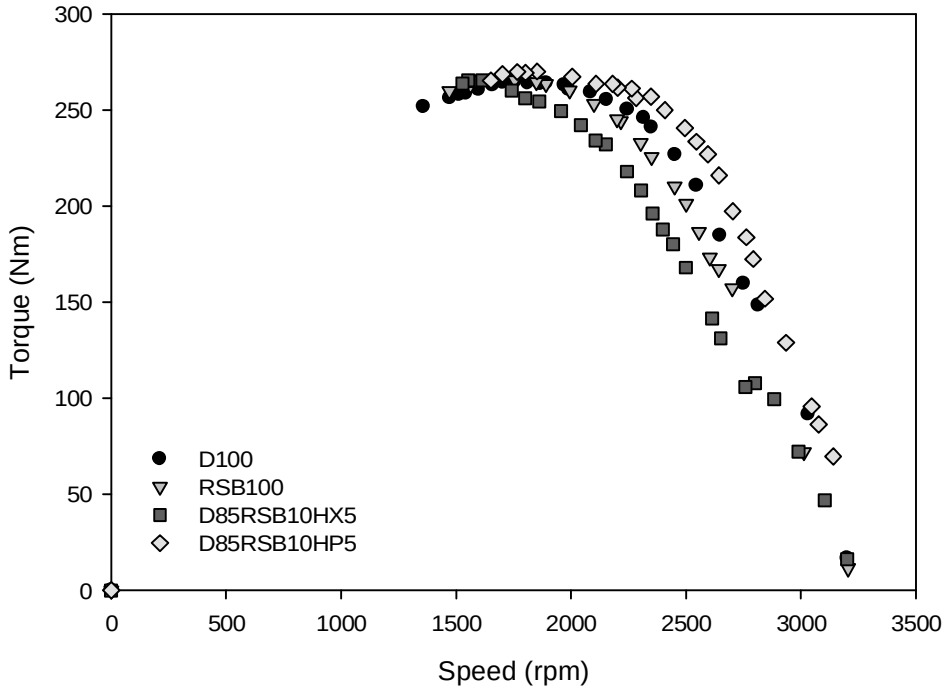


Figure 7.1. Torque-Speed Graphic of 85%Diesel, 10%RSB and 5%Alkenes

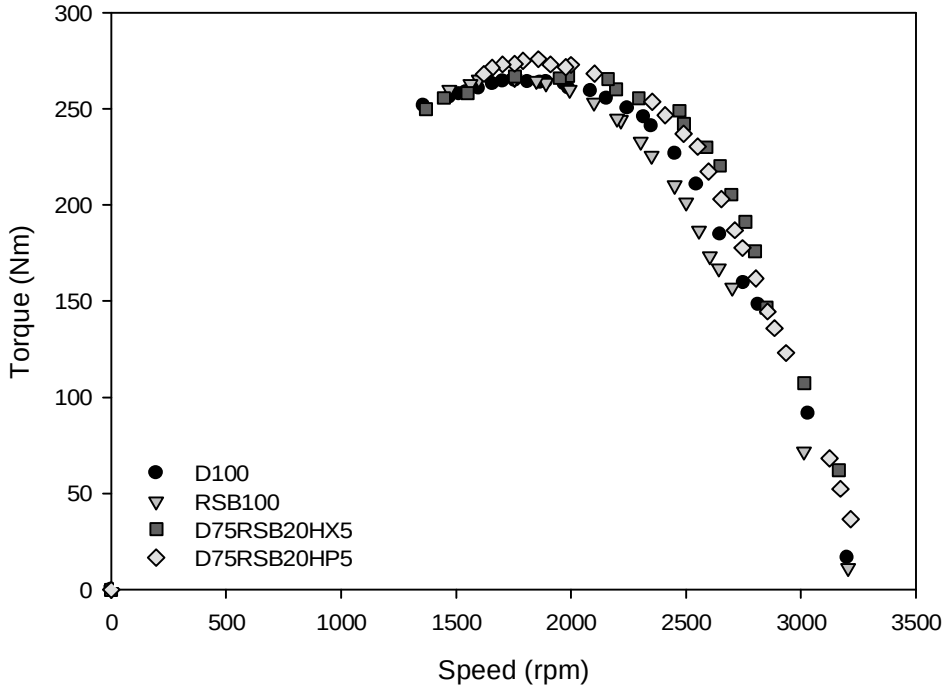


Figure 7.2. Torque-Speed Graphic of 75%Diesel, 20%RSB and 5%Alkenes

The results were tabulated for pure diesel D100 in table 7.1, for pure rapeseed biodiesel RSB100 table 7.2, for the blend coded D75RSB20HX5 in table 7.4, and for

the blend coded D75RSB20HP5 in table 7.19. The gained values, which were suitable for the engine torque characteristic curve, were shown in the torque versus speed graphic (Figure 7.2). The measured maximum torque values were for the sample coded D100 264.695 Nm at 1756 rpm, for the sample coded RSB100 265.588 Nm at 1754 rpm, for the sample coded D75RSB20HX5 267.227 Nm at 1986 rpm, and for the sample coded D75RSB20HP5 275.791 Nm at 1853 rpm respectively. The highest torque values were recorded from the blend D75RSB20HX5 until 2000 rpm. After 2000 rpm the highest torque values were measured from D75RSB20HP5.

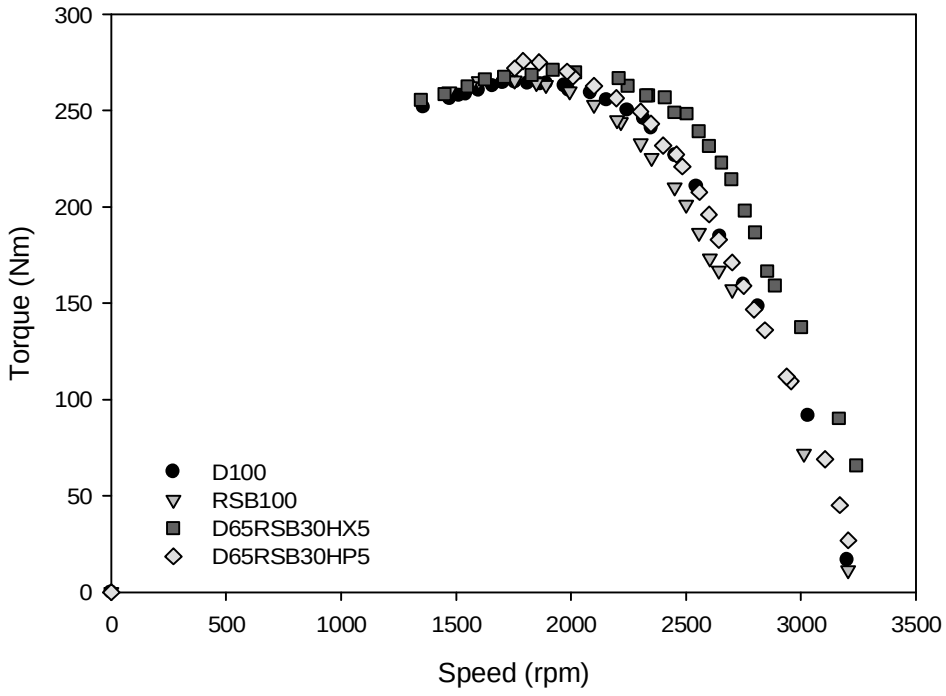


Figure 7.3. Torque-Speed Graphic of 65%Diesel, 30%RSB and 5%Alkenes

The results were tabulated for pure diesel D100 in table 7.1, for pure rapeseed biodiesel RSB100 table 7.2, for the blend coded D65RSB30HX5 in table 7.5, and for the blend coded D65RSB30HP5 in table 7.20. The gained values, which were suitable for the engine torque characteristic curve, were shown in the torque versus speed graphic (Figure 7.3). The measured maximum torque values were for the sample coded D100 264.695 Nm at 1756 rpm, for the sample coded RSB100 265.588 Nm at 1754 rpm, for the sample coded D65RSB30HX5 271.358 Nm at 1920 rpm, and for

the sample coded D65RSB30HP5 275.623 Nm at 1792 rpm respectively. The highest torque values were recorded from the blend D65RSB30HX5 until 1900 rpm. After 1900 rpm the highest torque values were measured from D65RSB30HP5.

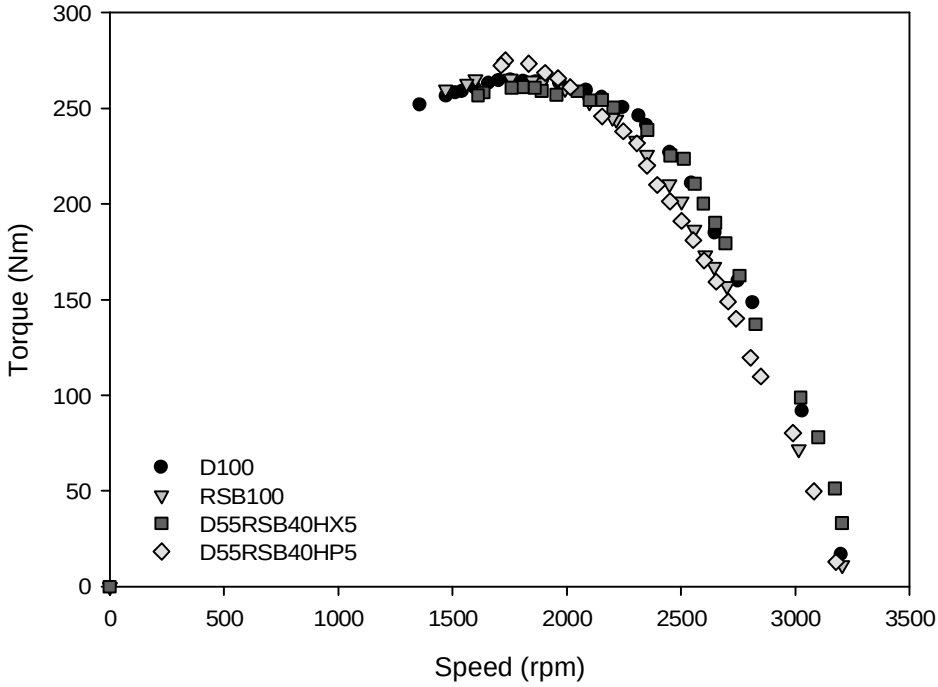


Figure 7.4. Torque-Speed Graphic of 55%Diesel, 40%RSB and 5%Alkenes

The results were tabulated for pure diesel D100 in table 7.1, for pure rapeseed biodiesel RSB100 table 7.2, for the blend coded D55RSB40HX5 in table 7.6, and for the blend coded D55RSB40HP5 in table 7.21. The gained values, which were suitable for the engine torque characteristic curve, were shown in the torque versus speed graphic (Figure 7.4). The measured maximum torque values were for the sample coded D100 264.695 Nm at 1756 rpm, for the sample coded RSB100 265.588 Nm at 1754 rpm, for the sample coded D55RSB40HX5 261.021 Nm at 1807 rpm, and for the sample coded D55RSB40HP5 274.870 Nm at 1731 rpm respectively. The torque curve of D55RSB40HX5 was closed to the sample coded D100 with minor changes, after 2047 rpm lower torque values were observed from the sample coded D55RSB40HX5. On the other hand, the lowest values of torque were measured from

the sample coded D55RSB40HP5 until 2015 rpm. After that speed, higher torque results were observed from the blend coded D50RSB40HP.

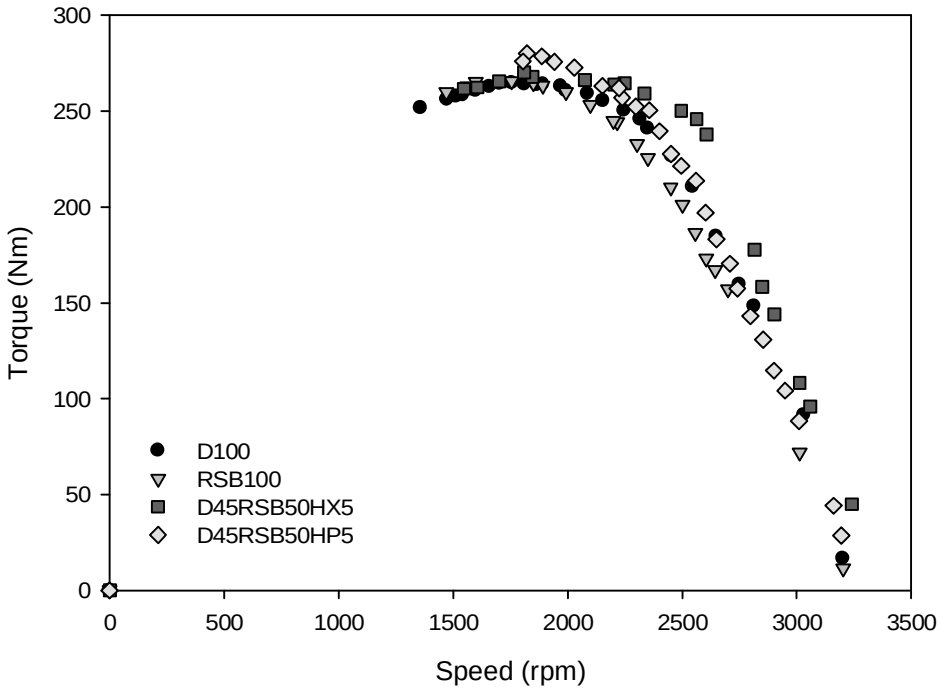


Figure 7.5. Torque-Speed Graphic of 45%Diesel, 50%RSB and 5%Alkenes

The results were tabulated for pure diesel D100 in table7.1, for pure rapeseed biodiesel RSB100 table 7.2, for the blend coded D45RSB50HX5 in table 7.7, and for the blend coded D45RSB50HP5 in table 7.22. The gained values, which were suitable for the engine torque characteristic curve, were shown in the torque versus speed graphic (Figure 7.5). The gained values were suitable for the engine torque characteristic curve. The measured maximum torque values were for the sample coded D100 264.695 Nm at 1756 rpm, for the sample coded RSB100 265.588 Nm at 1754 rpm, for the sample coded D45RSB50HX5 270.344 Nm at 1810 rpm, and for the sample coded D45RSB50HP5 280.129 Nm at 1822 rpm respectively. The highest values were taken from the sample coded D45RSB50HX5 blend until 1941 rpm. The torque curve of the sample coded D45RSB50HP5 was closed to the sample coded D100 with minor changes until 1941 rpm and after that speed the torque values which were measured reached the highest rate for D45RSB50HP5 blend.

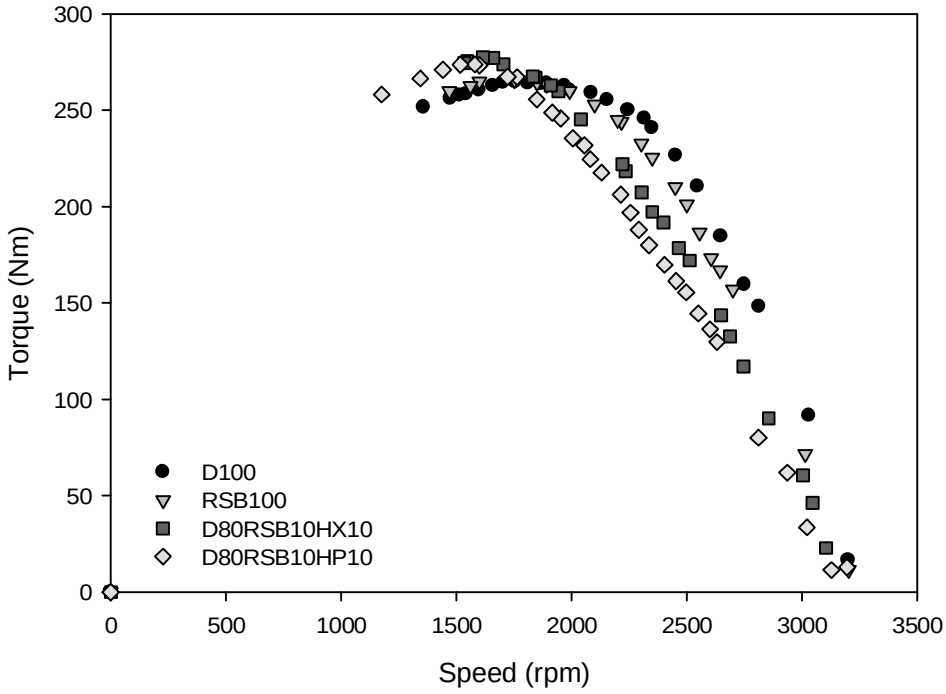


Figure 7.6. Torque-Speed Graphic of 80%Diesel, 10%RSB and 10%Alkenes

The results were tabulated for pure diesel D100 in table 7.1, for pure rapeseed biodiesel RSB100 table 7.2, for the blend coded D80RSB10HX10 in table 7.8, and for the blend coded D80RSB10HP10 in table 7.23. The gained values, which were suitable for the engine torque characteristic curve, were shown in the torque versus speed graphic (Figure 7.6). The measured maximum torque values were for the sample coded D100 264.695 Nm at 1756 rpm, for the sample coded RSB100 265.588 Nm at 1754 rpm, for the sample coded D80RSB10HX10 277.584 Nm at 1616 rpm, and for the sample coded D80RSB10HP10 273.899 Nm at 1579 rpm respectively. Although at the high speeds, the torque values were given lesser than both D100 and RSB100 by the blends. The inclination were begun at lower speeds, at 1844 rpm for the sample coded D80RSB10HX10 and 1763 rpm for the sample coded D80RSB10HP10.

The results were tabulated for pure diesel D100 in table 7.1, for pure rapeseed biodiesel RSB100 table 7.2, for the blend coded D70RSB20HX10 in table 7.9, and for the blend coded D70RSB20HP10 in table 7.24. The gained values, which were

suitable for the engine torque characteristic curve, were shown in the torque versus speed graphic (Figure 7.7). The measured maximum torque values were for the sample coded D100 264.695 Nm at 1756 rpm, for the sample coded RSB100 265.588 Nm at 1754 rpm, for the sample coded D70RSB20HX10 273.925 Nm at 1605 rpm, and for the sample coded D70RSB20HP10 275.542 Nm at 1759 rpm respectively. The highest values were taken from D70RSB20HP10 blend.

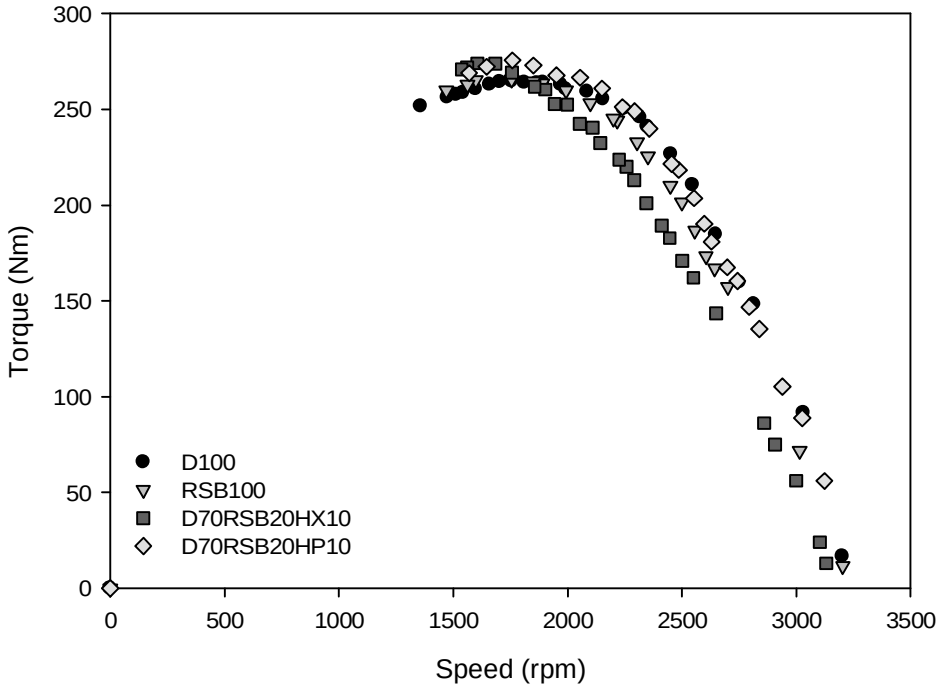


Figure 7.7. Torque-Speed Graphic of 70%Diesel, 20%RSB and 10%Alkenes

The results were tabulated for pure diesel D100 in table 7.1, for pure rapeseed biodiesel RSB100 table 7.2, for the blend coded D60RSB30HX10 in table 7.10, and for the blend coded D60RSB30HP10 in table 7.25. The gained values, which were suitable for the engine torque characteristic curve, were shown in the torque versus speed graphic (Figure 7.8). The measured maximum torque values were for the sample coded D100 264.695 Nm at 1756 rpm, for the sample coded RSB100 265.588 Nm at 1754 rpm, for the sample coded D60RSB30HX10 279.941 Nm at 1709 rpm, and for the sample coded D60RSB30HP10 274.642 Nm at 1800 rpm respectively. Higher torque values were observed till 1960 rpm from D100. After that speed,

higher torque results were measured from the blends D60RSB30HX10 and D60RSB30HP10. The highest values were taken from D60RSB30HX10 blend.

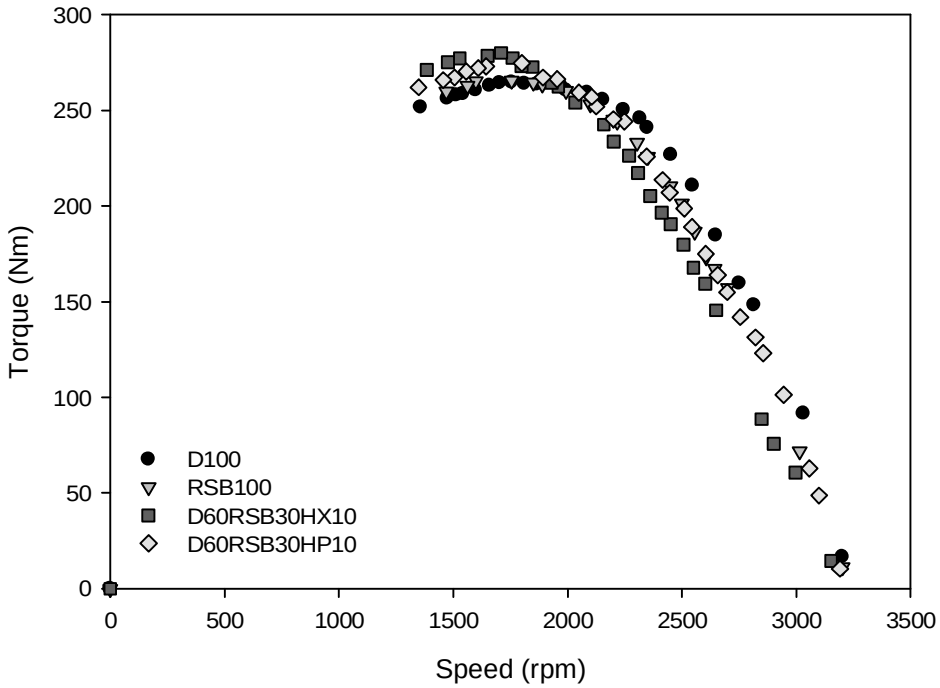


Figure 7.8. Torque-Speed Graphic of 60%Diesel, 30%RSB and 10%Alkenes

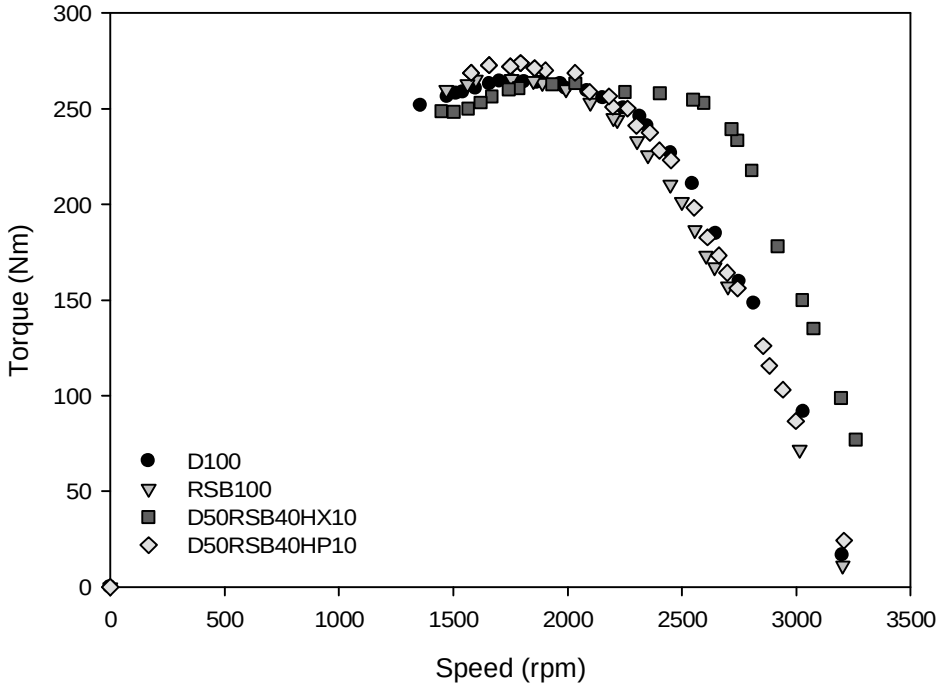


Figure 7.9. Torque-Speed Graphic of 50%Diesel, 40%RSB and 10%Alkenes

The results were tabulated for pure diesel D100 in table 7.1, for pure rapeseed biodiesel RSB100 table 7.2, for the blend coded D50RSB40HX10 in table 7.11, and for the blend coded D50RSB40HP10 in table 7.26. The gained values, which were suitable for the engine torque characteristic curve, were shown in the torque versus speed graphic (Figure 7.9). The gained values were suitable for the engine torque characteristic curve. The measured maximum torque values were for the sample coded D100 264.695 Nm at 1756 rpm, for the sample coded RSB100 265.588 Nm at 1754 rpm, for the sample coded D50RSB40HX10 263.191 Nm at 2034 rpm, and for the sample coded D50RSB40HP10 273.863 Nm at 1794 rpm respectively. Higher torque values were observed until 2034 rpm from D50RSB40HX10, maximum torque was measured at that speed. After that speed, higher torque results were observed from the blend D50RSB40HP.

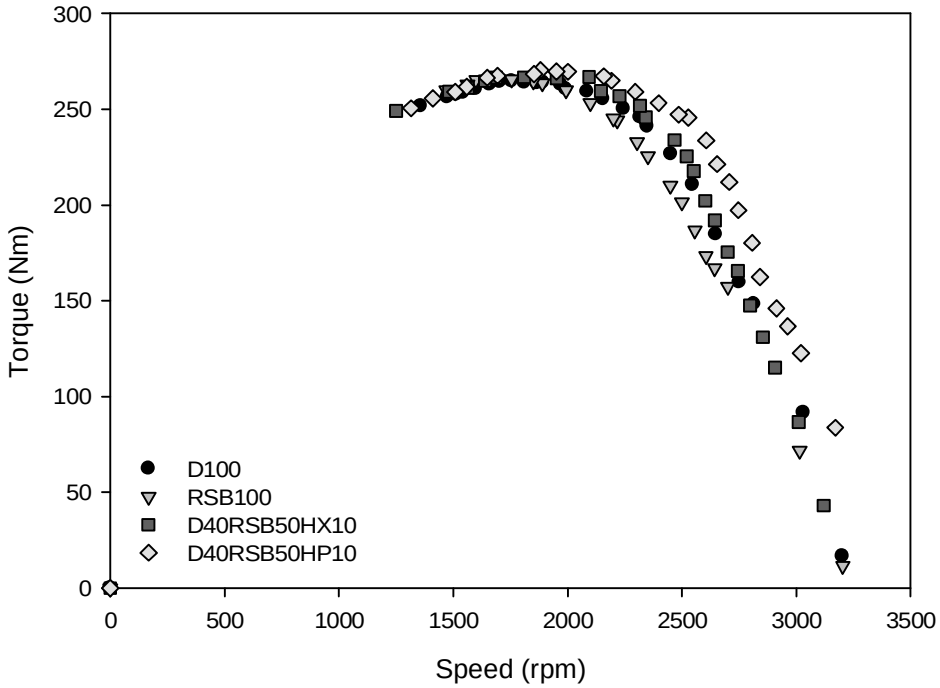


Figure 7.10. Torque-Speed Graphic of 40%Diesel, 50%RSB and 10%Alkenes

The results were tabulated for pure diesel D100 in table 7.1, for pure rapeseed biodiesel RSB100 table 7.2, for the blend coded D40RSB50HX10 in table 7.12, and for the blend coded D40RSB50HP10 in table 7.27. The gained values, which were

suitable for the engine torque characteristic curve, were shown in the torque versus speed graphic (Figure 7.10). The measured maximum torque values were for the sample coded D100 264.695 Nm at 1756 rpm, for the sample coded RSB100 265.588 Nm at 1754 rpm, for the sample coded D40RSB50HX10 266.804 Nm at 2094 rpm, and for the sample coded D40RSB50HP10 270.330 Nm at 1882 rpm respectively. The torque curve of D40RSB50HX10 was closed to D100 with minor changes nonetheless highest torque values were measured from D40RSB50HP10 blend.

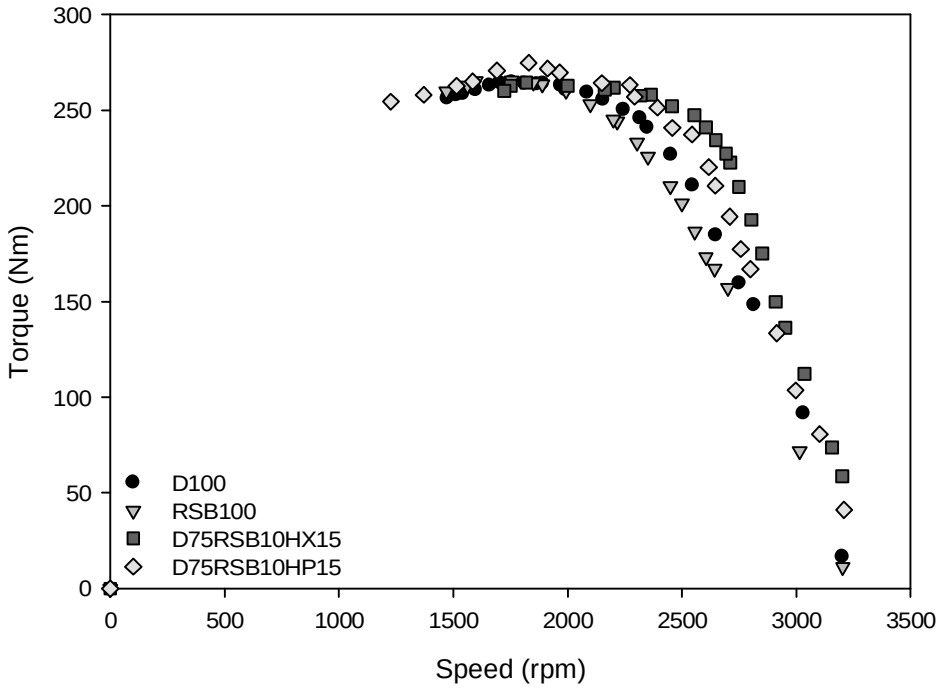


Figure 7.11. Torque-Speed Graphic of 75%Diesel, 10%RSB and 15%Alkenes

The results were tabulated for pure diesel D100 in table 7.1, for pure rapeseed biodiesel RSB100 table 7.2, for the blend coded D75RSB10HX15 in table 7.13, and for the blend coded D75RSB10HP15 in table 7.28. The gained values, which were suitable for the engine torque characteristic curve, were shown in the torque versus speed graphic (Figure 7.11). The measured maximum torque values were for the sample coded D100 264.695 Nm at 1756 rpm, for the sample coded RSB100 265.588 Nm at 1754 rpm, for the sample coded D75RSB10HX15 264.400 Nm at 1820 rpm,

and for the sample coded D75RSB10HX15 274.736 Nm at 1830 rpm respectively. Higher torque values were given by D75RSB10HX15 and D75RSB10HX15 blends.

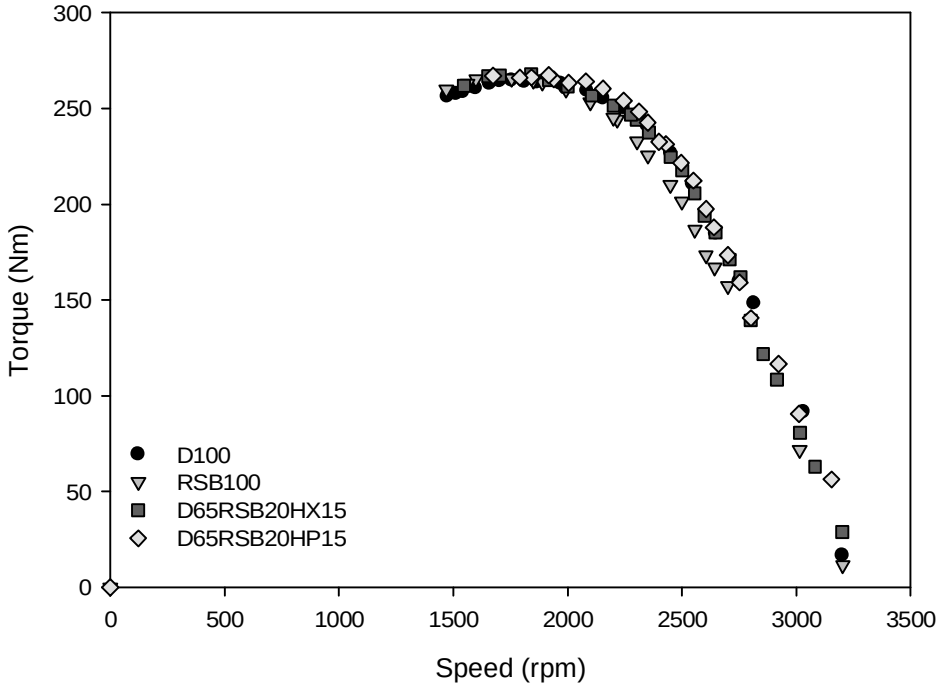


Figure 7.12. Torque-Speed Graphic of 65%Diesel, 20%RSB and 15%Alkenes

The results were tabulated for pure diesel D100 in table 7.1, for pure rapeseed biodiesel RSB100 table 7.2, for the blend coded D65RSB20HX15 in table 7.14, and for the blend coded D65RSB20HP15 in table 7.29. The gained values, which were suitable for the engine torque characteristic curve, were shown in the torque versus speed graphic (Figure 7.12). The measured maximum torque values were for the sample coded D100 264.695 Nm at 1756 rpm, for the sample coded RSB100 265.588 Nm at 1754 rpm, for the sample coded D65RSB20HX15 267.986 Nm at 1841 rpm, and for the sample coded D65RSB20HP15 267.388 Nm at 1918 rpm respectively. Both blends torque curve were closed to D100 torque curve with minor changes.

The results were tabulated for pure diesel D100 in table 7.1, for pure rapeseed biodiesel RSB100 table 7.2, for the blend coded D55RSB30HX15 in table 7.15, and for the blend coded D55RSB30HP15 in table 7.30. The gained values, which were suitable for the engine torque characteristic curve, were shown in the torque versus

speed graphic (Figure 7.13). The measured maximum torque values were for the sample coded D100 264.695 Nm at 1756 rpm, for the sample coded RSB100 265.588 Nm at 1754 rpm, for the sample coded D55RSB30HX15 272.171 Nm at 1822 rpm, and for the sample coded D55RSB30HP15 278.625 Nm at 1606 rpm respectively. Until 1962 rpm less torque were produced by D55RSB30HP15, the torque curve was beneath D100 torque curve.

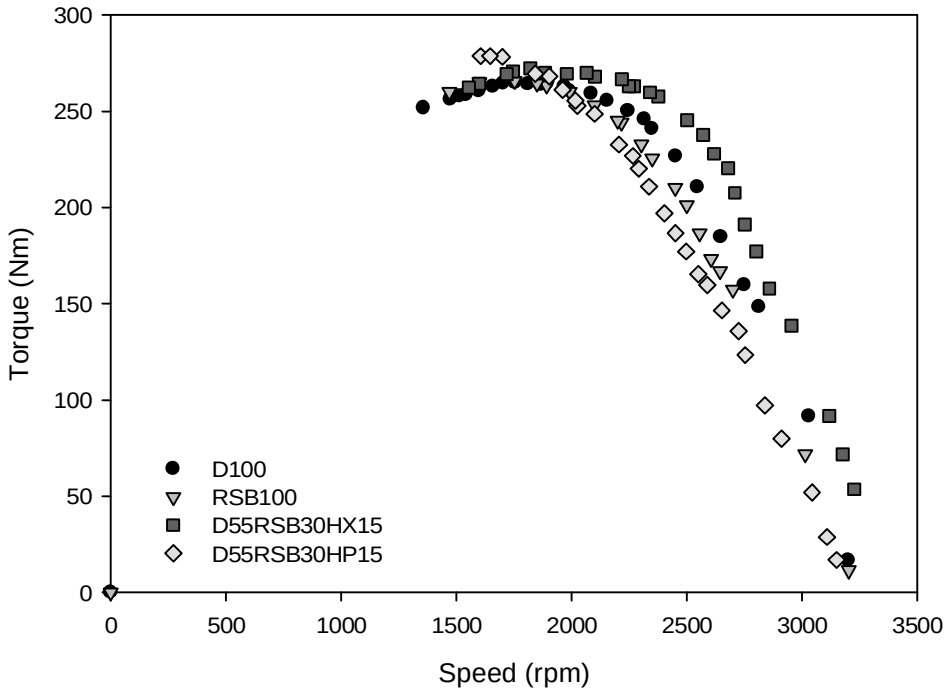


Figure 7.13. Torque-Speed Graphic of 55%Diesel, 30%RSB and 15%Alkenes

The results were tabulated for pure diesel D100 in table 7.1, for pure rapeseed biodiesel RSB100 table 7.2, for the blend coded D45RSB40HX15 in table 7.16, and for the blend coded D45RSB40HP15 in table 7.31. The gained values, which were suitable for the engine torque characteristic curve, were shown in the torque versus speed graphic (Figure 7.14). The measured maximum torque values were for the sample coded D100 264.695 Nm at 1756 rpm, for the sample coded RSB100 265.588 Nm at 1754 rpm, for the sample coded D45RSB40HX15 273.023 Nm at 1932 rpm, and for the sample coded D45RSB40HP15 274.743 Nm at 1864 rpm respectively. Both blends were produced more torque according to D100.

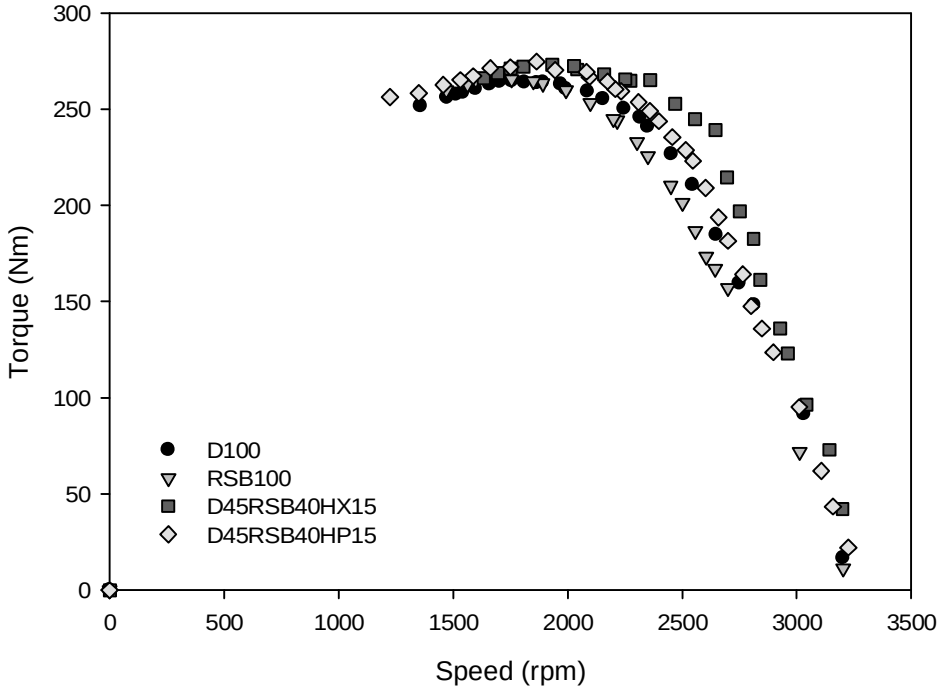


Figure 7.14. Torque-Speed Graphic of 45%Diesel, 40%RSB and 15%Alkenes

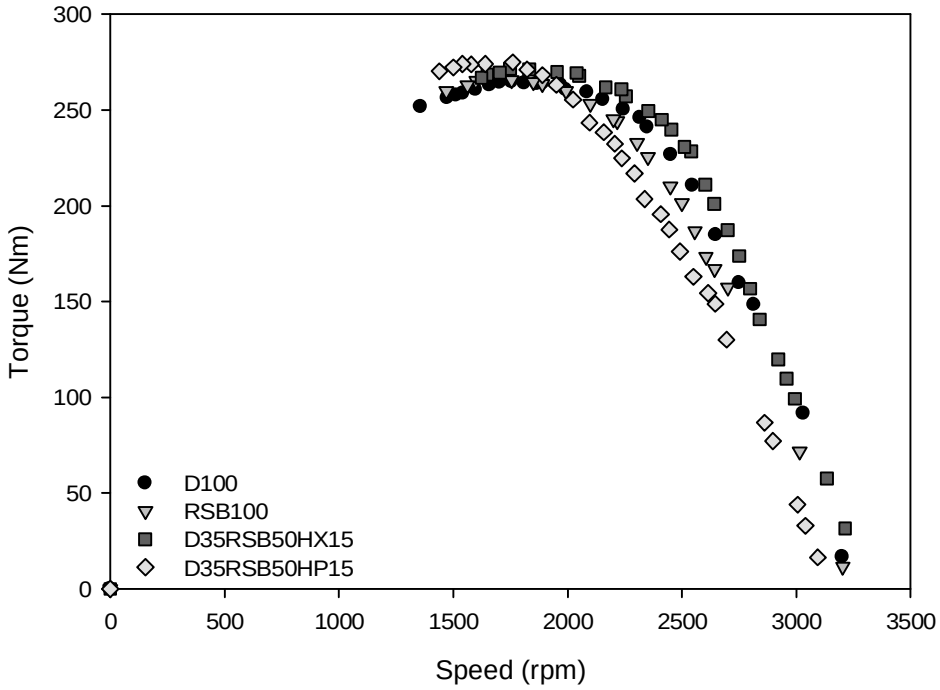


Figure 7.15. Torque-Speed Graphic of 35% Diesel, 50% RSB and 15% Alkenes

The results were tabulated for pure diesel D100 in table 7.1, for pure rapeseed biodiesel RSB100 table 7.2, for the blend coded D35RSB50HX15 in table 7.17, and for the blend coded D35RSB50HP15 in table 7.32. The gained values, which were suitable for the engine torque characteristic curve, were shown in the torque versus speed graphic (Figure 7.15). The measured maximum torque values were for the sample coded D100 264.695 Nm at 1756 rpm, for the sample coded RSB100 265.5885 Nm at 1754 rpm, for the sample coded D35RSB50HX15 271.40 Nm at 1748 rpm, and for the sample coded D35RSB50HP15 274.90 Nm at 1760 rpm respectively. At high speeds, D35RSB50HX15 was reached highest torque values. On the other hand D35RSB50HP15 at high speeds gave less torque values than D100 until 2000 rpm then produced more torque.

7.2. Power versus Speed

The improvements in the fuel quality of blends were showed tendency to increase the power.

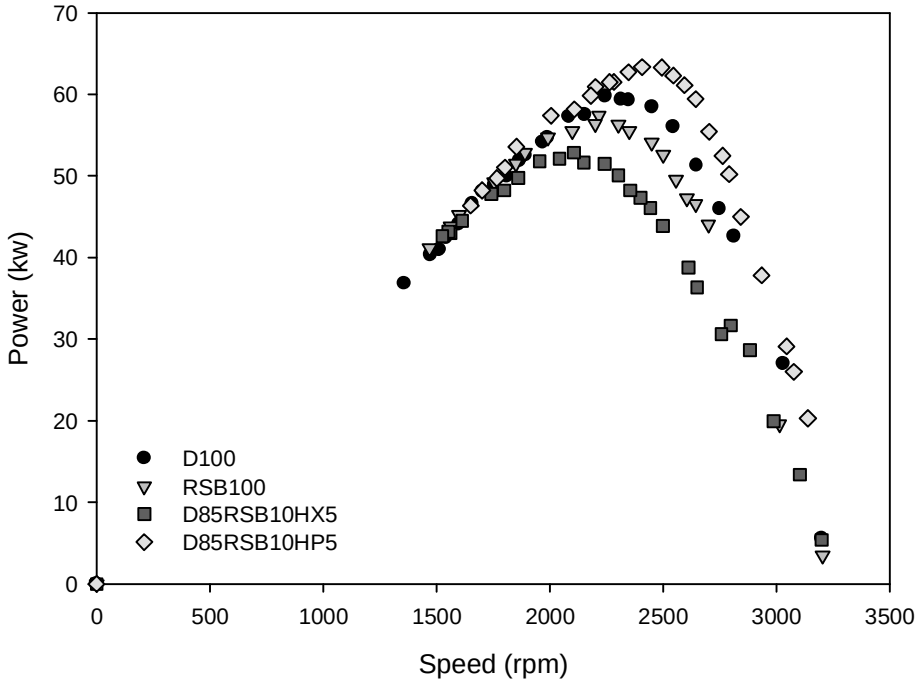


Figure 7.16. Power-Speed Graphic of 85%Diesel, 10%RSB and 5%Alkenes

The results were tabulated for pure diesel D100 in table 7.1, for pure rapeseed biodiesel RSB100 table 7.2, for the blend coded D85RSB10HX5 in table 7.3, and for the blend coded D85RSB10HP5 in table 7.18. The gained values, which were suitable for the engine power characteristic curve, were shown in the power versus speed graphic (Figure 7.16). The measured maximum power values were for the sample coded D100 59.774 kW at 2245 rpm, for the sample coded RSB100 57.355 kW at 2217 rpm, for the sample coded D85RSB10HX5 52.869 kW at 2106 rpm, for the sample coded D85RSB10HP5 63.337 kW at 2408 rpm respectively. For the sample coded D85RSB10HP5 maximum power inclination was 5.96%. At the speed of maximum torque the gained power values were for the sample coded D100 48.890 kW, for the sample coded RSB100 49.181 kW, for the sample coded D85RSB10HX5 44.478 kW and for the sample coded D85RSB10HP5 53.553 kW. At the maximum torque speed the best result was taken from the sample coded D85RSB10HP5 with an inclination of 9.53%.

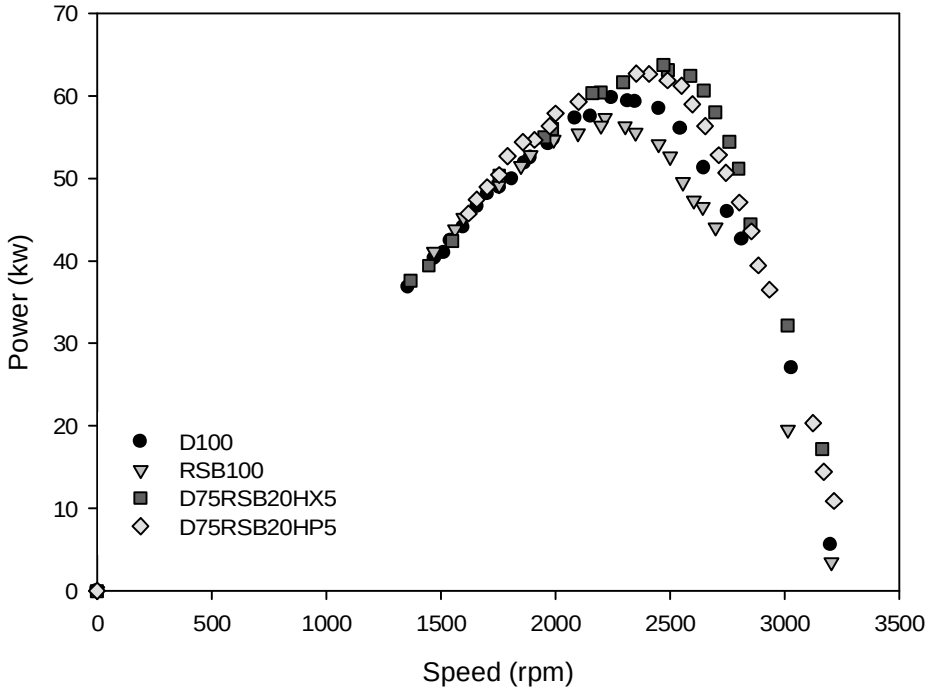


Figure 7.17. Power-Speed Graphic of 75%Diesel, 20%RSB and 5%Alkenes

The results were tabulated for pure diesel D100 in table 7.1, for pure rapeseed biodiesel RSB100 table 7.2, for the blend coded D75RSB20HX5 in table 7.4, and for the blend coded D75RSB20HP5 in table 7.19. The gained values, which were suitable for the engine power characteristic curve, were shown in the power versus speed graphic (Figure 7.17). The measured maximum power values were for the sample coded D100 59.774 kW at 2245 rpm, for the sample coded RSB100 57.355 kW at 2217 rpm, for the sample coded D75RSB20HX5 63.756 kW at 2471 rpm, for the sample coded D75RSB20HP5 62,695 kW at 2354 rpm respectively. For the sample coded D75RSB20HX5 maximum power inclination was 6.66%. At the speed of maximum torque the gained power values were for the sample coded D100 48.890 kW, for RSB100 49.181 kW, for D75RSB20HX5 56.011 kW and for the sample coded D75RSB20HP5 54.387 kW. At the maximum torque speed the best result was taken from D75RSB20HX5 with an increase of 14.56%.

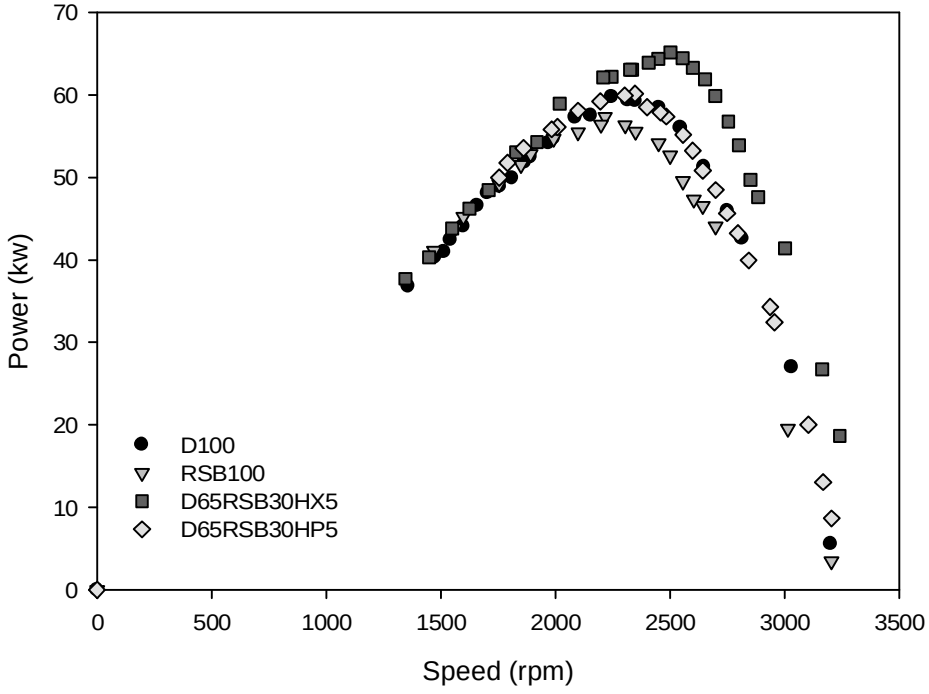


Figure 7.18. Power-Speed Graphic of 65%Diesel, 30%RSB and 5%Alkenes

The results were tabulated for pure diesel D100 in table 7.1, for pure rapeseed biodiesel RSB100 table 7.2, for the blend coded D65RSB30HX5 in table 7.5, and for

the blend coded D65RSB30HP5 in table 7.20. The gained values, which were suitable for the engine power characteristic curve, were shown in the power versus speed graphic (Figure 7.18). The measured maximum power values were for the sample coded D100 59.774 kW at 2245 rpm, for the sample coded RSB100 57.355 kW at 2217 rpm, for the sample coded D65RSB30HX5 65.130 kW at 2501 rpm, for the sample coded D65RSB30HP5 60.158 kW at 2348 rpm respectively. For the sample coded D65RSB30HX5 maximum power inclination was 8.96%. At the speed of maximum torque the gained power values were for the sample coded D100 48.890 kW, for the sample coded RSB100 49.181 kW, for the sample coded D65RSB30HX5 54.285 kW and for the sample coded D65RSB30HP5 51.767 kW. At the maximum torque speed the best result was taken from D85RSB10HP5 with an increase of 11.033%.

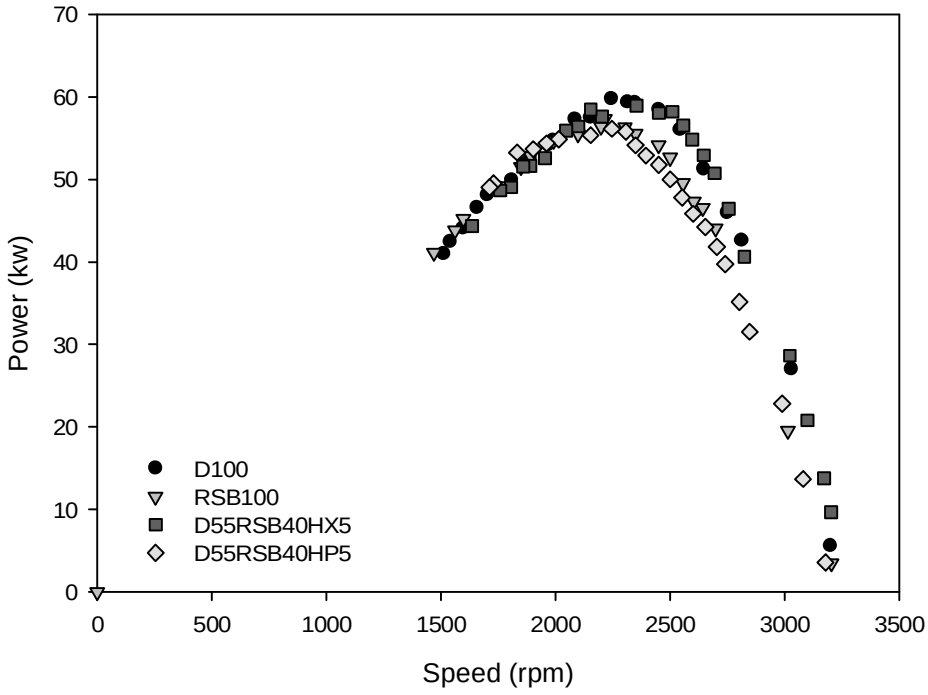


Figure 7.19. Power-Speed Graphic of 55%Diesel, 40%RSB and 5%Alkenes

The results were tabulated for pure diesel D100 in table 7.1, for pure rapeseed biodiesel RSB100 table 7.2, for the blend coded D55RSB40HX5 in table7.6, and for the blend coded D55RSB40HP5 in table 7.21. The gained values, which were suitable

for the engine power characteristic curve, were shown in the power versus speed graphic (Figure 7.19). The measured maximum power values were for the sample coded D100 59.774 kW at 2245 rpm, for the sample coded RSB100 57.355 kW at 2217 rpm, for the sample coded D55RSB40HX5 58.931 kW at 2353 rpm, for the sample coded D55RSB40HP5 56.137 kW at 2247 rpm respectively. For the sample coded D55RSB40HX5 maximum power inclination was 1.409%. At the speed of maximum torque the gained power values were for the sample coded D100 48.890 kW, for the sample coded RSB100 49.181 kW, for the sample coded D55RSB40HX5 49.050 kW and for the sample coded D55RSB40HP5 49.530 kW. At the maximum torque speed the best result was taken from D55RSB40HP5 with an increase of 1.309 %.

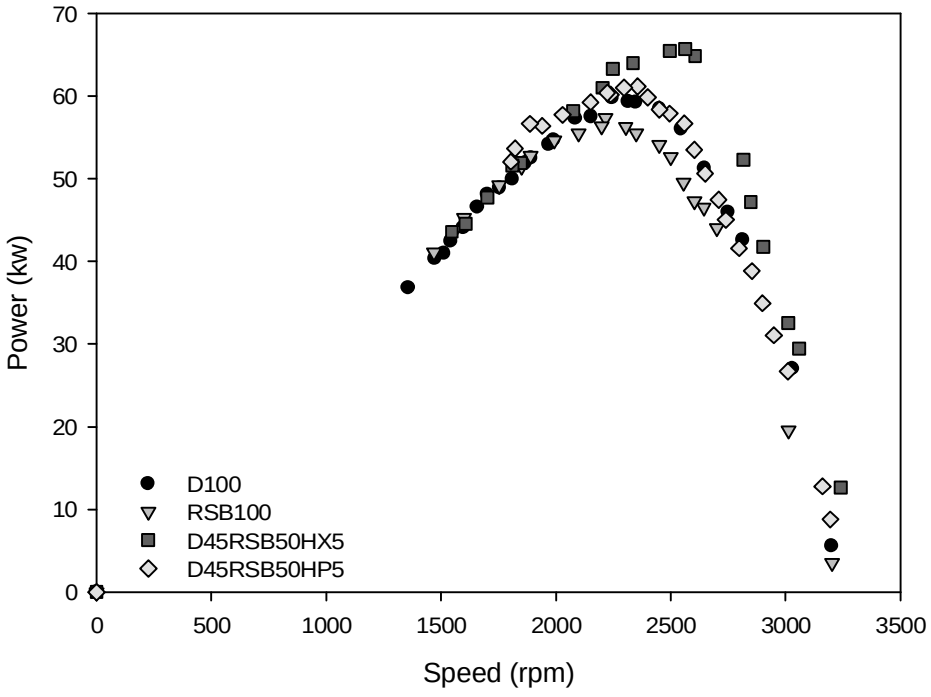


Figure 7.20. Power-Speed Graphic of 45%Diesel, 50%RSB and 5%Alkenes

The results were tabulated for pure diesel D100 in table7.1, for pure rapeseed biodiesel RSB100 table 7.2, for the blend coded D45RSB50HX5 in table 7.7, and for the blend coded D45RSB50HP5 in table 7.22. The gained values, which were suitable for the engine power characteristic curve, were shown in the power versus speed

graphic (Figure 7.20). The measured maximum power values were for the sample coded D100 59.774 kW at 2245 rpm, for the sample coded RSB100 57.355 kW at 2217 rpm for the sample coded D45RSB50HX5 65.73793 kW at 2563 rpm, for the sample coded D45RSB50HP5 61.19531 kW at 2357 rpm respectively. For the sample coded D45RSB50HX5 maximum power inclination was 9.98%. At the speed of maximum torque the gained power values were for the sample coded D100 48.890 kW, for the sample coded RSB100 49.181 kW, for the sample coded D45RSB50HX5 51.626 kW and for the sample coded D45RSB50HP5 53.645 kW. At the maximum torque speed the best result was taken from D45RSB50HP5 with an increase of 9.72%.

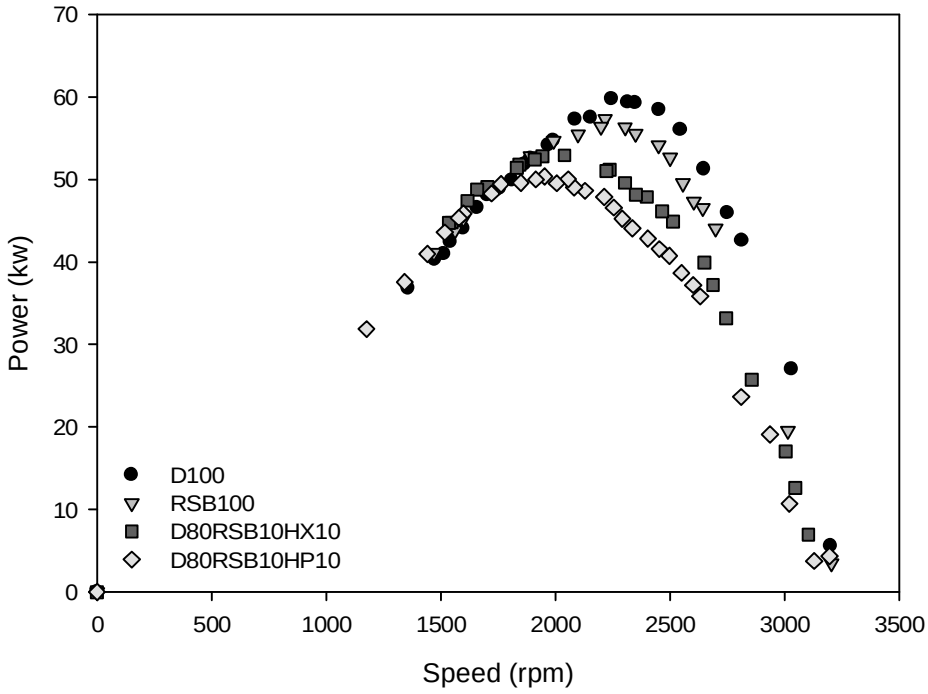


Figure 7.21. Power-Speed Graphic of 80%Diesel, 10%RSB and 10%Alkenes

The results were tabulated for pure diesel D100 in table 7.1, for pure rapeseed biodiesel RSB100 table 7.2, for the blend coded D80RSB10HX10 in table 7.8, and for the blend coded D80RSB10HP10 in table 7.23. The gained values, which were suitable for the engine power characteristic curve, were shown in the power versus speed graphic (Figure 7.21). The measured maximum power values were for the

sample coded D100 59.774 kW at 2245 rpm, for the sample coded RSB100 57.355 kW at 2217 rpm, for the sample coded D80RSB10HX10 52.917 kW at 2040 rpm, for the sample coded D80RSB10HP10 50.349 kW at 1953 rpm respectively. For the sample coded D80RSB10HX10 maximum power decline was 11.47%. At the speed of maximum torque the gained power values were for the sample coded D100 48.890 kW, for the sample coded RSB100 49.181 kW, for the sample coded D80RSB10HX10 44.781 kW and for the sample coded D80RSB10HP10 45.352 kW. At the maximum torque speed the best result was taken from the sample coded D80RSB10HX10 with a decrease of 3.02%.

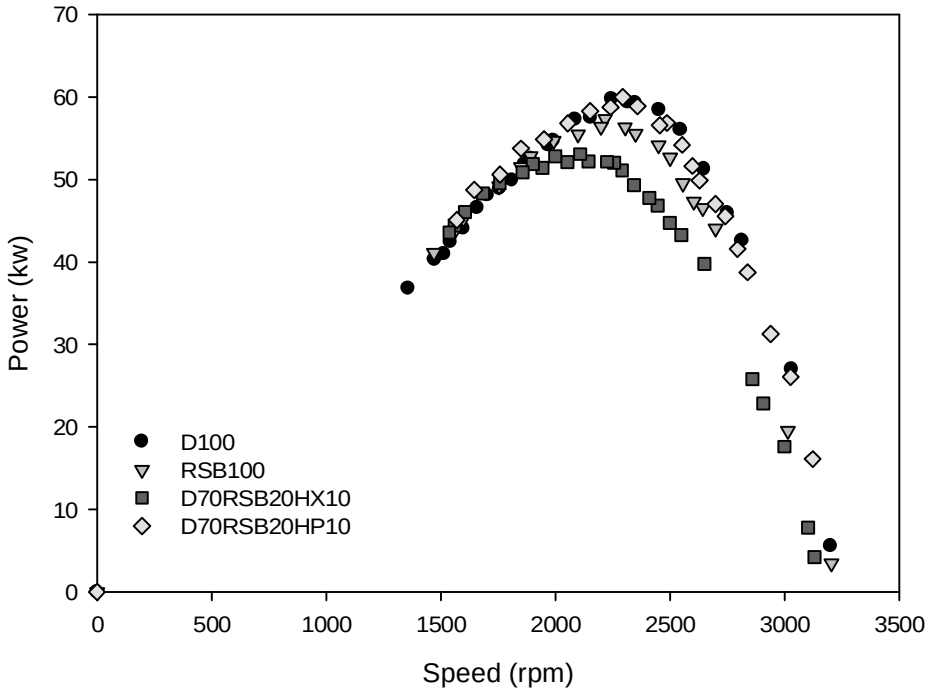


Figure 7.22. Power -Speed Graphic of 70%Diesel, 20%RSB and 10%Alkenes

The results were tabulated for pure diesel D100 in table 7.1, for pure rapeseed biodiesel RSB100 table 7.2, for the blend coded D70RSB20HX10 in table 7.9, and for the blend coded D70RSB20HP10 in table 7.24. The gained values, which were suitable for the engine power characteristic curve, were shown in the power versus speed graphic (Figure 7.22). The measured maximum power values were for the sample coded D100 59.774 kW at 2245 rpm, for the sample coded RSB100 57.355

kW at 2217 rpm, for the sample coded D70RSB20HX10 53.079 kW at 2109 rpm, for the sample coded D70RSB20HP10 59.974 kW at 2294 rpm respectively. For the sample coded D70RSB20HP10 maximum power inclination was 0.336 %. At the speed of maximum torque the gained power values were for the sample coded D100 48.890 kW, for the sample coded RSB100 49.181 kW, for the sample coded D70RSB20HX10 46.040 kW and for the sample coded D70RSB20HP10 50.582 kW. At the maximum torque speed the best result was taken from the sample coded D70RSB20HP10 with an increase of 3.46%.

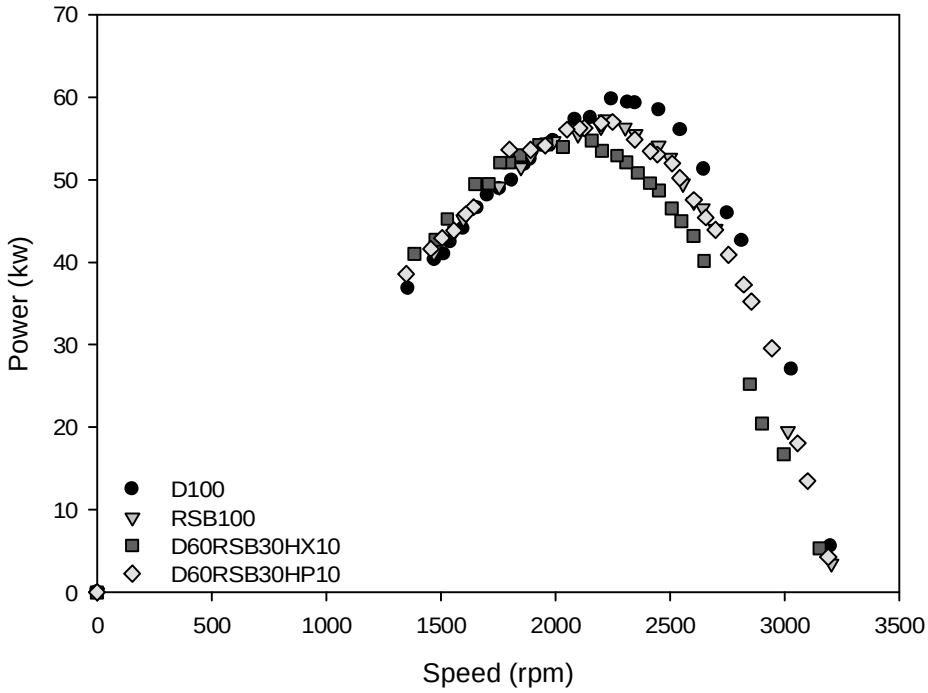


Figure 7.23. Power -Speed Graphic of 60%Diesel, 30%RSB and 10%Alkenes

The results were tabulated for pure diesel D100 in table 7.1, for pure rapeseed biodiesel RSB100 table 7.2, for the blend coded D60RSB30HX10 in table 7.10, and for the blend coded D60RSB30HP10 in table 7.25. The gained values, which were suitable for the engine power characteristic curve, were shown in the power versus speed graphic (Figure 7.23). The measured maximum power values were for the sample coded D100 59.774 kW at 2245 rpm, for the sample coded RSB100 57.355 kW at 2217 rpm for the sample coded D60RSB30HX10 54.784 kw at 2158 rpm, for

the sample coded D60RSB30HP10 57.017 kW at 2249 rpm respectively. For the sample coded D60RSB30HP10 maximum power decline was 4.61 %. At the speed of maximum torque, the gained power values were for the sample coded D100 48.890 kW, for the sample coded RSB100 49.181 kW, for the sample coded D60RSB30HX10 49.5 kW and for the sample coded D60RSB30HP10 53.658 kW. At the maximum torque speed the best result was taken from the sample coded D60RSB30HP10 with an increase of 9.75%.

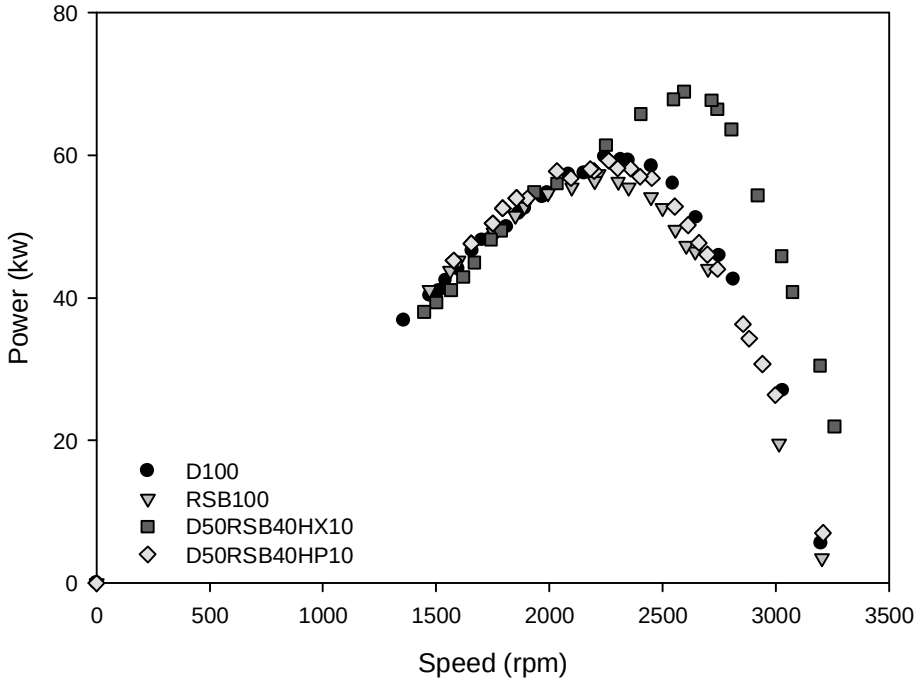


Figure 7.24. Torque-Speed Graphic of 50%Diesel, 40%RSB and 10%Alkenes

The results were tabulated for pure diesel D100 in table 7.1, for pure rapeseed biodiesel RSB100 table 7.2, for the blend coded D50RSB40HX10 in table 7.11, and for the blend coded D50RSB40HP10 in table 7.26. The gained values, which were suitable for the engine power characteristic curve, were shown in the power versus speed graphic (Figure 7.24). The measured maximum power values were for the sample coded D100 59.774 kW at 2245 rpm, for the sample coded RSB100 57.355 kW at 2217 rpm, for the sample coded D50RSB40HX10 68.922 kW at 2595 rpm, for the sample coded D50RSB40HP10 59.233 kW at 2263 rpm respectively. For the

sample coded D50RSB40HX10 maximum power inclination was 15.30%. At the speed of maximum torque the gained power values were for the sample coded D100 48.890 kW, for the sample coded RSB100 49.181 kW, for the sample coded D50RSB40HX10 56.064 kW and for the sample coded D50RSB40HP10 52.581 kW. At the maximum torque speed the best result was taken from the sample coded D50RSB40HX10 with an increase of 14.67%.

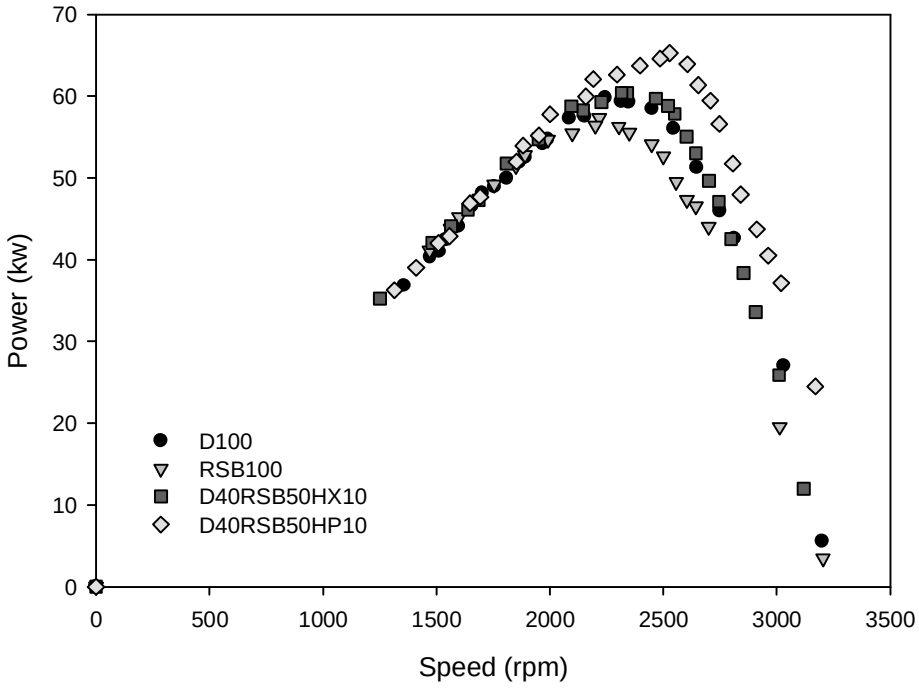


Figure 7.25. Power-Speed Graphic of 40%Diesel, 50%RSB and 10%Alkenes

The results were tabulated for pure diesel D100 in table 7.1, for pure rapeseed biodiesel RSB100 table 7.2, for the blend coded D40RSB50HX10 in table 7.12, and for the blend coded D40RSB50HP10 in table 7.27. The gained values, which were suitable for the engine power characteristic curve, were shown in the power versus speed graphic (Figure 7.25). The measured maximum power values were for the sample coded D100 59.774 kW at 2245 rpm, for the sample coded RSB100 57.355 kW at 2217 rpm for the sample coded D40RSB50HX10 60.433 kW at 2316 rpm, for the sample coded D40RSB50HP10 65.261 kW at 2528 rpm respectively. For the sample coded D40RSB50HP10 maximum power inclination was 9.18%. At the speed

of maximum torque the gained power values were for the sample coded D100 48.890 kW, for the sample coded RSB100 49.181 kW, for the sample coded D40RSB50HX10 58.767 kW and for the sample coded D40RSB50HP10 53.936 kW. At the maximum torque speed the best result was taken from the sample coded D40RSB50HX10 with an increase of 20.2%.

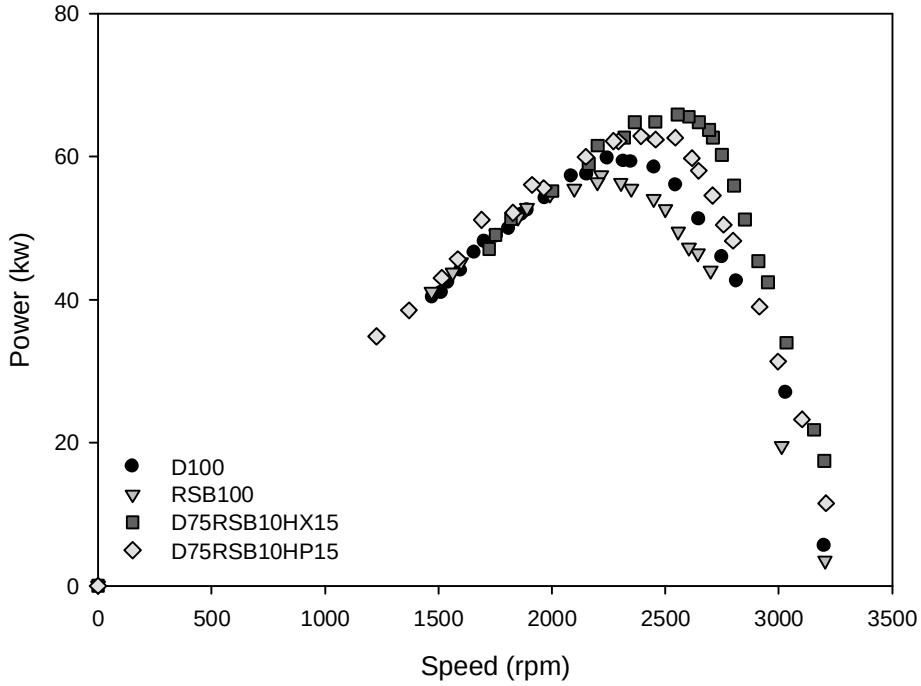


Figure 7.26. Power-Speed Graphic of 75%Diesel, 10%RSB and 15%Alkenes

The results were tabulated for pure diesel D100 in table 7.1, for pure rapeseed biodiesel RSB100 table 7.2, for the blend coded D75RSB10HX15 in table 7.13, and for the blend coded D75RSB10HP15 in table 7.28. The gained values, which were suitable for the engine power characteristic curve, were shown in the power versus speed graphic (Figure 7.26). The measured maximum power values were for the sample coded D100 59.774 kW at 2245 rpm, for the sample coded RSB100 57.355 kW at 2217 rpm for the sample coded D75RSB10HX15 65.886 kW at 2555 rpm, for the sample coded D75RSB10HP15 62.840 kW at 2544 rpm respectively. For the sample coded D75RSB10HX15 maximum power incline was 10.22%. At the speed of maximum torque the gained power values were for the sample coded D100 48.890

kW, for the sample coded RSB100 49.181 kW, for the sample coded D75RSB10HX15 51.283 kW and for the sample coded D75RSB10HP15 52.135 kW. At the maximum torque speed the best result was taken from the sample coded D75RSB10HP15 with an incline of 6.64%.

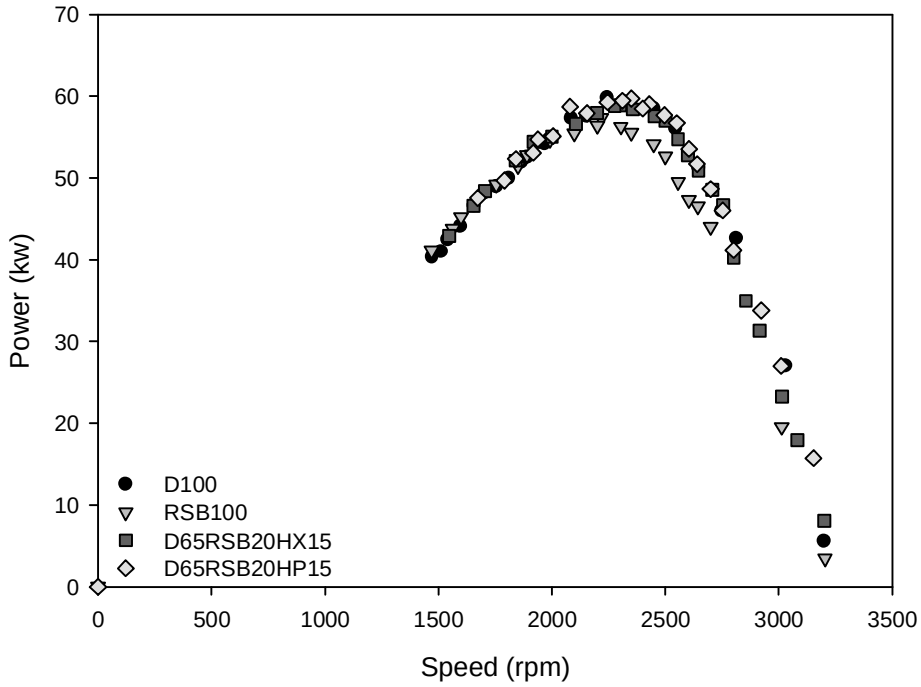


Figure 7.27. Power -Speed Graphic of 65%Diesel, 20%RSB and 15%Alkenes

The results were tabulated for pure diesel D100 in table 7.1, for pure rapeseed biodiesel RSB100 table 7.2, for the blend coded D65RSB20HX15 in table 7.14, and for the blend coded D65RSB20HP15 in table 7.29. The gained values, which were suitable for the engine power characteristic curve, were shown in the power versus speed graphic (Figure 7.27). The measured maximum power values were for the sample coded D100 59.774 kW at 2245 rpm, for the sample coded RSB100 57.355 kW at 2217 rpm, for the sample coded D65RSB20HX15 58.878 kW at 2301 rpm, for the sample coded D65RSB20HP15 59.71623kW at 2430 rpm respectively. the sample coded D65RSB20HP15 maximum power decline was 1.24%. At the speed of maximum torque the gained power values were for the sample coded D100 48.890 kW, for the sample coded RSB100 49.181 kW, for the sample coded

D65RSB20HX15 52.107 kW and for the sample coded D65RSB20HP15 53.087 kW. At the maximum torque speed the best result was taken from the sample coded D65RSB20HP15 with an increase of 8.58%.

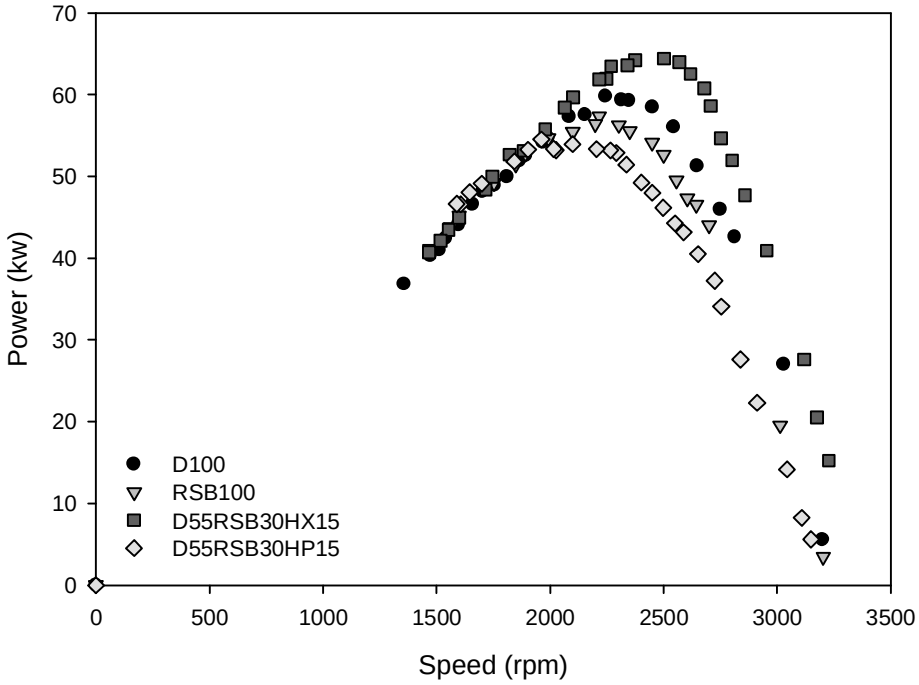


Figure 7.28. Power -Speed Graphic of 55%Diesel, 30%RSB and 15%Alkenes

The results were tabulated for pure diesel D100 in table 7.1, for pure rapeseed biodiesel RSB100 table 7.2, for the blend coded D55RSB30HX15 in table 7.15, and for the blend coded D55RSB30HP15 in table 7.30. The gained values, which were suitable for the engine power characteristic curve, were shown in the power versus speed graphic (Figure 7.28). The measured maximum power values were for the sample coded D100 59.77372 kW at 2245 rpm, for the sample coded RSB 57.35 kW at 2217 rpm, for the sample coded D55RSB30HX15 64.411 kW at 2502 rpm, for the sample coded D55RSB30HP15 53.937kW at 2100 rpm respectively. For the sample coded D55RSB30HX15 maximum power incline was 7.76%. At the speed of maximum torque the gained power values were for the sample coded D100 48.890 kW, for the sample coded RSB100 49.181 kW, for the sample coded D55RSB30HX15 52.668 kW and for the sample coded D55RSB30HP15 46.58678

kW. At the maximum torque speed the best result was taken from the sample coded D55RSB30HX15 with an incline of 7.73 %.

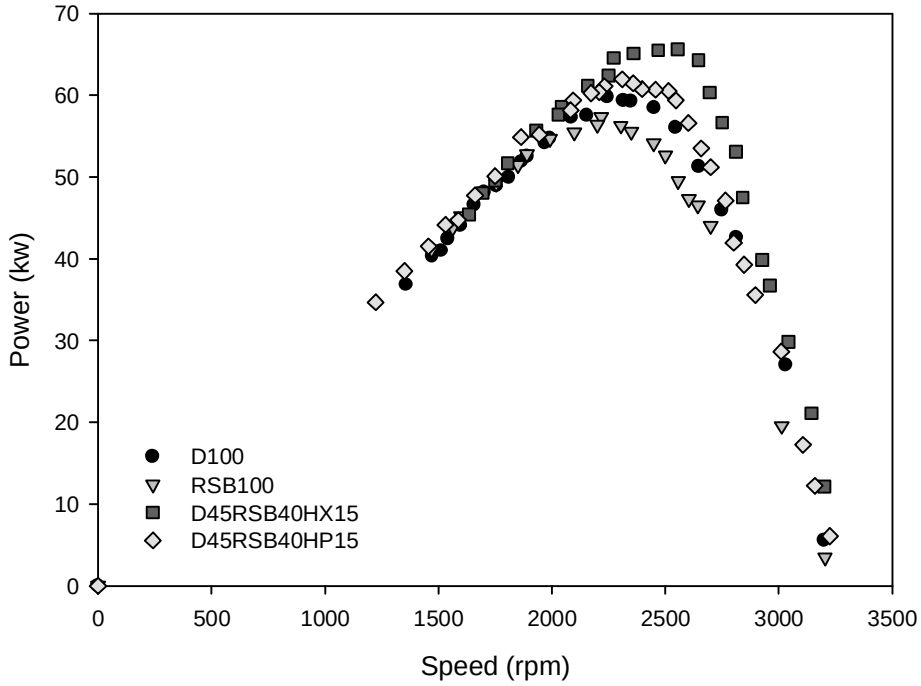


Figure 7.29. Power -Speed Graphic of 45%Diesel, 40%RSB and 15%Alkenes

The results were tabulated for pure diesel D100 in table 7.1, for pure rapeseed biodiesel RSB100 table 7.2, for the blend coded D45RSB40HX15 in table 7.16, and for the blend coded D45RSB40HP15 in table 7.31. The gained values, which were suitable for the engine power characteristic curve, were shown in the power versus speed graphic (Figure 7.29). The measured maximum power values were for the sample coded D100 59.774 kW at 2245 rpm, for the sample coded RSB100 57.355 kW at 2217 rpm for the sample coded D45RSB40HX15 65.631 kW at 2555 rpm, for the sample coded D45RSB40HP15 61.976 kW at 2359 rpm respectively. For the sample coded D45RSB40HX15 maximum power incline was 9.8%. At the speed of maximum torque the gained power values were for the sample coded D100 48.890 kW, for the sample coded RSB100 49.181 kW, for the sample coded D45RSB40HX15 55.676 kW and for the sample coded D45RSB40HP15 54.873 kW.

At the maximum torque speed the best result was taken from the sample coded D45RSB40HX15 with an increase of 13.88 %.

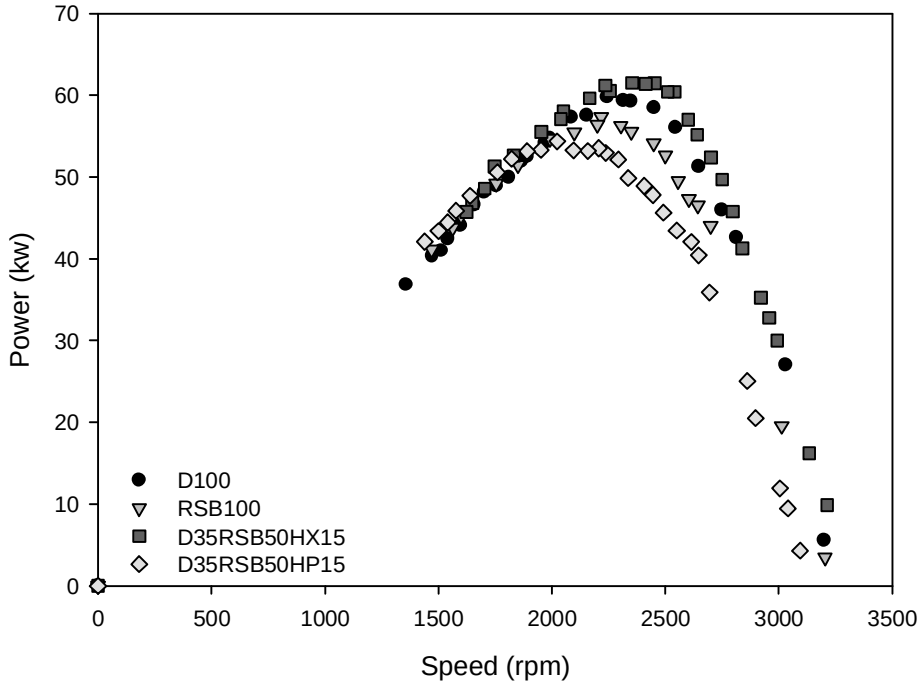


Figure 7.30. Power-Speed Graphic of 35%Diesel, 50%RSB and 15%Alkenes

The results were tabulated for pure diesel D100 in table 7.1, for pure rapeseed biodiesel RSB100 table 7.2, for the blend coded D35RSB50HX15 in table 7.17, and for the blend coded D35RSB50HP15 in table 7.32. The gained values, which were suitable for the engine power characteristic curve, were shown in the power versus speed graphic (Figure 7.30). The measured maximum power values were for the sample coded D100 59.774 kW at 2245 rpm, for the sample coded RSB100 57.355 kW at 2217 rpm for the sample coded D35RSB50HX15 61.515 kW at 2354 rpm, for the sample coded D35RSB50HP15 54.357 kW at 2024 rpm respectively. For the sample coded D35RSB50HX15 maximum power incline was 2.91%. At the speed of maximum torque the gained power values were for the sample coded D100 48.890 kW, for the sample coded RSB100 49.181 kW, for the sample coded D35RSB50HX15 51.274 kW and for the sample coded D35RSB50HP15 50.569 kW.

At the maximum torque speed the best result was taken from the sample coded D35RSB50HX15 with an incline of 4.43%.

7.3. Specific Fuel Consumption versus Speed

Specific Fuel Consumption (SFC) measures the amount of fuel needed to provide a given power for a given period. Most of the SFC values of blends were higher than biodiesel because the densities of blends were lower than biodiesel and the specific fuel consumption increases as density decreases.

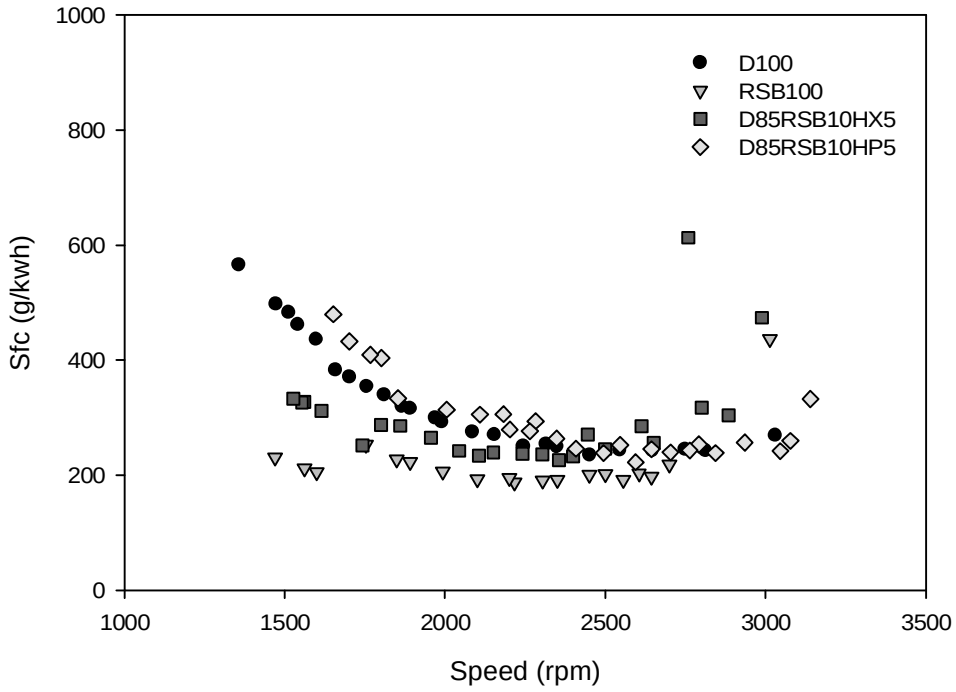


Figure 7.31. Specific Fuel Consumption-Speed Graphic of 85%Diesel, 10%RSB and 5%Alkenes

The results were tabulated for pure diesel D100 in table 7.1, for pure rapeseed biodiesel RSB100 table 7.2, for the blend coded D85RSB10HX5 in table 7.3, and for the blend coded D85RSB10HP5 in table 7.18. The gained values were shown in the Specific Fuel Consumption (SFC) versus speed graphic (Figure 7.31). The measured minimum SFC values were for the sample coded D100 234.957 g/kWh at 2452 rpm, for the sample coded RSB100 186.919 g/kWh at 2217 rpm, for the sample coded D85RSB10HX5 226.444 g/kWh at 2355 rpm and for the sample coded

D85RSB10HP5 222.685 g/kWh at 2595 rpm respectively. A decrease of 5.22 % was observed in the sample coded D85RSB10HP5.

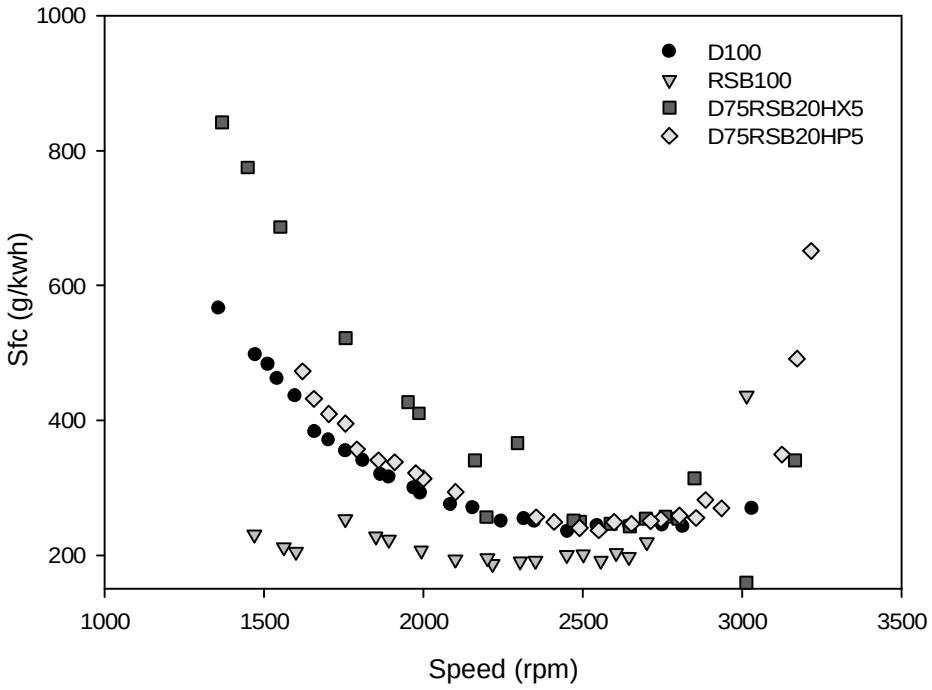


Figure 7.32. Specific Fuel Consumption-Speed Graphic of 75%Diesel, 20%RSB and 5%Alkenes

The results were tabulated for pure diesel D100 in table 7.1, for pure rapeseed biodiesel RSB100 table 7.2, for the blend coded D75RSB20HX5 in table 7.4, and for the blend coded D75RSB20HP5 in table 7.19. The gained values were shown in the Specific Fuel Consumption versus speed graphic (Figure 7.32). The measured minimum SFC values were for the sample coded D100 234.957 g/kWh at 2452 rpm, for the sample coded RSB100 186.919 g/kWh at 2217 rpm, for the sample coded D75RSB20HX5 242.933 g/kWh at 2648 rpm and for the sample coded D75RSB20HP5 237.009 g/kWh at 2550 rpm respectively. The minimum increase was observed for the sample coded D75RSB20HX5 as 3.35% nevertheless maximum increase was observed for the sample coded D75RSB20HP5 as 0.87%.

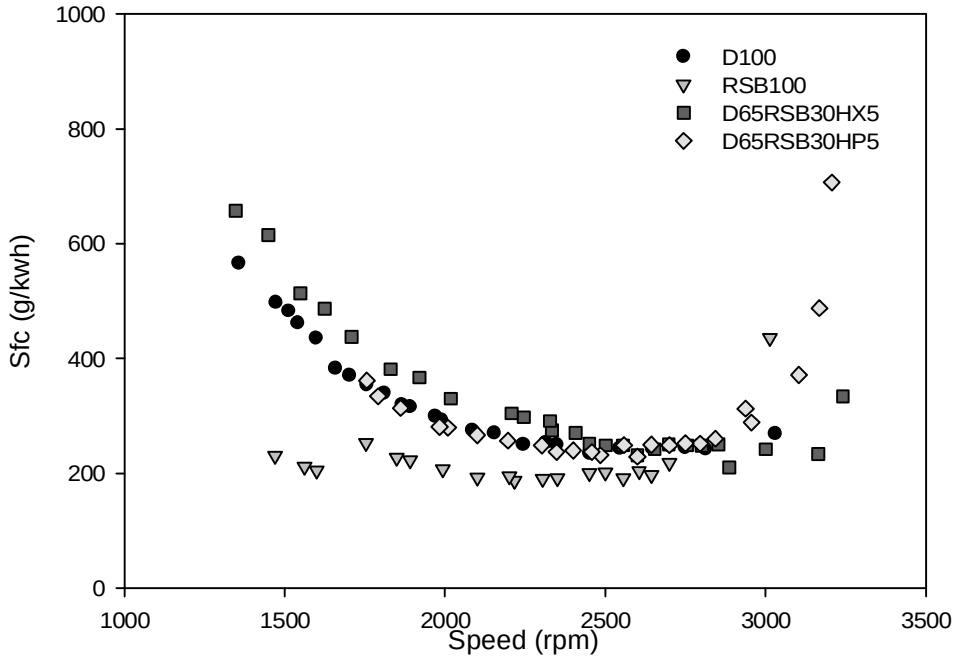


Figure 7.33. Specific Fuel Consumption-Speed Graphic of 65%Diesel, 30%RSB and 5%Alkenes

The results were tabulated for pure diesel D100 in table 7.1, for pure rapeseed biodiesel RSB100 table 7.2, for the blend coded D65RSB30HX5 in table 7.5, and for the blend coded D65RSB30HP5 in table 7.20. The gained values were shown in the Specific Fuel Consumption versus speed graphic (Figure 7.33). The measured minimum SFC values were for the sample coded D100 234.957 g/kWh at 2452 rpm, for the sample coded RSB100 186.919 g/kWh at 2217 rpm, for the sample coded D65RSB30HX5 210.335 g/kWh at 2886 rpm and for the sample coded D65RSB30HP5 229.158 g/kWh at 2600 rpm respectively. The maximum decrease was observed in the sample coded D65RSB30HX5 as 10.48 %.

The results were tabulated for pure diesel D100 in table 7.1, for pure rapeseed biodiesel RSB100 table 7.2, for the blend coded D55RSB40HX5 in table7.6, and for the blend coded D55RSB40HP5 in table 7.21. The gained values were shown in the Specific Fuel Consumption versus speed graphic (Figure 7.34). The measured minimum SFC values were for the sample coded D100 234.957 g/kWh at 2452 rpm, for the sample coded RSB100 186.919 g/kWh at 2217 rpm, for the sample coded D55RSB40HX5 233.956 g/kWh at 2756 rpm and for the sample coded

D55RSB40HP5 229.980 g/kWh at 2396 rpm respectively. The maximum decrease was observed the sample coded D55RSB40HP5 as 2.12%.

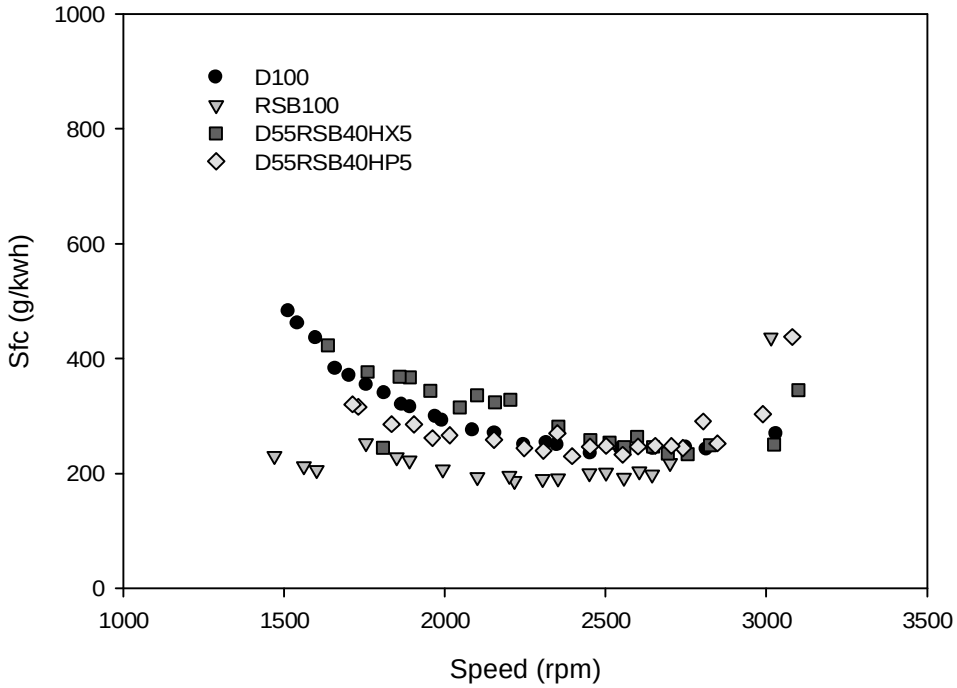


Figure 7.34. Specific Fuel Consumption-Speed Graphic of 55%Diesel, 40%RSB and 5%Alkenes

The results were tabulated for pure diesel D100 in table7.1, for pure rapeseed biodiesel RSB100 table 7.2, for the blend coded D45RSB50HX5 in table 7.7, and for the blend coded D45RSB50HP5 in table 7.22. The gained values were shown in the Specific Fuel Consumption versus speed graphic (Figure 7.35). The measured minimum SFC values were for the sample coded D100 234.957 g/kWh at 2452 rpm, for the sample coded RSB100 186.919 g/kWh at 2217 rpm, for the sample coded D45RSB50HX5 214.401 g/kWh at 2903 rpm and for the sample coded D45RSB50HP5 246.33 g/kWh at 2401 rpm respectively. The maximum decrease was observed in the sample coded D45RSB50HX5 as 8.75 %. Nevertheless, maximum increase was observed the sample coded D45RSB50HP5 as 4.84 %.

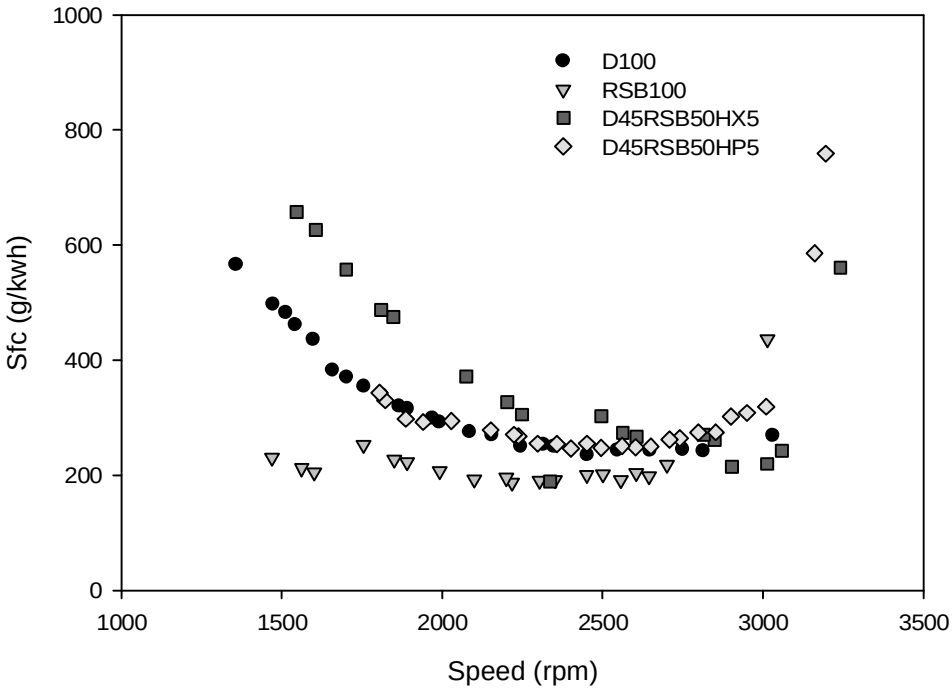


Figure 7.35. Specific Fuel Consumption-Speed Graphic of 45%Diesel, 50%RSB and 5%Alkenes

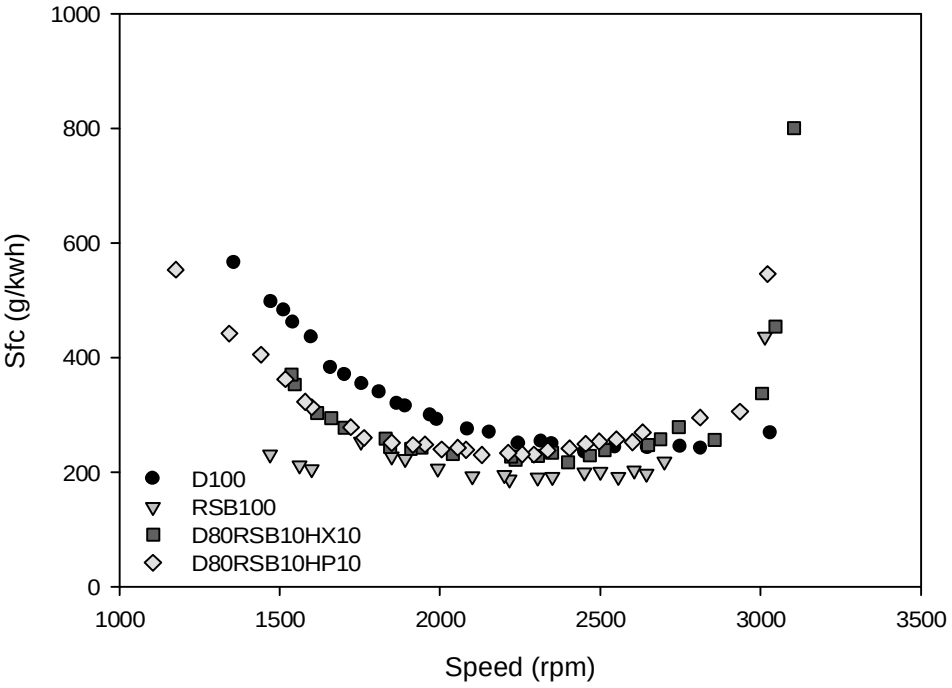


Figure 7.36. Specific Fuel Consumption-Speed Graphic of 80%Diesel, 10%RSB and 10%Alkenes

The results were tabulated for pure diesel D100 in table 7.1, for pure rapeseed biodiesel RSB100 table 7.2, for the blend coded D80RSB10HX10 in table 7.8, and for the blend coded D80RSB10HP10 in table 7.23. The gained values were shown in the Specific Fuel Consumption versus speed graphic (Figure 7.36). The measured minimum SFC values were for the sample coded D100 234.957 g/kWh at 2452 rpm, for the sample coded RSB100 186.919 g/kWh at 2217 rpm, for the sample coded D80RSB10HX10 217.505 g/kWh at 2399 rpm and for the sample coded D80RSB10HP10 231.026 g/kWh at 2293 rpm respectively. The maximum decrease was observed in the sample coded D80RSB10HX10 7.43%.

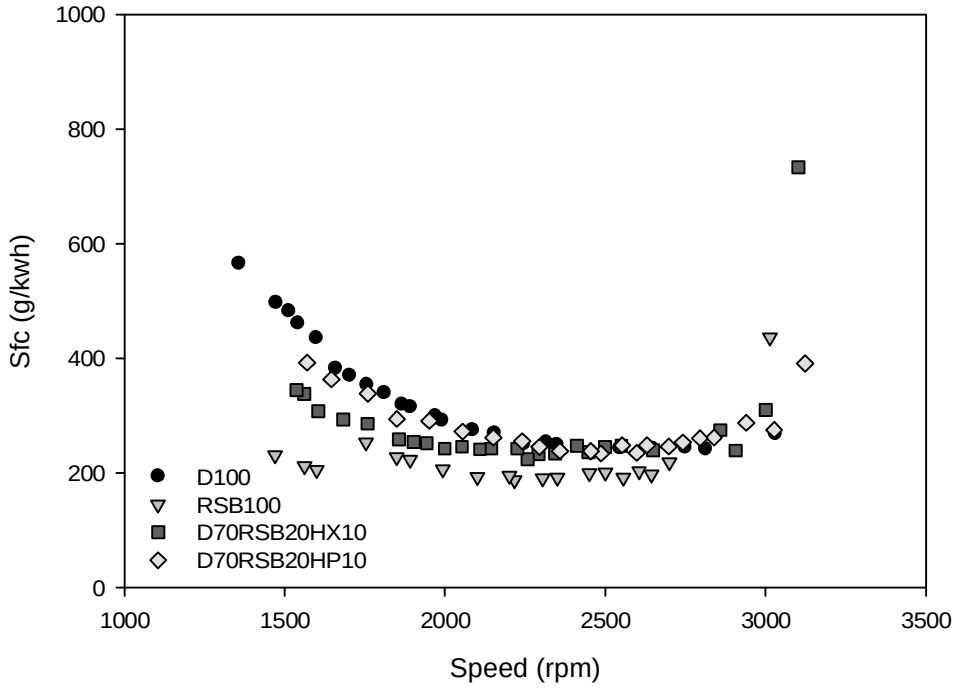


Figure 7.37. Specific Fuel Consumption-Speed Graphic of 70%Diesel, 20%RSB and 10%Alkenes

The results were tabulated for pure diesel D100 in table 7.1, for pure rapeseed biodiesel RSB100 table 7.2, for the blend coded D70RSB20HX10 in table 7.9, and for the blend coded D70RSB20HP10 in table 7.24. The gained values were shown in the Specific Fuel Consumption versus speed graphic (Figure 7.37). The measured minimum SFC values were for the sample coded D100 234.957 g/kWh at 2452 rpm,

for the sample coded RSB100 186.919 g/kWh at 2217 rpm, for the sample coded D70RSB20HX10 224.156 g/kWh at 2257 rpm and for the sample coded D70RSB20HP10 233.957 g/kWh at 2487 rpm respectively. The maximum decrease was observed in the sample coded D70RSB20HX10 as 4.59 %.

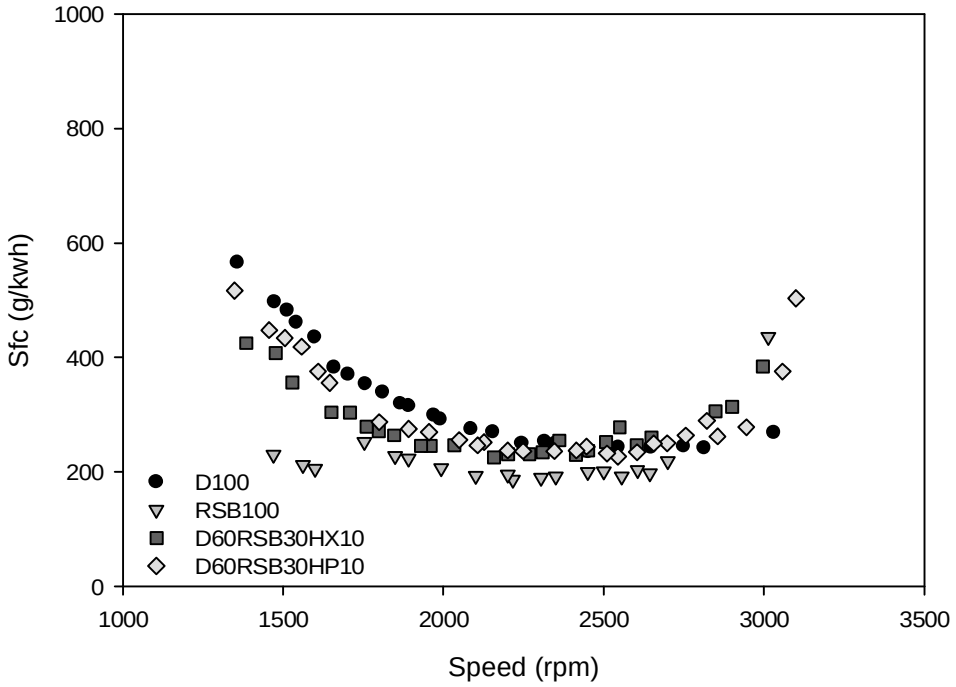


Figure 7.38. Specific Fuel Consumption-Speed Graphic of 60%Diesel, 30%RSB and 10%Alkenes

The results were tabulated for pure diesel D100 in table 7.1, for pure rapeseed biodiesel RSB100 table 7.2, for the blend coded D60RSB30HX10 in table 7.10, and for the blend coded D60RSB30HP10 in table 7.25. The gained values were shown in the Specific Fuel Consumption versus speed graphic (Figure 7.38). The measured minimum SFC values were for the sample coded D100 234.957 g/kWh at 2452 rpm, for the sample coded RSB100 186.919 g/kWh at 2217 rpm, for the sample coded D60RSB30HX10 226.018 g/kWh at 2158 rpm and for the sample coded D60RSB30HP10 227.223 g/kWh at 2544 rpm respectively. The maximum decrease was observed in the sample coded D60RSB30HX10 as 3.8%.

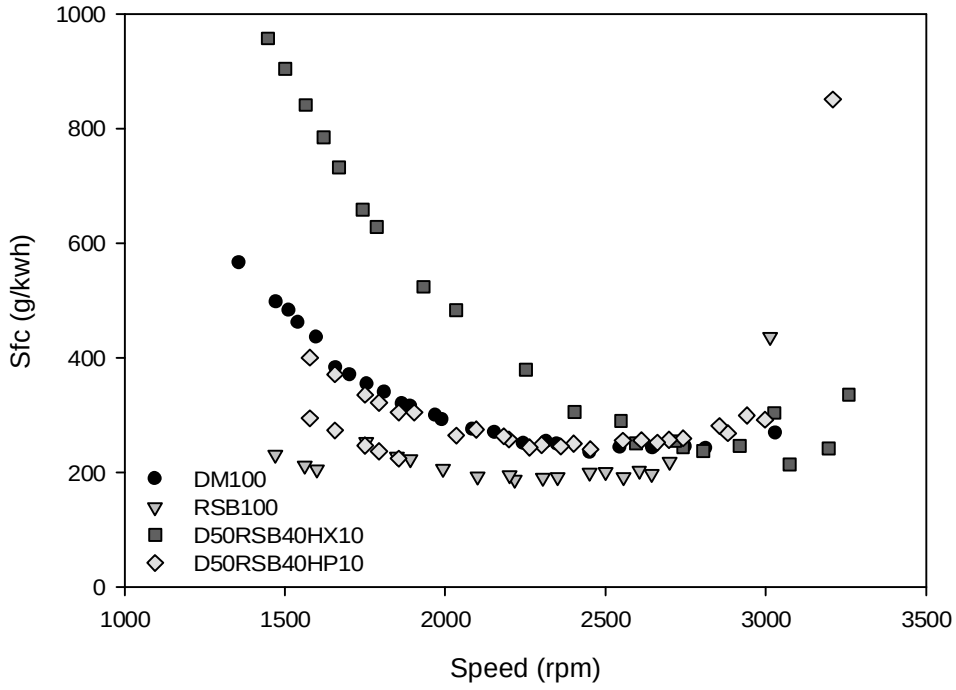


Figure 7.39. Specific Fuel Consumption-Speed Graphic of 50%Diesel, 40%RSB and 5%Alkenes

The results were tabulated for pure diesel D100 in table 7.1, for pure rapeseed biodiesel RSB100 table 7.2, for the blend coded D50RSB40HX10 in table 7.11, and for the blend coded D50RSB40HP10 in table 7.26. The gained values were shown in in the Specific Fuel Consumption versus speed graphic (Figure 7.39). The measured minimum SFC values were for the sample coded D100 234.957 g/kWh at 2452 rpm, for the sample coded RSB100 186.919 g/kWh at 2217 rpm, for the sample coded D50RSB40HX10 237.400 g/kWh at 2805 rpm and for the sample coded D50RSB40HP10 241.013 g/kWh at 2453 rpm respectively. The minimum increase in minimum SFC results was observed in the sample coded D50RSB40HX10 as 1.04 % nevertheless maximum increase in minimum SFC was observed in the sample coded D50RSB40HP10 as 2.58 %.

The results were tabulated for pure diesel D100 in table 7.1, for pure rapeseed biodiesel RSB100 table 7.2, for the blend coded D40RSB50HX10 in table 7.12, and for the blend coded D40RSB50HP10 in table 7.27. The gained values were shown in the Specific Fuel Consumption versus speed graphic (Figure 7.40). The measured

minimum SFC values were for the sample coded D100 234.957 g/kWh at 2452 rpm, for the sample coded RSB100 186.919 g/kWh at 2217 rpm, for the sample coded D40RSB50HX10 237.480 g/kWh at 2551 rpm and for the sample coded D40RSB50HP10 243.690 g/kWh at 2606 rpm respectively. The maximum increase in minimum SFC result was observed in the sample coded D40RSB50HP10 as 3.72%.

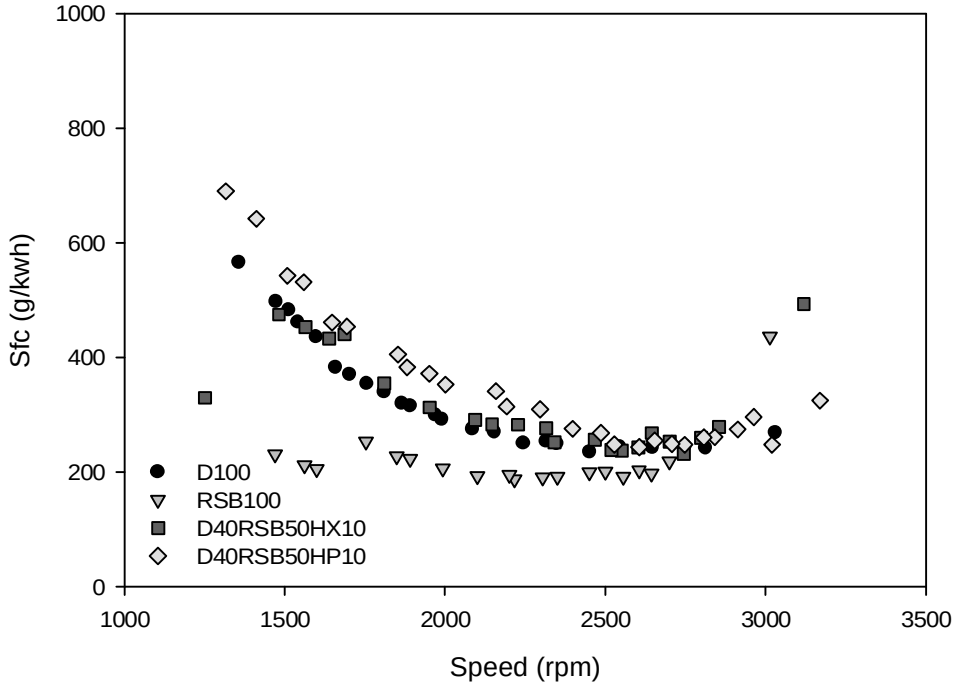


Figure 7.40. Specific Fuel Consumption-Speed Graphic of 40%Diesel, 50%RSB and 10%Alkenes

The results were tabulated for pure diesel D100 in table 7.1, for pure rapeseed biodiesel RSB100 table 7.2, for the blend coded D75RSB10HX15 in table 7.13, and for the blend coded D75RSB10HP15 in table 7.28. The gained values were shown in the Specific Fuel Consumption versus speed graphic (Figure 7.41). The measured minimum SFC values were for the sample coded D100 234.957 g/kWh at 2452 rpm, for the sample coded RSB100 186.919 g/kWh at 2217 rpm, for the sample coded D75RSB10HX15 201.344 g/kWh at 2911 rpm and for the sample coded D75RSB10HP15 242.271 g/kWh at 2618 rpm respectively. The maximum decrease in minimum SFC was observed in the sample coded D75RSB10HX15 14.31 %.

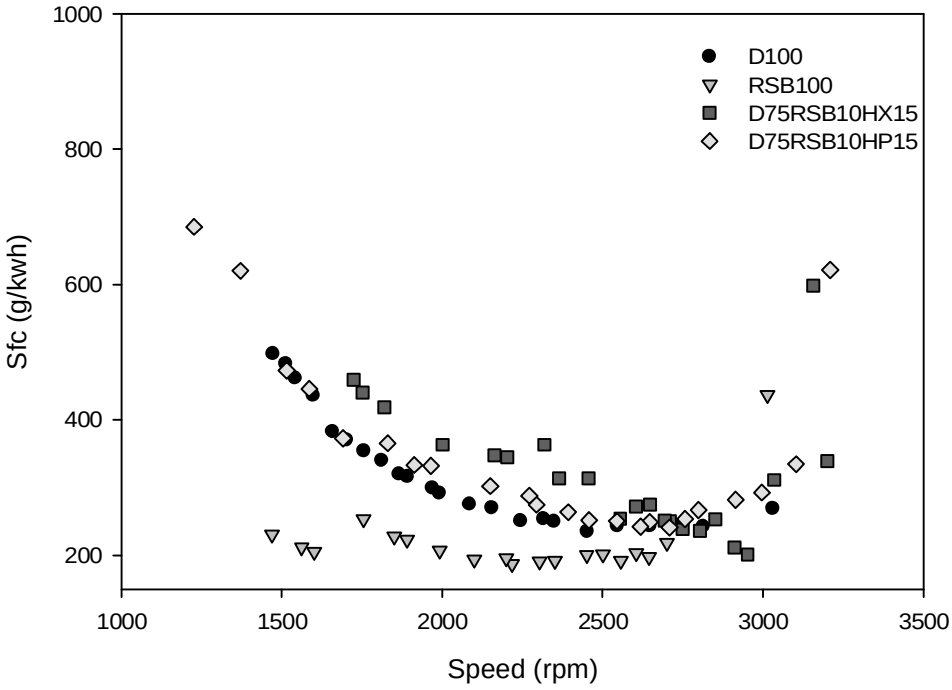


Figure 7.41. Specific Fuel Consumption-Speed Graphic of 75%Diesel, 10%RSB and 15%Alkenes

The results were tabulated for pure diesel D100 in table 7.1, for pure rapeseed biodiesel RSB100 table 7.2, for the blend coded D65RSB20HX15 in table 7.14, and for the blend coded D65RSB20HP15 in table 7.29. The gained values were shown in in the Specific Fuel Consumption versus speed graphic (Figure 7.42). The measured minimum SFC values were for the sample coded D100 234.957 g/kWh at 2452 rpm, for the sample coded RSB100 186.919 g/kWh at 2217 rpm, for the sample coded D65RSB20HX15 164.737 g/kWh at 2855 rpm and for the sample coded D65RSB20HP15 227.863 g/kWh at 2551 rpm respectively. The maximum decrease was observed in the sample coded D65RSB20HX15 as 29.89%.

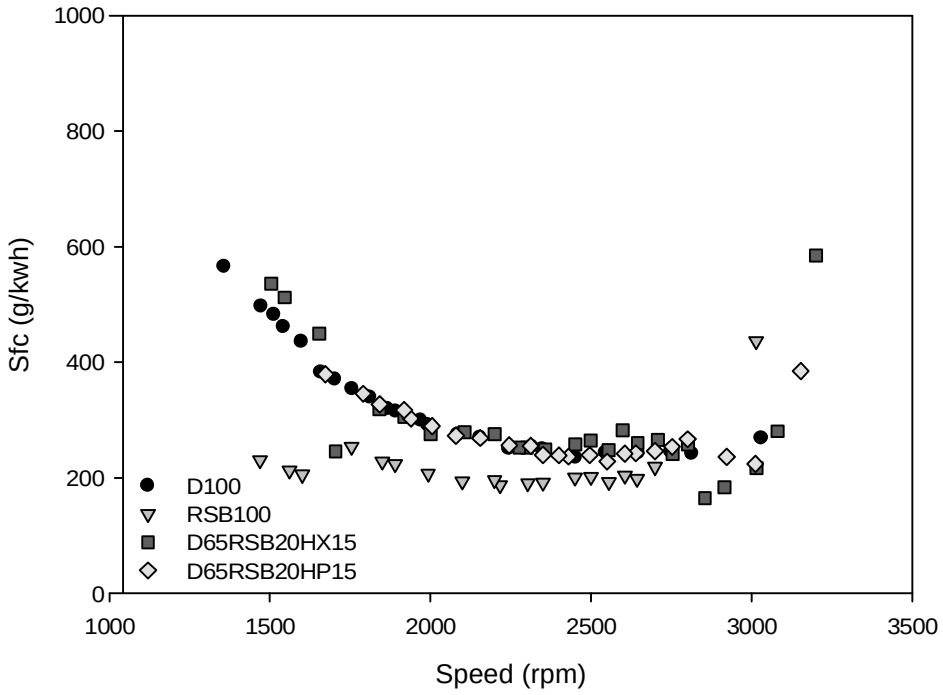


Figure 7.42. Specific Fuel Consumption-Speed Graphic of 65%Diesel, 20%RSB and 15%Alkenes

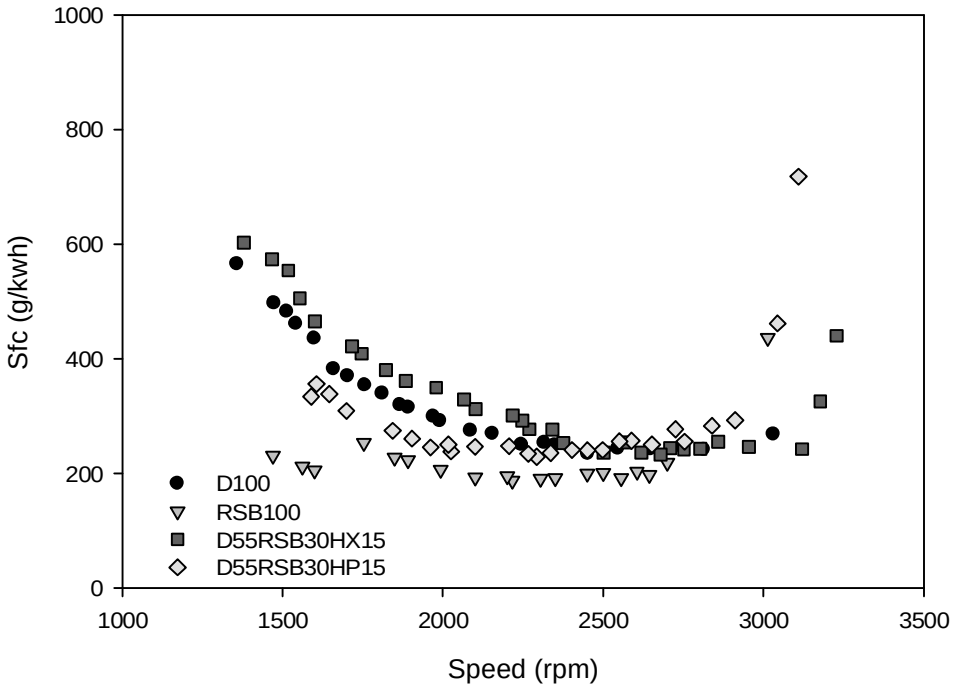


Figure 7.43. Specific Fuel Consumption-Speed Graphic of 55%Diesel, 40%RSB and 15%Alkenes

The results were tabulated for pure diesel D100 in table 7.1, for pure rapeseed biodiesel RSB100 table 7.2, for the blend coded D55RSB30HX15 in table 7.15, and for the blend coded D55RSB30HP15 in table 7.30. The gained values were shown in the Specific Fuel Consumption versus speed graphic (Figure 7.43). The measured minimum SFC values were for the sample coded D100 234.957 g/kWh at 2452 rpm, for the sample coded RSB100 186.919 g/kWh at 2217 rpm, for the sample coded D55RSB30HX15 233.179 g/kWh at 2355 rpm and for the sample coded D55RSB30HP15 229.358 g/kWh at 2292 rpm respectively. The maximum decrease was observed in the sample coded D55RSB30HP15 as 2.38%.

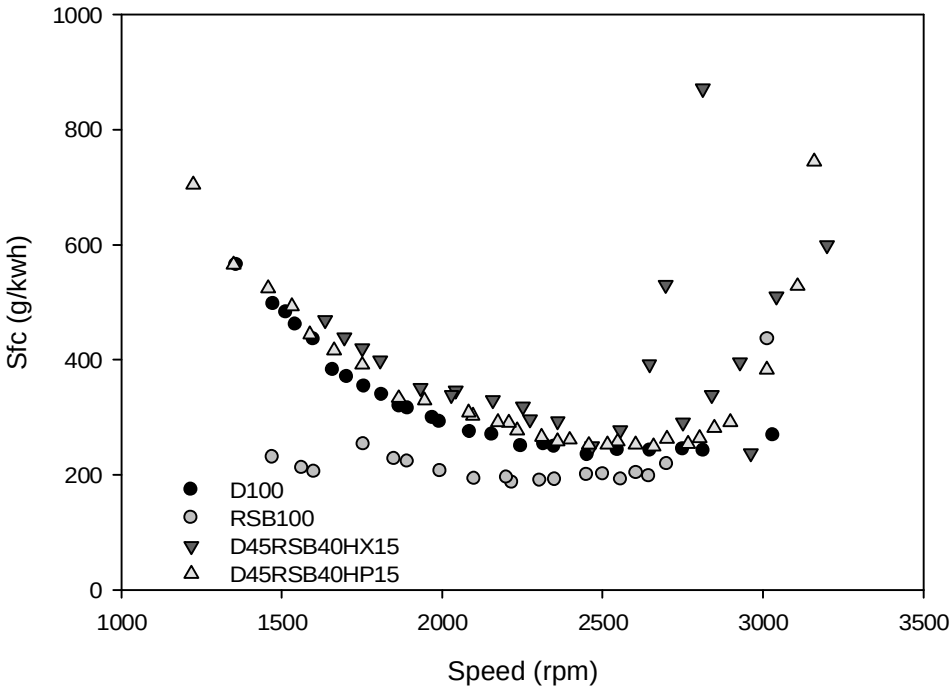


Figure 7.44. Specific Fuel Consumption -Speed Graphic of 45%Diesel, 40%RSB and 15%Alkenes

The results were tabulated for pure diesel D100 in table 7.1, for pure rapeseed biodiesel RSB100 table 7.2, for the blend coded D45RSB40HX15 in table 7.16, and for the blend coded D45RSB40HP15 in table 7.31. The gained values were shown in the Specific Fuel Consumption versus speed graphic (Figure 7.44). The measured minimum SFC values were for the sample coded D100 234.957 g/kWh at 2452 rpm, for the sample coded RSB100 186.919 g/kWh at 2217 rpm, for the sample coded

D45RSB40HX15 249.957 g/kWh at 2468 rpm and for the sample coded D45RSB40HP15 251.914 g/kWh at 2457 rpm respectively. The maximum increase was observed in the sample coded D45RSB40HP15 as 7.22%.

The results were tabulated for pure diesel D100 in table 7.1, for pure rapeseed biodiesel RSB100 table 7.2, for the blend coded D35RSB50HX15 in table 7.17, and for the blend coded D35RSB50HP15 in table 7.32. The gained values were shown in the Specific Fuel Consumption versus speed graphic (Figure 7.45). The measured minimum SFC values were for the sample coded D100 234.957 g/kWh at 2452 rpm, for the sample coded RSB100 186.919 g/kWh at 2217 rpm, for the sample coded D35RSB50HX15 214.894 g/kWh at 2958 rpm and for the sample coded D35RSB50HP15 230.282 g/kWh at 2207 rpm respectively. The maximum decrease was observed in the sample coded D35RSB50HX15 as 8.54%.

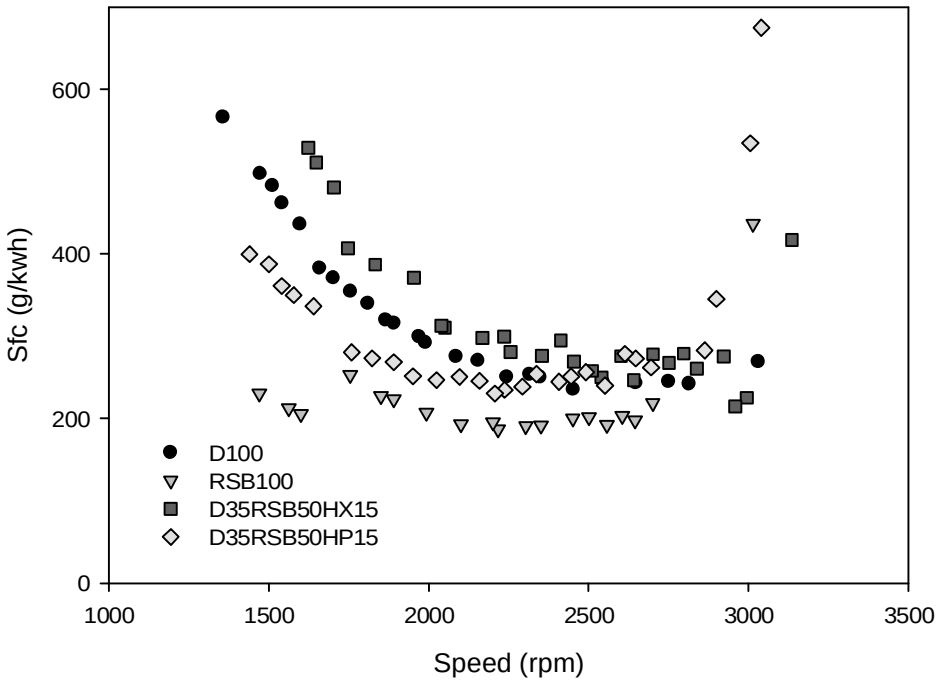


Figure 7.45. Specific Fuel Consumption-Speed Graphic of 35%Diesel, 50%RSB and 15%Alkenes

7.4. CO Emission

Carbon monoxide (CO) is produced from incomplete combustion. Most of the CO emission was turned to CO_2 during and after expansion period. The exhaust gas analyzer equipment which was used during tests lasted measuring before the test ends because of the dense emission. Therefore some of the samples emissions could not measured. The reason for the dense emission was the blended alkenes.

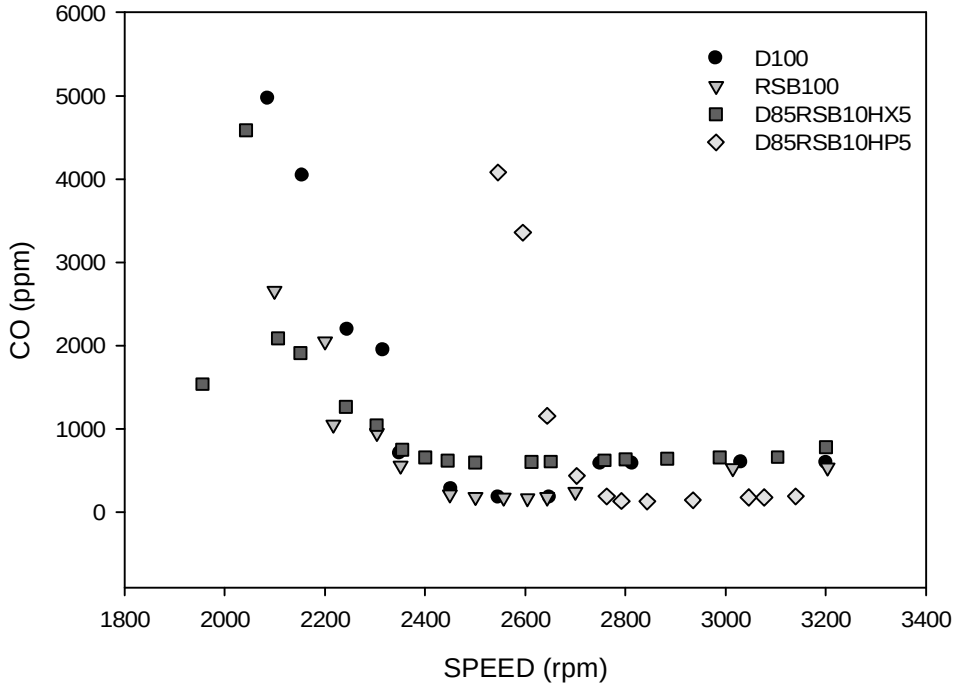


Figure 7.46. CO-Speed Graphic of 85%Diesel, 10%RSB and 5%Alkenes

The results were tabulated for pure diesel D100 in table 7.1, for pure rapeseed biodiesel RSB100 table 7.2, for the blend coded D85RSB10HX5 in table 7.3, and for the blend coded D85RSB10HP5 in table 7.18. The gained values were shown in in CO emission versus speed graphic (figure 7.46). The measured maximum CO emission rates were for the sample coded D100 4969 ppm at 2086 rpm, for the sample coded RSB100 2656 ppm at 2100 rpm, for the sample coded D85RSB10HX5 4586 ppm at 2043 rpm, for the sample coded D85RSB10HP5 4078 ppm at 2546 rpm respectively. Minimum CO emission was obtained from the sample coded D100 181 ppm at 2648 rpm, the sample coded RSB100 168 ppm at 2605 rpm, the sample coded

D85RSB10HX5 600 ppm at 2500 rpm, and the sample coded D85RSB10HP5 132 ppm at 2844 rpm.

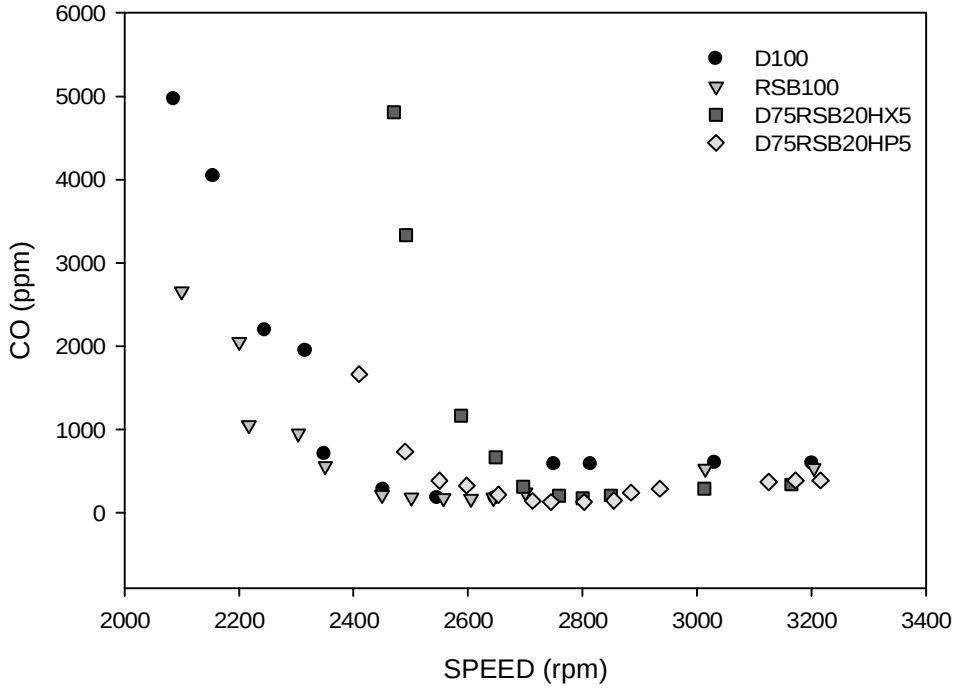


Figure 7.47. CO-Speed Graphic of 75%Diesel, 20%RSB and 5%Alkenes

The results were tabulated for pure diesel D100 in table 7.1, for pure rapeseed biodiesel RSB100 table 7.2, for the blend coded D75RSB20HX5 in table 7.4, and for the blend coded D75RSB20HP5 in table 7.19. The gained values were shown in CO emission versus speed graphic (figure 7.47). The measured maximum CO emission rates were for the sample coded D100 4969 ppm at 2086 rpm, for the sample coded RSB100 2656 ppm at 2100 rpm, for the sample coded D75RSB20HX5 4812 ppm at 2471 rpm, for the sample coded D75RSB20HP5 1666 ppm at 2410 rpm. Minimum CO emission was obtained from the sample coded D100 181 ppm at 2648 rpm, the sample coded RSB100 168 ppm at 2605 rpm, the sample coded D75RSB20HX5 174 ppm at 2800 rpm, and the sample coded D75RSB20HP5 132 ppm at 2803 rpm.

The results were tabulated for pure diesel D100 in table 7.1, for pure rapeseed biodiesel RSB100 table 7.2, for the blend coded D65RSB30HX5 in table 7.5, and for the blend coded D65RSB30HP5 in table 7.20. The gained values were shown in CO

emission versus speed graphic (figure 7.48). The measured maximum CO emission rates were for the sample coded D100 4969 ppm at 2086 rpm, for the sample coded RSB100 2656 ppm at 2100 rpm, for the sample coded D65RSB30HX5 2112 ppm at 2450 rpm, for the sample coded D65RSB30HP5 4996 ppm at 2348 rpm. Minimum CO emission was obtained from the sample coded D100 181 ppm at 2648 rpm, the sample coded RSB100 168 ppm at 2605 rpm, the sample coded D65RSB30HX5 162 ppm at 2800 rpm, and the sample coded D65RSB30HP5 142 ppm at 2750 rpm.

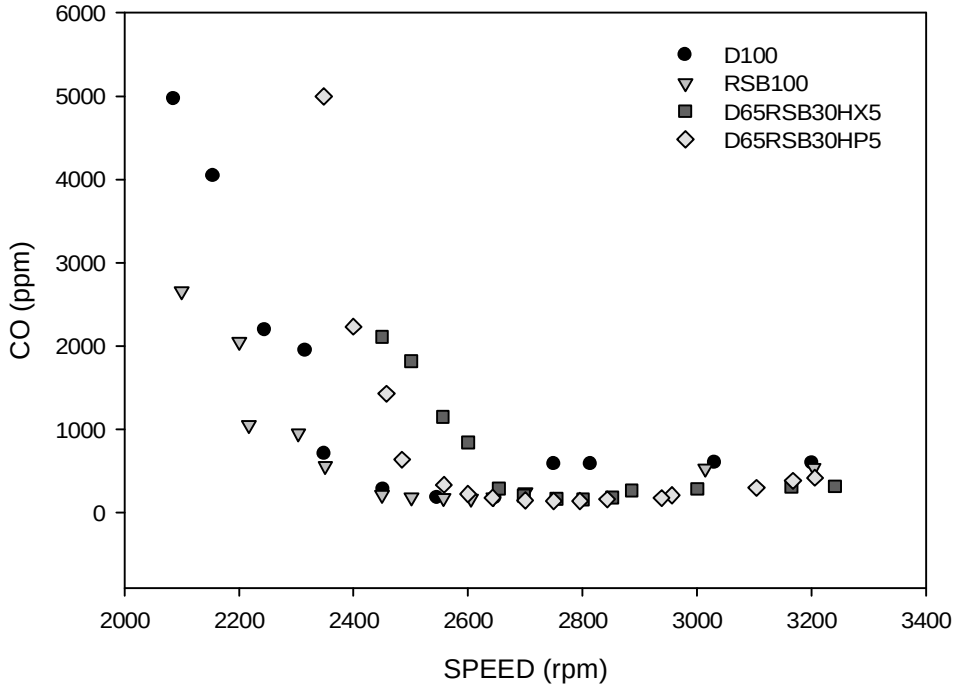


Figure 7.48. CO-Speed Graphic of 65%Diesel, 30%RSB and 5%Alkenes

The results were tabulated for pure diesel D100 in table 7.1, for pure rapeseed biodiesel RSB100 table 7.2, for the blend coded D55RSB40HX5 in table7.6, and for the blend coded D55RSB40HP5 in table 7.21. The gained values were shown in CO emission versus speed graphic (figure 7.49). The measured maximum CO emission rates were for the sample coded D100 4969 ppm at 2086 rpm, for the sample coded RSB100 2656 ppm at 2100 rpm, for the sample coded D55RSB40HX5 4265 ppm at 2452 rpm, for the sample coded D55RSB40HP5 3673 ppm at 1961 rpm respectively. Minimum CO emission was obtained from the sample coded D100 181 ppm at 2648

rpm, the sample coded RSB100 168 ppm at 2605 rpm, the sample coded D55RSB40HX5 603 ppm at 3023 rpm, and the sample coded D55RSB40HP5 105 ppm at 2553 rpm.

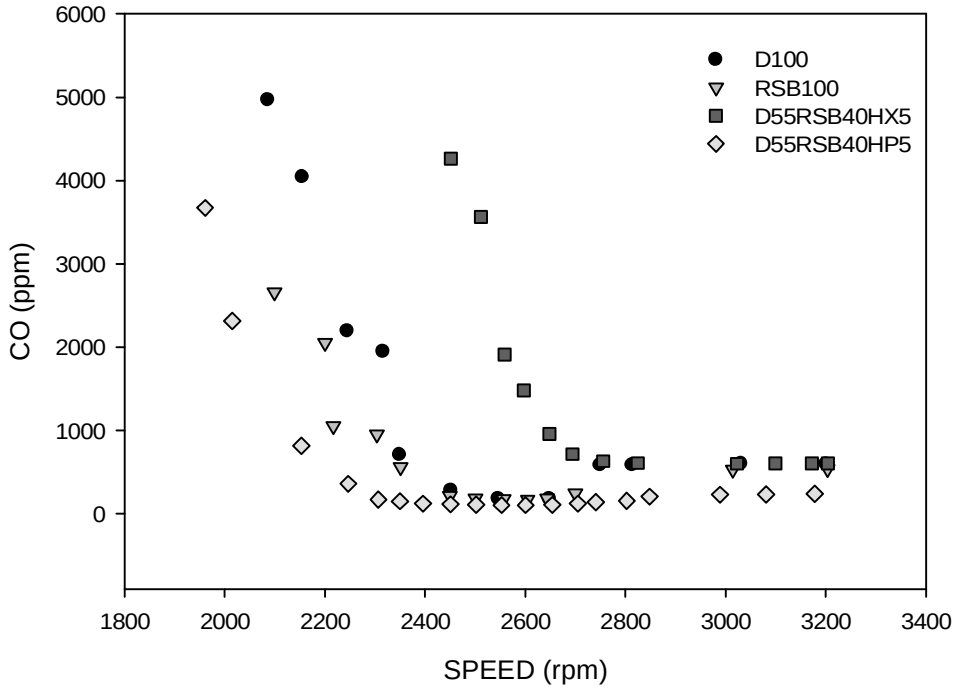


Figure 7.49. CO-Speed Graphic of 55%Diesel, 40%RSB and 5%Alkenes

The results were tabulated for pure diesel D100 in table7.1, for pure rapeseed biodiesel RSB100 table 7.2, for the blend coded D45RSB50HX5 in table 7.7, and for the blend coded D45RSB50HP5 in table 7.22. The gained values were shown in CO emission versus speed graphic (figure 7.50). The measured maximum CO emission rates were for the sample coded D100 4969 ppm at 2086 rpm, for the sample coded RSB100 2656 ppm at 2100 rpm, for the sample coded D45RSB50HX5 3766 ppm at 2496 rpm and for the sample coded D45RSB50HP5 3748 ppm at 2151 rpm respectively. Minimum CO emission was obtained from the sample coded D100 181 ppm at 2648 rpm, the sample coded RSB100 168 ppm at 2605 rpm, the sample coded D45RSB50HX5 144 ppm at 2816, and the sample coded D45RSB50HP5 125 ppm at 2650 rpm.

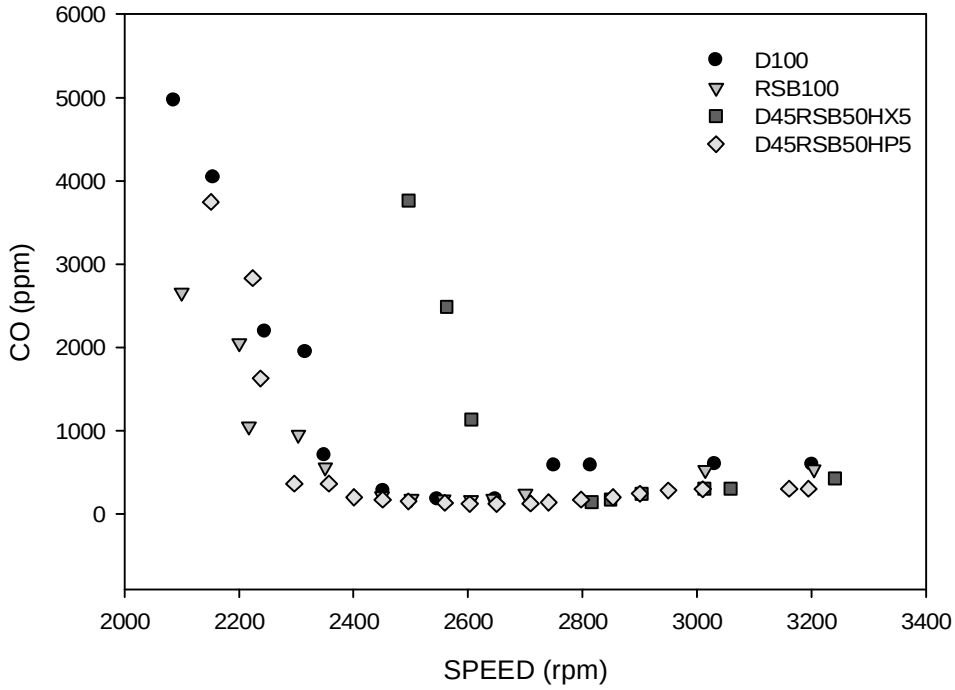


Figure 7.50. CO-Speed Graphic of 45%Diesel, 10%RSB and 5%Alkenes

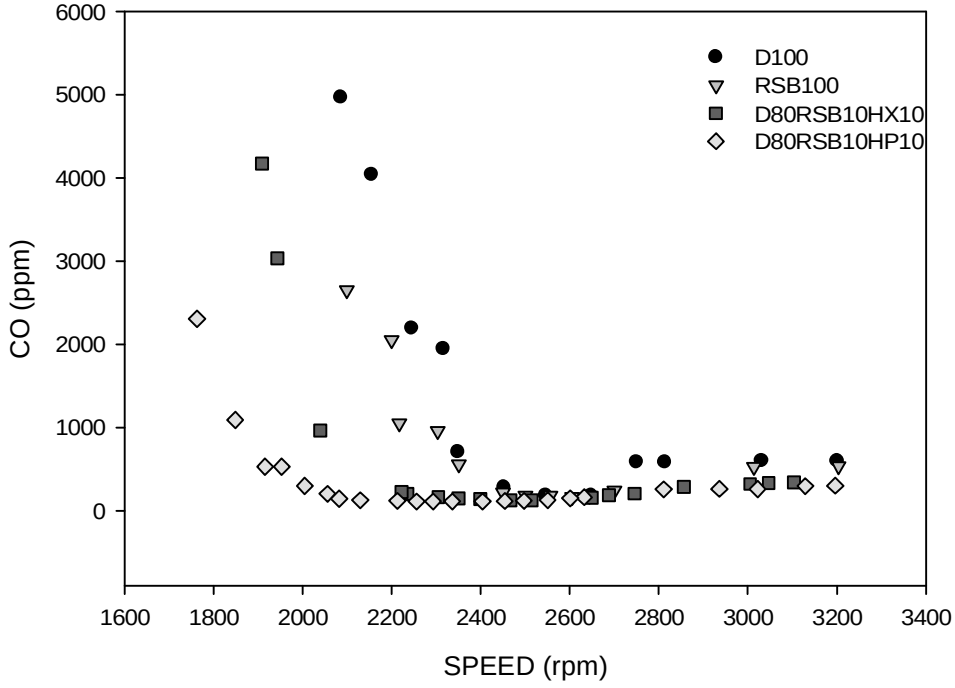


Figure 7.51. CO-Speed Graphic of 80%Diesel, 10%RSB and 10%Alkenes

The results were tabulated for pure diesel D100 in table 7.1, for pure rapeseed biodiesel RSB100 table 7.2, for the blend coded D80RSB10HX10 in table 7.8, and

for the blend coded D80RSB10HP10 in table 7.23. The gained values were shown in in CO emission versus speed graphic (figure 7.51). The measured maximum CO emission rates were for the sample coded D100 4969 ppm at 2086 rpm, for the sample coded RSB100 2656 ppm at 2100 rpm, for the sample coded D80RSB10HX10 4176 ppm at 1909 rpm and for the sample coded D80RSB10HP10 3882 ppm at 2161 rpm respectively. Minimum CO emissions were obtained from the sample coded D100 181 ppm at 2648 rpm, the sample coded RSB100 168 ppm at 2605 rpm, the sample coded D80RSB10HX10 127 ppm at 2514 rpm, and the sample coded D80RSB10HP10 111 ppm at 2336 rpm.

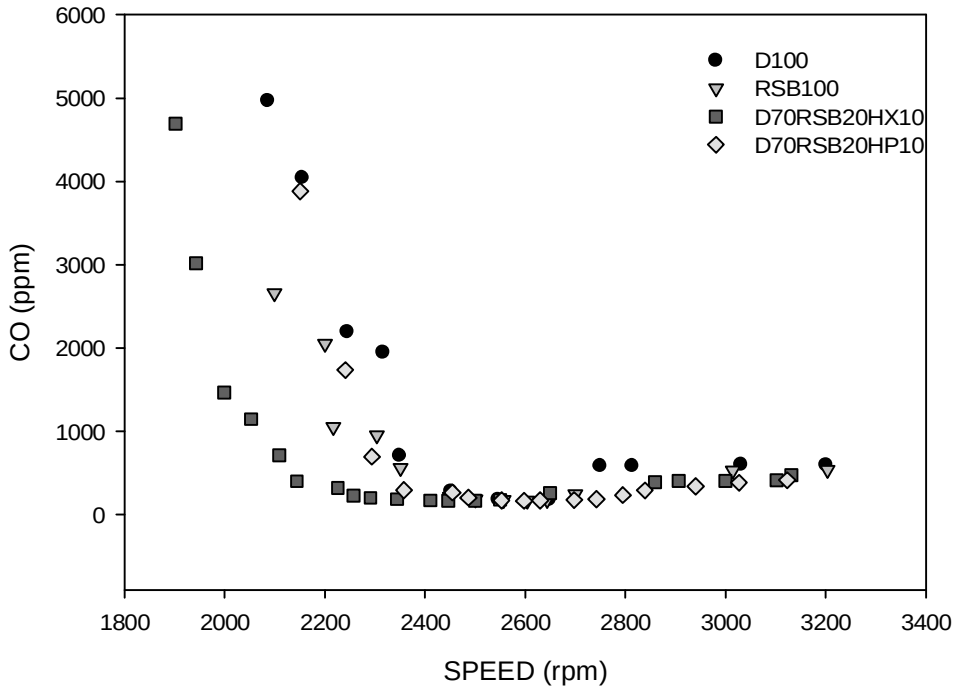


Figure 7.52. CO-Speed Graphic of 70%Diesel, 20%RSB and 10%Alkenes

The results were tabulated for pure diesel D100 in table 7.1, for pure rapeseed biodiesel RSB100 table 7.2, for the blend coded D70RSB20HX10 in table 7.9, and for the blend coded D70RSB20HP10 in table 7.24. The gained values were shown in CO emission versus speed graphic (figure 7.52). The measured maximum CO emission rates were for the sample coded D100 4969 ppm at 2086 rpm, for the sample coded RSB100 2656 ppm at 2100 rpm, for the sample coded

D70RSB20HX10 4691 ppm at 1902 rpm and for the sample coded D70RSB20HP10 3882 ppm at 2161 rpm respectively. Minimum CO emission was obtained from the sample coded D100 181 ppm at 2648 rpm, the sample coded RSB100 168 ppm at 2605 rpm, the sample coded D70RSB20HX10 167 ppm at 2500 rpm, the sample coded D70RSB20HP10 169 ppm at 2598 rpm.

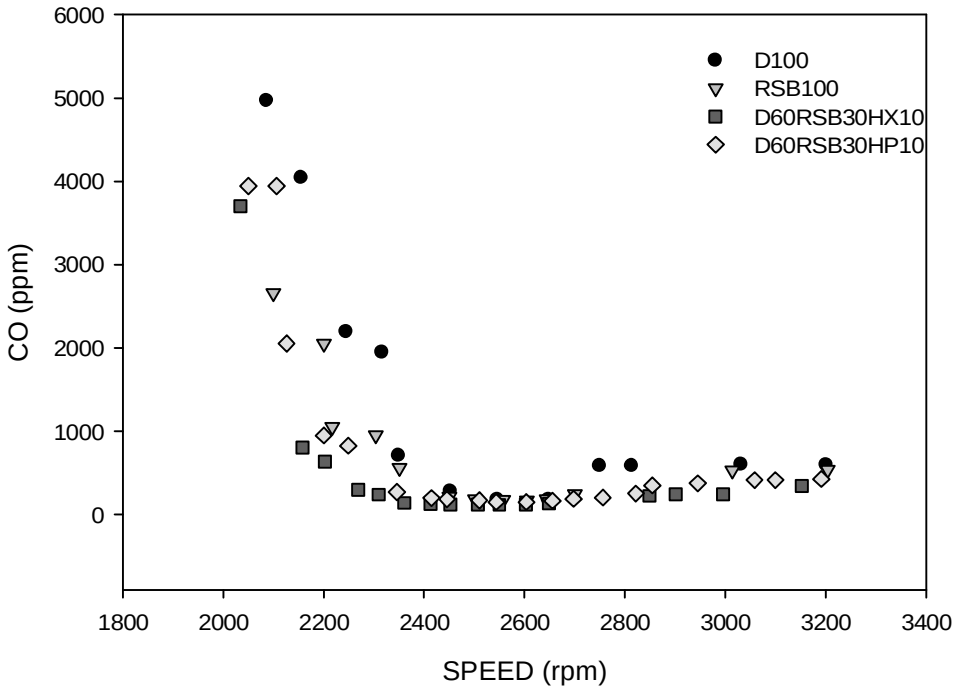


Figure 7.53. CO-Speed Graphic of 60%Diesel, 30%RSB and 10%Alkenes

The results were tabulated for pure diesel D100 in table 7.1, for pure rapeseed biodiesel RSB100 table 7.2, for the blend coded D60RSB30HX10 in table 7.10, and for the blend coded D60RSB30HP10 in table 7.25. The gained values were shown in CO emission versus speed graphic (figure 7.53). The measured maximum CO emission rates were for the sample coded D100 4969 ppm at 2086 rpm, for RSB100 2656 ppm at 2100 rpm, for the sample coded D60RSB30HX10 3702 ppm at 2034 rpm and for the sample coded D60RSB30HP10 3944 ppm at 2050 rpm respectively. Minimum CO emission was obtained from the sample coded D100 181 ppm at 2648 rpm, the sample coded RSB100 168 ppm at 2605 rpm, the sample coded

D60RSB30HX10 121 ppm at 2550 rpm, and the sample coded D60RSB30HP10 152 ppm at 2604 rpm.

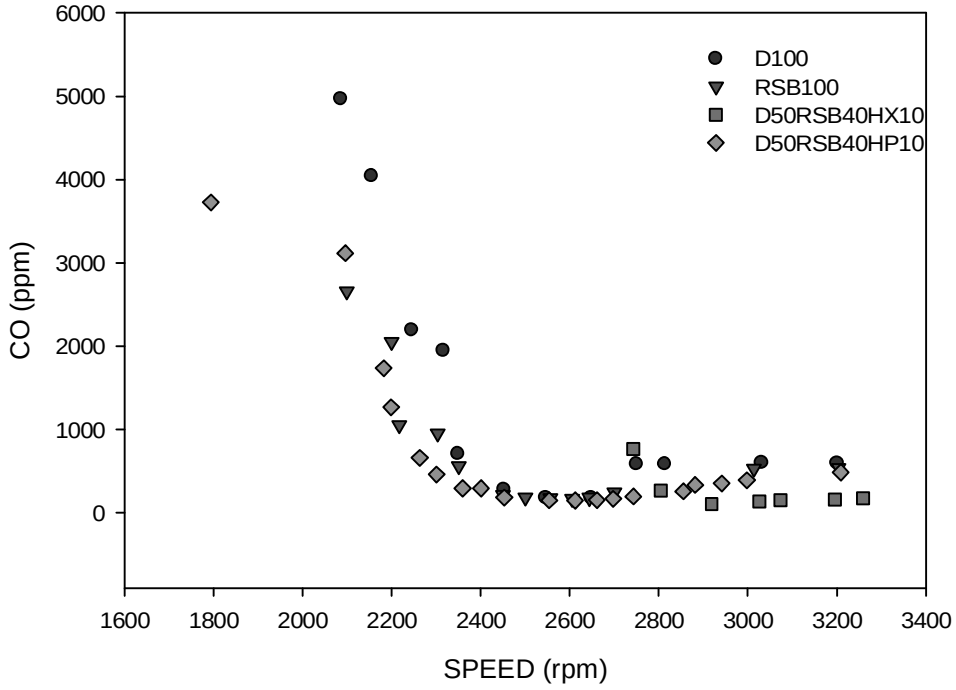


Figure 7.54. CO-Speed Graphic of 50%Diesel, 40%RSB and 10%Alkenes

The results were tabulated for pure diesel D100 in table 7.1, for pure rapeseed biodiesel RSB100 table 7.2, for the blend coded D50RSB40HX10 in table 7.11, and for the blend coded D50RSB40HP10 in table 7.26. The gained values were shown in CO emission versus speed graphic (figure 7.54). The measured maximum CO emission rates were for the sample coded D100 4969 ppm at 2086 rpm, for the sample coded RSB100 2656 ppm at 2100 rpm, for the sample coded D50RSB40HX10 766 ppm at 2742 rpm and for the sample coded D50RSB40HP10 3116 ppm at 2096 rpm respectively. Minimum CO emission was obtained from the sample coded D100 181 ppm at 2648 rpm, the sample coded RSB100 168 ppm at 2605 rpm, the sample coded D50RSB40HX10 603 ppm at 3023 rpm, the sample coded D50RSB40HP10 148 ppm at 2612 rpm.

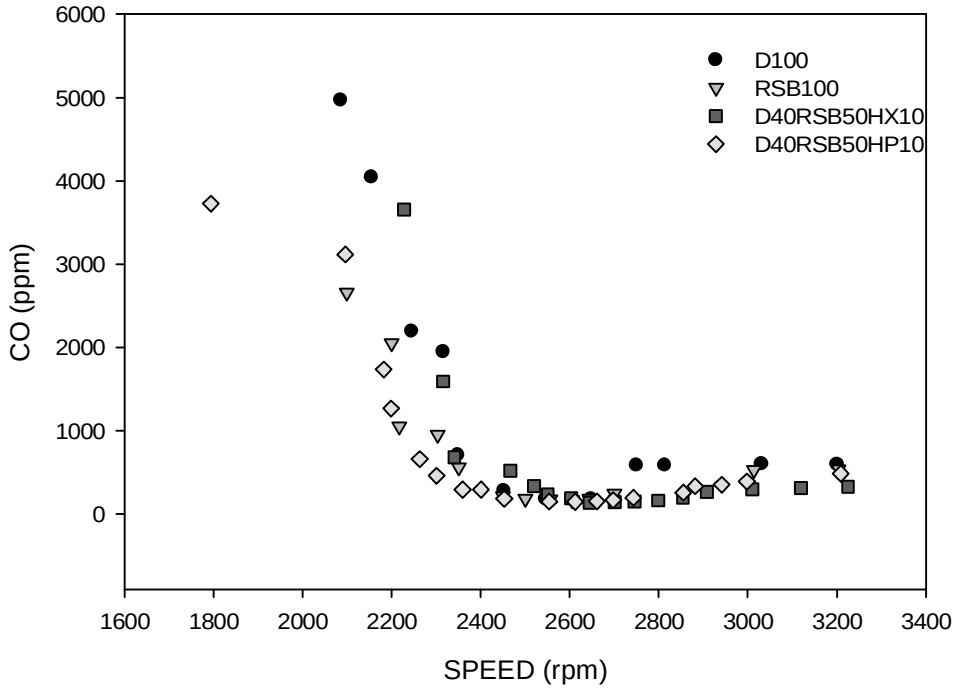


Figure 7.55. CO-Speed Graphic of 40%Diesel, 50%RSB and 10%Alkenes

The results were tabulated for pure diesel D100 in table 7.1, for pure rapeseed biodiesel RSB100 table 7.2, for the blend coded D40RSB50HX10 in table 7.12, and for the blend coded D40RSB50HP10 in table 7.27. The gained values were shown in CO emission versus speed graphic (figure 7.55). The measured maximum CO emission rates were for the sample coded D100 4969 ppm at 2086 rpm, for the sample coded RSB100 2656 ppm at 2100 rpm, for the sample coded D40RSB50HX10 3657 ppm at 2228 rpm and for the sample coded D40RSB50HP10 3646 ppm at 2398 rpm respectively. Minimum CO emission was obtained from the sample coded D100 181 ppm at 2648 rpm, the sample coded RSB100 168 ppm at 2605 rpm, the sample coded D40RSB50HX10 141 ppm at 2644 rpm, and the sample coded D40RSB50HP10 154 ppm at 2807 rpm.

The results were tabulated for pure diesel D100 in table 7.1, for pure rapeseed biodiesel RSB100 table 7.2, for the blend coded D75RSB10HX15 in table 7.13, and for the blend coded D75RSB10HP15 in table 7.28. The gained values were shown in CO emission versus speed graphic (figure 7.56). The measured maximum CO emission rates were for the sample coded D100 4969 ppm at 2086 rpm, for the

sample coded RSB100 2656 ppm at 2100 rpm, for the sample coded D75RSB10HX15 4127 ppm at 2555 rpm, for the sample coded D75RSB10HP15 1895 ppm at 2294 rpm respectively. Minimum CO emission was obtained from the sample coded D100 181 ppm at 2648 rpm, the sample coded RSB100 168 ppm at 2605 rpm, the sample coded D75RSB10HX15 170 ppm at 2852 rpm, the sample coded D75RSB10HP15 165 ppm at 2709 rpm.

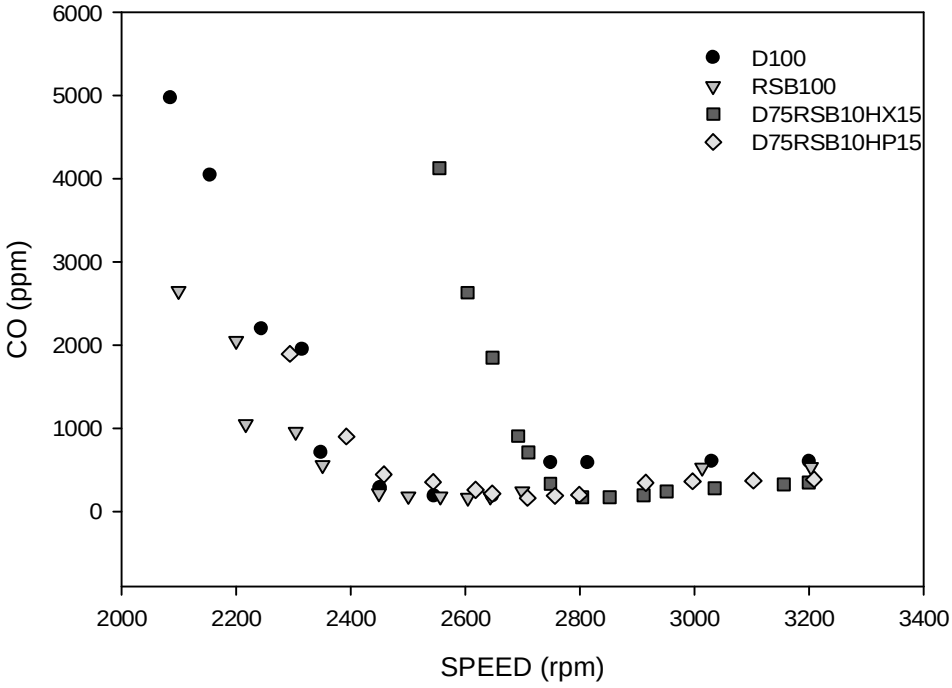


Figure 7.56. CO-Speed Graphic of 75%Diesel, 10%RSB and 15%Alkenes

The results were tabulated for pure diesel D100 in table 7.1, for pure rapeseed biodiesel RSB100 table 7.2, for the blend coded D65RSB20HX15 in table 7.14, and for the blend coded D65RSB20HP15 in table 7.29. The gained values were shown in CO emission versus speed graphic (figure 7.57). The measured maximum CO emission rates were for the sample coded D100 4969 ppm at 2086 rpm, for the sample coded RSB100 2656 ppm at 2100 rpm, for the sample coded D65RSB20HX15 4503 ppm at 2277 rpm, for the sample coded D65RSB20HP15 2152 ppm at 2155 rpm respectively. Minimum CO emission was obtained from the sample coded D100 181 ppm at 2648 rpm, the sample coded RSB100 168 ppm at

2605 rpm, the sample coded D65RSB20HX15 91 ppm at 2708 rpm, and the sample coded D65RSB20HP15 206 ppm at 2605 rpm.

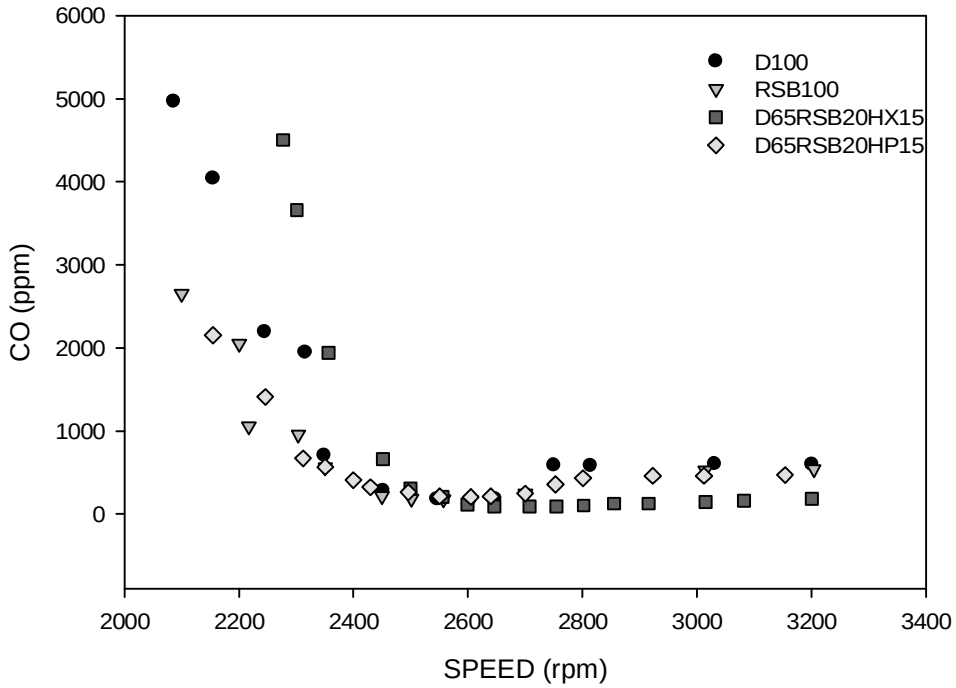


Figure 7.57. CO-Speed Graphic of 65%Diesel, 20%RSB and 15%Alkenes

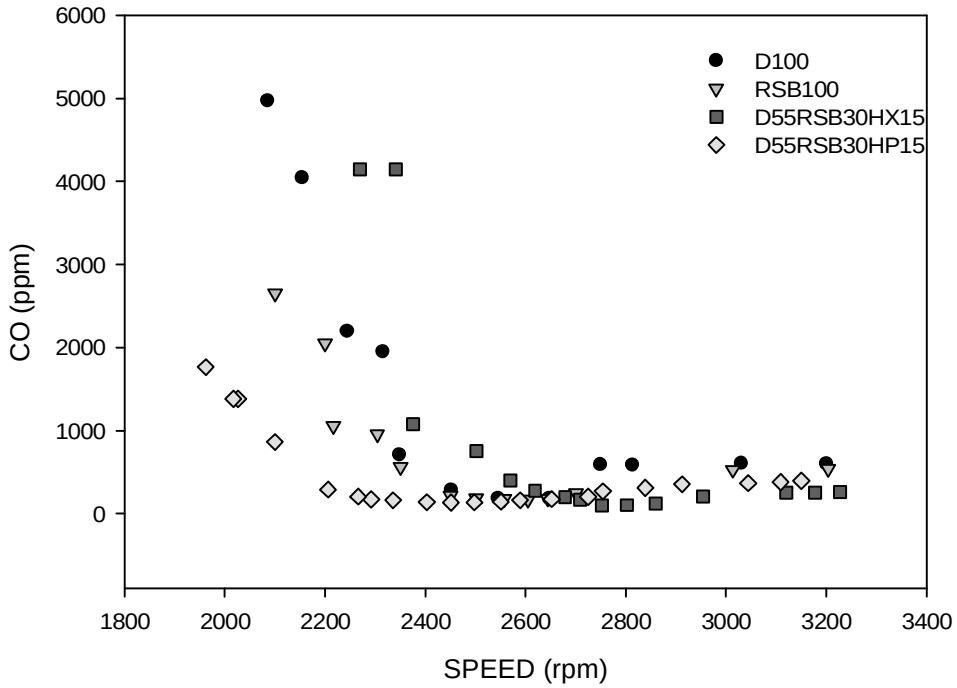


Figure 7.58. CO-Speed Graphic of 55%Diesel, 30%RSB and 15%Alkenes

The results were tabulated for pure diesel D100 in table 7.1, for pure rapeseed biodiesel RSB100 table 7.2, for the blend coded D55RSB30HX15 in table 7.15, and for the blend coded D55RSB30HP15 in table 7.30. The gained values were shown in CO emission versus speed graphic (figure 7.58). The measured maximum CO emission rates were for the sample coded D100 4969 ppm at 2086 rpm, for the sample coded RSB100 2656 ppm at 2100 rpm, for the sample coded D55RSB30HX15 4147 ppm at 2270 rpm, for the sample coded D55RSB30HP15 1766 ppm at 1962 rpm respectively. Minimum CO emission was obtained from the sample coded D100 181 ppm at 2648 rpm, the sample coded RSB100 168 ppm at 2605 rpm, the sample coded D55RSB30HX15 101 ppm at 2752 rpm, and the sample coded D55RSB30HP15 136 ppm at 2451 rpm.

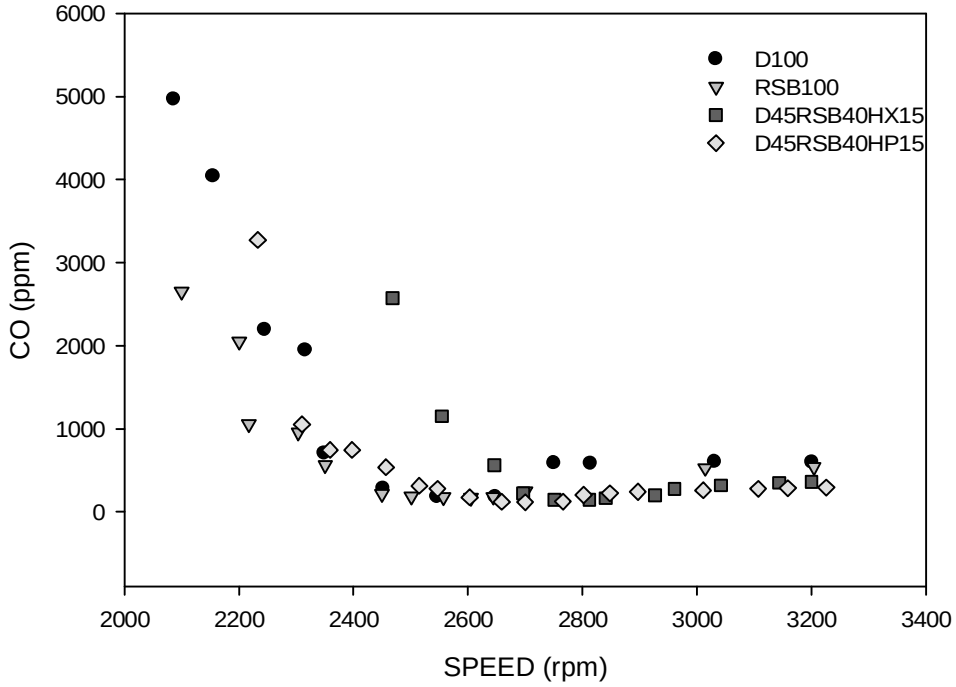


Figure 7.59. CO-Speed Graphic of 45%Diesel, 40%RSB and 15%Alkenes

The results were tabulated for pure diesel D100 in table 7.1, for pure rapeseed biodiesel RSB100 table 7.2, for the blend coded D45RSB40HX15 in table 7.16, and for the blend coded D45RSB40HP15 in table 7.31. The gained values were shown in CO emission versus speed graphic (figure 7.59). The measured maximum CO

emission rates were for the sample coded D100 4969 ppm at 2086 rpm, for the sample coded RSB100 2656 ppm at 2100 rpm, for the sample coded D45RSB40HX15 2572 ppm at 2468 rpm, for the sample coded D45RSB40HP15 3274 ppm at 2233 rpm respectively. Minimum CO emission was obtained from the sample coded D100 181 ppm at 2648 rpm, the sample coded RSB100 168 ppm at 2605 rpm, the sample coded D45RSB40HX15 144 ppm at 2812 rpm, and the sample coded D45RSB40HP15 115 ppm at 2700 rpm.

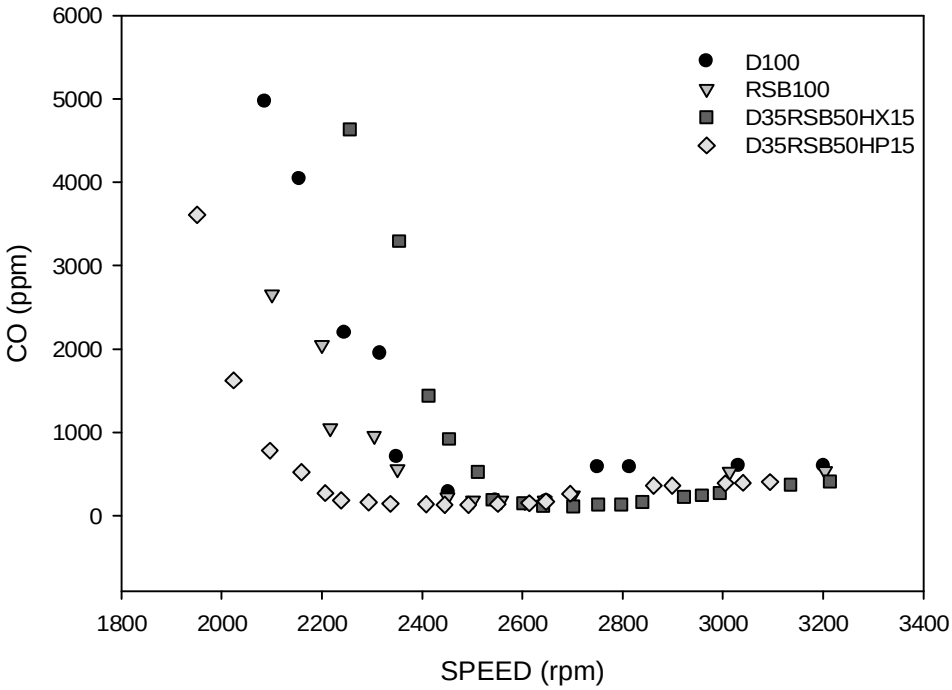


Figure 7.60. CO-Speed Graphic of 35%Diesel, 50%RSB and 15%Alkenes

The results were tabulated for pure diesel D100 in table 7.1, for pure rapeseed biodiesel RSB100 table 7.2, for the blend coded D35RSB50HX15 in table 7.17, and for the blend coded D35RSB50HP15 in table 7.32. The gained values were shown in in CO emission versus speed graphic (figure 7.60). The measured maximum CO emission rates were for the sample coded D100 4969 ppm at 2086 rpm, for the sample coded RSB100 2656 ppm at 2100 rpm, for the sample coded D35RSB50HX15 4632 ppm at 2256 rpm, for the sample coded D35RSB50HP15 3610 ppm at 1951 rpm respectively. Minimum CO emissions were obtained from the

sample coded D100 181 ppm at 2648 rpm, the sample coded RSB100 168 ppm at 2605 rpm, from the sample coded D35RSB50HX15 115 ppm at 2701 rpm, from the sample coded D35RSB50HP15 133 ppm at 2445 rpm.

7.5 NO_x Emission

In this study, high NO_x emissions were measured between 2800-2200 rpm engine speed. At high speeds low NO_x emissions were measured nevertheless, the emission rate were shown rapid increase as the engine speed decreases. After 2200 rpm NO_x emissions were lowered.

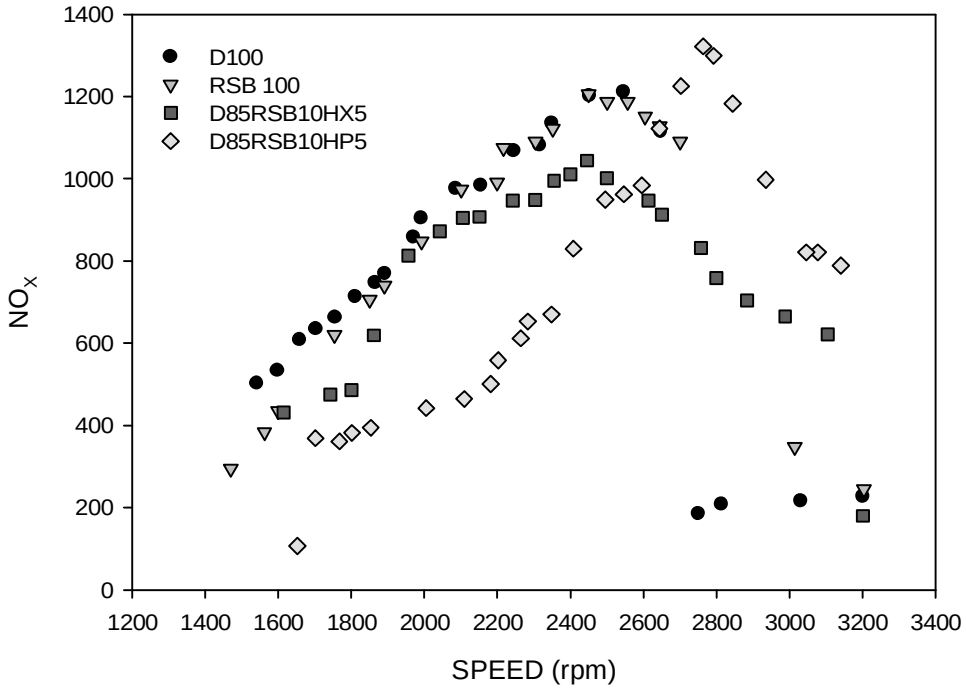


Figure 7.61. NO_x-Speed Graphic of 85%Diesel, 10%RSB and 5%Alkenes

The results were tabulated for pure diesel D100 in table 7.1, for pure rapeseed biodiesel RSB100 table 7.2, for the blend coded D85RSB10HX5 in table 7.3, and for the blend coded D85RSB10HP5 in table 7.18. The gained values were shown in NO_x emission versus speed graphic (figure 7.61). At the speed of maximum torque, the measured NO_x emission rates were for the sample coded D100 662 ppm, for the sample coded RSB100 260 ppm, for the sample coded D85RSB10HX5 431 ppm, for

the sample coded D85RSB10HP5 394 ppm respectively. Maximum NO_x emission were obtained from the sample coded D100 1211 ppm at 2546 rpm, the sample coded RSB100 1205 ppm at 2450 rpm, the sample coded D85RSB10HX5 1044 ppm at 2445 rpm, the sample coded D85RSB10HP5 1322 ppm at 2763 rpm.

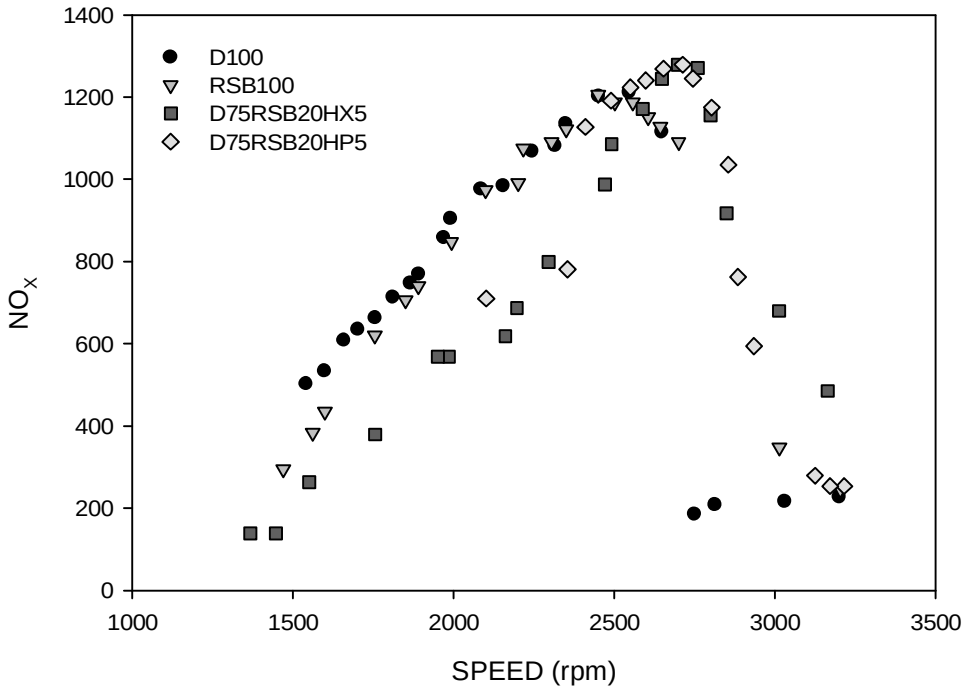


Figure 7.62. NO_x-Speed Graphic of 75%Diesel, 20%RSB and 5%Alkenes

The results were tabulated for pure diesel D100 in table 7.1, for pure rapeseed biodiesel RSB100 table 7.2, for the blend coded D75RSB20HX5 in table 7.4, and for the blend coded D75RSB20HP5 in table 7.19. The gained values were shown in NO_x emission versus speed graphic (figure 7.62). At the speed of maximum torque, the measured NO_x emission rates were for the sample coded D100 662 ppm, for the sample coded RSB100 260 ppm, for the sample coded D75RSB20HX5 568 ppm, for the sample coded D75RSB20HP5 could not measured. Maximum NO_x emission were obtained from the sample coded D100 1211 ppm at 2546 rpm, the sample coded RSB100 1205 ppm at 2450 rpm, the sample coded D75RSB20HX5 1279 ppm at 2697 rpm, the sample coded D75RSB20HP5 1279 ppm at 2713 rpm.

The results were tabulated for pure diesel D100 in table 7.1, for pure rapeseed biodiesel RSB100 table 7.2, for the blend coded D65RSB30HX5 in table 7.5, and for the blend coded D65RSB30HP5 in table 7.20. The gained values were shown in NO_x emission versus speed graphic (figure 7.63). At the speed of maximum torque, the measured NO_x emission rates were for the sample coded D100 662 ppm, for the sample coded RSB100 260 ppm, for the sample coded D65RSB30HX5 976 ppm, for the sample coded D65RSB30HP5 could not measured. Maximum NO_x emission were obtained from the sample coded D100 1211 ppm at 2546 rpm, the sample coded RSB100 1205 ppm at 2450 rpm, the sample coded D65RSB30HX5 931 ppm at 2407 rpm, the sample coded D65RSB30HP5 1358 ppm at 2700 rpm.

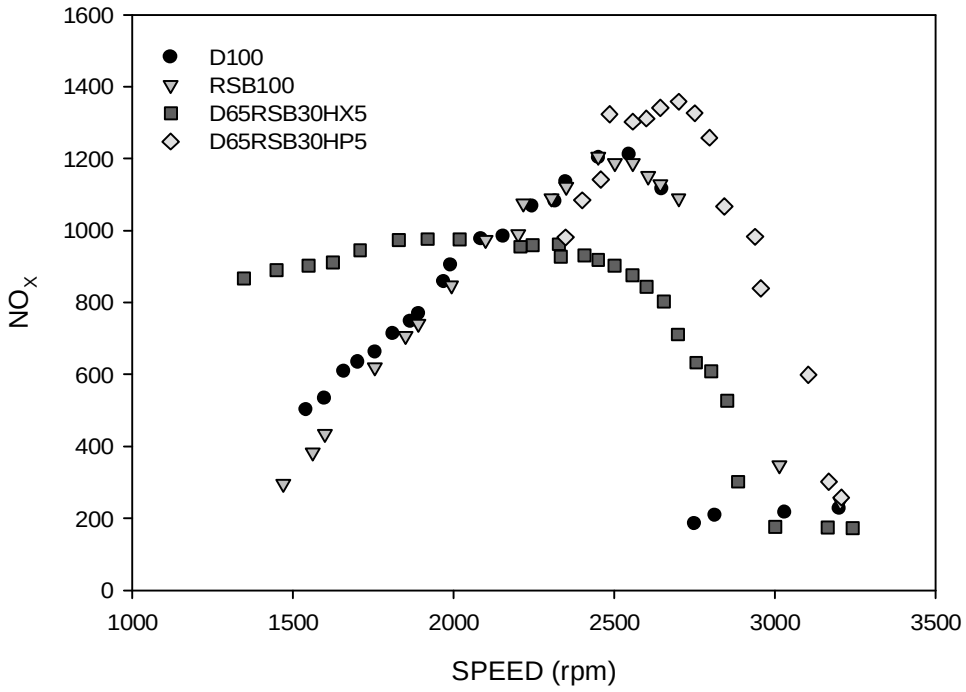


Figure 7.63. NO_x-Speed Graphic of 65%Diesel, 30%RSB and 5%Alkenes

The results were tabulated for pure diesel D100 in table 7.1, for pure rapeseed biodiesel RSB100 table 7.2, for the blend coded D55RSB40HX5 in table7.6, and for the blend coded D55RSB40HP5 in table 7.21. The gained values were shown in NO_x emission versus speed graphic (figure 7.64). At the speed of maximum torque, the measured NO_x emission rates were for the sample coded D100 662 ppm, for the

sample coded RSB100 260 ppm, for the sample coded D55RSB40HX5 467 ppm, for the sample coded D55RSB40HP5 735 ppm respectively. Maximum NO_x emission were obtained from the sample coded D100 1211 ppm at 2546 rpm, the sample coded RSB100 1205 ppm at 2450 rpm, the sample coded D55RSB40HX5 1031 ppm at 2756 rpm, the sample coded D55RSB40HP5 1296 ppm at 2396 rpm.

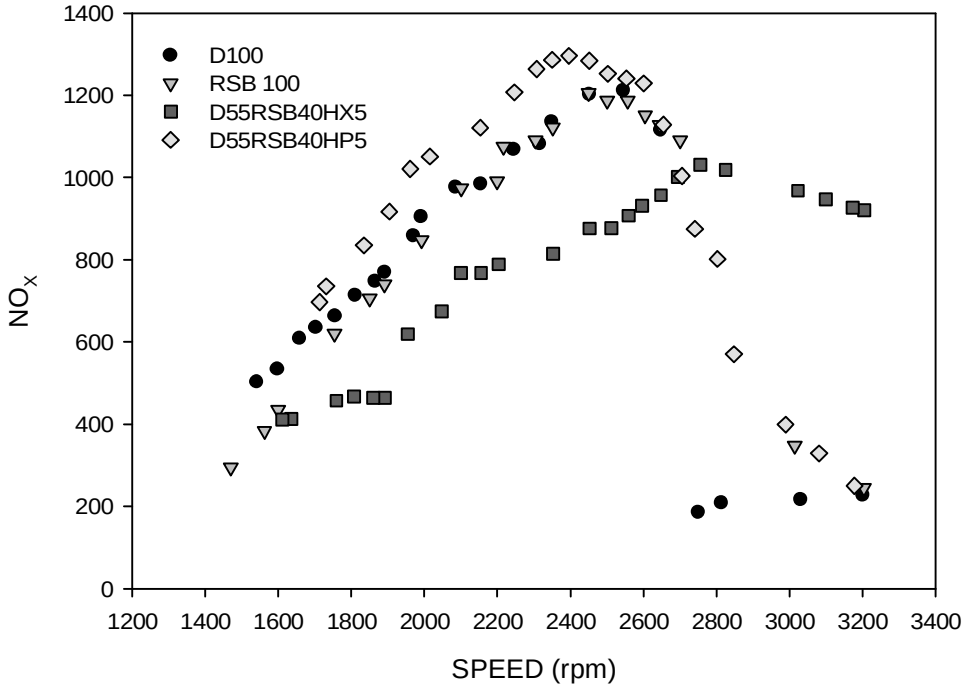


Figure 7.64. NO_x -Speed Graphic of 55%Diesel, 40%RSB and 5%Alkenes

The results were tabulated for pure diesel D100 in table7.1, for pure rapeseed biodiesel RSB100 table 7.2, for the blend coded D45RSB50HX5 in table 7.7, and for the blend coded D45RSB50HP5 in table 7.22. The gained values were shown in NO_x emission versus speed graphic (figure 7.65). At the speed of maximum torque, the measured NO_x emission rates were for the sample coded D100 662 ppm, for the sample coded RSB100 260 ppm, for the sample coded D45RSB50HX5 348 ppm, for the sample coded D45RSB50HP5 671 ppm respectively. Maximum NO_x emission were obtained from the sample coded D100 1211 ppm at 2546 rpm, the sample coded RSB100 1205 ppm at 2450 rpm, the sample coded D45RSB50HX5 1178 ppm at 2606 rpm, the sample coded D45RSB50HP5 1307 ppm at 2560 rpm.

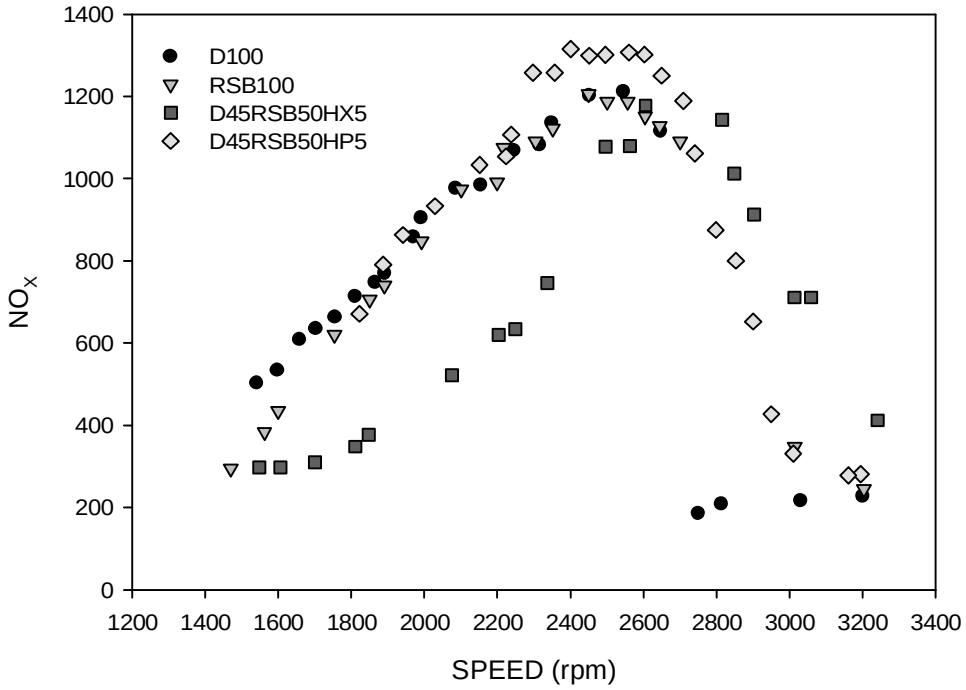


Figure 7.65. NO_x-Speed Graphic of 45%Diesel, 50%RSB and 5%Alkenes

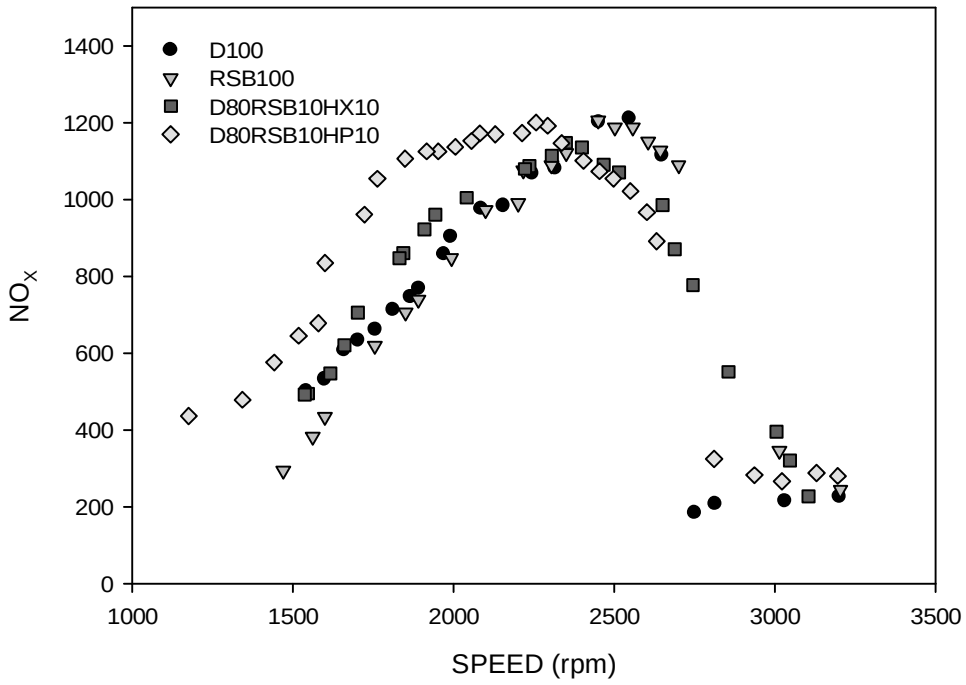


Figure 7.66. NO_x-Speed Graphic of 80%Diesel, 10%RSB and 10%Alkenes

The results were tabulated for pure diesel D100 in table 7.1, for pure rapeseed biodiesel RSB100 table 7.2, for the blend coded D80RSB10HX10 in table 7.8, and for the blend coded D80RSB10HP10 in table 7.23. The gained values were shown in NO_x emission versus speed graphic (figure 7.66). At the speed of maximum torque, the measured NO_x emission rates were for the sample coded D100 662 ppm, for the sample coded RSB100 260 ppm, for the sample coded D80RSB10HX10 547 ppm, for the sample coded D80RSB10HP10 678 ppm respectively. Maximum NO_x emission were obtained from the sample coded D100 1211 ppm at 2546 rpm, the sample coded RSB100 1205 ppm at 2450 rpm, the sample coded D80RSB10HX10 1148 ppm at 2350 rpm, the sample coded D80RSB10HP10 1200 ppm at 2256 rpm.

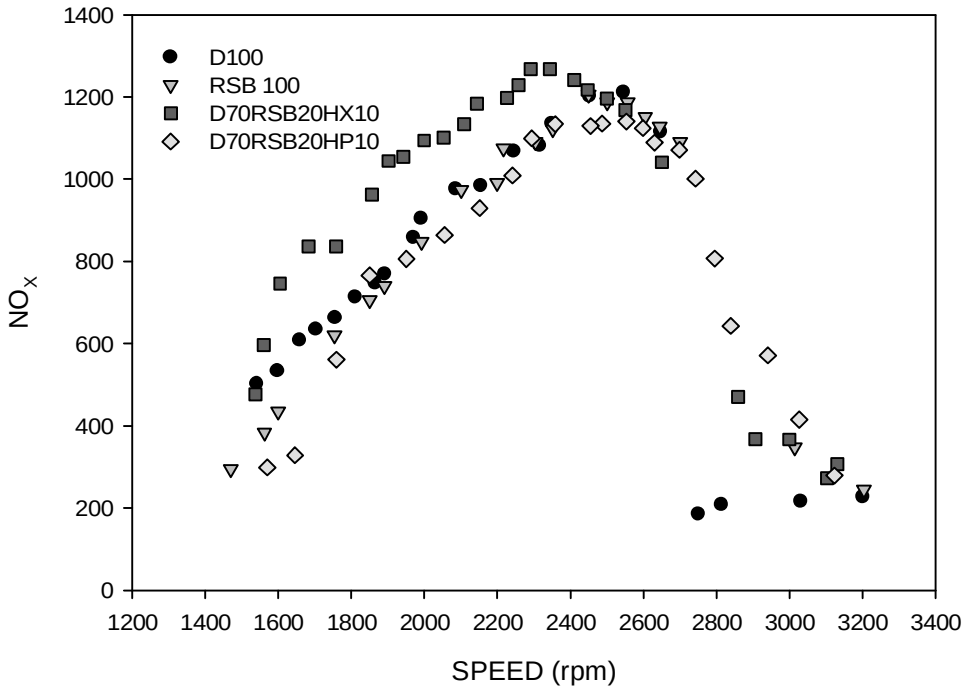


Figure 7.67. NO_x-Speed Graphic of 70%Diesel, 20%RSB and 10%Alkenes

The results were tabulated for pure diesel D100 in table 7.1, for pure rapeseed biodiesel RSB100 table 7.2, for the blend coded D70RSB20HX10 in table 7.9, and for the blend coded D70RSB20HP10 in table 7.24. The gained values were shown in NO_x emission versus speed graphic (figure 7.67). At the speed of maximum torque, the measured NO_x emission rates were for the sample coded D100 662 ppm, for the

sample coded RSB100 260 ppm, for the sample coded D70RSB20HX10 746 ppm, for the sample coded D70RSB20HP10 561 ppm respectively. Maximum NO_x emission were obtained from the sample coded D100 1211 ppm at 2546 rpm, the sample coded RSB100 1205 ppm at 2450 rpm, the sample coded D70RSB20HX10 1267 ppm at 2291 rpm, the sample coded D70RSB20HP10 1140 ppm at 2553 rpm.

The results were tabulated for pure diesel D100 in table 7.1, for pure rapeseed biodiesel RSB100 table 7.2, for the blend coded D60RSB30HX10 in table 7.10, and for the blend coded D60RSB30HP10 in table 7.25. The gained values were shown in NO_x emission versus speed graphic (figure 7.68). At the speed of maximum torque, the measured NO_x emission rates were for the sample coded D100 662 ppm, for the sample coded RSB100 260 ppm, for the sample coded D60RSB30HX10 506 ppm, for the sample coded D60RSB30HP10 713 ppm respectively. Maximum NO_x emission were obtained from the sample coded D100 1211 ppm at 2546 rpm, the sample coded RSB100 1205 ppm at 2450 rpm, the sample coded D60RSB30HX10 1137 ppm at 2413 rpm, the sample coded D60RSB30HP10 1156 ppm at 2346 rpm.

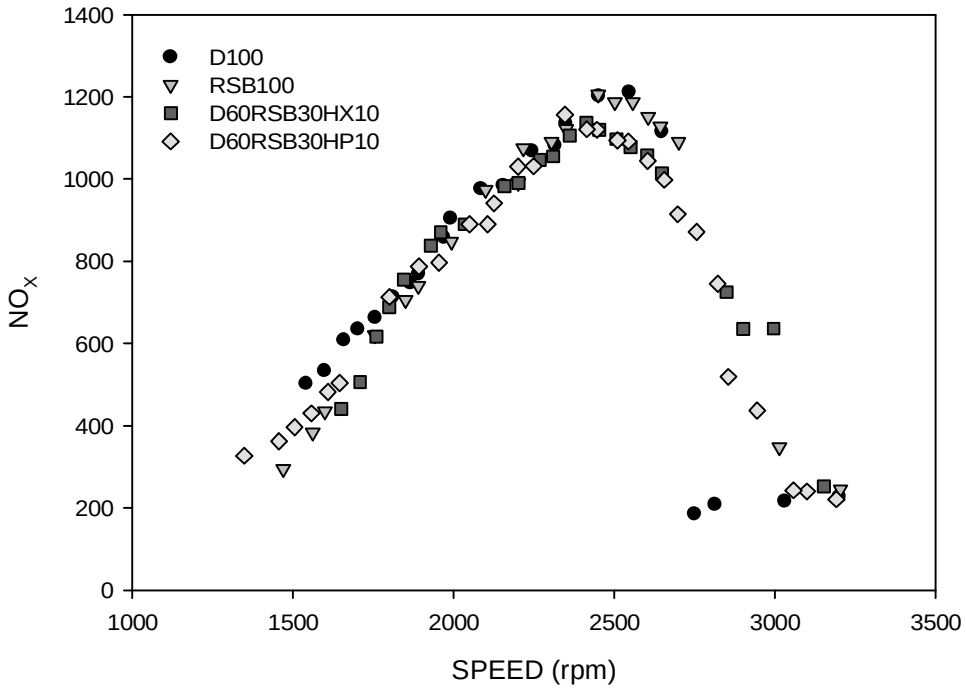


Figure 7.68. NO_x-Speed Graphic of 60%Diesel, 30%RSB and 10%Alkenes

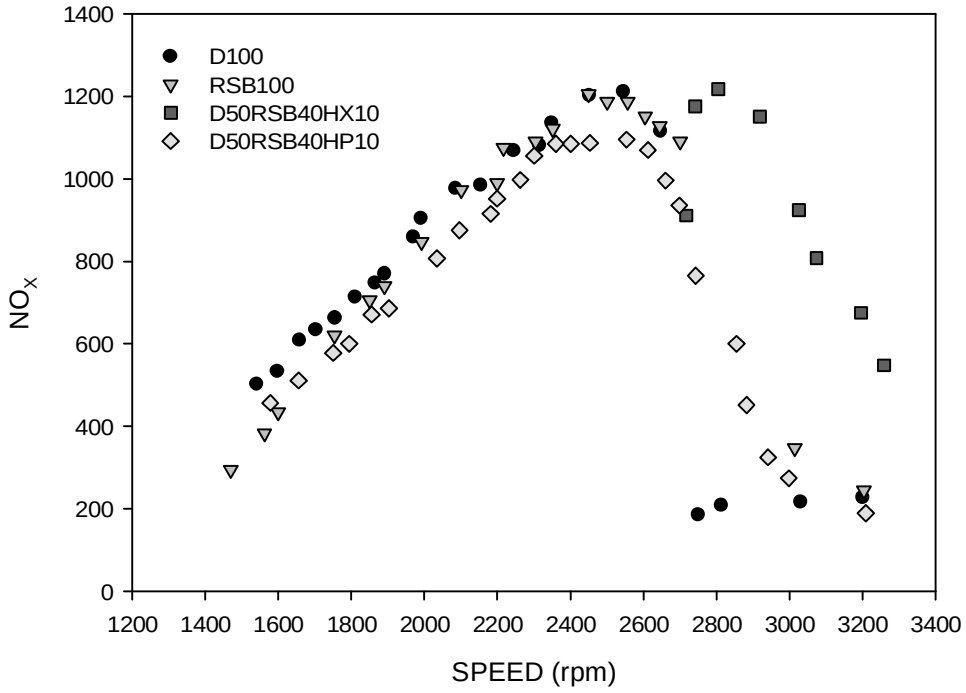


Figure 7.69. NO_x-Speed Graphic of 50%Diesel, 40%RSB and 10%Alkenes

The results were tabulated for pure diesel D100 in table 7.1, for pure rapeseed biodiesel RSB100 table 7.2, for the blend coded D50RSB40HX10 in table 7.11, and for the blend coded D50RSB40HP10 in table 7.26. The gained values were shown in NO_x emission versus speed graphic (figure 7.69). At the speed of maximum torque, the measured NO_x emission rates were for the sample coded D100 662 ppm, for the sample coded RSB100 260 ppm, for the sample coded D50RSB40HX10 could not measured, for the sample coded D50RSB40HP10 600 ppm respectively. Maximum NO_x emission were obtained from the sample coded D100 1211 ppm at 2546 rpm, the sample coded RSB100 1205 ppm at 2450 rpm, the sample coded D50RSB40HX10 1217 ppm at 2805 rpm, the sample coded D50RSB40HP10 1095 ppm at 2554 rpm.

The results were tabulated for pure diesel D100 in table 7.1, for pure rapeseed biodiesel RSB100 table 7.2, for the blend coded D40RSB50HX10 in table 7.12, and for the blend coded D40RSB50HP10 in table 7.27. The gained values were shown in NO_x emission versus speed graphic (figure 7.70). At the speed of maximum torque, the measured NO_x emission rates were for the sample coded D100 662 ppm, for the

sample coded RSB100 260 ppm, for the sample coded D40RSB50HX10 762 ppm, for the sample coded D40RSB50HP10 461 ppm respectively. Maximum NO_x emission were obtained from the sample coded D100 1211 ppm at 2546 rpm, the sample coded RSB100 1205 ppm at 2450 rpm, the sample coded D40RSB50HX10 1195 ppm at 2603 rpm, the sample coded D40RSB50HP10 1174 ppm at 2654 rpm.

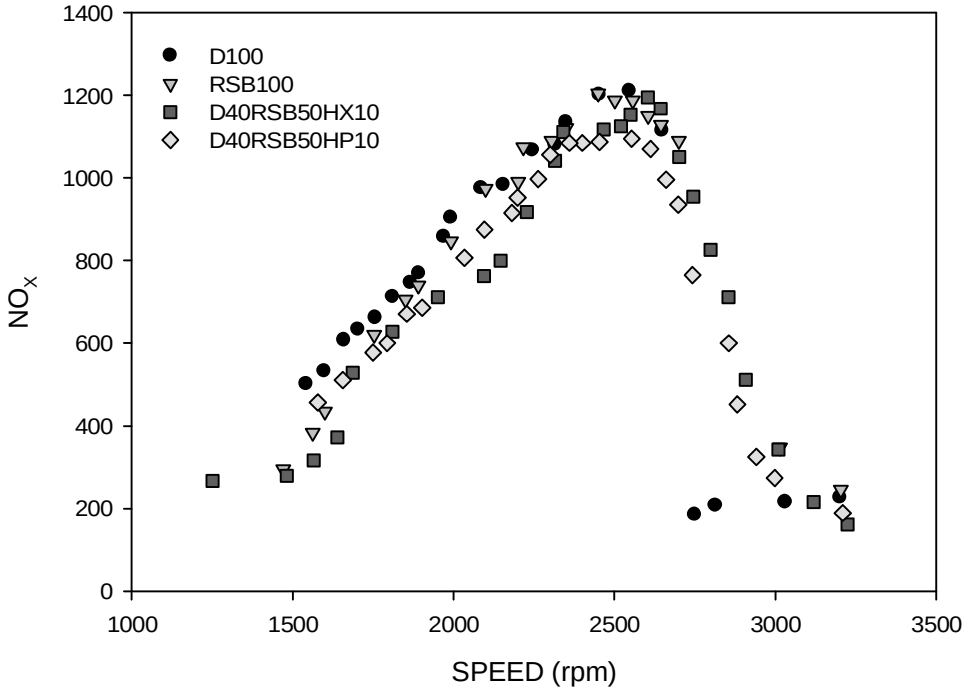


Figure 7.70. NO_x-Speed Graphic of 40%Diesel, 50%RSB and 10%Alkenes

The results were tabulated for pure diesel D100 in table 7.1, for pure rapeseed biodiesel RSB100 table 7.2, for the blend coded D75RSB10HX15 in table 7.13, and for the blend coded D75RSB10HP15 in table 7.28. The gained values were shown in NO_x emission versus speed graphic (figure 7.71). At the speed of maximum torque, the measured NO_x emission rates were for the sample coded D100 662 ppm, for the sample coded RSB100 260 ppm, for the sample coded D75RSB10HX15 364 ppm, for the sample coded D75RSB10HP15 502 ppm respectively. Maximum NO_x emission were obtained from the sample coded D100 1211 ppm at 2546 rpm, the sample coded RSB100 1205 ppm at 2450 rpm, the sample coded D75RSB10HX15 1182 ppm at 2749 rpm, the sample coded D75RSB10HP15 1205 ppm at 2618 rpm.

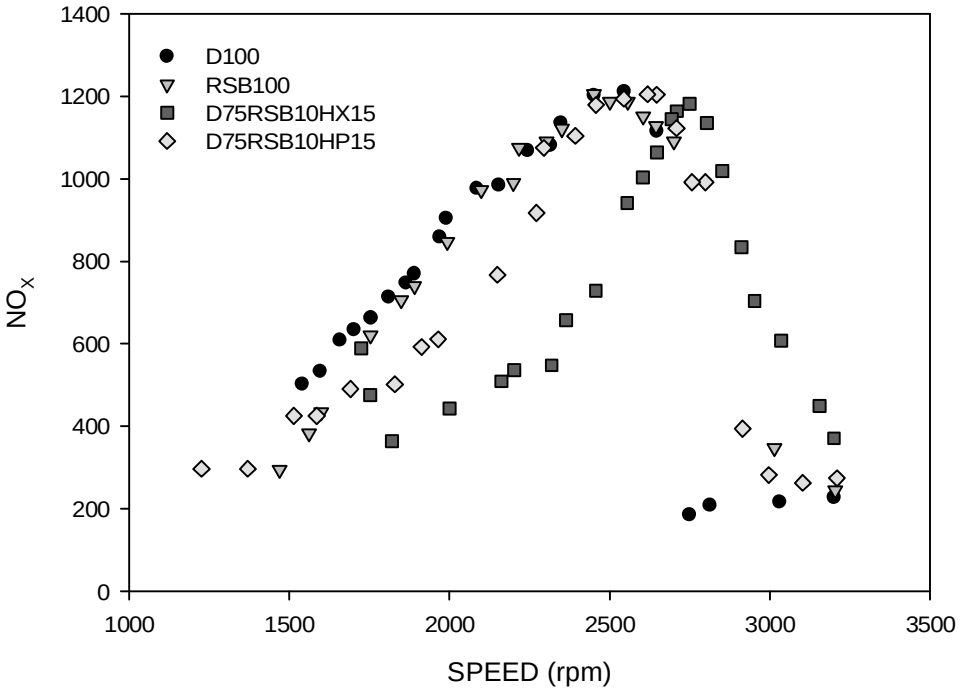


Figure 7.71. NO_x-Speed Graphic of 75%Diesel, 10%RSB and 15%Alkenes

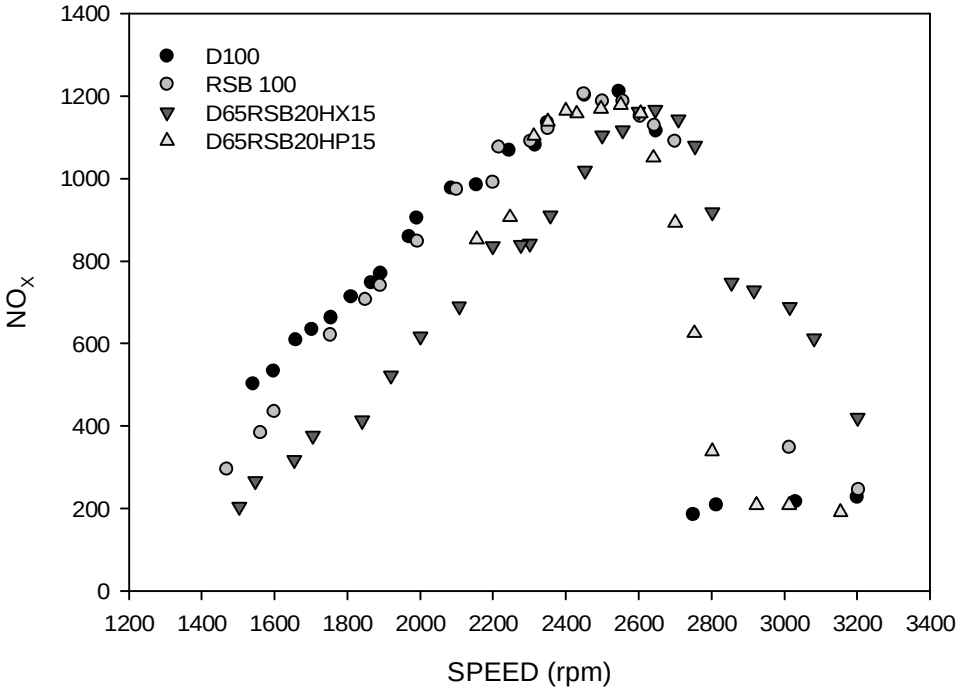


Figure 7.72. NO_x-Speed Graphic of 65%Diesel, 20%RSB and 15%Alkenes

The results were tabulated for pure diesel D100 in table 7.1, for pure rapeseed biodiesel RSB100 table 7.2, for the blend coded D65RSB20HX15 in table 7.14, and

for the blend coded D65RSB20HP15 in table 7.29. The gained values were shown in NO_x emission versus speed graphic (figure 7.72). At the speed of maximum torque, the measured NO_x emission rates were for the sample coded D100 662 ppm, for the sample coded RSB100 260 ppm, for the sample coded D65RSB20HX15 413 ppm, for D65RSB20HP15 could not measured respectively. Maximum NO_x emission were obtained from the sample coded D100 1211 ppm at 2546 rpm, the sample coded RSB100 1205 ppm at 2450 rpm, the sample coded D65RSB20HX15 1167 ppm at 2646 rpm, the sample coded D65RSB20HP15 1178 ppm at 2551 rpm.

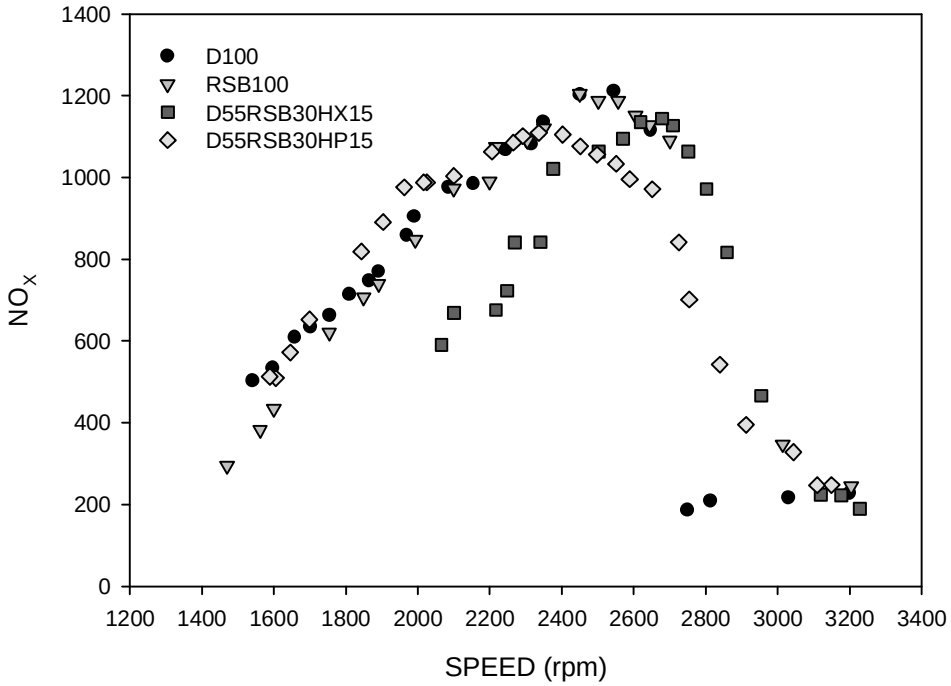


Figure 7.73. NO_x-Speed Graphic of 55%Diesel, 30%RSB and 15%Alkenes

The results were tabulated for pure diesel D100 in table 7.1, for pure rapeseed biodiesel RSB100 table 7.2, for the blend coded D55RSB30HX15 in table 7.15, and for the blend coded D55RSB30HP15 in table 7.30. The gained values were shown in NO_x emission versus speed graphic (figure 7.73). At the speed of maximum torque, the measured NO_x emission rates were for the sample coded D100 662 ppm, for the sample coded RSB100 260 ppm, for the sample coded D55RSB30HX15 could not measured, for the sample coded D55RSB30HP15 509 ppm respectively. Maximum

NO_x emission were obtained from the sample coded D100 1211 ppm at 2546 rpm, the sample coded RSB100 1205 ppm at 2450 rpm, the sample coded D55RSB30HX15 1144 ppm at 2676 rpm, the sample coded D55RSB30HP15 1109 ppm at 2336 rpm.

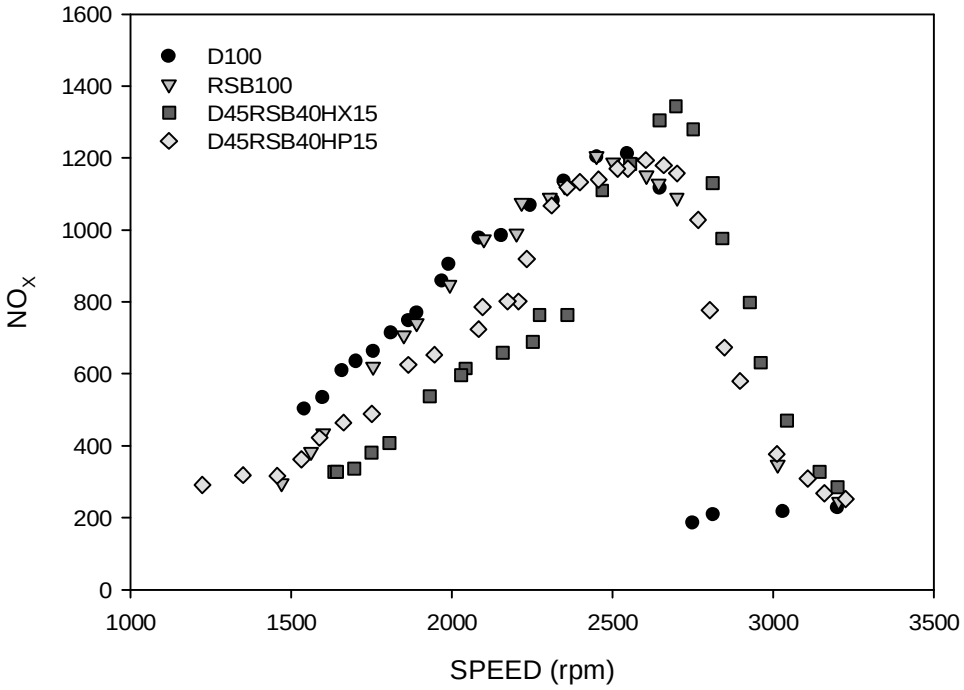


Figure 7.74. NO_x-Speed Graphic of 45%Diesel, 40%RSB and 15%Alkenes

The results were tabulated for pure diesel D100 in table 7.1, for pure rapeseed biodiesel RSB100 table 7.2, for the blend coded D45RSB40HX15 in table 7.16, and for the blend coded D45RSB40HP15 in table 7.31. The gained values were shown in in NO_x emission versus speed graphic (figure 7.74). At the speed of maximum torque, the measured NO_x emission rates were for the sample coded D100 662 ppm, for the sample coded RSB100 260 ppm, for the sample coded D45RSB40HX15 538 ppm, for the sample coded D45RSB40HP15 625 ppm respectively. Maximum NO_x emission were obtained from the sample coded D100 1211 ppm at 2546 rpm, the sample coded RSB100 1205 ppm at 2450 rpm, the sample coded D45RSB40HX15 1344 ppm at 2697 rpm, the sample coded D45RSB40HP15 1194 ppm at 2603 rpm.

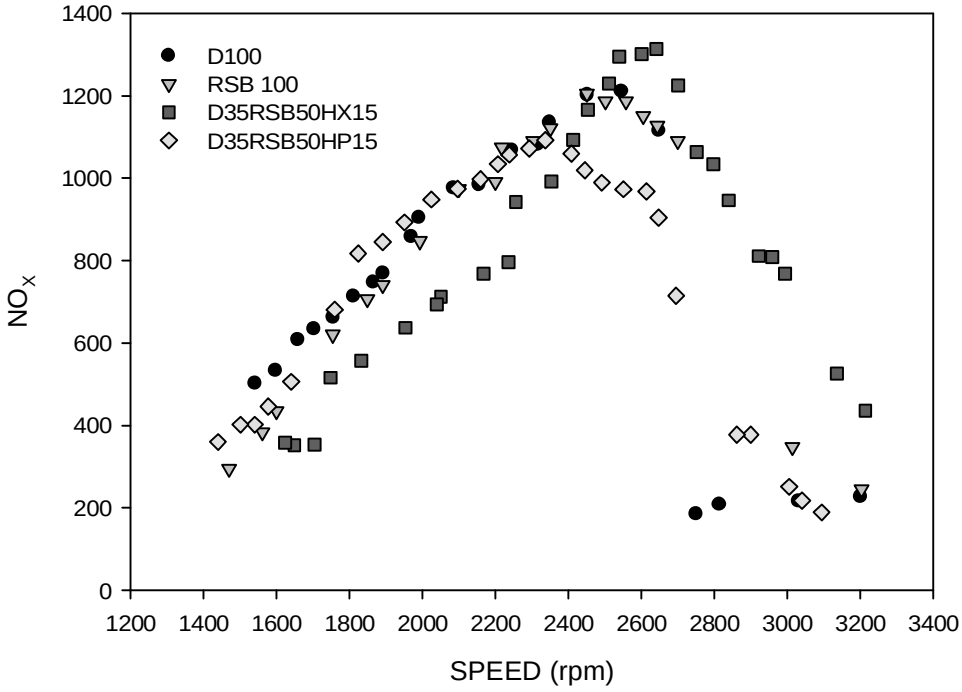


Figure 7.75. NO_x-Speed Graphic of 35%Diesel, 50%RSB and 15%Alkenes

The results were tabulated for pure diesel D100 in table 7.1, for pure rapeseed biodiesel RSB100 table 7.2, for the blend coded D35RSB50HX15 in table 7.17, and for the blend coded D35RSB50HP15 in table 7.32. The gained values were shown in NO_x emission versus speed graphic (figure 7.75). At the speed of maximum torque, the measured NO_x emission rates were for the sample coded D100 662 ppm, for the sample coded RSB100 260 ppm, for the sample coded D35RSB50HX15 516 ppm, for the sample coded D35RSB50HP15 681 ppm respectively. Maximum NO_x emission were obtained from the sample coded D100 1211 ppm at 2546 rpm, the sample coded RSB100 1205 ppm at 2450 rpm, the sample coded D35RSB50HX15 1314 ppm at 2641 rpm, the sample coded D35RSB50HP15 1092 ppm at 2337 rpm.

7.6 CO_2 Emission

The results were tabulated for pure diesel D100 in table 7.1, for pure rapeseed biodiesel RSB100 table 7.2, for the blend coded D85RSB10HX5 in table 7.3, and for the blend coded D85RSB10HP5 in table 7.18. The gained values were shown in CO_2

emission versus speed graphic (figure 7.76). At the speed of maximum torque, the measured CO_2 emission rates were for the sample coded D100 11.72 %, for the sample coded RSB100 11.69%, for the sample coded D85RSB10HX5 11.77%, and for the sample coded D85RSB10HP5 11.9% respectively. Minimum CO_2 emission were obtained from the sample coded D100 3.38 % at 3201 rpm, the sample coded RSB100 2.99% at 3204 rpm, the sample coded D85RSB10HX5 2.67% at 3201 rpm, the sample coded D85RSB10HP5 5.97% at 3140 rpm.

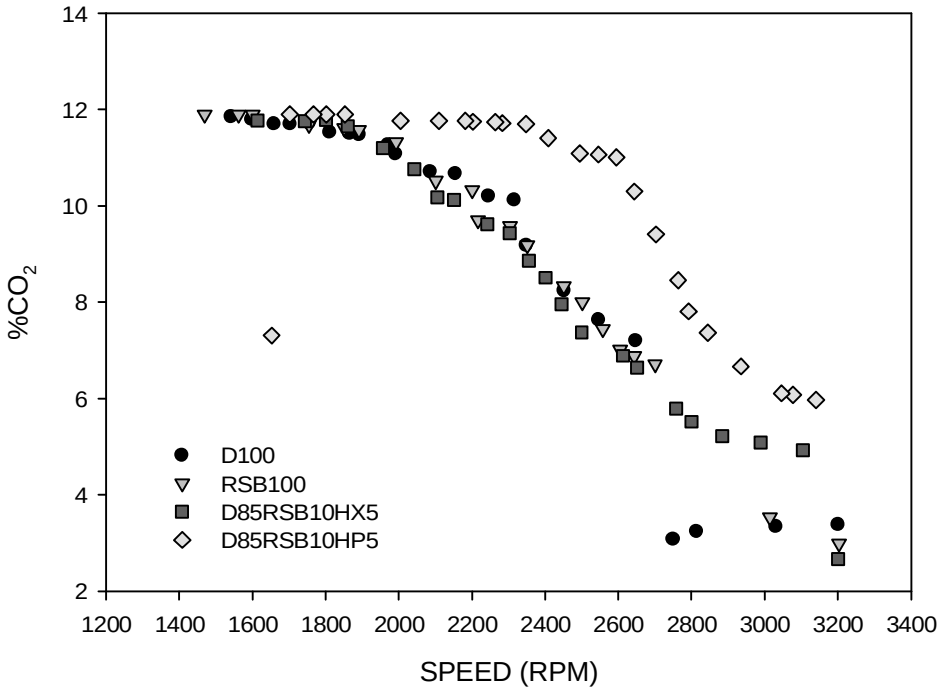


Figure 7.76. CO_2-Speed Graphic of 85%Diesel, 10%RSB and 5%Alkenes

The results were tabulated for pure diesel D100 in table 7.1, for pure rapeseed biodiesel RSB100 table 7.2, for the blend coded D75RSB20HX5 in table 7.4, and for the blend coded D75RSB20HP5 in table 7.19. The gained values were shown in CO_2 emission versus speed graphic (figure 7.77). At the speed of maximum torque, the measured CO_2 emission rates were for the sample coded D100 11.72 %, for the sample coded RSB100 11.69%, for the sample coded D75RSB20HX5 11.87%, for the sample coded D75RSB20HP5 could not measured. Minimum CO_2 emission were obtained from the sample coded D100 3.38 % at 3201 rpm, the sample coded

RSB100 2.99% at 3204 rpm, the sample coded D75RSB20HX5 4.69% at 3165 rpm, the sample coded D75RSB20HP5 3.37% at 3216 rpm.

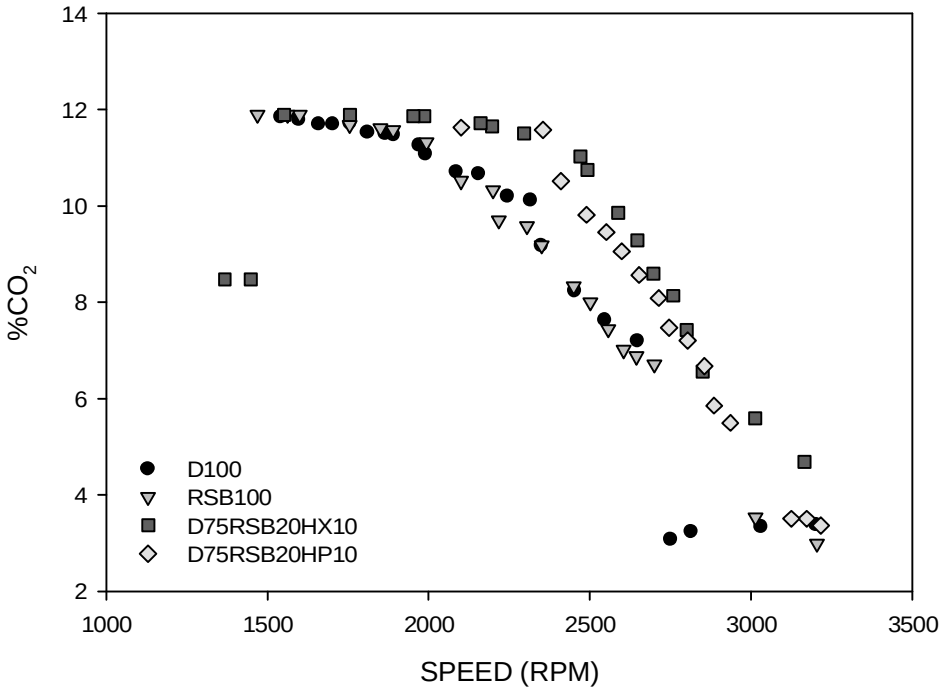


Figure 7.77. CO_2-Speed Graphic of 75%Diesel, 20%RSB and 5%Alkenes

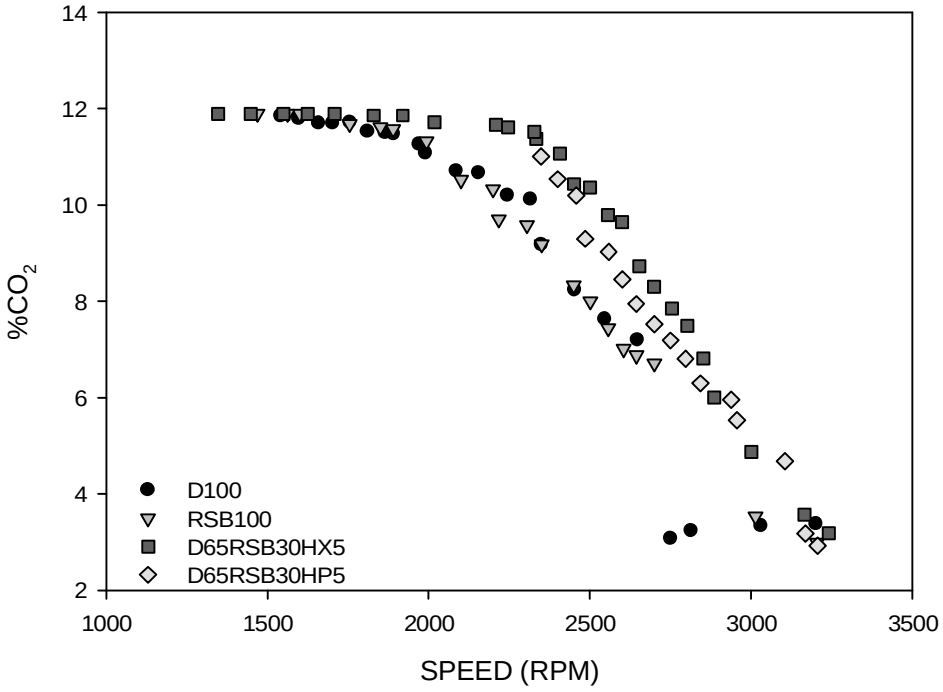


Figure 7.78. CO_2-Speed Graphic of 65%Diesel, 30%RSB and 5%Alkenes

The results were tabulated for pure diesel D100 in table 7.1, for pure rapeseed biodiesel RSB100 table 7.2, for the blend coded D65RSB30HX5 in table 7.5, and for the blend coded D65RSB30HP5 in table 7.20. The gained values were shown in CO_2 emission versus speed graphic (figure 7.78). At the speed of maximum torque, the measured CO_2 emission rates were for the sample coded D100 11.72 %, for the sample coded RSB100 11.69%, for the sample coded D65RSB30HX5 11.86%, for the sample coded D65RSB30HP5 could not measured. Minimum CO_2 emission were obtained from the sample coded D100 3.38 % at 3201 rpm, the sample coded RSB100 2.99% at 3204 rpm, the sample coded D65RSB30HX5 3.19% at 3241 rpm, the sample coded D65RSB30HP5 2.93% at 3206 rpm.

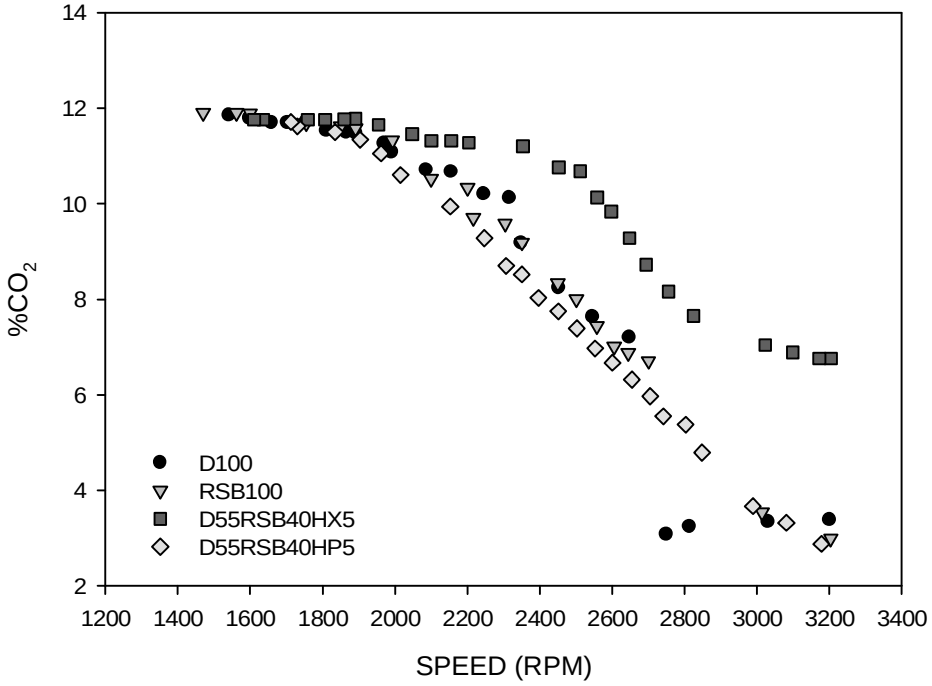


Figure 7.79. CO_2-Speed Graphic of 55%Diesel, 40%RSB and 5%Alkenes

The results were tabulated for pure diesel D100 in table 7.1, for pure rapeseed biodiesel RSB100 table 7.2, for the blend coded D55RSB40HX5 in table7.6, and for the blend coded D55RSB40HP5 in table 7.21. The gained values were shown in CO_2 emission versus speed graphic (figure 7.79). At the speed of maximum torque, the measured CO_2 emission rates were for the sample coded D100 11.72 %, for the

sample coded RSB100 11.69%, for the sample coded D55RSB40HX5 11.76%, for the sample coded D55RSB40HP5 11.62% measured respectively. Minimum CO_2 emission were obtained from the sample coded D100 3.38 % at 3201 rpm, the sample coded RSB100 2.99% at 3204 rpm, the sample coded D55RSB40HX5 6.76% at 3204 rpm, the sample coded D55RSB40HP5 2.88% at 3178 rpm.

The results were tabulated for pure diesel D100 in table7.1, for pure rapeseed biodiesel RSB100 table 7.2, for the blend coded D45RSB50HX5 in table 7.7, and for the blend coded D45RSB50HP5 in table 7.22. The gained values were shown in CO_2 emission versus speed graphic (figure 7.80). At the speed of maximum torque, the measured CO_2 emission rates were for the sample coded D100 11.72 %, for the sample coded RSB100 11.69%, for the sample coded D45RSB50HX5 11.87%, for the sample coded D45RSB50HP5 11.74% measured respectively. Minimum CO_2 emission were obtained from the sample coded D100 3.38 % at 3201 rpm, the sample coded RSB100 2.99% at 3204 rpm, the sample coded D45RSB50HX5 4.34% at 3241 rpm, the sample coded D45RSB50HP5 3.1% at 3195 rpm.

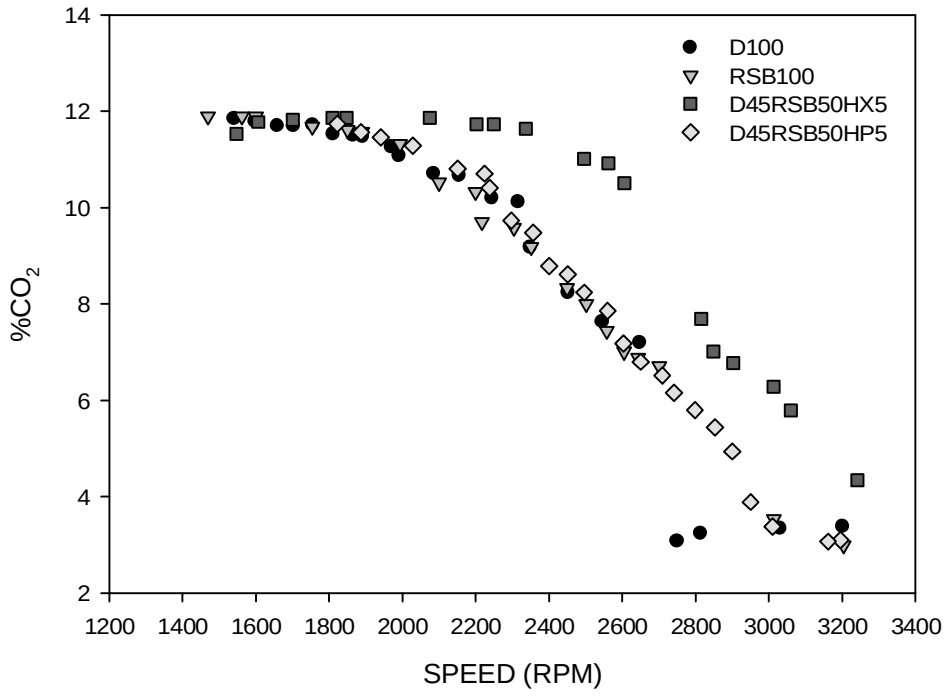


Figure 7.80. CO_2-Speed Graphic of 45%Diesel, 50%RSB and 5%Alkenes

The results were tabulated for pure diesel D100 in table 7.1, for pure rapeseed biodiesel RSB100 table 7.2, for the blend coded D80RSB10HX10 in table 7.8, and for the blend coded D80RSB10HP10 in table 7.23. The gained values were shown in CO_2 emission versus speed graphic (figure 7.81). At the speed of maximum torque, the measured CO_2 emission rates were for the sample coded D100 11.72 %, for the sample coded RSB100 11.69%, the sample coded D80RSB10HX10 11.76%, for the sample coded D80RSB10HP10 11.6% measured respectively. Minimum CO_2 emission were obtained from the sample coded D100 3.38 % at 3201 rpm, the sample coded RSB100 2.99% at 3204 rpm, the sample coded D80RSB10HX10 3.06% at 3104 rpm, the sample coded D80RSB10HP10 3% at 3196 rpm.

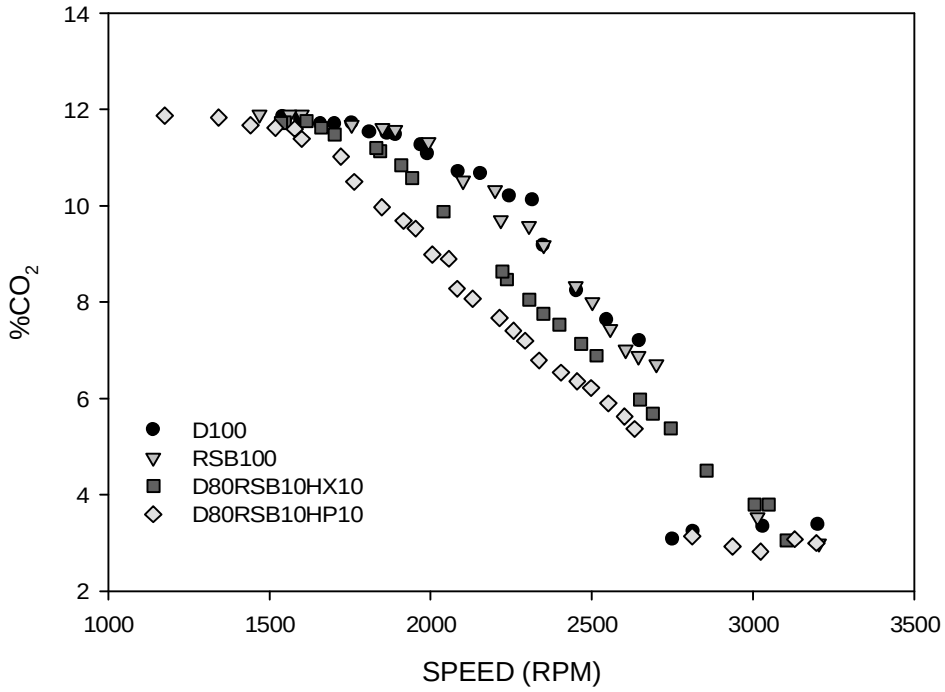


Figure 7.81. CO_2-Speed Graphic of 80%Diesel, 10%RSB and 10%Alkenes

The results were tabulated for pure diesel D100 in table 7.1, for pure rapeseed biodiesel RSB100 table 7.2, for the blend coded D70RSB20HX10 in table 7.9, and for the blend coded D70RSB20HP10 in table 7.24. The gained values were shown in CO_2 emission versus speed graphic (figure 7.82). At the speed of maximum torque, the measured CO_2 emission rates were for the sample coded D100 11.72 %, for the

sample coded RSB100 11.69%, for the sample coded D70RSB20HX10 11.56%, for the sample coded D70RSB20HP10 11.78% measured respectively. Minimum CO_2 emission were obtained from the sample coded D100 3.38 % at 3201 rpm, the sample coded RSB100 2.99% at 3204 rpm, the sample coded D70RSB20HX10 3.35% at 3131 rpm, the sample coded D70RSB20HP10 3.73% at 3123 rpm.

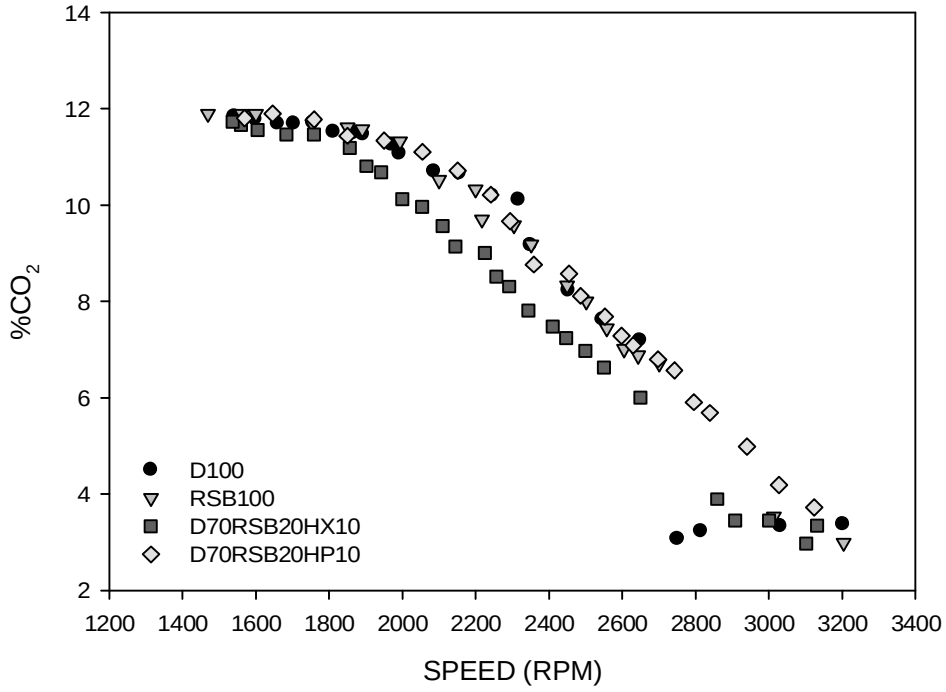


Figure 7.82. CO_2-Speed Graphic of 70%Diesel, 20%RSB and 10%Alkenes

The results were tabulated for pure diesel D100 in table 7.1, for pure rapeseed biodiesel RSB100 table 7.2, for the blend coded D60RSB30HX10 in table 7.10, and for the blend coded D60RSB30HP10 in table 7.25. The gained values were shown in CO_2 emission versus speed graphic (figure 7.83). At the speed of maximum torque, the measured CO_2 emission rates were for the sample coded D100 11.72 %, for the sample coded RSB100 11.69%, for the sample coded D60RSB30HX10 11.75%, for the sample coded D60RSB30HP10 11.62% measured respectively. Minimum CO_2 emission were obtained from the sample coded D100 3.38 % at 3201 rpm, the sample coded RSB100 2.99% at 3204 rpm, the sample coded D60RSB30HX10 3.09% at 3152 rpm, the sample coded D60RSB30HP10 3.27% at 3191 rpm.

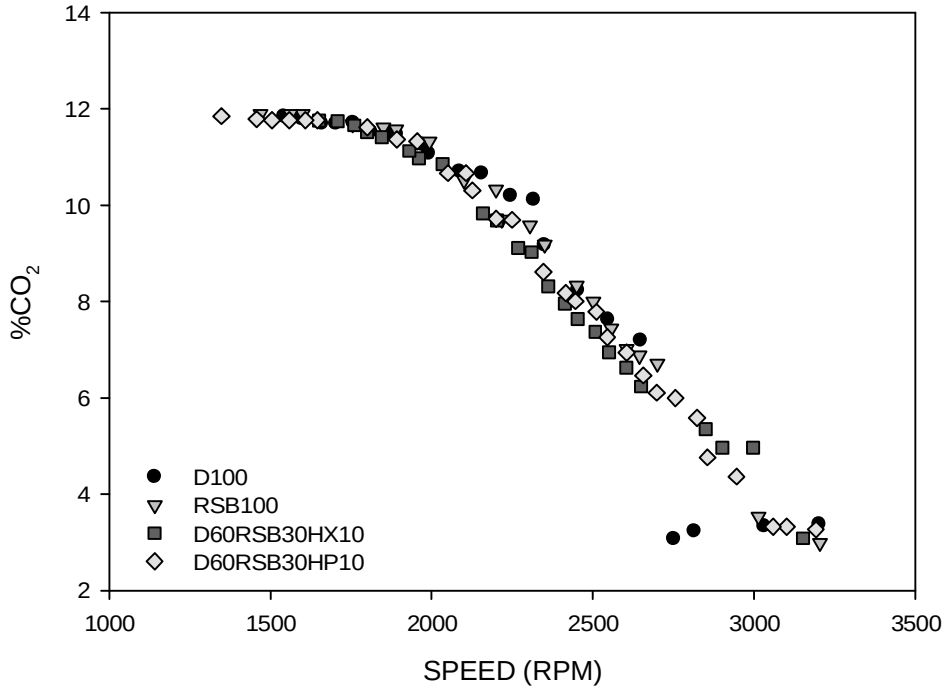


Figure 7.83. CO_2-Speed Graphic of 60%Diesel, 30%RSB and 10%Alkenes

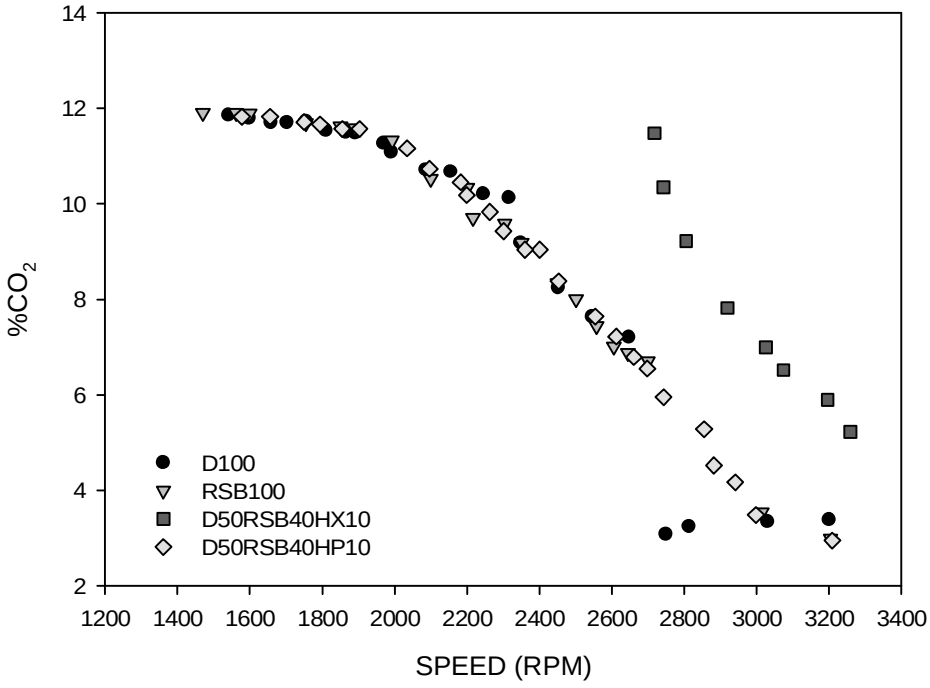


Figure 7.84. CO_2-Speed Graphic of 50%Diesel, 40%RSB and 10%Alkenes

The results were tabulated for pure diesel D100 in table 7.1, for pure rapeseed biodiesel RSB100 table 7.2, for the blend coded D50RSB40HX10 in table 7.11, and

for the blend coded D50RSB40HP10 in table 7.26. The gained values were shown in CO_2 emission versus speed graphic (figure 7.84). At the speed of maximum torque, the measured CO_2 emission rates were for the sample coded D100 11.72 %, for the sample coded RSB100 11.69%, the sample coded D50RSB40HX10 could not measured, for the sample coded D50RSB40HP10 11.66% respectively. Minimum CO_2 emission were obtained from the sample coded D100 3.38 % at 3201 rpm, the sample coded RSB100 2.99% at 3204 rpm, the sample coded D50RSB40HX10 5.23% at 3259 rpm, the sample coded D50RSB40HP10 2.95% at 3209 rpm.

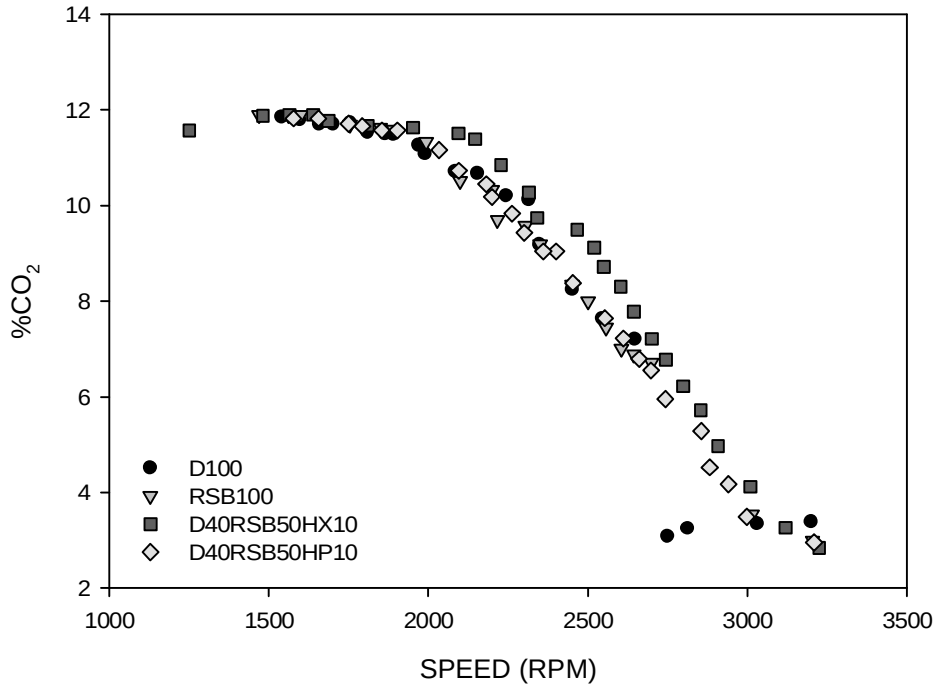


Figure 7.85. CO_2-Speed Graphic of 40%Diesel, 50%RSB and 10%Alkenes

The results were tabulated for pure diesel D100 in table 7.1, for pure rapeseed biodiesel RSB100 table 7.2, for the blend coded D40RSB50HX10 in table 7.12, and for the blend coded D40RSB50HP10 in table 7.27. The gained values were shown in CO_2 emission versus speed graphic (figure 7.85). At the speed of maximum torque, the measured CO_2 emission rates were for the sample coded D100 11.72 %, for the sample coded RSB100 11.69%, for the sample coded D40RSB50HX10 11.51%, for the sample coded D40RSB50HP10 11.79% measured respectively. Minimum CO_2 emission were obtained from the sample coded D100 3.38 % at 3201 rpm, the sample

coded RSB100 2.99% at 3204 rpm, the sample coded D40RSB50HX10 2.84% at 3225 rpm, the sample coded D40RSB50HP10 4.21% at 3170 rpm.

The results were tabulated for pure diesel D100 in table 7.1, for pure rapeseed biodiesel RSB100 table 7.2, for the blend coded D75RSB10HX15 in table 7.13, and for the blend coded D75RSB10HP15 in table 7.28. The gained values were shown in CO_2 emission versus speed graphic (figure 7.86). At the speed of maximum torque, the measured CO_2 emission rates were for the sample coded D100 11.72 %, for the sample coded RSB100 11.69%, for the sample coded D75RSB10HX15 11.9%, for the sample coded D75RSB10HP15 11.86% measured respectively. Minimum CO_2 emission were obtained from the sample coded D100 3.38 % at 3201 rpm, the sample coded RSB100 2.99% at 3204 rpm, the sample coded D75RSB10HX15 4.41% at 3200 rpm, the sample coded D75RSB10HP15 3.67% at 3209 rpm.

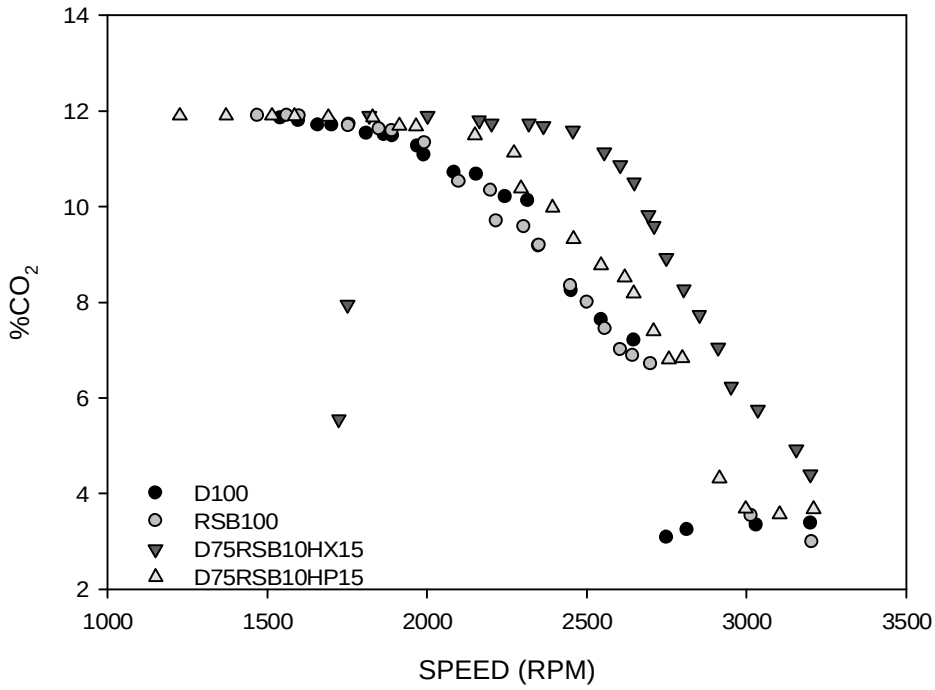


Figure 7.86. CO_2-Speed Graphic of 75%Diesel, 10%RSB and 15%Alkenes

The results were tabulated for pure diesel D100 in table 7.1, for pure rapeseed biodiesel RSB100 table 7.2, for the blend coded D65RSB20HX15 in table 7.14, and for the blend coded D65RSB20HP15 in table 7.29. The gained values were shown in

CO_2 emission versus speed graphic (figure 7.87). At the speed of maximum torque, the measured CO_2 emission rates were for the sample coded D100 11.72 %, for the sample coded RSB100 11.69%, for the sample coded D65RSB20HX15 11.83%, the sample coded D65RSB20HP15 could not measured. Minimum CO_2 emission were obtained from the sample coded D100 3.38 % at 3201 rpm, the sample coded RSB100 2.99% at 3204 rpm, the sample coded D65RSB20HX15 4.31% at 3201 rpm, the sample coded D65RSB20HP15 2.98% at 3154 rpm.

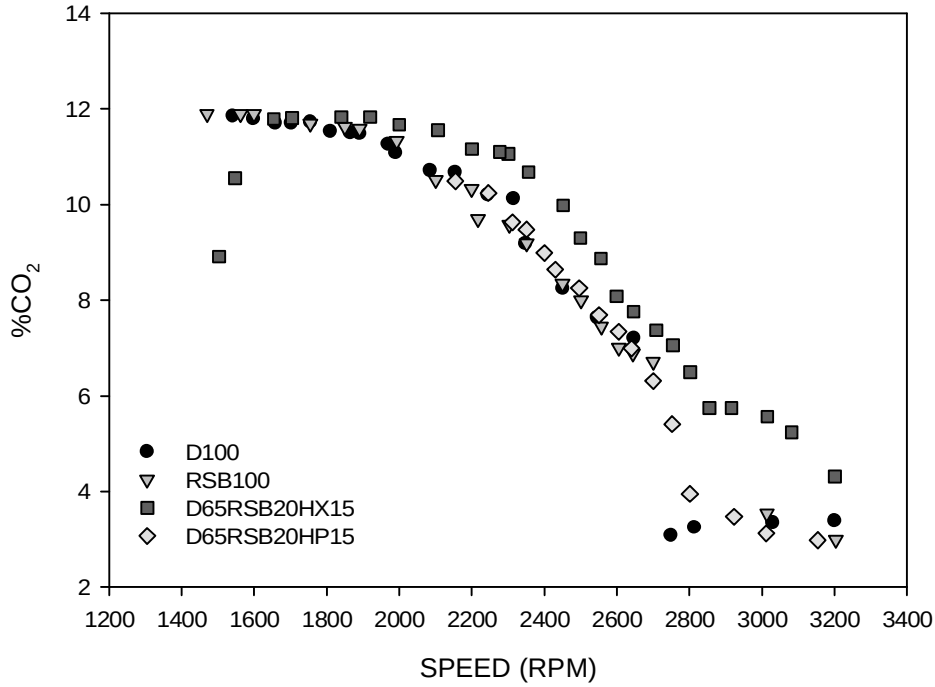


Figure 7.87. CO_2-Speed Graphic of 65% Diesel, 20% RSB and 15% Alkenes

The results were tabulated for pure diesel D100 in table 7.1, for pure rapeseed biodiesel RSB100 table 7.2, for the blend coded D55RSB30HX15 in table 7.15, and for the blend coded D55RSB30HP15 in table 7.30. The gained values were shown in CO_2 emission versus speed graphic (figure 7.88). At the speed of maximum torque, the measured CO_2 emission rates were for the sample coded D100 11.72 %, for the sample coded RSB100 11.69%, the sample coded D55RSB30HX15 could not measured, for the sample coded D55RSB30HP15 11.71% respectively. Minimum CO_2 emission were obtained from the sample coded D100 3.38 % at 3201 rpm, the

sample coded RSB100 2.99% at 3204 rpm, the sample coded D55RSB30HX15 3.06% at 3228 rpm, the sample coded D55RSB30HP15 3.12% at 3150 rpm.

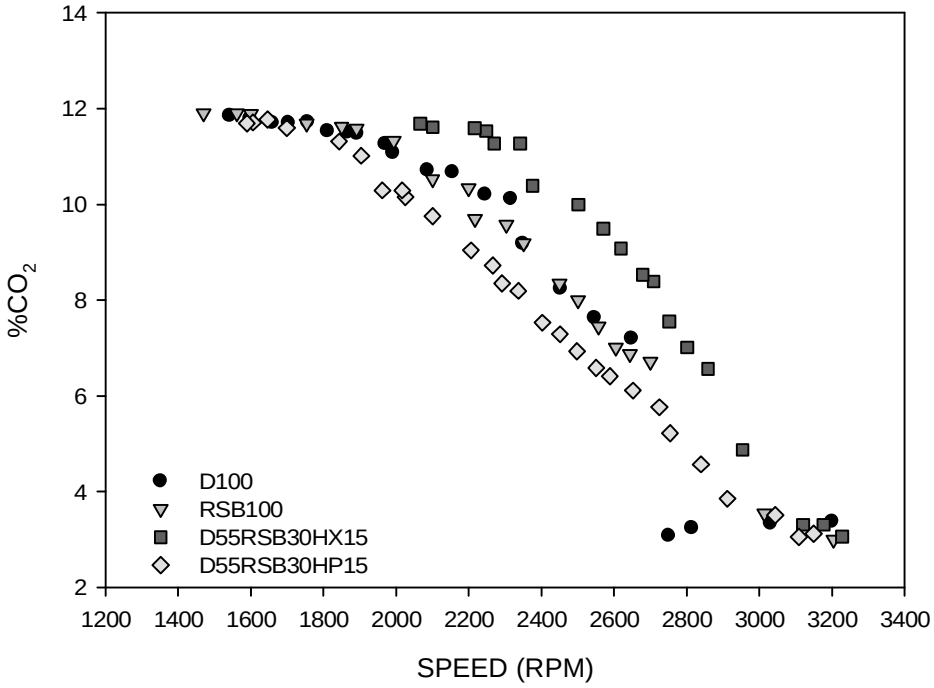


Figure 7.88. CO_2-Speed Graphic of 55% Diesel, 30% RSB and 15% Alkenes

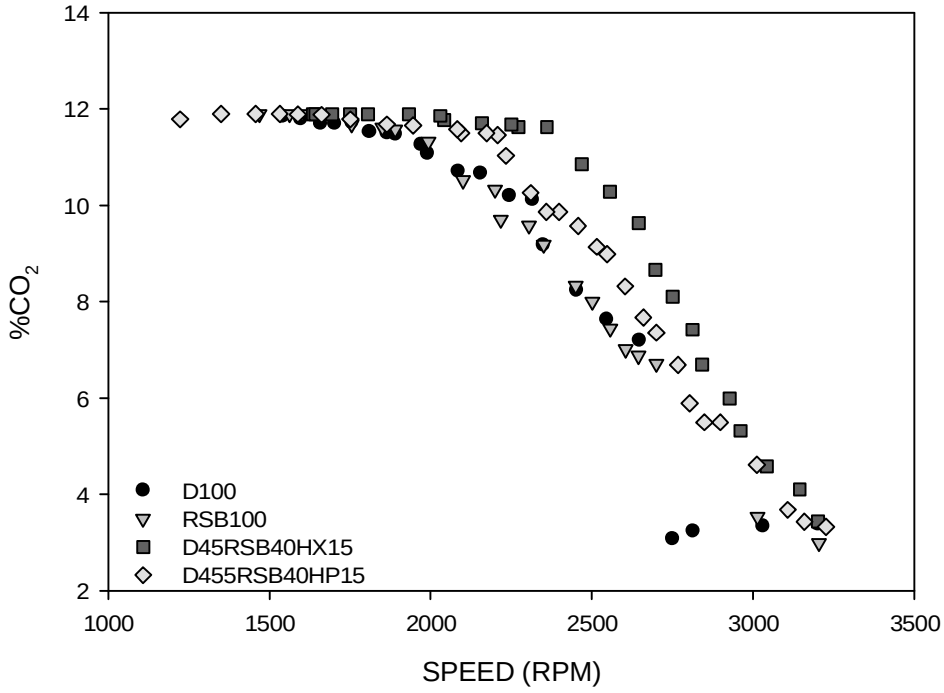


Figure 7.89. CO_2-Speed Graphic of 45% Diesel, 40% RSB and 15% Alkenes

The results were tabulated for pure diesel D100 in table 7.1, for pure rapeseed biodiesel RSB100 table 7.2, for the blend coded D45RSB40HX15 in table 7.16, and for the blend coded D45RSB40HP15 in table 7.31. The gained values were shown in CO_2 emission versus speed graphic (figure 7.89). At the speed of maximum torque, the measured CO_2 emission rates were for the sample coded D100 11.72 %, for the sample coded RSB100 11.69%, for the sample coded D45RSB40HX15 11.89%, for the sample coded D45RSB40HP15 11.68% measured respectively. Minimum CO_2 emission were obtained from the sample coded D100 3.38 % at 3201 rpm, the sample coded RSB100 2.99% at 3204 rpm, the sample coded D45RSB40HX15 3.44% at 3200 rpm, the sample coded D45RSB40HP15 3.33% at 3226 rpm.

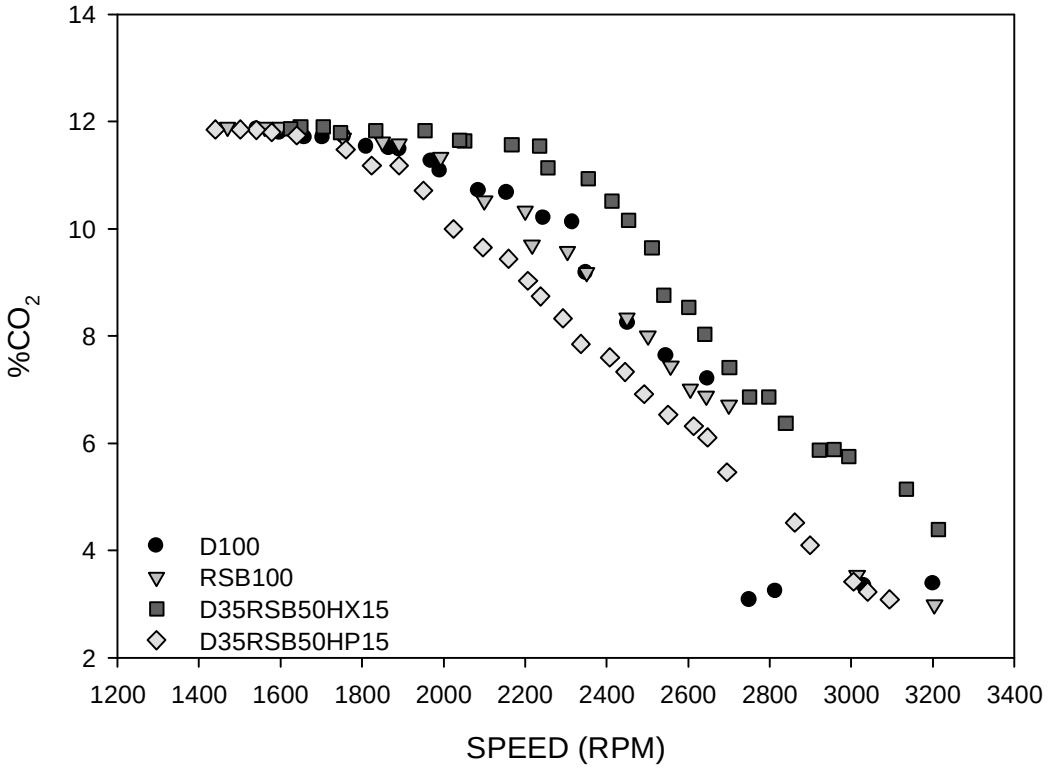


Figure 7.90. CO_2-Speed Graphic of 35% Diesel, 50% RSB and 15% Alkenes

The results were tabulated for pure diesel D100 in table 7.1, for pure rapeseed biodiesel RSB100 table 7.2, for the blend coded D35RSB50HX15 in table 7.17, and for the blend coded D35RSB50HP15 in table 7.32. The gained values were shown in CO_2 emission versus speed graphic (figure 7.90). At the speed of maximum torque,

the measured CO_2 emission rates were for the sample coded D100 11.72 %, for the sample coded RSB100 11.69%, for the sample coded D35RSB50HX15 11.79%, for the sample coded D35RSB50HP15 11.48% measured respectively. Minimum CO_2 emission were obtained from the sample coded D100 3.38% at 3201 rpm, the sample coded RSB100 2.99% at 3204 rpm, the sample coded D35RSB50HX15 4.39% at 3214 rpm, the sample coded D35RSB50HP15 3.09% at 3094 rpm.

8. CONCLUSION AND RECOMMENDATIONS

Nowadays, the need of energy is increased paralel to the development of technology and industry. Fossil fuels which are the oldest and widely used energy source is decreasing rapidly while the need is increasing. Due to the increase in the price of the petroleum and the environmental concerns about pollution coming from the car gasses alternative fuels are becoming a developing area of high concern. Biodiesel is the one of the most important alternative fuel, since it can be produced different kinds of raw materials including refine, crude or frying oils. The raw materials are natural and renewable that makes biodiesel biodegradable and nontoxic. Producing biodiesel from refine, crude or frying oils will give social and economic benefits. These include:

- A reduced dependence on imports of foreign oil;
- Alternative market opportunities for agricultural crops;
- Rural economic development including job creation and increased rural income;
- Reducing carbon emissions;
- The replacement of fossil fuel with renewable fuel

The purpose of this study was to improve cold flow properties of high rated biodiesel – eurodiesel by using three different substances. The increased amount of biodiesel in the blend effects on fuel specifications, engine performance and emissions were also in concern.

In order to produce biodiesel from Rapeseed Oil, the used oil/ alcohol molar rate was 6:1. The used catalyst was NaOH with 0.4%. 25 liter of rapeseed oil was filled in the reactor and heated up to 50 °C. The methoxide (the mixture of methanol and sodium hydroxide) send to the reactor. Heater was set to 65 °C. The reaction took 2 hours. The produced biodiesel and eurodiesel were tested according to quality standards TS EN 14214 and European petrodiesel standard EN 590. 45 samples were prepared by mixing Eurodiesel, rapeseed biodiesel (10% to 50%) and three different substances. These substances were n-hexane, n-heptane and xylene with percentages

changing from 5%, 10% and 15%. The prepared mixtures were tested for their physical characteristics in order to evaluate the blends before engine performance tests. The blends with xylene had lower cetane ratings according to the other blends. Also the blends could not reach the desired value of standards. So a cetane improver (tert butyl peroxide) was added in order to increase the cetane number but this addition made the cetane results worse. This result was implied that blends of Xylene could not use in diesel engine. Adding n-hexane and n-heptane had positive effects on the physical characteristics of the blends, lowering density and viscosity, increasing cetane number and lower heating value of the blends, decreasing the pour point of the blend. But blends with %15 alkanes had lowered the densities below European petrodiesel standard EN 590 standards so blends with %15 would not be used as diesel fuel although the other physical specification stayed within the limits of the standards.

The performance test measurements showed that most of the blends had tendency to increase torque values according to pure Eurodiesel (D100). The reason for this increase was the improvement of the quality of fuel by adding alkenes to the mixture of biodiesel – eurodiesel blends. Being saturated hydrocarbons alkenes have tendency to ignite. Having more hydrogen atoms caused higher heating capacity. Cetane numbers of alkenes were high (n-heptane is accepted as 100 cetane) because of these specifications the blends combustion efficiency were increased. The measured maximum torque values were D100 264.695 Nm at 1756 rpm, RSB100 265.5885 Nm at 1754 rpm. Except M50RSB40HX10, M75RSB10HX15 and M55RSB40HX15 rest of the results showed an incline in the torque values. The decline was M50RSB40HX10 0.57% (263.191 Nm), M75RSB10HX15 0.11% (264.4 Nm) and M55RSB40HX15 1.39 % (261.021 Nm) respectively. The maximum incline was given by M45RSB50HP5 with 5.83% (280.13 Nm)

The improvements in the fuel quality of blends were showed tendency to increase the power. The measured maximum power values were D100 59.774 kW at 2245 rpm, RSB100 57.35 kW at 2217 rpm. Except M85RSB10HX5, M55RSB40HX5, M80RSB10HX10, M70RSB20HX10, M60RSB30HX10,

M55RSB40HP5, M60RSB30HP10, M50RSB40HP10, M65RSB20HP15, M55RSB30HP15 and M35RSB50HP15 rest of the results showed an incline in the power values. The decline was M85RSB10HX5 11.55% (52.869 kW), M55RSB40HX5 1.40% (58.981 kW), M80RSB10HX10 11.47% (52.917 kW), M70RSB20HX10 11.19% (53.079 kW), M60RSB30HX10 8.34% (54.784 kW), M55RSB40HP5 6.08% (56.137 kW), M60RSB30HP10 4.61% (57.017 kW), M50RSB40HP10 0.95% (59.234 kW), M65RSB20HP15 1.23% (59.033 kW), M55RSB30HP15 8.79% (54.516 kW), M35RSB50HP15 9.05% (54.36 kW) respectively. Maximum incline was given by M50RSB40HX10 with 15.31% (68.922 kW)

Specific Fuel Consumption (SFC) measures the amount of fuel needed to provide a given power for a given period. Most of the SFC values of blends were higher than biodiesel because the densities of blends were lower than biodiesel and the specific fuel consumption increases as density decreases. The measured minimum sfc values were D100 234.957 g/kWh at 2452 rpm, RSB100 186.919 g/kWh at 2217 rpm. Except M75RSB20HX5, M50RSB40HX10, M40RSB50HX10, M450RSB30HX15, M75RSB20HP5, M45RSB50HP5, M50RSB40HP10, M40RSB50HP10, M75RSB10HP15 and M45RSB40HP15 rest of the results showed an decline in the sfc values. The incline was M75RSB20HX5 3.39% (242.933 g/kWh), M50RSB40HX10 1.04% (237.400 g/kWh), M40RSB50HX10 1.07% (237.48 g/kWh), M45RSB40HX15 6.39% (249.957 g/kWh), M75RSB20HP5 0.87% (237.009 g/kWh), M45RSB50HP5 5.47% (246.33 g/kWh), M50RSB40HP10 2.58% (241.013 g/kWh), M40RSB50HP10 3.72% (243.690 g/kWh), M75RSB10HP15 3.11% (242.271 g/kWh) and M45RSB40HP15 7.22% (251.914 g/kWh) respectively.

The exhaust gas analyzer, which was used during tests, lasted measuring before the test ends because of the dense emission. Therefore, some of the samples CO emissions could not measured. The maximum CO emission results were taken at different engine speeds where the CO sensor cut off the measuring.

CO_2 was calculated by the exhaust gas analyzer with measuring O_2 in the exhaust. As the load was increased on the dynamometer, the value of $\%O_2$ decreased and $\%$ CO_2 level increased which means good combustion.

High NO_x emissions were measured between 2800-2200 rpm engine speed. At high speeds low NO_x emissions were measured nevertheless, the emission rate were shown rapid increase as the engine speed decreases. After 2200 rpm NO_x emissions were lowered.

The obtained results showed that all the blends, which were prepared from n-hexane and n-heptane up to a percentage of 10 (except D45RSB50HP5 which had higher density value than the limitation of the standart European petrodiesel standard EN 590), had physical characteristics within the limits of EN 590. The blends even with high percentages of rapeseed biodiesel could be used in engines as fuel without any modification. The fuel quality results showed that blends of n-hexane had better results than n-heptane. Although the performance results indicated that there was a decrease in maximum torque 0.57% and increase in specific fuel consumption 1.04% the suitable blend was D50RSB40HX10 with an increased power rating 15.31%.

In the European Union diesel fuel ought to mix with %5 biodiesel from the beginning of 2010. The firms which are distributing the fuels could mix the eurodiesel fuel with biodiesel and also might add n-hexane as %25 of biodiesel could achieve the EN 590 standarts. If this mixture prepared and marketed, the dependence on imports of foreign oil could be reduced. Besides when hexane is used as fuel additives by fuel distribution firms, this mixture of fuel will be taxed and the income from taxes will be increased.

Having poor cold flow properties and high viscosities, biodiesels, which are produced from animal fat, would be investigated by using n-hexane in order to improve the poor specifications of the biodiesel for future works. On the other hand, emission test would be carried out for unregulated emissions.

REFERENCES

ABDULVAHITOĞLU A., DEMIRAY A, AYDIN K. "Fuel quality investigation of diesel fuel, biodiesel and different hydrocarbon blends" University of Çukurova Faculty of Engineering and Architecture, 30th Annual Symposium, Pages 606-610, 16-17 October 2008, ADANA

ADEBANJO A. "Production of Fuels and Chemicals from Biomass Derived Oil and Lard" A Thesis Submitted to the College of Graduate Studies and Research in partial fulfillment of the requirements for the degree of Master of Science in the Department of Chemical Engineering University of Saskatchewan Saskatoon, Saskatchewan, January 2005

AGARWAL D., SINHA S., AGARWAL A. K. "Experimental investigation of control of NOx emissions in biodiesel-fueled compression ignition engine" Renewable Energy 31, Pages 2356–2369, 2006

ALBUQUERQUE M.C.G. , MACHADO Y.L., TORRES A.E.B., AZEVEDO D.C.S., CAVALCANTE JR. C.L., FİRMİANO L.R., PARENTE, JR. E.J.S. "Properties of biodiesel oils formulated using different biomass sources and their blends" Renewable Energy, Volume 34, Issue 3, , Pages 857-85, March 2009

ALPTEKIN E, ÇANAKÇI M. "Determination of the density and the viscosities of biodiesel– diesel fuel blends ination of the density and the viscosities of biodiesel–diesel fuel blends", Renewable Energy, Volume 33, Issue 12, Pages 2623-2630, December 2008

ALPTEKIN, E. ÇANAKÇI M. "Characterization of the key fuel properties of methyl ester–diesel fuel blends", Fuel, Volume 88, Issue 1, Pages 75-80, January 2009

Anonymous, 2008a http://hood.eas.asu.edu/che211/wiki/index.php/Biofuels

Anonymous, 2008b http://www.biofuels.ru/biodiesel/what_bd/

Anonymous, 2008c http://www.eere.energy.gov/afdc/fuels/biodiesel/alternative.html

Anonymous, 2008d http://www.eere.energy.gov/afdc/fuels/biodiesel/production.html

Anonymous, 2008e http://www.eere.energy.gov/afdc/fuels/properties.html

Anonymous, 2008f http://www.fueleconomy.gov/feg/biodiesel.shtml

Anonymous, 2008i http://www.euromot.org/download/news/positions/fuels/BIOFUELS position EMAtestspecificationsmay06.pdf

Anonymous, 2008g http://www.dieselnet.com/tech/diesel_fund.html

Anonymous, 2008h http://cu-ocw.eng.chula.ac.th/cu/eng/me/2103471/lecture-notes-1/9-2013471-Compression Ignition Engine Combustion

Anonymous, 2008j http://www.sigmaaldrich.com/catalog/search/Productdetail/riedel/15677 23.07.2008

Anonymous, 2008k http://www.sigmaaldrich.com/catalog/search/Productdetail/riedel/16446 23.07.2008

Anonymous, 2008 l http://www.carloerbareagenti.com/Repository/DIRI199/ENCH0023.htm 23.07.2008

Anonymous, 2009 a http://en.wikipedia.org/wiki/hexane 13.03.2009

Anonymous, 2009 b http://en.wikipedia.org/wiki/heptane 13.03.2009

Anonymous, 2009 c http://en.wikipedia.org/wiki/Xylene 13.03.2009

Anonymous, 2009d http://www.mitsubishi-Motors.co.nz/Trucks/pdf/canter/old%20models/7700%20MID%20Canter%202.0%20C4_FA2.pdf 31.08.2009

BALAT M, BALAT H, "A critical review of bio-diesel as a vehicular fuel", Energy Conversion and Management, Volume 49, Issue 10, Pages 2727-2741, October 2008

BHALE P. V, DESHPANDE N. V., THOMBRE S. B. "Improving the low temperature properties of biodiesel fuel" Renewable Energy, Volume 34, Issue 3, Pages 794-800, March 2009

BOZBAŞ K. "Biodiesel as an alternative motor fuel: Production and policies in the European Union" Renewable and Sustainable Energy Reviews 12, Pages 542–552 2008

BROWN R.C. “Biorenewable Resources Engineering New Products from Agriculture” Page 179, Iowa State Press, 2003

CANOIRA L., ALCÁNTARA R., TORCAL S., TSIOUVARAS N., LOIS E., KORRES D.M. “Nitration of biodiesel of waste oil: Nitrated biodiesel as a cetane number enhancer” Fuel, Volume 86, Issues 7-8, Pages 965-971, May 2007

CAO P., DUBÉ M. A., TREMBLAY A. Y. “High-purity fatty acid methyl ester production from canola, soybean, palm, and yellow grease lipids by means of a membrane reactor” Biomass and Bioenergy, Volume 32, Issue 11, Pages 1028-1036 November 2008

CHIU C., SCHUMACHER L.G., SUPPES G. J.; “Impact of cold flow improvers on soybean biodiesel blend” Biomass and Bioenergy, 27, Pages 485–491,2004

CROOKES R.J. “Comparative bio-fuel performance in internal combustion engines” Biomass and Bioenergy, 30, Pages 461–468, 2006

DEMIRBAŞ A. “Importance of biodiesel as transportation fuel” Energy Policy 35 , Pages 4661–4670, 2007

DOE/GO-102006-2358 “Biodiesel Handling And Usage” http://www.nrel.gov/docs/fy06osti/40555.pdf

DZIDA M., PRUSAKIEWICZ P. “The effect of temperature and pressure on the physicochemical properties of petroleum diesel oil and biodiesel fuel” Fuel 87, Pages 1941–1948, 2008

GERPEN J. V. “Biodiesel production” P. Ranalli (ed.), Improvement of Crop Plants for Industrial End Uses, Pages 281–289, Springer, 2007.

GERPEN J. V, SHANKS B., PRUSZKO R., CLEMENTS D., KNOTHE G. “USDA/NCAUR Biodiesel Production Technology” August 2002–January 2004, NREL/SR-510-36244, July 2004

GERPEN J. V, “Basics of Diesel engines and Diesel Fuels” KNOTHE, G., GERPEN J.V., KRAHL J. as editors The Biodiesel Handbook Chapter 3 Pages 17-25, ISBN 1-893997-79-0, 2004

GUO, Y. “Volatility of blended fuel of biodiesel and ethanol”, Energy & Fuels 21, 2, pages 1188-1192. Retrieved November 25, 2007, from ACS Publications Web of Science database.

International Energy Outlook 2007 http://www.eia.doe.gov/oiaf/archive/ieo07/pdf/0484(2007).pdf

ISSARIYAKUL T., KULKARNI M. G., MEHER L. C., DALAI A. K., BAKHSHI N. N., “Biodiesel production from mixtures of canola oil and used cooking oil” Chemical Engineering Journal 140, Pages 77–85, 2008

KESKIN A., GÜRÜ M., ALTIPARMAK D. “Biodiesel production from tall oil with synthesized Mn and Ni based additives: Effects of the additives on fuel consumption and emissions” Fuel, Volume 86, Issues 7-8, Pages 1139-1143, May 2007

KESKIN A., GÜRÜ M., ALTIPARMAK D., AYDIN K. “Using of cotton oil soapstock biodiesel–diesel fuel blends as an alternative diesel fuel” Renewable Energy, Volume 33, Issue 4, , Pages 553-557, April 2008

KLEINOVÁ A., PALIGOVÁ J. M. VRBOVÁ, MIKULEC J. AND CVENGROS J. “Cold Flow Properties of Fatty Esters” Trans IChemE, Part B, Process Safety and Environmental Protection, 85(B5): Pages 390–395, 2007

KNOTHE, G., DUNN, R.O. “Biodiesel: an alternative diesel fuel from vegetable oils or animal fats”. In: Erhan, S.Z., editor. Industrial Uses of Vegetable Oils. Chapter 4. Champaign, IL: AOCS Press. Pages 42-89 2005.

LABECKAS G., SLAVINSKAS S. “The effect of rapeseed oil methyl ester on direct injection Diesel engine performance and exhaust emissions” Energy Conversion and Management, Volume 47, Issues 13-14, Pages 1954-1967, 2006

MA F., HANNA M. A. “Biodiesel production: a review” Bioresource Technology 70 Pages 1-15 , 1999

MAKAREVICIENE V., JANULIS P. “Environmental effect of rapeseed oil ethyl ester” Renewable Energy 28 , Pages 2395–2403, 2003

MEHER L.C., SAGAR D. V., NAIK S.N. "Technical aspects of biodiesel production by transesterification-a review" Renewable and Sustainable Energy Reviews 10 , Pages 248–268, 2006

MÉNDEZ M. C. "Feasibility Study of a Biodiesel Production Plant from Oilseed" Master Thesis University of Strathclyde Glasgow, December 2006

MURUGESAN, A., C. UMARANI SUBRAMANIAN R. NEDUNCHEZHIAN N., Bio-diesel as an alternative fuel for diesel engines—A review, Renew Sustain Energy Rev (2008), doi:10.1016/j.rser.2007.10.007

NABI N., AKHTER S., SHAHADAT Z. "Improvement of engine emissions with conventional diesel fuel and diesel–biodiesel blends" Bioresource Technology 97 , Pages 372–378, 2006

NWAFOR O.M.I., "Emission characteristics of diesel engine operating on rapeseed methyl ester" Renewable Energy 29 , Pages 119–129, 2004

OZSEZEN A. N., CANAKCI M., TURKCAN A., SAYIN C. "Performance and combustion characteristics of a DI diesel engine fueled with waste palm oil and canola oil methyl esters" Fuel, Volume 88, Issue 4, Pages 629-636, April 2009

RADICH, A. "Biodiesel Performance, Costs, and Use", http://www.eia.doe.gov/oiaf/analysispaper/biodiesel/ 2008

RAKOPOULOS C.D., ANTONOPOULOS K.A., RAKOPOULOS D.C., HOUNTALAS D.T., GIAKOUMIS E.G. "Comparative performance and emissions study of a direct injection Diesel engine using blends of Diesel fuel with vegetable oils or bio-diesels of various origins" Energy Conversion and Management 47, Pages 3272–3287, 2006

SOLTIC P., EDENHAUSER D., THURNHEER T, SCHREIBER D, SANKOWSKI A, "Experimental investigation of mineral diesel fuel, GTL fuel, RME and neat soybean and rapeseed oil combustion in a heavy duty on-road engine with exhaust gas aftertreatment" Fuel 88 Pages 1–8, 2009

SRIVASTAVA A., PRASAD R. "Triglycerides-based diesel fuels" Renewable and Sustainable Energy Reviews 4, Pages 111-133, 2000

STRONG C., ERICKSON C, SHUKLA D. http://www.mdt.mt.gov/research/ docs/ research_proj/ biodiesel/final_report.pdf 2009

TSOLAKIS A., MEGARITIS A. WYSZYNSKI M.L., THEINNOI K.; "Engine performance and emissions of a diesel engine operating on diesel-RME (rapeseed methyl ester) blends with EGR (exhaust gas recirculation)" Energy, Volume 32, Issue 11, Pages 2072-2080, November 2007

TÜCCAR G., GÜNGÖR C., DEMIRAY A., ABDULVAHITOĞLU A., ÖZGÜR T., AYDIN K. "Investigation of fuel properties and engine performance of rapeseed oil biodiesel, diisoprophylether and diesel fuel blends" New and Renewable Energy Resources Symposium Proceedings Book, ISBN 978-9944-89-798-3, MMO Yayın No:E/2009/512, Pages 86-92, 16-17 Ekim, Kayseri,2009

VAN BASSHUYSEN R., and SCHÄFER F, "Internal combustion engine handbook : basics, components, systems, and perspectives", SAE International and Professional Engineering Publishing ISBN: 978-0-7680-1139-5, Pages 629-634 , 2004

WU F., WANG J., CHEN W., SHUAI S. "A study on emission performance of a diesel engine fueled with five typical methyl ester biodiesels" Atmospheric Environment 43 Pages 1481–1485, 2009

ZHENG M., MULENGA M. C., READER G. T., WANG M., TING D. S-K. TJONG J. "Biodiesel engine performance and emissions in low temperature combustion" Fuel, Volume 87, Issue 6, Pages 714-722, May 2008

CIRRICULUM VITAE

Aslı Abdulvahitoğlu was born on November 24, 1972 in Adana. After completing her education in Adana Anadolu High School, she enrolled in Çukurova University Mechanical Engineering Department in 1991. She had graduated from the Mechanical Engineering Department with a Bachelor Degree of Science in 1995. She worked in ELBA Basincli Dőkűm Sanayii A.S. as a quality control engineer (Bursa-1997), Bayraktarlar A.Ş. FARBA Otomotiv Aydınlatma ve Plâstik Fabrikaları as production planning engineer (Bursa, 1998-1999), TUBITAK UNIVERSITE SANAYİ Ortak Araştırma Merkezi (USAM) as a specialist (ADANA 2000-2002). She had obtained Master of Science degree from Mechanical Engineering Department of Çukurova University in 2003. She had commenced the study to the degree of Doctor of Philosophy in 2004 at the Department of Mechanical Engineering in Çukurova University.

APPENDIXES

Table 7.1. Performance and Emission Results for Fuel Coded D100

Speed (rpm)	Torque (Nm)	PB (kW)	mf (g/s)	Sfc (g/kWh)	bmep	ma (kg/s)	AFR	v (%)	b (%)	O_2 %	CO_2 %	CO ppm	NO ppm	NO_2 ppm	NO_x ppm
3201	16.640	5.564	1.78	1151.667	58.59	0.12	67.04	60.52	6.85	15.04	3.38	598	226	0.90	227
3031	91.561	26.997	2.02	268.777	322.40	0.12	57.60	62.19	29.34	15.11	3.34	602	214	2.00	216
2814	148.281	42.595	2.86	241.963	522.12	0.11	39.07	64.54	32.59	15.28	3.24	585	204	4.00	208
2750	159.618	45.944	3.12	244.757	562.04	0.11	35.40	65.28	32.22	15.57	3.08	587	18	4.90	185
2648	184.697	51.253	3.46	242.999	650.35	0.11	31.36	66.53	32.46	8.29	7.20	181	1100	14.90	1115
2546	210.642	56.030	3.79	243.541	741.71	0.11	28.07	67.84	32.38	7.54	7.63	183	1194	16.90	1211
2452	226.748	58.461	3.82	234.957	798.42	0.10	27.36	69.13	33.57	6.46	8.24	284	1184	18.00	1202
2349	241.007	59.264	4.11	249.744	848.62	0.10	24.85	70.62	31.58	4.79	9.18	708	1118	17.10	1135
2316	245.829	59.350	4.18	253.639	865.60	0.10	24.26	71.12	31.09	3.14	10.12	1948	1065	15.40	1081
2245	250.255	59.774	4.16	250.333	881.19	0.10	24.03	72.23	31.51	3.01	10.20	2195	1053	15.20	1068
2155	255.427	57.497	4.31	269.975	899.40	0.10	22.69	73.72	29.21	2.18	10.67	4041	970	13.80	984
2086	259.248	57.278	4.38	275.106	912.86	0.10	21.99	74.92	28.67	2.10	10.71	4969	963	13.10	976
1991	260.551	54.707	4.44	291.992	917.44	0.09	21.19	76.68	27.01	1.45	11.08		892	11.80	904
1970	262.922	54.147	4.50	299.345	925.79	0.09	20.77	77.09	26.35	1.12	11.26		848	10.70	858
1892	264.030	52.512	4.60	315.542	929.69	0.09	19.91	78.66	24.99	0.74	11.48		759	9.80	769
1866	263.721	51.860	4.60	319.507	928.61	0.09	19.78	79.20	24.68	0.71	11.50		738	9.30	747
1811	264.097	49.934	4.71	339.786	929.93	0.09	19.03	80.39	23.21	0.65	11.53		704	8.70	713
1756	264.695	48.890	4.81	354.053	932.04	0.09	18.36	81.63	22.28	0.31	11.72		654	7.80	662
1703	264.400	48.106	4.95	370.330	931.00	0.09	17.57	82.89	21.30	0.36	11.70		626	7.10	634
1659	262.868	46.569	4.95	382.554	925.60	0.09	17.34	83.97	20.62	0.35	11.70		602	6.50	608
1598	260.578	44.040	5.33	435.741	917.54	0.08	15.80	85.55	18.10	0.19	11.79		527	5.80	533
1542	258.536	42.427	5.44	461.337	910.35	0.08	15.21	87.09	17.10	0.08	11.85		496	5.60	502
1513	257.784	40.975	5.49	482.524	907.70	0.08	14.92	87.91	16.34						
1473	256.212	40.313	5.57	497.239	902.17	0.08	14.52	89.09	15.86						
1358	251.699	36.813	5.79	565.877	886.27	0.08	13.41	92.77	13.94						

Table 7.2. Performance and Emission Results for Fuel Coded RSB100

Speed (rpm)	Torque (Nm)	PB (kW)	mf (g/s)	Sfc (g/kWh)	bmep	ma (kg/s)	AFR	v (%)	b (%)	O_2 %	CO_2 %	CO ppm	NO ppm	NO_2 ppm	NO_x ppm
3204	11.415	3.491	1.795	1362.186	40.194	0.116	65	58.90	4.93	15.72	2.99	539	186	59	245
3014	71.721	19.552	3.219	436.217	252.542	0.113	35	60.63	15.40	14.76	3.54	528	288	59.5	347
2700	157.106	44.032	3.635	218.736	553.197	0.106	29	63.85	30.72	9.17	6.71	244	1046	44.5	1090
2644	166.986	46.511	3.470	197.652	587.985	0.105	30	64.48	34.00	8.87	6.88	181	1091	37	1128
2605	173.172	47.285	3.630	203.406	609.766	0.104	29	64.93	33.04	8.64	7.01	168	1118	33.2	1151
2557	186.551	49.526	3.590	192.059	656.875	0.103	29	65.49	34.99	7.86	7.44	179	1156	30.7	1187
2501	201.219	52.631	4.001	201.425	708.526	0.102	26	66.17	33.36	6.88	8	186	1160	27.4	1187
2450	210.078	54.101	4.086	200.127	739.719	0.101	25	66.81	33.58	6.28	8.34	218	1180	24.9	1205
2351	225.546	55.501	4.016	191.728	794.184	0.099	25	68.10	35.05	4.78	9.19	562	1100	21	1121
2304	232.887	56.280	4.046	190.488	820.032	0.098	24	68.74	35.28	4.1	9.58	957	1071	19.2	1090
2217	244.103	57.355	4.046	186.919	859.527	0.096	24	69.97	35.95	3.88	9.7	1054	1057	18.3	1075
2200	244.989	56.377	4.156	195.346	862.649	0.096	23	70.52	34.40	2.76	10.33	2049	974	16.3	990
2100	253.096	55.461	4.046	193.301	891.193	0.095	24	73.57	34.76	2.44	10.52	2656	957	15.6	973
1993	259.994	54.678	4.267	206.759	915.481	0.093	22	75.59	32.50	1	11.33		835	11.4	847
1891	263.359	52.813	4.447	223.116	927.330	0.090	20	77.44	30.12	0.56	11.58		733	7.4	740
1850	264.460	51.497	4.422	227.530	931.208	0.088	20	76.93	29.53	0.5	11.62		700	6.5	706
1754	265.588	49.181	4.698	253.099	935.181	0.087	18	80.17	26.55	0.37	11.69		615	5.1	620
1600	265.152	45.227	3.505	205.322	933.644	0.084	24	85.35	32.73	0.02	11.89		430	3.8	434
1562	262.828	43.792	3.505	212.048	925.461	0.080	23	83.10	31.69	-0.01	11.9		379	3.8	383
1470	259.940	41.126	7.161	230.747	915.292	0.079	11	87.13	14.56	-0.02	11.9		290	4.4	295

Table 7.3. Performance and Emission Results for Fuel Coded D85RSB10HX5

Speed (rpm)	Torque (Nm)	PB (kW)	mf (g/s)	Sfc (g/kWh)	bmep	ma (kg/s)	AFR	v (%)	b (%)	O_2 %	CO_2 %	CO ppm	NO ppm	NO_2 ppm	NO_x ppm
3201	16.090	5.399	2.778	1852.292	56.654	0.115	41	58.18	4.34	16.28	2.67	785	171	8.7	180
3104	46.777	13.395	3.896	1046.981	164.708	0.113	29	59.01	7.68	12.29	4.93	665	598	23.6	621
2988	72.138	19.918	2.621	473.767	254.008	0.111	42	60.05	43.48	12.03	5.09	659	641	24.3	665
2884	99.446	28.634	2.417	303.833	350.167	0.109	45	61.03	26.46	11.79	5.22	647	679	25.9	704
2800	107.949	31.661	2.790	317.286	380.107	0.107	38	61.85	69.80	11.27	5.52	636	731	27.4	758
2758	105.713	30.600	5.209	612.877	372.232	0.106	20	62.28	13.12	10.77	5.80	625	804	27.9	832
2651	131.221	36.362	2.587	256.138	462.052	0.104	40	63.41	31.38	9.28	6.64	610	885	27	912
2613	141.484	38.752	3.068	285.059	498.188	0.103	34	63.82	28.20	8.85	6.89	605	921	26.5	947
2500	167.987	43.849	2.993	245.746	591.509	0.100	34	65.10	32.71	8.00	7.37	600	978	24.8	1002
2445	179.969	46.084	3.470	271.038	633.699	0.099	29	65.76	29.66	6.95	7.96	623	1021	23	1044
2400	187.880	47.299	3.058	232.783	661.558	0.098	32	66.30	34.53	5.98	8.51	663	988	21.9	1010
2355	196.101	48.224	3.033	226.444	690.505	0.097	32	66.87	35.50	5.37	8.86	752	975	20.1	995
2303	208.184	50.067	3.284	236.137	733.050	0.096	29	67.53	34.04	4.36	9.43	1048	931	17.9	949
2242	217.936	51.477	3.394	237.382	767.389	0.095	28	68.34	33.86	4.02	9.62	1265	930	17.6	947
2151	232.074	51.659	3.439	239.691	817.171	0.092	27	69.60	33.54	3.12	10.13	1914	891	15.2	907
2106	234.149	52.869	3.439	234.206	824.478	0.091	27	70.25	34.32	3.04	10.18	2088	890	14.9	905
2043	242.068	52.097	3.505	242.182	852.361	0.090	26	71.19	33.19	2.01	10.76	4586	861	11.8	872
1956	249.395	51.789	3.816	265.228	878.163	0.088	23	72.54	30.31	1.24	11.20		804	8.9	813
1861	254.339	49.772	3.951	285.770	895.569	0.085	22	74.12	28.13	0.44	11.65		613	5.8	619
1800	256.085	48.229	3.851	287.425	901.717	0.084	22	75.18	27.97	0.21	11.78		480	5.3	486
1743	260.195	47.797	3.344	251.884	916.191	0.082	25	76.21	31.91	0.25	11.76		471	4.7	475
1614	265.474	44.478	3.858	312.248	934.779	0.078	20	78.71	825.35	0.23	11.77		428	3.6	431
1561	264.910	42.957	3.906	327.301	932.793	0.077	20	79.81	255.08						
1554	265.434	43.140	3.912	326.436	934.637	0.077	20	79.96	256.17						
1527	263.802	42.607	3.936	332.575	928.890	0.076	19	80.53	253.00						

Table 7.4. Performance and Emission Results for Fuel Coded D75RSB20HX5

Speed (rpm)	Torque (Nm)	PB (kW)	mf (g/s))	Sfc (g/kWh)	bmep	ma (kg/s)	AFR	v (%)	b (%)	O_2 %	CO_2 %	CO ppm	NO ppm	NO_2 ppm	NO_x ppm
3165	62.097	17.152	1.624	340.962	218.653	0.115	71	60.19	23.90	12.72	4.69	341	466	18.5	485
3013	107.459	32.137	1.419	158.946	378.380	0.112	79	61.56	51.27	11.14	5.59	291	657	22.9	680
2850	146.561	44.469	3.876	313.758	516.067	0.109	28	63.15	25.97	9.42	6.56	211	893	23.2	917
2800	175.999	51.197	3.620	254.543	619.722	0.108	30	63.66	32.02	7.88	7.43	174	1133	23.4	1156
2759	191.319	54.448	3.886	256.919	673.666	0.107	28	64.09	31.72	6.63	8.14	207	1247	23.2	1271
2697	205.336	57.983	4.091	254.019	723.023	0.106	26	64.75	32.08	5.83	8.6	314	1256	22.7	1279
2648	220.361	60.628	4.091	242.933	775.926	0.105	26	65.29	33.55	4.61	9.29	668	1224	20.5	1244
2588	230.012	62.414	4.277	246.682	809.910	0.103	24	65.97	33.04	3.61	9.86	1170	1152	18.7	1171
2492	242.330	63.104	4.372	249.420	853.283	0.101	23	67.10	32.68	2.03	10.75	3332	1068	16.7	1085
2471	249.013	63.756	4.452	251.398	876.815	0.101	23	67.35	32.42	1.54	11.03	4812	972	15.1	987
2295	255.628	61.639	6.272	366.333	900.109	0.097	15	69.61	22.25	0.7	11.51		787	12.5	799
2197	260.269	60.407	4.307	256.671	916.451	0.094	22	70.97	31.75	0.45	11.65		676	10.9	686
2161	265.588	60.317	5.704	340.446	935.181	0.094	16	71.49	23.94	0.32	11.72		609	9.4	618
1986	267.227	56.012	6.387	410.480	940.952	0.089	14	74.17	19.85	0.05	11.87		560	7.8	568
1952	266.005	54.998	6.519	426.724	936.647	0.088	14	74.73	19.10	0.04	11.87		560	7.8	568
1755	266.972	50.288	7.288	521.698	940.053	0.083	11	78.21	15.62	0	11.9		373	6	379
1551	258.201	42.388	8.083	686.500	909.167	0.077	10	82.36	11.87	0	11.9		256	7.1	263
1448	255.655	39.425	8.485	774.775	900.204	0.074	9	84.70	10.52	6.04	8.48		131	8	139
1368	249.778	37.633	8.797	841.511	879.511	0.072	8	86.66	9.68	6.04	8.48		131	8.3	139

Table 7.5. Performance and Emissions Results for Fuel Coded D65RSB30HX5

Speed (rpm)	Torque (Nm)	PB (kW)	mf (g/s)	Sfc (g/kWh)	bmep	ma (kg/s)	AFR	v (%)	b (%)	O_2 %	CO_2 %	CO ppm	NO ppm	NO_2 ppm	NO_x ppm
3241	65.891	18.688	1.73	334.19	232.01	0.12	70	60.74	24.78	15.37	3.19	319	231	39.5	173
3165	90.198	26.724	1.73	233.69	317.60	0.12	69	61.47	35.43	14.7	3.57	314	291	40.8	174
3001	137.716	41.397	2.78	241.99	484.92	0.12	42	63.13	34.22	12.39	4.88	288	526	42.6	177
2886	159.148	47.627	2.78	210.34	560.39	0.11	41	64.38	39.37	10.39	6.01	268	658	42.2	302
2852	166.684	49.703	3.45	250.21	586.92	0.11	33	64.76	33.09	8.97	6.82	186	1020	33.7	527
2801	186.893	53.869	3.72	248.62	658.08	0.11	30	65.35	33.30	7.77	7.5	162	1204	29.9	609
2755	198.170	56.745	3.92	248.74	697.79	0.11	28	65.90	33.29	7.15	7.85	169	1265	28.5	633
2698	214.423	59.897	4.16	250.12	755.02	0.11	26	66.59	33.10	6.35	8.3	209	1298	26.5	711
2654	223.161	61.891	4.16	242.06	785.79	0.11	26	67.14	34.21	5.6	8.73	291	1300	25	803
2600	231.503	63.266	4.07	231.66	815.16	0.11	27	67.84	35.74	3.96	9.65	844	1216	20.5	843
2556	239.448	64.450	4.45	248.69	843.14	0.11	24	68.42	33.29	3.71	9.8	1152	1196	19.4	875
2501	248.509	65.130	4.50	248.87	875.04	0.11	24	69.17	33.27	2.71	10.36	1818	1133	17.4	903
2450	249.187	64.390	4.50	251.73	877.43	0.10	23	69.89	32.89	2.57	10.44	2112	1128	16.9	918
2407	256.958	63.931	4.81	270.76	904.79	0.10	22	70.51	30.58	1.47	11.07		1049	12.7	931
2334	257.838	63.023	4.81	274.66	907.89	0.10	21	71.61	30.15	0.93	11.37		1013	12.3	928
2327	257.918	63.058	5.10	291.11	908.17	0.10	20	71.72	28.44	0.67	11.52		830	10.7	962
2246	262.794	62.207	5.15	297.99	925.34	0.10	20	73.01	27.79	0.52	11.61		808	8.3	960
2208	267.012	62.106	5.25	304.58	940.19	0.10	19	73.63	27.19	0.4	11.67		716	7.6	955
2019	269.773	58.953	5.40	330.06	949.91	0.10	18	77.01	25.09	0.32	11.72		640	6.2	975
1920	271.358	54.285	5.54	367.08	955.50	0.09	17	78.98	22.56	0.07	11.86		571	5.8	976
1830	268.644	53.063	5.62	381.32	945.94	0.09	16	80.91	21.71	0.07	11.86		549	5.4	973
1709	267.577	48.470	5.90	437.93	942.18	0.09	15	83.74	18.91	-0.02	11.9		427	5.1	945
1625	266.193	46.209	6.25	487.10	937.31	0.09	14	85.88	17.00	-0.07	11.9		344	4.7	911
1549	262.633	43.826	6.25	513.58	924.78	0.08	13	87.97	16.12	-0.06	11.9		317	4.7	902
1449	258.691	40.316	6.89	615.16	910.89	0.08	12	90.97	13.46	-0.05	11.9		291	5.4	890
1347	255.527	37.700	6.89	657.84	899.75	0.08	11	94.37	12.59	-0.02	11.9		291	5.4	867

Table 7.6. Performance and Emission Results for Fuel Coded D55RSB40HX5

Speed (rpm)	Torque (Nm)	PB (kW)	mf (g/s)	Sfc (g/kWh)	bmep	ma (kg/s)	AFR	v (%)	b (%)	O_2 %	CO_2 %	CO ppm	NO ppm	NO_2 ppm	NO_x ppm
3204	33.109	9.690	6.603	2453.227	116.582	0.122	18	61.36	3.44	9.06	6.76	607	893	26.6	920
3172	51.230	13.802	6.603	1722.339	180.388	0.121	18	61.68	4.91	9.06	6.76	606	901	26.5	927
3099	78.202	20.785	1.990	344.755	275.364	0.120	60	62.44	24.51	8.85	6.89	605	921	26.3	947
3023	98.956	28.645	1.990	250.155	348.440	0.118	59	63.25	33.78	8.58	7.04	603	942	26.1	968
2825	137.091	40.609	2.808	248.906	482.721	0.115	41	65.53	33.95	7.5	7.65	610	994	23.7	1018
2756	162.546	46.445	3.018	233.956	572.353	0.113	38	66.39	36.12	6.6	8.16	634	1009	22.5	1031
2694	179.391	50.753	3.304	234.366	631.665	0.112	34	67.18	36.06	5.61	8.72	718	981	20.7	1001
2648	190.224	52.921	3.620	246.254	669.812	0.111	31	67.79	34.31	4.62	9.28	963	939	18.3	957
2597	200.252	54.790	4.021	264.207	705.120	0.110	27	68.49	31.98	3.64	9.84	1480	914	16.5	931
2559	210.494	56.554	3.861	245.756	741.185	0.109	28	69.02	34.38	3.12	10.13	1914	891	15.2	907
2512	223.511	58.198	4.106	254.008	787.018	0.108	26	69.70	33.27	2.15	10.68	3566	865	12.5	877
2452	225.384	58.034	4.161	258.147	793.616	0.107	26	70.59	32.73	2.01	10.76	4265	863	12.3	876
2353	238.555	58.931	4.613	281.783	839.992	0.105	23	72.14	29.99	1.24	11.2		804	10	814
2204	250.228	57.602	5.249	328.080	881.095	0.102	19	74.69	25.76	1.1	11.28		780	8.2	789
2155	254.480	58.470	5.265	324.136	896.065	0.101	19	75.58	26.07	1.02	11.32		760	8.2	768
2100	254.258	56.424	5.265	335.894	895.285	0.100	19	76.63	25.16	1.02	11.32		760	8	768
2047	258.852	55.910	4.883	314.441	911.461	0.098	20	77.67	26.87	0.78	11.46		667	6.7	674
1955	257.139	52.609	5.024	343.781	905.430	0.096	19	79.60	24.58	0.44	11.65		613	5.8	619
1891	258.980	51.608	5.270	367.586	911.910	0.095	18	81.03	22.99	0.21	11.78		459	5.1	464
1860	260.786	51.538	5.270	368.087	918.272	0.094	18	81.75	22.96	0.23	11.77		459	5.1	464
1807	261.021	49.050	3.334	244.712	919.100	0.093	28	83.02	34.53	0.25	11.76		462	4.7	467
1759	260.639	48.651	5.094	376.929	917.752	0.092	18	84.23	350.40	0.25	11.76		453	4.5	457
1636	258.174	44.372	5.217	423.257	909.072	0.089	17	87.58	1298.32	0.24	11.76		409	4	413
1611	256.615	43.659	5.242	432.235	903.586	0.088	17	88.31	757.00	0.24	11.76		407	4	411

Table 7.7. Performance and Emission Results for Fuel Coded D45RSB50HX5

Speed (rpm)	Torque (Nm)	PB (kW)	mf (g/s)	Sfc (g/kWh)	bmep	ma (kg/s)	AFR	v (%)	b (%)	O_2 %	CO_2 %	CO ppm	NO ppm	NO_2 ppm	NO_x ppm
3241	45.004	12.676	1.975	561.009	158.465	0.121	61	61.17	15.19	13.35	4.34	432	363	48.5	412
3059	96.014	29.477	1.985	242.487	338.082	0.117	59	62.97	35.15	10.77	5.8	307	668	42.3	711
3013	108.319	32.529	1.985	219.737	381.408	0.117	59	63.45	38.79	9.9	6.29	307	668	42.3	711
2903	143.982	41.757	2.487	214.401	506.986	0.114	46	64.64	39.76	9.03	6.78	245	876	36.7	913
2849	158.375	47.224	3.429	261.439	557.666	0.113	33	65.25	32.60	8.62	7.02	175	983	29.6	1012
2816	177.786	52.313	3.931	270.506	626.013	0.113	29	65.63	31.51	7.43	7.69	144	1117	26.3	1143
2606	237.682	64.879	4.803	266.524	836.918	0.113	23	70.92	31.98	2.45	10.51	1134	1160	18.4	1178
2563	245.970	65.738	4.994	273.474	866.101	0.108	22	69.37	31.17	1.72	10.92	2488	1063	15.8	1079
2496	250.154	65.495	5.500	302.325	880.835	0.108	20	70.65	28.19	1.55	11.02	3766	1063	14.4	1078
2336	259.255	63.986	3.364	189.282	912.880	0.106	32	74.49	45.03	0.45	11.64		735	10.9	746
2249	264.668	63.318	5.368	305.187	931.941	0.103	19	74.86	27.93	0.31	11.73		625	9.3	634
2203	263.977	61.020	5.538	326.722	929.505	0.101	18	74.99	26.09	0.29	11.74		611	8.9	620
2075	266.193	58.191	6.012	371.904	937.310	0.100	17	78.79	22.92	0.06	11.87		514	8	522
1847	267.758	51.923	6.855	475.285	942.820	0.097	14	85.92	17.93	0.06	11.87		369	7.3	377
1810	270.344	51.626	6.992	487.565	951.925	0.091	13	82.72	17.48	0.06	11.87		341	7.3	348
1701	265.656	47.767	7.395	557.349	935.418	0.090	12	87.14	15.29	0.13	11.83		302	8	310
1606	262.344	44.553	7.747	625.967	923.759	0.088	11	89.48	13.62	0.21	11.78		287	10	297
1547	261.666	43.598	7.965	657.698	921.370	0.085	11	90.27	12.96	0.64	11.54		287	10	297

Table 7.8. Performance and Emission Results for Fuel Coded D80RSB10HX10

Speed (rpm)	Torque (Nm)	PB (kW)	mf (g/s)	Sfc (g/kWh)	bmep	ma (kg/s)	AFR	v (%)	b (%)	O_2 %	CO_2 %	CO ppm	NO ppm	NO_2 ppm	NO_x ppm
3104	22.934	6.942	1.544	800.840	80.753	0.115	75	60.609	10.078	15.6	3.06	343	224	4.5	228
3047	46.468	12.623	1.594	454.699	163.620	0.114	72	61.149	17.750	14.29	3.8	332	312	9.4	321
3005	60.653	17.016	1.594	337.316	213.568	0.113	71	61.555	23.927	14.29	3.8	323	385	11.2	396
2856	90.198	25.727	1.835	256.780	317.602	0.110	60	63.066	31.432	13.07	4.5	289	538	14.7	552
2745	117.097	33.157	2.572	279.261	412.317	0.108	42	64.267	28.901	11.5	5.38	207	759	18.5	777
2688	132.773	37.212	2.662	257.563	467.515	0.107	40	64.911	31.336	10.95	5.69	187	852	19.4	871
2650	143.720	39.912	2.743	247.374	506.063	0.106	39	65.351	32.627	10.45	5.98	157	966	20.5	986
2514	172.124	44.903	2.978	238.770	606.077	0.103	35	67.002	33.803	8.85	6.89	127	1050	21.9	1071
2467	178.652	46.147	2.938	229.205	629.064	0.102	35	67.602	35.213	8.4	7.14	128	1069	21.6	1090
2399	191.809	47.883	2.893	217.505	675.393	0.101	35	68.500	37.107	7.69	7.54	142	1115	21.2	1136
2350	197.344	48.134	3.129	233.996	694.880	0.100	32	69.169	34.492	7.3	7.76	151	1127	21	1148
2305	207.425	49.587	3.149	228.595	730.378	0.099	31	69.801	35.307	6.8	8.05	164	1094	20.1	1114
2236	218.339	51.168	3.154	221.882	768.808	0.097	31	70.805	36.375	6.05	8.47	201	1069	19	1088
2222	222.013	51.016	3.224	227.500	781.744	0.097	30	71.014	35.477	5.75	8.64	228	1062	18.5	1080
2040	245.278	52.917	3.414	232.289	863.666	0.092	27	73.909	34.746	3.57	9.88	964	990	14.9	1005
1943	259.953	52.802	3.560	242.706	915.339	0.090	25	75.603	33.254	2.32	10.58	3035	948	12.5	960
1909	262.936	52.434	3.510	240.967	925.840	0.089	25	76.225	33.494	1.88	10.84	4176	910	12	922
1844	267.140	51.788	3.510	243.971	940.644	0.088	25	77.457	33.082	1.33	11.14		851	10.5	861
1831	267.590	51.438	3.695	258.617	942.229	0.087	24	77.711	31.208	1.23	11.2		837	10	847
1703	274.004	49.065	3.790	278.112	964.814	0.084	22	80.348	29.021	0.74	11.48		698	8.2	706
1660	277.194	48.774	3.996	294.945	976.047	0.083	21	81.295	27.365	0.49	11.62		614	7.3	621
1616	277.584	47.412	4.001	303.800	977.419	0.082	20	82.299	26.567	0.24	11.76		541	6.7	547
1547	275.770	44.781	4.392	353.091	971.034	0.080	18	83.951	22.858	0.29	11.74		489	5.8	495
1536	274.703	44.728	4.603	370.452	967.273	0.079	17	84.224	21.787	0.32	11.72		487	5.6	493

Table 7.9. Performance and Emission Results for Fuel Coded D70RSB20HX10

Speed (rpm)	Torque (Nm)	PB (kW)	mf (g/s)	Sfc (g/kWh)	bmep	ma (kg/s)	AFR	v (%)	b (%)	O_2 %	CO_2 %	CO ppm	NO ppm	NO_2 ppm	NO_x ppm
3131	12.989	4.259	1.735	1466.430	45.736	0.119	69	62.48	5.59	15.09	3.35	474	300	7.5	307
3102	24.004	7.797	1.589	733.807	84.521	0.117	74	62.03	11.18	15.73	2.98	416	242	30.2	273
3000	56.074	17.616	1.519	310.457	197.447	0.115	76	63.16	26.42	14.91	3.45	409	336	31.1	367
2907	75.082	22.856	1.519	239.281	264.375	0.114	75	64.65	34.28	14.91	3.45	409	336	32.6	368
2859	86.184	25.803	1.970	274.914	303.467	0.110	56	63.34	29.84	14.11	3.90	395	436	33.8	470
2650	143.454	39.810	2.652	239.851	505.126	0.108	41	67.06	34.20	10.39	6.01	262	1006	34.9	1041
2550	162.052	43.274	2.973	247.346	570.611	0.107	36	69.02	33.17	9.30	6.63	179	1138	29.5	1168
2500	170.957	44.757	3.048	245.200	601.970	0.106	35	69.66	33.46	8.70	6.97	167	1169	27.5	1196
2447	182.751	46.830	3.073	236.271	643.498	0.105	34	70.66	34.72	8.22	7.24	168	1190	26.7	1217
2411	189.260	47.784	3.284	247.418	666.414	0.104	32	70.74	33.16	7.80	7.48	173	1216	25.5	1241
2344	200.933	49.322	3.199	233.484	707.517	0.102	32	71.95	35.13	7.22	7.81	188	1243	24.6	1267
2291	213.103	51.126	3.314	233.363	750.369	0.102	31	73.08	35.15	6.34	8.31	203	1244	23.6	1267
2257	220.088	52.018	3.239	224.156	774.965	0.101	31	73.68	36.60	5.97	8.52	230	1206	22.2	1229
2226	223.681	52.141	3.515	242.666	787.617	0.099	28	73.36	33.81	5.10	9.01	323	1177	20	1197
2144	232.365	52.170	3.515	242.531	818.196	0.098	28	75.55	33.82	4.87	9.14	404	1164	18.9	1183
2109	240.337	53.079	3.560	241.438	846.268	0.097	27	75.81	33.98	4.11	9.57	713	1117	16.7	1134
2053	242.292	52.090	3.560	246.023	853.150	0.096	27	76.87	33.34	3.41	9.97	1147	1086	15.5	1101
1999	252.339	52.823	3.560	242.608	888.529	0.095	27	77.87	33.81	3.12	10.13	1466	1079	14.9	1094
1943	252.836	51.445	3.605	252.267	890.279	0.094	26	79.29	32.52	2.13	10.69	3020	1041	12.9	1054
1902	260.318	51.849	3.660	254.128	916.625	0.093	25	80.04	32.28	1.93	10.81	4691	1032	11.5	1044
1856	261.689	50.862	3.660	259.062	921.449	0.090	25	79.90	31.67	1.25	11.19		951	10.9	962
1758	269.144	49.549	3.936	285.964	947.700	0.088	22	82.59	28.69	0.76	11.47		827	8.9	836
1683	273.879	48.269	3.936	293.543	964.373	0.086	22	84.32	27.95	0.76	11.47		827	8.9	836
1605	273.925	46.040	3.936	307.757	964.536	0.085	22	87.21	26.66	0.61	11.56		738	7.8	746
1560	271.830	44.407	4.172	338.178	957.160	0.084	20	89.09	24.26	0.41	11.67		589	6.9	596
1537	270.890	43.601	4.172	344.430	953.849	0.083	20	88.44	23.82	0.31	11.73		469	6.5	476
1468	269.110	41.370	4.653	404.889	947.582	0.081	17	90.30	20.26	0.17	11.80		469	6.5	476
1393	265.960	38.797	4.653	431.742	936.490	0.016	3	19.06	19.00	0.17	11.80		379	6.2	385

Table 7.10. Performance and Emission Results for Fuel Coded D60RSB30HX10

Speed (rpm)	Torque (Nm)	PB (kW)	mf (g/s)	Sfc (g/kWh)	bmep	ma (kg/s)	AFR	v (%)	b (%)	O_2 %	CO_2 %	CO ppm	NO ppm	NO_2 ppm	NO_x ppm
3152	14.572	5.320	1.745	1180.646	51.310	0.119	68	62.65	7.04	15.55	3.09	344	214	37.9	252
2996	60.599	16.730	1.785	384.085	213.379	0.116	65	64.26	21.65	12.22	4.97	248	595	40.5	636
2901	75.778	20.475	1.785	313.833	266.826	0.115	64	65.30	26.49	12.22	4.97	248	595	40.1	635
2849	88.579	25.211	2.146	306.424	311.902	0.114	53	65.89	27.13	11.56	5.35	227	686	39.4	725
2649	145.487	40.176	2.908	260.575	512.283	0.109	38	68.32	31.91	9.98	6.24	136	980	34.1	1014
2603	159.343	43.162	2.963	247.151	561.072	0.109	37	68.92	33.64	9.3	6.63	126	1025	32.7	1058
2550	167.765	44.971	3.470	277.748	590.728	0.107	31	69.63	29.94	8.74	6.95	119	1048	30.6	1078
2507	179.747	46.520	3.259	252.204	632.919	0.106	33	70.22	32.97	8	7.37	121	1068	28.5	1097
2452	190.547	48.703	3.209	237.190	670.947	0.105	33	71.00	35.05	7.52	7.64	124	1093	27.4	1120
2413	196.504	49.583	3.164	229.706	691.924	0.104	33	71.57	36.20	6.95	7.96	130	1110	26.8	1137
2361	205.202	50.831	3.605	255.314	722.550	0.103	29	72.35	32.57	6.31	8.32	143	1081	25.2	1106
2309	217.224	52.132	3.394	234.399	764.882	0.102	30	73.16	35.47	5.07	9.03	242	1031	23.2	1055
2269	226.291	52.913	3.394	230.940	796.809	0.101	30	73.80	36.00	4.9	9.12	296	1025	21.5	1046
2202	233.699	53.526	3.439	231.329	822.894	0.100	29	74.91	35.94	3.89	9.69	638	973	19	991
2158	242.478	54.784	3.439	226.018	853.804	0.099	29	75.67	36.79	3.66	9.83	805	965	18.2	983
2034	254.070	53.958	3.705	247.207	894.623	0.096	26	77.93	33.63	1.84	10.86	3702	875	15.1	890
1960	262.405	54.308	3.705	245.615	923.971	0.094	25	79.38	33.85	1.62	10.98		856	14.2	870
1930	264.386	54.244	3.705	245.902	930.948	0.093	25	79.99	33.81	1.35	11.13		824	13.5	838
1846	272.567	52.968	3.891	264.438	959.753	0.091	23	81.78	31.44	0.87	11.41		744	10.9	755
1799	272.923	52.063	3.921	271.115	961.006	0.090	23	82.84	30.67	0.67	11.52		678	10	688
1760	277.275	52.064	4.036	279.084	976.331	0.089	22	83.74	29.79	0.43	11.66		608	9.1	617
1709	279.941	49.500	4.182	304.113	985.720	0.088	21	84.98	27.34	0.27	11.75		498	7.8	506
1651	278.423	49.472	4.182	304.284	980.375	0.086	21	86.45	27.32	0.25	11.76		433	7.5	441
1529	277.201	45.234	4.482	356.734	976.071	0.083	19	89.81	23.31						
1477	275.173	42.736	4.843	407.995	968.929	0.082	17	91.37	20.38						
1385	271.049	41.017	4.843	425.098	954.408	0.079	16	94.34	19.56						

Table 7.11. Performance and Emission Results for Fuel Coded D50RSB40HX10

Speed (rpm)	Torque (Nm)	PB (kW)	mf (g/s)	Sfc (g/kWh)	bmep	ma (kg/s)	AFR	v (%)	b (%)	O_2 %	CO_2 %	CO ppm	NO ppm	NO_2 ppm	NO_x ppm
3259	77.061	21.976	2.051	335.926	271.343	0.120	59	59.64	25.05	11.77	5.23	174	506	42.3	548
3196	98.768	30.524	2.051	241.851	347.778	0.119	58	60.22	34.80	10.59	5.9	163	635	39.9	675
3074	135.137	40.783	2.427	214.211	475.839	0.117	48	61.40	39.29	9.5	6.52	152	771	37.4	808
3026	150.047	45.867	3.876	304.195	528.341	0.116	30	61.88	27.66	8.66	6.99	140	889	34.8	924
2919	178.155	54.363	3.720	246.360	627.314	0.114	31	63.00	34.16	7.2	7.82	106	1124	26.7	1151
2805	217.761	63.638	4.197	237.400	766.774	0.111	27	64.26	35.45	4.72	9.22	268	1194	22.9	1217
2742	233.484	66.461	4.497	243.611	822.137	0.110	24	64.98	34.54	2.73	10.35	766	1156	19.4	1176
2717	239.334	67.730	4.798	255.037	842.736	0.110	23	65.28	33.00	0.73	11.48		897	14.7	911
2595	253.150	68.922	4.813	251.411	891.383	0.107	22	66.79	33.47						
2548	254.842	67.859	5.460	289.662	897.342	0.106	19	67.39	29.05						
2404	258.046	65.819	5.590	305.770	908.623	0.103	18	69.37	27.52						
2251	258.792	61.431	6.478	379.618	911.248	0.100	15	71.66	22.17						
2034	263.191	56.064	7.533	483.737	926.738	0.095	13	75.35	17.40						
1933	262.781	54.808	7.978	524.012	925.296	0.092	12	77.28	16.06						
1786	260.793	49.424	8.625	628.206	918.296	0.089	10	80.36	13.40						
1742	260.162	48.202	8.818	658.594	916.073	0.088	10	81.35	12.78						
1669	256.300	44.934	9.139	732.223	902.474	0.086	9	83.09	11.49						
1620	253.190	42.918	9.355	784.703	891.524	0.084	9	84.32	10.72						
1565	249.913	41.070	9.597	841.226	879.984	0.083	9	85.77	10.00						
1501	248.341	39.328	9.879	904.259	874.450	0.081	8	87.56	9.31						
1448	248.636	38.020	10.112	957.468	875.490	0.080	8	89.12	8.79						

Table 7.12. Performance and Emission Results for Fuel Coded D40RSB50HX10

Speed (rpm)	Torque (Nm)	PB (kW)	mf (g/s)	Sfc (g/kWh)	bmep	ma (kg/s)	AFR	v (%)	b (%)	O_2 %	CO_2 %	CO ppm	NO ppm	NO_2 ppm	NO_x ppm
3119	43.08	11.99	1.64	493.65	151.70	0.12	71	60.27	17.34	15.24	3.26	316	215	1.6	216
3010	86.67	25.89	13.99	1944.81	305.16	0.11	8	61.32	4.40	13.73	4.12	297	340	2.7	343
2908	115.10	33.62	13.75	1472.50	405.27	0.11	8	62.36	5.81	12.24	4.97	270	508	3.6	511
2854	130.95	38.35	2.97	278.60	461.11	0.11	37	62.92	30.73	10.9	5.72	197	705	6	711
2799	147.34	42.54	3.07	260.13	518.81	0.11	36	63.52	32.91	10.02	6.22	164	819	7.4	827
2745	165.67	47.09	3.03	231.89	583.35	0.11	36	64.77	36.92	9.06	6.77	152	946	8.7	955
2701	175.41	49.64	3.49	253.09	617.64	0.11	31	65.17	33.83	8.28	7.21	146	1041	9.8	1051
2644	191.90	53.04	3.95	268.18	675.70	0.11	27	66.02	31.92	7.27	7.78	141	1156	12.3	1168
2603	202.13	55.08	3.73	243.48	711.74	0.11	29	66.32	35.16	6.35	8.3	190	1183	12.9	1195
2551	217.65	57.84	3.82	237.48	766.40	0.11	28	67.13	36.05	5.61	8.72	239	1141	12.7	1153
2520	225.26	58.78	3.90	238.59	793.19	0.10	27	67.25	35.88	4.9	9.12	340	1113	12	1125
2467	233.94	59.72	4.25	256.31	823.75	0.10	24	68.26	33.40	4.25	9.49	521	1106	11.8	1118
2341	245.81	60.36	4.23	252.07	865.53	0.10	24	71.15	33.96	3.82	9.74	682	1099	11.6	1111
2316	251.74	60.43	4.64	276.57	886.42	0.10	22	69.99	30.95	2.87	10.27	1593	1030	10.5	1041
2228	256.70	59.26	4.65	282.65	903.87	0.10	21	72.35	30.29	1.85	10.85	3657	907	9.8	917
2147	259.53	58.27	4.59	283.42	913.85	0.10	21	73.58	30.21	0.89	11.39		790	8.7	799
2094	266.80	58.77	4.76	291.48	939.46	0.10	20	74.00	29.37	0.68	11.51		754	8.3	762
1952	266.21	54.76	4.76	312.80	937.38	0.09	20	78.36	27.37	0.48	11.63		704	7.8	712
1810	266.69	51.78	5.11	355.23	939.06	0.09	18	81.46	24.10	0.41	11.67		620	7.6	628
1687	266.48	47.24	5.78	440.14	938.30	0.09	15	84.00	19.45	0.22	11.77		521	6.9	528
1639	264.63	46.11	5.55	432.96	931.82	0.08	15	83.32	19.77	0	11.9		367	6	373
1565	261.16	44.07	5.55	452.96	919.60	0.08	15	85.94	18.90	0.01	11.9		310	6.5	316
1482	259.27	42.05	5.55	474.80	912.93	0.08	15	88.57	18.03	0.03	11.88		271	7.8	279
1251	248.97	35.24	3.23	329.83	876.65	0.08	24	101.93	25.96	0.58	11.57		257	10	267

Table 7.13. Performance and Emission Results for Fuel Coded D75RSB10HX15

Speed (rpm)	Torque (Nm)	PB (kW)	mf (g/s)	Sfc (g/kWh)	bmep	ma (kg/s)	AFR	v (%)	b (%)	O_2 %	CO_2 %	CO ppm	NO ppm	NO_2 ppm	NO_x ppm
3200	58.611	17.468	1.645	338.923	206.379	0.122	74	62.623	24.042	13.21	4.41	347	339	31.9	371
3156	73.743	21.806	3.625	598.455	259.661	0.122	34	63.076	13.616	12.32	4.92	326	419	30.8	449
3035	112.187	33.972	2.938	311.355	395.030	0.119	41	64.372	26.170	10.84	5.76	283	580	27.1	607
2952	136.373	42.403	2.372	201.344	480.191	0.118	50	65.308	40.469	9.99	6.24	244	680	23.7	704
2911	149.852	45.346	2.662	211.363	527.655	0.117	44	65.786	38.551	8.55	7.05	195	813	20.6	834
2852	175.092	51.218	3.600	253.031	616.530	0.116	32	66.493	32.203	7.35	7.73	170	999	19.9	1019
2804	192.669	55.920	3.665	235.954	678.420	0.116	32	67.631	34.533	6.41	8.27	171	1115	20	1135
2749	209.782	60.256	3.991	238.445	738.679	0.115	29	68.427	34.173	5.24	8.93	331	1163	19.3	1182
2710	222.658	62.642	4.347	249.820	784.014	0.114	26	68.758	32.617	4.07	9.6	709	1145	18.8	1164
2693	227.218	63.731	4.442	250.933	800.072	0.113	25	68.722	32.472	3.66	9.82	909	1127	17.9	1145
2648	234.230	64.812	4.954	275.154	824.762	0.113	23	69.680	29.614	2.47	10.5	1853	1048	16	1064
2604	241.101	65.555	4.954	272.037	848.956	0.112	23	70.290	29.953	1.82	10.87	2632	987	16	1003
2555	247.347	65.886	4.648	253.958	870.950	0.111	24	71.069	32.085	1.36	11.13	4127	927	14.4	941
2457	252.001	64.844	5.646	313.433	887.339	0.110	19	73.239	25.997	0.55	11.59		718	11.7	729
2365	258.080	64.760	5.646	313.839	908.741	0.108	19	74.686	25.963	0.39	11.68		645	11.1	657
2319	257.515	62.679	6.322	363.132	906.755	0.106	17	74.802	22.439	0.3	11.73		539	9.5	548
2203	261.680	61.536	5.886	344.357	921.417	0.105	18	78.011	23.662	0.3	11.73		528	9.3	537
2163	260.712	58.998	5.691	347.241	918.012	0.102	18	77.550	23.466	0.17	11.8		500	8.6	509
2001	262.821	55.181	5.565	363.084	925.438	0.102	18	83.107	22.442	0.02	11.89		435	7.8	443
1820	264.400	51.283	5.966	418.839	930.995	0.098	16	88.085	19.454	-0.02	11.9		357	7.6	364
1752	262.821	49.062	6.002	440.371	925.438	0.094	16	87.533	18.503	6.98	7.95		467	7.8	475
1724	259.987	47.073	6.002	458.980	915.458	0.092	15	87.390	17.753	11.21	5.55		580	8.4	589

Table 7.14. Performance and Emission Results for Fuel Coded D65RSB20HX15

Speed (rpm)	Torque (Nm)	PB (kW)	mf (g/s)	Sfc (g/kWh)	bmep	ma (kg/s)	AFR	v (%)	b (%)	O_2 %	CO_2 %	CO ppm	NO ppm	NO_2 ppm	NO_x ppm
3201	28.925	8.058	1.309	584.669	101.848	0.118	90	59.84	14.00	13.39	4.31	183	404	15.6	420
3082	62.849	17.959	1.399	280.410	221.301	0.116	83	60.96	30.53	11.74	5.24	160	595	16.1	612
3015	80.687	23.262	1.399	216.484	284.114	0.114	82	61.61	39.55	11.19	5.56	147	672	15.8	688
2916	108.507	31.327	1.599	183.798	382.070	0.113	70	62.62	46.58	10.88	5.74	128	714	15.2	729
2855	121.711	34.952	1.599	164.737	428.564	0.111	70	63.27	51.97	10.88	5.74	128	734	14.9	748
2802	139.341	40.264	2.883	257.765	490.644	0.110	38	63.85	33.21	9.55	6.49	104	903	15.2	918
2755	161.740	46.719	3.134	241.468	569.515	0.109	35	64.38	35.45	8.55	7.06	93	1062	17	1079
2708	171.123	48.525	3.580	265.584	602.553	0.108	30	64.92	32.24	7.99	7.37	91	1125	18	1143
2646	185.315	50.902	3.670	259.569	652.524	0.107	29	65.66	32.98	7.31	7.76	95	1148	18.3	1167
2599	193.871	52.809	4.141	282.322	682.653	0.106	26	66.23	30.32	6.75	8.08	113	1144	18.1	1162
2556	205.612	54.758	3.765	247.554	723.992	0.105	28	66.77	34.58	5.35	8.87	209	1100	16.9	1117
2500	217.486	57.013	4.192	264.673	765.804	0.104	25	67.49	32.35	4.59	9.30	309	1089	16	1105
2452	224.511	57.551	4.121	257.803	790.542	0.103	25	68.13	33.21	3.38	9.98	662	1004	15	1019
2357	237.413	58.399	4.041	249.117	835.972	0.101	25	69.44	34.37	2.16	10.68	1940	897	13.1	910
2301	243.875	58.878	4.126	252.304	858.723	0.100	24	70.25	33.93	1.48	11.06	3658	830	12	842
2277	246.722	58.812	4.126	252.584	868.750	0.099	24	70.61	33.89	1.40	11.10	4503	827	11.4	839
2200	251.531	57.941	4.442	276.007	885.683	0.097	22	71.79	31.02	1.31	11.16		826	10.2	836
2107	256.636	56.607	4.382	278.685	903.657	0.095	22	73.31	30.72	0.60	11.56		683	7.1	690
2000	261.518	55.064	4.207	275.022	920.850	0.093	22	75.17	31.13	0.41	11.67		611	6.7	617
1920	264.635	54.449	4.613	304.978	931.823	0.091	20	76.66	28.07	0.12	11.83		516	5.8	522
1841	267.986	52.107	4.618	319.036	943.624	0.089	19	78.22	26.83	0.13	11.83		408	5.6	413
1705	267.153	48.425	3.304	245.635	940.692	0.085	26	81.14	34.85	0.16	11.81		371	5.6	377
1654	266.952	46.596	5.818	449.514	939.982	0.084	14	82.33	502.29	0.19	11.79		313	5.8	318
1547	261.753	42.920	6.107	512.250	921.677	0.081	13	84.99	442.54	2.38	10.55		259	8.7	267
1504	259.712	41.756	6.223	536.535	914.488	0.080	13	86.14	19804.43	5.28	8.91		196	8.7	205

Table 7.15. Performance and Emission Results for Fuel Coded D55RSB30HX15

Speed (rpm)	Torque (Nm)	PB (kW)	mf (g/s)	Sfc (g/kWh)	bmep	ma (kg/s)	AFR	v (%)	b (%)	O_2 %	CO_2 %	CO ppm	NO ppm	NO_2 ppm	NO_x ppm
3228	53.587	15.216	1.860	440.101	188.689	0.122	65.4	62.03	18.91	15.61	3.06	260	174	15.3	189
3177	71.647	20.525	1.860	326.268	252.282	0.121	64.9	62.54	25.51	15.16	3.31	252	207	15.3	222
3120	91.548	27.612	1.860	242.522	322.355	0.120	64.3	63.11	34.32	15.16	3.31	252	207	17.5	224
2954	138.616	40.931	2.808	246.952	488.090	0.116	41.5	64.89	33.70	12.41	4.87	210	445	20.9	466
2859	157.818	47.678	3.384	255.539	555.703	0.115	33.9	65.97	32.57	9.43	6.56	122	797	20.5	817
2802	177.242	51.967	3.505	242.786	624.097	0.113	32.4	66.65	34.28	8.64	7.01	103	952	20.5	972
2752	191.212	54.670	3.680	242.339	673.288	0.112	30.6	67.26	34.35	7.68	7.55	101	1042	20.5	1063
2709	207.620	58.608	3.976	244.223	731.063	0.112	28.1	67.80	34.08	6.2	8.39	170	1107	19.6	1127
2679	220.495	60.765	3.936	233.179	776.399	0.111	28.2	68.19	35.70	5.95	8.53	197	1126	18.5	1144
2619	227.937	62.532	4.111	236.692	802.603	0.110	26.7	68.98	35.17	4.97	9.08	275	1118	18	1136
2570	237.642	63.994	4.517	254.132	836.776	0.109	24.1	69.64	32.75	4.26	9.49	399	1079	16.2	1095
2502	245.372	64.411	4.227	236.232	863.997	0.107	25.4	70.60	35.23	3.37	9.99	756	1048	14.9	1063
2376	257.529	64.201	4.517	253.311	906.802	0.105	23.2	72.48	32.86	2.66	10.39	1075	1007	13.5	1021
2341	259.839	63.567	4.888	276.851	914.937	0.104	21.2	73.03	30.06	1.12	11.27	4147	830	11.6	842
2270	262.936	63.473	4.888	277.260	925.840	0.102	20.9	74.19	30.02	1.12	11.27	4147	830	11.1	841
2248	262.922	61.938	5.034	292.583	925.792	0.102	20.2	74.55	28.45	0.65	11.53		714	9.1	723
2217	266.724	61.852	5.174	301.159	939.178	0.101	19.5	75.08	27.64	0.55	11.59		667	8.5	676
2101	268.067	59.649	5.174	312.282	943.908	0.098	19.0	77.17	26.65	0.52	11.61		660	8.2	669
2066	270.068	58.408	5.345	329.426	950.955	0.098	18.3	77.83	25.27	0.39	11.68		583	7.1	590
1979	269.504	55.763	5.420	349.905	948.969	0.096	17.6	79.56	23.79						
1884	270.021	53.146	5.340	361.703	950.790	0.093	17.5	81.59	23.01						
1822	272.171	52.668	5.565	380.407	958.358	0.092	16.5	83.00	21.88						
1746	270.579	49.954	5.676	409.021	952.753	0.090	15.9	84.83	20.35						
1717	269.323	48.414	5.676	422.038	948.330	0.089	15.7	85.56	19.72						
1600	264.185	44.965	5.816	465.646	930.238	0.086	14.8	88.72	17.87						
1554	262.459	43.472	6.102	505.307	924.161	0.085	13.9	90.05	16.47						
1518	261.317	42.148	6.488	554.153	920.140	0.084	13.0	91.15	15.02						
1467	259.618	40.731	6.488	573.438	914.157	0.083	12.7	92.76	14.51						

Table 7.16. Performance and Emission Results for Fuel Coded D45RSB40HX15

Speed (rpm)	Torque (Nm)	PB (kW)	mf (g/s)	Sfc (g/kWh)	bmep	ma (kg/s)	AFR	v (%)	b (%)	O_2 %	CO_2 %	CO ppm	NO ppm	NO_2 ppm	NO_x ppm
3200	42.129	12.131	2.021	599.646	148.343	0.121	60	62.16	14.10	14.92	3.44	363	245	40.7	285
3144	72.984	21.116	7.275	1240.331	256.988	0.119	16	62.71	6.82	13.76	4.1	350	285	41.6	327
3042	96.417	29.846	4.234	510.753	339.501	0.118	28	63.77	16.55	12.93	4.58	318	429	41.6	470
2961	123.162	36.735	2.417	236.832	433.673	0.116	48	64.64	35.70	11.62	5.32	275	592	38.9	631
2927	136.104	39.833	4.372	395.167	479.245	0.115	26	65.02	21.39	10.43	5.99	198	766	32	798
2841	161.431	47.515	4.476	339.100	568.427	0.114	25	66.01	24.93	9.18	6.7	167	947	28.3	976
2812	182.662	53.074	12.845	871.300	643.182	0.113	9	66.35	9.70	7.91	7.42	144	1105	25.1	1130
2751	196.827	56.662	4.584	291.216	693.059	0.112	24	67.09	29.03	6.69	8.11	144	1256	23.6	1280
2697	214.611	60.344	8.885	530.035	755.682	0.111	12	67.76	15.95	5.71	8.66	221	1321	22.7	1344
2646	239.274	64.316	7.004	392.056	842.523	0.110	16	68.42	21.56	4	9.63	564	1285	20.2	1305
2555	244.909	65.631	5.049	276.944	862.365	0.108	21	69.64	30.53	2.85	10.29	1152	1165	17.6	1183
2468	252.962	65.496	4.548	249.957	890.720	0.106	23	70.87	33.82	1.84	10.86	2572	1095	15.3	1110
2360	265.266	65.108	5.310	293.584	934.046	0.104	20	72.50	28.80	0.47	11.63		753	10.7	763
2273	264.877	64.547	5.310	296.136	932.674	0.102	19	73.89	28.55	0.47	11.63		753	10.7	763
2251	265.649	62.404	5.530	319.032	935.394	0.101	18	74.25	26.50	0.38	11.68		679	9.4	689
2158	268.006	61.132	5.610	330.395	943.695	0.099	18	75.86	25.59	0.34	11.71		649	9.1	658
2042	270.659	58.568	5.636	346.399	953.036	0.097	17	78.01	24.41	0.22	11.77		607	8	615
2029	272.466	57.632	5.430	339.183	959.398	0.096	18	78.26	24.93	0.07	11.86		590	7.6	597
1932	273.023	55.676	5.430	351.100	961.361	0.094	17	80.23	24.08	0.02	11.89		531	7.3	538
1806	272.050	51.672	5.718	398.347	957.932	0.091	16	83.03	21.22	-0.05	11.9		401	6.4	407
1750	271.056	49.547	5.785	420.315	954.432	0.089	15	84.36	20.11	-0.05	11.9		375	6.2	381
1695	268.772	48.039	5.851	438.455	946.391	0.088	15	85.75	19.28	-0.07	11.9		330	6.2	336
1635	266.065	45.416	5.923	469.487	936.860	0.087	15	87.33	18.01	-0.06	11.9		322	5.8	327

Table 7.17. Performance and Emission Results for Fuel Coded D35RSB50HX15

Speed (rpm)	Torque (Nm)	PB (kW)	mf (g/s)	Sfc (g/kWh)	bmep	ma (kg/s)	AFR	v (%)	b (%)	O_2 %	CO_2 %	CO ppm	NO ppm	NO_2 ppm	NO_x ppm
3214	31.66	9.86	2.07	755.95	111.50	0.11	55	57.21	11.38	13.25	4.39	413	426	10.7	436
3135	57.66	16.19	1.88	416.96	203.02	0.11	60	57.85	20.63	11.93	5.14	373	514	12.1	526
2994	99.21	29.97	1.88	225.23	349.34	0.11	58	59.04	38.19	10.85	5.75	275	753	14.5	768
2958	109.76	32.76	1.96	214.89	386.47	0.11	55	59.36	40.02	10.62	5.88	249	794	14.9	809
2922	119.82	35.25	2.70	275.48	421.92	0.11	40	59.68	31.22	10.64	5.87	228	797	14.9	811
2839	140.66	41.26	2.98	260.30	495.30	0.11	36	60.44	33.04	9.76	6.37	165	930	15.2	946
2797	156.71	45.76	3.54	278.87	551.80	0.11	30	60.83	30.84	8.9	6.86	137	1019	15.2	1034
2751	173.74	49.67	3.69	267.44	611.78	0.10	28	61.27	32.16	8.9	6.86	137	1048	15.4	1063
2701	187.15	52.37	4.05	278.13	659.00	0.10	25	61.76	30.92	7.92	7.41	115	1209	15.8	1225
2641	201.00	55.18	3.78	246.64	707.77	0.10	27	62.37	34.87	6.83	8.03	117	1298	16	1314
2601	210.92	57.02	4.37	275.70	742.70	0.10	23	62.78	31.19	5.94	8.54	151	1286	15.2	1301
2540	228.53	60.43	4.20	250.01	804.71	0.10	24	63.42	34.40	5.53	8.76	194	1281	14.5	1295
2511	230.72	60.43	4.33	257.78	812.42	0.10	23	63.74	33.36	3.97	9.65	526	1217	12.5	1229
2454	239.77	61.48	4.59	268.91	844.27	0.10	21	64.36	31.98	3.07	10.16	924	1154	11.6	1166
2413	244.90	61.42	5.02	294.48	862.32	0.10	19	64.83	29.21	2.46	10.51	1441	1082	10.9	1093
2354	249.34	61.52	4.72	276.40	877.97	0.10	20	65.51	31.12	1.71	10.93	3294	983	9.6	992
2256	257.10	60.53	4.72	280.89	905.29	0.09	20	66.69	30.62	1.34	11.14	4632	933	9.1	942
2236	260.92	61.19	5.09	299.40	918.74	0.09	18	66.94	28.73	0.64	11.54		789	7.1	796
2167	261.69	59.63	4.93	297.84	921.46	0.09	18	67.82	28.88	0.59	11.57		762	6.7	768
2051	267.72	58.06	5.00	310.27	942.70	0.09	18	69.38	27.72	0.47	11.64		705	6.5	712
2040	269.30	57.12	4.96	312.86	948.26	0.09	18	69.53	27.49	0.44	11.65		688	6	694
1954	269.71	55.54	5.72	370.81	949.68	0.09	15	70.76	23.19	0.12	11.83		631	5.6	637
1833	271.09	52.62	5.66	386.90	954.55	0.08	15	72.59	22.23	0.12	11.83		552	5.3	557
1748	271.40	51.27	5.80	406.94	955.64	0.08	14	73.95	21.13	0.2	11.79		511	4.5	516
1704	269.58	48.60	6.49	480.49	949.25	0.08	12	74.69	17.90	-0.01	11.9		350	4.2	354
1649	268.38	46.84	6.65	510.83	945.02	0.08	12	75.64	16.84	-0.02	11.9		348	4	352

Table 7.18. Performance and Emission Results for Fuel Coded D85RSB10HX5

Speed (rpm)	Torque (Nm)	PB (kW)	mf (g/s)	Sfc (g/kWh)	bmep	ma (kg/s)	AFR	v (%)	b (%)	O_2 %	CO_2 %	CO ppm	NO ppm	NO_2 ppm	NO_x ppm
3140	69.619	20.298	1.875	332.570	245.140	0.121	65	62.546	24.455	10.46	5.97	193	766	23.2	789
3077	86.302	25.983	1.875	259.808	303.885	0.120	64	63.218	31.303	10.27	6.08	182	798	23.2	821
3046	95.598	29.096	1.955	241.934	336.616	0.120	61	63.557	33.616	10.23	6.11	182	798	23.2	821
2935	128.797	37.820	2.697	256.762	453.514	0.118	44	64.817	31.675	9.22	6.67	146	974	22.6	997
2844	151.686	44.996	2.983	238.680	534.112	0.116	39	65.907	34.074	7.99	7.37	132	1160	22.8	1183
2792	172.372	50.198	3.535	253.498	606.952	0.115	33	66.555	32.083	7.21	7.81	137	1277	22.1	1299
2763	183.689	52.467	3.545	243.225	646.801	0.114	32	66.925	33.438	6.07	8.46	194	1301	21.4	1322
2703	197.283	55.424	3.690	239.692	694.667	0.113	31	67.710	33.931	4.4	9.41	439	1206	18.1	1225
2644	215.995	59.428	4.046	245.106	760.554	0.112	28	68.510	33.181	2.82	10.3	1157	1107	15	1122
2595	226.842	61.116	3.780	222.685	798.748	0.111	29	69.195	36.522	1.58	11.01	3359	970	13.6	984
2546	233.484	62.301	4.367	252.344	822.137	0.110	25	69.902	32.229	1.47	11.07	4078	949	12.5	962
2495	240.557	63.290	4.197	238.705	847.040	0.109	26	70.661	34.071	1.43	11.09		937	11.4	949
2408	249.946	63.337	4.327	245.937	880.102	0.107	25	72.014	33.069	0.86	11.41		820	9.6	830
2348	256.918	62.716	4.593	263.626	904.650	0.106	23	72.994	30.850	0.35	11.7		663	6.7	670
2283	256.186	61.497	5.024	294.096	902.072	0.105	21	74.102	27.654	0.32	11.72		647	6.3	653
2264	261.082	61.483	4.723	276.545	919.312	0.104	22	74.435	29.409	0.29	11.74		606	5.8	612
2202	261.518	60.911	4.723	279.145	920.850	0.103	22	75.555	29.135	0.26	11.75		553	5.6	558
2182	263.513	59.841	5.089	306.153	927.874	0.102	20	75.927	26.565	0.23	11.77		495	5.4	501
2109	263.567	58.149	4.934	305.438	928.063	0.101	20	77.332	26.627	0.24	11.77		460	4.5	464
2005	267.254	57.383	5.004	313.919	941.046	0.099	20	79.476	25.908	0.23	11.77		437	4.2	442
1853	269.988	53.553	4.964	333.675	950.672	0.095	19	82.953	24.374	-0.02	11.9		390	3.6	394
1802	269.329	51.024	5.721	403.632	948.354	0.094	16	84.225	20.149	-0.02	11.9		378	3.6	382
1767	269.826	49.716	5.656	409.532	950.104	0.093	16	85.132	19.859	-0.03	11.9		357	3.4	361
1702	268.537	48.214	5.796	432.771	945.563	0.091	16	86.897	18.793	-0.03	11.9		366	2.9	369
1652	265.320	46.353	6.178	479.795	934.235	0.090	15	88.331	286.107	8.11	7.31		105	2	107

Table 7.19. Performance and Emission Results for Fuel Coded D75RSB20HP5

Speed (rpm)	Torque (Nm)	PB (kW)	mf (g/s)	Sfc (g/kWh)	bmep	ma (g/s)	AFR	v (%)	b (%)	O_2 %	CO_2 %	CO ppm	NO ppm	NO_2 ppm	NO_x ppm
3216	36.615	10.894	1.970	651.172	128.927	0.126	64	64.37	12.55	15.05	3.37	390	228	25.1	254
3172	52.445	14.442	1.970	491.183	184.668	0.125	63	64.85	16.64	14.81	3.51	390	228	25.1	254
3125	68.282	20.316	1.970	349.156	240.434	0.124	63	65.38	23.41	14.81	3.51	372	250	28.6	279
2935	123.074	36.498	2.733	269.525	433.365	0.121	44	67.65	30.32	11.29	5.50	291	561	33.5	594
2885	135.976	39.448	3.089	281.855	478.796	0.120	39	68.29	29.00	10.66	5.86	244	730	31.7	762
2855	144.620	43.584	3.089	255.109	509.232	0.119	39	68.68	32.04	9.21	6.68	148	1010	25.3	1035
2803	161.767	47.064	3.379	258.491	569.609	0.118	35	69.37	31.62	8.27	7.21	132	1149	24.9	1174
2745	177.678	50.697	3.565	253.141	625.635	0.117	33	70.17	32.29	7.82	7.47	132	1220	25.1	1245
2713	186.927	52.816	3.675	250.501	658.200	0.117	32	70.63	32.63	6.73	8.09	144	1254	24.9	1279
2653	203.019	56.344	3.861	246.671	714.864	0.115	30	71.50	33.13	5.87	8.57	219	1246	23.1	1269
2598	217.285	58.959	4.076	248.895	765.095	0.114	28	72.33	32.84	5.01	9.06	329	1218	21.3	1240
2550	230.449	61.230	4.031	237.009	811.448	0.113	28	73.08	34.48	4.31	9.46	389	1203	20.6	1223
2490	237.031	61.874	4.131	240.377	834.624	0.112	27	74.04	34.00	3.67	9.82	737	1172	18.9	1191
2410	246.702	62.639	4.337	249.255	868.679	0.111	25	75.40	32.79	2.44	10.52	1666	1110	17.1	1127
2354	253.640	62.695	4.462	256.232	893.109	0.109	25	76.39	31.90	0.57	11.58		769	11.3	781
2101	268.248	59.280	4.833	293.523	944.546	0.104	22	81.39	27.84	0.48	11.63		700	10	710
2000	272.889	57.863	5.039	313.501	960.888	0.102	20	83.68	26.07						
1976	271.613	56.340	5.039	321.974	956.395	0.101	20	84.25	25.38						
1910	273.131	54.659	5.129	337.823	961.739	0.100	19	85.89	24.19						
1859	275.791	54.387	5.144	340.504	971.105	0.099	19	87.22	24.00						
1792	274.891	52.679	5.224	357.026	967.936	0.097	19	89.06	22.89						
1755	273.447	50.409	5.530	394.951	962.851	0.096	17	90.13	20.69						
1703	273.097	48.927	5.565	409.496	961.621	0.095	17	91.70	19.96						
1656	271.257	47.451	5.691	431.745	955.141	0.094	16	93.18	18.93						
1621	268.121	45.730	6.007	472.853	944.097	0.093	15	94.79	17.28						

Table 7.20. Performance and Emission Results for Fuel Coded D65RSB30HP5

Speed (rpm)	Torque (Nm)	PB (kW)	mf (g/s)	Sfc (g/kWh)	bmep	ma (kg/s)	AFR	v (%)	b (%)	O_2 %	CO_2 %	CO ppm	NO ppm	NO_2 ppm	NO_x ppm
3206	26.916	8.660	1.700	706.590	94.777	0.122	72	62.67	11.88	15.83	2.93	421	215	43.2	258
3168	45.205	13.070	1.770	487.486	159.174	0.122	69	63.06	17.22	15.39	3.18	384	257	44.3	302
3104	68.974	20.018	2.066	371.491	242.870	0.120	58	63.73	22.60	12.75	4.68	300	553	45.6	599
2956	109.339	32.444	2.602	288.737	385.002	0.118	45	65.36	29.07	11.24	5.53	212	802	36.9	839
2938	111.918	34.285	2.978	312.720	394.084	0.117	39	65.57	26.84	10.49	5.96	178	948	34.3	983
2843	136.044	39.931	2.888	260.363	479.032	0.116	40	66.70	32.24	9.88	6.30	163	1033	33.6	1067
2796	146.776	43.209	3.023	251.891	516.824	0.115	38	67.28	33.32	8.98	6.81	143	1226	32	1258
2750	158.926	45.646	3.199	252.285	559.606	0.114	36	67.86	33.27	8.30	7.19	142	1295	30.5	1326
2700	171.137	48.469	3.354	249.134	602.600	0.113	34	68.51	33.69	7.71	7.53	150	1329	29.1	1358
2643	182.991	50.831	3.530	249.987	644.341	0.112	32	69.28	33.58	6.98	7.95	181	1315	26.5	1341
2600	196.101	53.246	3.389	229.158	690.505	0.111	33	69.87	36.63	6.06	8.46	226	1287	23.6	1311
2558	207.680	55.171	3.816	248.969	731.276	0.110	29	70.47	33.72	5.07	9.03	336	1281	21.3	1302
2485	220.931	57.358	3.695	231.923	777.937	0.108	29	71.54	36.19	4.59	9.30	637	1304	18.2	1323
2458	227.124	57.856	3.816	237.416	799.741	0.108	28	71.95	35.36	3.00	10.20	1431	1127	15.3	1142
2400	231.859	58.512	3.901	239.997	816.414	0.107	27	72.86	34.98	2.41	10.54	2235	1070	13.8	1084
2348	243.129	60.158	3.966	237.332	856.098	0.105	27	73.70	35.37	1.57	11.01	4996	969	11.8	981
2302	249.409	59.931	4.141	248.770	878.210	0.104	25	74.46	33.74						
2196	256.495	59.208	4.227	256.993	903.160	0.102	24	76.33	32.66						
2100	262.660	58.097	4.302	266.568	924.870	0.100	23	78.14	31.49						
2009	267.778	56.098	4.362	279.929	942.891	0.098	22	79.99	29.99						
1983	270.223	55.820	4.362	281.324	951.499	0.097	22	80.54	29.84						
1862	275.085	53.556	4.673	314.108	968.621	0.094	20	83.27	26.72						
1792	275.623	51.767	4.808	334.381	970.513	0.093	19	84.98	25.10						
1756	271.922	49.957	5.019	361.666	957.483	0.092	18	85.90	23.21						

Table 7.21. Performance and Emission Results for Fuel Coded D55RSB40HP5

Speed (rpm)	Torque (Nm)	PB (kW)	mf (g/s)	Sfc (g/kWh)	bmep	ma (kg/s)	AFR	v (%)	b (%)	O_2 %	CO_2 %	CO ppm	NO ppm	NO_2 ppm	NO_x ppm
3178	12.899	3.559	1.660	1678.847	45.421	0.122	73	62.57	5.02	15.91	2.88	243	217	32.8	250
3081	49.812	13.689	1.665	437.748	175.398	0.120	72	63.58	19.27	15.13	3.32	235	292	37.2	329
2989	80.311	22.804	1.920	303.150	282.790	0.118	61	64.58	27.83	14.52	3.67	230	359	39.5	399
2848	109.810	31.535	2.211	252.413	386.658	0.115	52	66.22	33.42	12.55	4.79	210	530	40.3	570
2803	119.642	35.158	2.838	290.583	421.280	0.114	40	66.77	29.03	11.51	5.38	159	765	37.2	802
2741	140.033	39.739	2.692	243.912	493.080	0.113	42	67.55	34.58	11.21	5.55	141	842	33.2	875
2705	148.912	41.840	2.883	248.054	524.344	0.112	39	68.01	34.01	10.47	5.97	123	973	31.4	1004
2654	159.322	44.218	3.048	248.187	561.001	0.111	37	68.69	33.99	9.86	6.32	109	1097	30.5	1128
2601	170.465	45.836	3.139	246.512	600.235	0.110	35	69.41	34.22	9.22	6.67	105	1200	29.6	1229
2553	181.117	47.807	3.089	232.574	637.743	0.109	35	70.08	36.27	8.69	6.97	105	1213	28.5	1241
2502	191.158	50.000	3.439	247.642	673.099	0.108	31	70.82	34.06	7.95	7.39	111	1225	26.8	1252
2451	201.300	51.766	3.550	246.865	708.809	0.107	30	71.59	34.17	7.32	7.75	118	1259	25.4	1284
2396	209.944	52.898	3.379	229.980	739.246	0.106	31	72.44	36.68	6.82	8.03	125	1272	23.9	1296
2350	219.978	54.134	4.061	270.078	774.578	0.105	26	73.18	31.23	5.96	8.52	152	1265	21.8	1286
2307	231.711	55.807	3.710	239.340	815.894	0.104	28	73.89	35.24	5.64	8.7	174	1243	20.9	1264
2247	237.897	56.137	3.806	244.043	837.675	0.103	27	74.91	34.56	4.63	9.28	363	1189	18.3	1207
2153	245.688	55.352	3.976	258.591	865.108	0.101	25	76.60	32.62	3.46	9.94	818	1105	15.8	1121
2015	261.001	54.849	4.056	266.225	919.029	0.098	24	79.31	31.68	2.29	10.6	2316	1039	12.2	1051
1961	265.662	54.359	3.951	261.653	935.441	0.096	24	80.45	32.24	1.5	11.05	3673	1009	11.6	1021
1904	268.423	53.672	4.257	285.516	945.161	0.095	22	81.71	29.54	0.98	11.34		907	10.3	917
1834	273.285	53.256	4.227	285.717	962.283	0.093	22	83.34	29.52	0.7	11.5		825	9.4	835
1731	274.870	49.530	4.342	315.587	967.865	0.091	21	85.92	26.73	0.5	11.62		727	8	735
1713	272.332	49.053	4.362	320.128	958.925	0.090	21	86.40	26.35	0.34	11.71		690	6.3	697

Table 7.22. Performance and Emission Results for Fuel Coded D45RSB50HP5

Speed (rpm)	Torque (Nm)	PB (kW)	mf (g/s)	Sfc (g/kWh)	bmep	ma (kg/s)	AFR	v (%)	b (%)	O_2 %	CO_2 %	CO ppm	NO ppm	NO_2 ppm	NO_x ppm
3195	28.690	8.777	1.85	758.84	101.02	0.12	65	60.87	11.26	15.53	3.1	307	231	49.9	281
3161	44.124	12.796	2.08	585.41	155.37	0.12	58	61.20	14.59	15.58	3.07	307	227	50.3	278
3010	88.465	26.708	2.37	318.99	311.50	0.12	49	62.75	26.78	15.03	3.38	301	280	51.7	331
2950	104.175	31.069	2.66	308.49	366.82	0.12	43	63.40	27.69	14.14	3.89	286	374	53.2	427
2900	114.618	34.934	2.93	301.74	403.59	0.11	39	63.95	28.31	12.28	4.94	247	602	49.7	652
2853	130.805	38.838	2.96	274.67	460.59	0.11	38	64.49	31.10	11.41	5.44	203	757	43.4	800
2798	143.096	41.618	3.17	274.10	503.86	0.11	36	65.13	31.17	10.76	5.8	176	835	40.1	875
2741	157.348	45.041	3.30	264.09	554.05	0.11	34	65.82	32.35	10.12	6.16	141	1024	36.6	1061
2709	170.431	47.495	3.45	261.85	600.12	0.11	32	66.22	32.63	9.49	6.52	130	1153	36.1	1189
2650	183.145	50.656	3.52	250.14	644.89	0.11	31	66.97	34.15	9	6.8	125	1215	35	1250
2603	197.062	53.522	3.70	248.88	693.89	0.11	29	67.59	34.33	8.32	7.18	125	1268	34.1	1302
2560	213.725	56.671	3.95	250.98	752.56	0.11	27	68.16	34.04	7.12	7.86	137	1276	30.8	1307
2496	221.422	57.908	3.99	247.80	779.66	0.11	27	69.05	34.48	6.45	8.24	154	1273	28.2	1301
2451	227.641	58.384	4.14	255.05	801.56	0.11	26	69.70	33.50	5.8	8.62	176	1273	26.4	1299
2401	239.509	59.865	4.10	246.33	843.35	0.10	26	70.44	34.68	5.48	8.79	203	1290	25.1	1315
2357	250.430	61.195	4.32	254.25	881.80	0.10	24	71.11	33.60	4.28	9.48	367	1235	22.4	1257
2297	252.391	61.028	4.32	254.95	888.71	0.10	24	72.06	33.51	3.83	9.73	367	1235	22.4	1257
2238	257.025	60.205	4.48	268.03	905.03	0.10	23	73.03	31.87	2.63	10.41	1628	1089	18.4	1107
2224	262.042	60.417	4.54	270.67	922.69	0.10	22	73.26	31.56	2.1	10.71	2833	1038	16.2	1054
2151	263.103	59.262	4.58	278.38	926.43	0.10	22	74.53	30.69	1.92	10.81	3748	1018	14.9	1033
2029	272.762	57.741	4.72	294.16	960.44	0.10	20	76.80	29.04	1.07	11.29		920	12.4	933
1941	275.717	56.389	4.58	292.24	970.84	0.09	21	78.58	29.23	0.77	11.46		852	11.5	863
1887	278.618	56.648	4.69	297.92	981.06	0.09	20	79.73	28.68	0.59	11.57		781	10	791
1822	280.129	53.645	4.92	330.08	986.38	0.09	19	81.19	25.88	0.29	11.74		662	8.6	671
1805	275.885	52.076	4.97	343.49	971.44	0.09	18	81.58	24.87						

Table 7.23. Performance and Emission Results for Fuel Coded D80RSB10HP10

Speed (rpm)	Torque (Nm)	PB (kW)	mf (g/s)	Sfc (g/kWh)	bmep	ma (kg/s)	AFR	v (%)	b (%)	O_2 %	CO_2 %	CO ppm	NO ppm	NO_2 ppm	NO_x ppm
3196	13.016	4.362	1.640	1353.051	45.831	0.123	75	62.631	5.942	15.7	3	303	253	27.4	281
3129	11.492	3.771	1.640	1565.284	40.465	0.122	74	63.333	5.136	15.57	3.08	296	260	29.2	289
3022	33.696	10.678	1.619	545.976	118.650	0.120	74	64.505	14.725	16.02	2.82	262	228	39.2	267
2936	61.931	19.067	1.619	305.763	218.069	0.118	73	65.495	26.293	15.84	2.93	263	242	40.6	283
2811	80.173	23.633	1.940	295.577	282.301	0.116	60	67.019	27.199	15.46	3.14	260	283	41.9	325
2632	129.800	35.825	2.682	269.551	457.046	0.112	42	69.398	29.825	11.53	5.37	164	854	37.5	892
2601	136.355	37.191	2.612	252.856	480.128	0.111	43	69.836	31.794	11.07	5.63	150	931	35.9	967
2550	144.663	38.683	2.768	257.566	509.382	0.110	40	70.575	31.213	10.59	5.9	130	989	32.8	1022
2497	155.570	40.735	2.873	253.896	547.789	0.109	38	71.369	31.664	10.03	6.22	120	1023	30.6	1054
2454	161.495	41.558	2.883	249.736	568.650	0.108	38	72.032	32.191	9.77	6.36	117	1044	29.6	1074
2404	169.883	42.826	2.878	241.922	598.186	0.107	37	72.828	33.231	9.45	6.54	114	1073	28.5	1101
2336	179.964	44.084	2.923	238.702	633.683	0.106	36	73.953	33.679	9.02	6.79	111	1120	27.6	1147
2293	188.131	45.237	2.903	231.026	662.441	0.105	36	74.692	34.799	8.3	7.2	112	1166	26.1	1192
2256	196.896	46.580	2.993	231.337	693.304	0.104	35	75.345	34.752	7.93	7.41	114	1175	25.2	1200
2213	206.225	47.857	3.104	233.461	726.153	0.103	33	76.127	34.436	7.47	7.67	119	1149	24.1	1173
2130	217.757	48.638	3.109	230.084	766.758	0.102	33	77.706	34.941	6.76	8.07	130	1148	21.9	1170
2082	224.668	49.051	3.259	239.187	791.094	0.100	31	78.666	33.611	6.38	8.28	146	1151	21	1172
2056	231.962	50.011	3.379	243.258	816.777	0.100	30	79.200	33.049	5.29	8.9	206	1133	19.4	1152
2005	235.622	49.540	3.304	240.105	829.666	0.099	30	80.281	33.483	5.14	8.99	298	1119	18.9	1137
1953	245.845	50.349	3.475	248.437	865.660	0.098	28	81.429	32.360	4.18	9.53	530	1108	17	1125
1916	248.820	49.993	3.439	247.679	876.137	0.097	28	82.277	32.459	3.9	9.69	530	1108	17	1125
1849	255.711	49.581	3.465	251.558	900.401	0.095	27	83.881	31.958	3.4	9.97	1092	1090	15.6	1106
1763	267.357	49.428	3.570	260.005	941.409	0.093	26	86.083	30.920	2.48	10.5	2308	1040	14	1054
1722	267.438	48.293	3.740	278.824	941.693	0.092	25	87.195	28.833	1.56	11.02		948	12.5	961
1600	273.375	45.868	3.996	313.636	962.599	0.089	22	90.775	25.633	0.9	11.39		825	10.2	835
1579	273.899	45.352	4.071	323.169	964.444	0.089	22	91.437	24.877	0.54	11.6		669	9.4	678
1518	273.684	43.566	4.387	362.521	963.687	0.087	20	93.442	22.176	0.49	11.62		637	9.1	646
1441	271.058	40.959	4.613	405.423	954.440	0.085	18	96.170	19.830	0.4	11.67		568	8.3	576
1343	266.626	37.550	4.613	442.238	938.834	0.082	18	100.009	18.179	0.12	11.83		471	7.8	479

Table 7.24. Performance and Emission Results for Fuel Coded D70RSB20HP10

Speed (rpm)	Torque (Nm)	PB (kW)	mf (g/s)	Sfc (g/kWh)	bmep	ma (kg/s)	AFR	v (%)	b (%)	O_2 %	CO_2 %	CO ppm	NO ppm	NO_2 ppm	NO_x ppm
3123	56.038	16.113	1.750	390.958	197.321	0.118	67	61.68	20.97	14.41	3.73	416	244	34.4	279
3027	88.828	26.088	1.996	275.371	312.777	0.115	58	62.26	29.78	13.61	4.19	387	379	36.2	415
2940	105.169	31.293	2.502	287.823	370.316	0.113	45	63.16	28.49	12.20	4.99	342	536	35.8	571
2839	135.291	38.753	2.818	261.758	476.383	0.111	40	64.26	31.33	10.95	5.69	292	609	33.5	643
2795	146.743	41.564	3.008	260.561	516.706	0.111	37	64.76	31.47	10.57	5.91	237	780	27.1	807
2742	160.343	45.560	3.209	253.554	564.596	0.110	34	65.37	32.34	9.40	6.57	188	976	25.1	1001
2698	167.483	47.003	3.214	246.152	589.735	0.109	34	65.89	33.31	9.00	6.80	177	1047	24.9	1071
2630	180.795	49.852	3.439	248.378	636.608	0.107	31	66.72	33.02	8.49	7.09	172	1064	24.9	1089
2598	190.251	51.641	3.369	234.880	669.906	0.107	32	67.13	34.91	8.13	7.29	169	1099	24.6	1124
2553	203.576	54.178	3.740	248.535	716.827	0.106	28	67.71	32.99	7.44	7.69	172	1116	24	1140
2487	218.279	56.860	3.695	233.957	768.595	0.104	28	68.58	35.05	6.67	8.12	207	1113	22	1135
2455	221.509	56.563	3.740	238.058	779.970	0.104	28	69.02	34.45	5.86	8.58	268	1109	20.7	1129
2358	239.898	58.873	3.901	238.525	844.722	0.101	26	70.40	34.38	5.52	8.77	296	1114	20.4	1134
2294	249.019	59.974	4.086	245.281	876.838	0.100	24	71.36	33.43	3.93	9.67	697	1080	18.2	1099
2241	251.155	58.772	4.172	255.519	884.359	0.099	24	72.18	32.09	2.96	10.22	1738	993	15.5	1009
2151	260.840	58.274	4.237	261.731	918.461	0.097	23	73.65	31.33	2.08	10.72	3882	915	13.8	929
2055	266.509	56.815	4.302	272.583	938.421	0.095	22	75.32	30.08	1.39	11.11		852	12.2	864
1951	267.744	54.874	4.437	291.106	942.773	0.092	21	77.26	28.17	0.99	11.34		794	11.3	806
1850	272.876	53.753	4.397	294.492	960.841	0.090	20	79.29	27.85	0.82	11.44		755	10.9	766
1759	275.542	50.582	4.758	338.641	970.230	0.087	18	81.27	24.22	0.20	11.78		552	8.4	561
1646	272.312	48.736	4.919	363.322	958.854	0.084	17	83.94	22.57	-0.01	11.90		321	7.6	328
1570	268.920	45.072	4.919	392.854	946.911	0.082	17	85.90	20.87	0.17	11.81		290	8.5	299

Table 7.25. Performance and Emission Results for Fuel Coded D60RSB30HP10

Speed (rpm)	Torque (Nm)	PB (kW)	mf (g/s)	Sfc (g/kWh)	bmep	ma (kg/s)	AFR	v (%)	b (%)	O_2 %	CO_2 %	CO ppm	NO ppm	NO_2 ppm	NO_x ppm
3191	10.421	4.277	1.875	1578.257	36.694	0.121	65	62.13	5.24	15.23	3.27	430	218	3.3	221
3100	48.758	13.479	1.885	503.507	171.685	0.119	63	63.05	16.43	15.13	3.33	416	231	9.4	240
3058	62.876	18.056	1.885	375.873	221.396	0.118	63	63.49	22.01	15.13	3.33	416	231	12.3	243
2945	101.340	29.557	2.286	278.465	356.836	0.116	51	64.72	29.71	13.28	4.37	376	417	19.8	437
2855	123.115	35.231	2.567	262.312	433.507	0.115	45	65.75	31.54	12.58	4.77	352	497	21.2	519
2822	131.382	37.281	2.998	289.524	462.619	0.114	38	66.14	28.58	11.13	5.59	255	723	21.8	745
2756	141.840	40.914	2.998	263.818	499.442	0.113	38	66.95	31.36	10.42	6.00	207	849	21.9	871
2698	154.977	43.938	3.058	250.591	545.700	0.111	36	67.68	33.02	10.22	6.11	189	893	21.8	914
2656	163.856	45.433	3.159	250.287	576.964	0.111	35	68.22	33.06	9.59	6.47	168	976	22.1	998
2604	174.945	47.551	3.104	234.966	616.009	0.109	35	68.91	35.21	8.76	6.94	152	1024	20.5	1044
2544	189.156	50.204	3.169	227.223	666.051	0.108	34	69.74	36.41	8.19	7.26	153	1071	19.8	1091
2510	198.721	51.948	3.354	232.452	699.728	0.108	32	70.22	35.59	7.25	7.79	172	1075	18.5	1094
2446	206.914	53.034	3.600	244.366	728.580	0.106	29	71.16	33.86	6.87	8.01	186	1102	18.1	1120
2415	213.711	53.441	3.530	237.779	752.513	0.106	30	71.62	34.80	6.57	8.18	202	1103	17.6	1121
2346	225.794	54.857	3.605	236.577	795.059	0.104	29	72.69	34.97	5.78	8.62	273	1140	16.9	1156
2249	244.183	57.017	3.750	236.793	859.811	0.102	27	74.28	34.94	3.89	9.70	829	1016	14.1	1031
2200	245.332	56.846	3.750	237.504	863.855	0.101	27	75.13	34.84	3.84	9.72	952	1017	13.8	1030
2126	251.927	56.267	3.941	252.141	887.078	0.099	25	76.46	32.81	2.80	10.31	2053	928	12.3	941
2106	257.018	56.220	3.856	246.891	905.005	0.099	26	76.83	33.51	2.17	10.67	3944	879	10.9	890
2050	259.215	56.075	3.986	255.900	912.738	0.097	24	77.90	32.33	2.17	10.67	3944	879	10.9	890
1955	266.247	54.132	4.056	269.753	937.499	0.095	23	79.83	30.67	1.00	11.33		787	9.1	797
1892	267.153	53.615	4.101	275.386	940.692	0.094	23	81.19	30.04	0.94	11.37		778	8.5	787
1800	274.642	53.658	4.282	287.273	967.061	0.091	21	83.30	28.80	0.50	11.62		706	7.1	713
1645	272.909	46.667	4.613	355.836	960.959	0.088	19	87.27	23.25	0.24	11.77		498	5.8	504
1609	272.070	45.821	4.783	375.800	958.003	0.087	18	88.27	22.02	0.24	11.77		476	5.4	482
1558	270.276	43.854	5.099	418.585	951.688	0.085	17	89.76	19.77	0.24	11.77		425	5.1	430
1505	267.227	42.943	5.179	434.190	940.952	0.084	16	91.38	19.06	0.23	11.77		391	4.9	396

Table 7.26. Performance and Emission Results for Fuel Coded D50RSB40HP10

Speed (rpm)	Torque (Nm)	PB (kW)	mf (g/s)	Sfc (g/kWh)	bmep	ma (kg/s)	AFR	v (%)	b (%)	O_2 %	CO_2 %	CO ppm	NO ppm	NO_2 ppm	NO_x ppm
3209	24.324	7.020	1.660	851.016	85.648	0.121	73	61.01	9.95	15.8	2.95	488	175	13.6	189
2998	86.719	26.395	2.141	291.997	305.351	0.117	55	63.15	29.00	14.85	3.49	392	249	24.5	274
2941	103.086	30.717	2.557	299.687	362.985	0.116	45	63.77	28.26	13.65	4.17	356	299	26.3	325
2882	115.606	34.273	2.557	268.593	407.067	0.115	45	64.42	31.53	13.02	4.52	335	424	28	452
2855	125.976	36.310	2.838	281.358	443.582	0.114	40	64.73	30.10	11.68	5.28	260	574	26.5	600
2743	156.125	44.030	3.179	259.904	549.744	0.112	35	66.06	32.58	10.5	5.95	199	743	22.5	765
2698	164.185	46.074	3.294	257.382	578.123	0.111	34	66.61	32.90	9.43	6.55	170	913	22	935
2661	173.299	47.714	3.344	252.319	610.215	0.110	33	67.08	33.56	9.02	6.79	155	975	21.1	996
2612	182.763	50.206	3.575	256.333	643.537	0.109	31	67.72	33.04	8.26	7.22	148	1049	20.9	1070
2554	198.163	52.793	3.750	255.740	697.765	0.108	29	68.49	33.11	7.51	7.64	152	1074	20.7	1095
2453	223.067	56.768	3.800	241.013	549.744	0.106	28	69.91	35.14	6.2	8.38	186	1068	18.7	1087
2401	228.037	56.993	3.966	250.511	578.123	0.105	26	70.67	33.80	5.05	9.04	296	1068	17.4	1085
2360	237.440	58.138	3.966	245.576	610.215	0.104	26	71.30	34.48	5.05	9.04	296	1068	17.1	1085
2301	241.034	58.157	4.011	248.291	643.537	0.103	26	72.22	34.11	4.36	9.43	463	1040	16.2	1056
2263	250.107	59.234	4.011	243.778	697.765	0.102	25	72.83	34.74	3.65	9.83	663	981	15.4	997
2199	250.907	57.766	4.136	257.783	785.457	0.101	24	73.90	32.85	3.04	10.18	1269	937	14.5	952
2182	256.401	58.089	4.252	263.496	802.958	0.100	24	74.19	32.14	2.56	10.45	1735	901	13.8	915
2096	258.765	56.787	4.337	274.939	836.067	0.098	23	75.73	30.80	2.06	10.73	3116	862	12.5	875
2034	268.712	57.777	4.247	264.607	848.719	0.097	23	76.89	32.00	1.3	11.16		796	11.3	807
1903	270.001	53.940	4.568	304.847	880.669	0.094	20	79.55	27.78	0.58	11.57		676	9.1	686
1855	271.143	53.972	4.568	304.664	883.484	0.092	20	80.59	27.80	0.58	11.57		663	8.4	671
1794	273.863	52.581	4.703	321.992	902.829	0.091	19	81.98	26.30	0.43	11.66		593	7.1	600
1750	272.016	50.428	4.703	335.738	911.153	0.090	19	83.02	25.22	0.34	11.71		571	6.9	578
1656	272.728	47.638	4.919	371.695	946.178	0.087	18	85.40	22.78	0.14	11.82		505	6.2	511
1578	268.725	45.248	5.034	400.501	950.719	0.085	17	87.53	21.14	0.15	11.82		451	6.2	457

Table 7.27. Performance and Emission Results for Fuel Coded D40RSB50HP10

Speed (rpm)	Torque (Nm)	PB (kW)	mf (g/s)	Sfc (g/kWh)	bmep	ma (kg/s)	AFR	v (%)	b (%)	O_2 %	CO_2 %	CO ppm	NO ppm	NO_2 ppm	NO_x ppm
3170	83.68	24.49	2.21	325.04	294.66	0.12	54	61.20	26.27	13.58	4.21	309	262	28.5	291
3020	122.52	37.12	2.56	247.96	431.43	0.12	46	62.72	34.43	11.9	5.16	282	476	28.8	505
2963	136.62	40.51	3.33	296.29	481.07	0.12	35	63.32	28.81	10.33	6.05	200	684	21.6	706
2913	146.04	43.72	3.33	274.55	514.25	0.12	35	63.87	31.10	10.26	6.09	192	697	20.9	718
2841	162.36	47.96	3.48	261.17	571.71	0.11	33	64.68	32.69	9.3	6.63	172	819	19.4	838
2807	180.15	51.73	3.74	260.31	634.34	0.11	30	65.08	32.80	8.34	7.17	154	982	18.5	1001
2747	197.29	56.59	3.90	247.85	694.69	0.11	29	65.79	34.45	6.97	7.95	158	1092	18	1110
2707	211.90	59.46	4.12	249.24	746.13	0.11	27	66.28	34.25	5.94	8.54	264	1146	16.3	1162
2654	221.27	61.35	4.35	255.07	779.14	0.11	25	66.95	33.47	5	9.07	414	1159	15.1	1174
2606	233.63	63.92	4.33	243.69	822.66	0.11	25	67.57	35.03	4.42	9.39	467	1159	14.5	1173
2528	245.58	65.26	4.50	248.37	864.73	0.11	24	68.61	34.37	3.26	10.05	999	1067	13.1	1080
2486	247.25	64.60	4.81	268.24	870.59	0.11	22	69.20	31.83	2.68	10.38	1433	1030	12.2	1042
2398	253.12	63.72	4.88	275.90	891.26	0.10	21	70.47	30.94	1.65	10.97	3646	958	10.5	968
2296	259.08	62.64	5.39	309.76	912.26	0.10	19	72.04	27.56	0.6	11.56		770	8.2	778
2192	264.90	62.08	5.42	314.59	932.77	0.10	18	73.75	27.14	0.53	11.6		684	7.1	691
2159	267.22	59.95	5.68	341.11	940.93	0.10	17	74.32	25.03	0.3	11.73		591	6	597
2002	269.56	57.79	5.66	352.64	949.18	0.10	17	77.23	24.21	0.12	11.83		543	5.3	549
1951	269.68	55.18	5.70	371.90	949.58	0.09	17	78.24	22.96	0.18	11.8		496	4.7	501
1882	270.33	53.94	5.74	382.84	951.88	0.09	16	79.69	22.30	0.19	11.79		457	4.5	461
1853	268.42	51.99	5.86	405.53	945.14	0.09	16	80.32	21.05	0.22	11.78		410	4.2	414
1694	267.46	47.66	6.01	454.08	941.78	0.09	15	84.07	18.80	0.22	11.77		300	4.4	305
1648	266.45	46.90	6.01	461.45	938.23	0.09	14	85.25	18.50	0.21	11.78		281	5.1	286
1559	261.69	42.89	6.33	531.57	921.44	0.08	13	87.70	16.06	0.48	11.63		260	6.5	267
1509	258.96	42.01	6.33	542.62	911.84	0.08	13	89.17	15.73	5.8	8.61		203	6.5	210
1411	255.57	39.01	6.95	641.83	899.90	0.08	12	92.28	13.30	10.64	5.87		150	5.3	155
1316	250.49	36.27	6.95	690.24	882.02	0.08	11	95.63	12.37	9.83	6.33		150	5.3	155

Table 7.28. Performance and Emission Results for Fuel Coded D75RSB10HP15

Speed (rpm)	Torque (Nm)	PB (kW)	mf (g/s)	Sfc (g/kWh)	bmep	ma (kg/s)	AFR	v (%)	b (%)	O_2 %	CO_2 %	CO ppm	NO ppm	NO_2 ppm	NO_x ppm
3209	41.068	11.535	1.990	621.197	144.606	0.113	57	57.815	13.026	14.52	3.67	386	271	2.6	274
3103	80.627	23.252	2.161	334.578	283.901	0.111	51	58.664	24.184	14.7	3.57	370	258	5.5	263
2997	103.516	31.343	2.547	292.547	364.498	0.109	43	59.551	27.659	14.5	3.68	364	275	7.5	282
2915	133.512	39.018	3.058	282.190	470.116	0.107	35	60.263	28.674	13.37	4.32	345	382	12.1	394
2799	166.952	48.209	3.575	266.951	587.867	0.105	29	61.315	30.311	8.94	6.83	201	975	16.8	992
2757	177.342	50.465	3.555	253.587	624.452	0.104	29	61.709	31.908	9	6.8	189	976	16.4	992
2709	194.362	54.544	3.650	240.912	684.380	0.103	28	62.169	33.587	7.96	7.39	165	1107	15.9	1123
2647	210.528	57.997	4.016	249.288	741.304	0.101	25	62.777	32.459	6.57	8.18	214	1189	14.8	1204
2618	220.206	59.751	4.021	242.271	775.382	0.101	25	63.067	33.399	5.97	8.52	261	1191	14.1	1205
2544	237.333	62.626	4.357	250.461	835.688	0.099	23	63.825	32.307	5.53	8.77	355	1181	13	1194
2458	240.718	62.345	4.362	251.877	847.608	0.097	22	64.740	32.125	4.56	9.32	447	1167	12.1	1179
2393	251.263	62.840	4.603	263.680	884.737	0.096	21	65.456	30.687	3.39	9.98	902	1094	10	1104
2294	257.039	62.119	4.738	274.587	905.076	0.093	20	66.591	29.468	2.68	10.38	1895	1066	8.4	1075
2272	263.117	62.144	4.969	287.837	926.478	0.093	19	66.851	28.112	1.37	11.12		911	6.8	917
2150	264.151	59.946	5.034	302.304	930.120	0.090	18	68.344	26.766	0.73	11.49		762	4.7	767
1965	269.524	55.579	5.129	332.228	949.040	0.085	17	70.791	24.355	0.41	11.67		608	3.5	611
1913	271.673	56.031	5.189	333.413	956.608	0.083	16	71.522	24.269	0.37	11.69		588	3.3	592
1830	274.736	52.135	5.295	365.598	967.392	0.081	15	72.730	22.132	0.07	11.86		499	2.6	502
1691	270.606	51.161	5.295	372.558	952.847	0.077	15	74.874	21.719	0.05	11.87		488	2.4	490
1586	264.903	45.640	5.651	445.712	932.769	0.074	13	76.598	18.154	0.02	11.89		423	2.4	425
1515	262.539	43.022	5.651	472.828	924.444	0.072	13	77.816	17.113	-0.01	11.9		423	2.4	425
1371	258.019	38.512	6.633	620.065	908.528	0.067	10	80.411	13.050	0	11.9		293	3.7	297
1227	254.379	34.857	6.633	685.092	895.710	0.062	9	83.150	11.811	0	11.9		293	3.7	297

Table 7.29. Performance and Emission Results for Fuel Coded D65RSB20HP15

Speed (rpm)	Torque (Nm)	PB (kW)	mf (g/s)	Sfc (g/kWh)	bmep	ma (kg/s)	AFR	v (%)	b (%)	O_2 %	CO_2 %	CO ppm	NO ppm	NO_2 ppm	NO_x ppm
3154	56.334	15.708	1.680	384.938	198.361	0.118	70	61.21	21.40	15.75	2.98	471	190	1.3	192
3012	90.594	27.000	1.680	223.951	318.997	0.115	68	62.59	36.78	15.50	3.12	460	207	1.3	208
2923	116.640	33.802	2.216	236.024	410.709	0.113	51	63.51	34.90	14.88	3.47	460	207	1.3	208
2801	140.497	41.177	3.053	266.956	494.712	0.111	36	64.84	30.85	14.03	3.95	431	337	2	339
2753	159.175	46.051	3.244	253.594	560.481	0.110	34	65.38	32.48	11.46	5.41	357	621	4.2	625
2700	173.427	48.662	3.329	246.294	610.665	0.109	33	66.00	33.44	9.87	6.31	249	884	7.4	892
2640	187.860	51.693	3.480	242.325	661.487	0.107	31	66.72	33.99	8.66	6.99	214	1041	9.4	1050
2605	197.498	53.551	3.595	241.671	695.424	0.107	30	67.15	34.08	8.05	7.34	206	1148	10.5	1158
2551	212.301	56.717	3.590	227.863	747.547	0.105	29	67.83	36.15	7.43	7.69	215	1167	10.5	1178
2496	221.583	57.685	3.831	239.059	780.231	0.104	27	68.55	34.45	6.44	8.25	262	1159	10.2	1169
2430	231.288	59.033	3.881	236.655	814.404	0.103	26	69.44	34.80	5.75	8.64	324	1148	9.8	1157
2400	232.517	58.493	3.876	238.533	818.732	0.102	26	69.86	34.53	5.14	8.99	409	1155	9.3	1164
2351	242.511	59.716	3.971	239.390	853.922	0.101	25	70.55	34.41	4.27	9.48	569	1129	9.3	1138
2312	248.186	59.452	4.212	255.028	873.906	0.100	24	71.12	32.30	4.01	9.63	671	1094	8.7	1103
2246	254.016	59.265	4.212	255.831	894.433	0.099	23	72.12	32.19	2.93	10.24	1411	899	7.6	906
2155	260.256	57.925	4.322	268.605	916.404	0.097	22	73.56	30.66	2.49	10.49	2152	845	7.1	852
2080	264.144	58.735	4.447	272.585	930.097	0.095	21	74.82	30.22						
2005	263.318	55.104	4.432	289.562	927.188	0.093	21	76.15	28.44						
1939	265.239	54.737	4.593	302.056	933.951	0.091	20	77.37	27.27						
1918	267.388	53.087	4.673	316.883	941.519	0.091	19	77.77	25.99						
1842	266.213	52.333	4.758	327.312	937.381	0.089	19	79.29	25.16						
1791	266.065	49.685	4.768	345.484	936.860	0.088	18	80.35	23.84						
1674	266.952	47.556	5.004	378.793	939.982	0.085	17	82.96	21.74						

Table 7.30. Performance and Emission Results for Fuel Coded D55RSB30HP15

Speed (rpm)	Torque (Nm)	PB (kW)	mf (g/s)	Sfc (g/kWh)	bmep	ma (kg/s)	AFR	v (%)	b (%)	O_2 %	CO_2 %	CO ppm	NO ppm	NO_2 ppm	NO_x ppm
3150	16.902	5.592	1.745	1123.368	59.516	0.122	70	64.03	7.37	15.49	3.12	396	217	31.3	248
3109	28.743	8.246	1.645	717.990	101.210	0.121	74	64.47	11.53	15.62	3.05	381	214	33.3	247
3044	51.874	14.147	1.815	461.854	182.658	0.120	66	65.18	17.92	14.81	3.51	367	292	35.1	328
2912	79.794	22.321	1.815	292.735	280.969	0.118	65	66.71	28.28	14.21	3.85	355	359	35.8	395
2839	97.183	27.606	2.171	283.113	342.197	0.116	54	67.60	29.24	12.93	4.57	313	507	35.1	542
2754	123.336	34.089	2.422	255.746	434.288	0.115	47	68.69	32.37	11.80	5.22	270	668	33.3	701
2725	135.741	37.230	2.868	277.319	477.968	0.114	40	69.07	29.85	10.83	5.76	203	813	28	841
2652	146.488	40.515	2.818	250.377	515.807	0.113	40	70.07	33.06	10.22	6.11	175	944	26.3	971
2589	159.746	43.183	3.084	257.060	562.491	0.111	36	70.96	32.20	9.69	6.41	162	971	24.7	996
2551	165.407	44.247	3.149	256.184	582.427	0.111	35	71.51	32.31	9.39	6.58	145	1010	22.9	1033
2498	177.087	46.159	3.094	241.270	623.553	0.109	35	72.31	34.31	8.77	6.93	137	1035	21.8	1056
2451	186.571	47.991	3.204	240.334	656.946	0.108	34	73.04	34.45	8.13	7.29	136	1056	20.3	1076
2403	197.035	49.248	3.299	241.165	693.792	0.107	33	73.80	34.33	7.70	7.53	140	1086	19.9	1105
2336	210.810	51.428	3.369	235.852	742.297	0.106	31	74.92	35.10	6.55	8.19	162	1090	18.8	1109
2292	220.099	52.884	3.369	229.358	775.004	0.105	31	75.67	36.09	6.26	8.35	172	1082	18.1	1101
2266	226.822	53.202	3.465	234.436	798.677	0.105	30	76.13	35.31	5.60	8.72	208	1068	17.2	1085
2206	232.618	53.356	3.670	247.630	819.086	0.103	28	77.22	33.43	5.04	9.04	291	1046	16.1	1063
2100	248.677	53.937	3.695	246.636	875.632	0.101	27	79.27	33.57	3.80	9.75	864	991	13.2	1004
2026	252.861	53.222	3.530	238.757	890.366	0.099	28	80.80	34.67	3.08	10.15	1384	976	12.1	988
2017	255.494	53.368	3.715	250.615	899.636	0.099	27	80.99	33.03	2.84	10.29	1384	976	12.1	988
1962	261.068	54.516	3.715	245.340	919.265	0.098	26	82.20	33.74	2.84	10.29	1766	964	11.7	976
1904	268.107	53.258	3.861	260.961	944.050	0.096	25	83.53	31.72	1.57	11.01		882	9.5	891
1843	269.457	51.834	3.951	274.400	948.803	0.095	24	85.00	30.17	1.03	11.31		811	8.4	819
1699	278.269	49.101	4.217	309.154	979.831	0.091	22	88.80	26.78	0.55	11.59		645	6.9	652
1606	278.625	46.587	4.613	356.450	981.085	0.089	19	91.54	23.22	0.34	11.71		503	6	509
1646	278.591	48.041	4.517	338.521	980.966	0.090	20	90.33	24.45	0.24	11.77		566	5.8	572
1589	277.403	46.640	4.327	333.986	976.780	0.089	20	92.07	24.79	0.37	11.69		507	6	513

Table 7.31. Performance and Emission Results for Fuel Coded D45RSB40HP15

Speed (rpm)	Torque (Nm)	PB (kW)	mf (g/s)	Sfc (g/kWh)	bmep	ma (kg/s)	AFR	v (%)	b (%)	O_2 %	CO_2 %	CO ppm	NO ppm	NO_2 ppm	NO_x ppm
3226	22.134	6.076	2.031	1203.092	77.939	0.121	59	61.19	7.01	15.13	3.33	292	225	26.9	252
3159	43.499	12.226	2.527	744.091	153.167	0.119	47	61.83	11.34	14.96	3.43	286	240	28.3	268
3107	61.915	17.233	2.527	527.887	218.014	0.118	47	62.35	15.99	14.5	3.68	280	280	29.6	309
3011	95.134	28.635	3.043	382.622	334.984	0.116	38	63.33	22.06	12.86	4.62	260	346	30.7	377
2897	123.632	35.544	2.878	291.484	435.328	0.114	40	64.57	28.95	11.29	5.5	243	549	31.4	580
2848	135.909	39.265	3.073	281.794	478.559	0.113	37	65.12	29.95	11.29	5.5	224	642	30.9	673
2802	147.636	41.957	3.073	263.713	519.851	0.112	37	65.66	32.00	10.61	5.89	204	748	29.6	777
2766	164.165	47.108	3.319	253.653	578.052	0.112	34	66.08	33.27	9.2	6.69	123	1004	24.1	1028
2700	181.580	51.207	3.730	262.249	639.375	0.110	30	66.89	32.18	8.01	7.36	115	1133	23.6	1157
2659	193.697	53.495	3.700	249.011	682.038	0.109	30	67.40	33.89	7.47	7.67	122	1157	22.5	1180
2603	209.084	56.595	3.971	252.594	736.219	0.108	27	68.12	33.41	6.31	8.32	174	1173	20.9	1194
2547	223.168	59.351	4.247	257.590	785.812	0.107	25	68.87	32.76	5.13	8.99	280	1152	18.7	1170
2515	228.675	60.501	4.247	252.691	805.204	0.106	25	69.30	33.40	4.87	9.14	314	1152	18.7	1170
2457	235.533	60.688	4.247	251.914	829.350	0.105	25	70.12	33.50	4.12	9.57	538	1123	17.2	1140
2398	243.821	60.757	4.402	260.840	858.534	0.104	24	70.98	32.35	3.58	9.87	747	1116	16.9	1133
2359	249.107	61.454	4.402	257.878	877.146	0.103	23	71.56	32.73	3.58	9.87	747	1101	16.5	1118
2310	253.761	61.976	4.573	265.610	893.535	0.102	22	72.32	31.77	2.9	10.26	1055	1052	16	1068
2233	259.329	61.104	4.708	277.374	913.140	0.100	21	73.55	30.43	1.53	11.03	3274	905	14.2	919
2208	260.397	60.412	4.873	290.414	916.900	0.100	20	73.97	29.06	0.77	11.46		789	12	801
2173	264.507	60.261	4.873	291.139	931.374	0.099	20	74.56	28.99	0.71	11.5		789	12	801
2095	266.791	59.373	4.989	302.489	939.414	0.097	19	75.94	27.90	0.71	11.5		775	11.3	786
2083	269.417	58.176	4.989	308.710	948.661	0.097	19	76.16	27.34	0.56	11.58		714	10.2	724
1945	270.263	55.190	5.044	329.010	951.641	0.094	19	78.82	25.65	0.42	11.66		643	9.6	653
1864	274.743	54.873	5.079	333.216	967.415	0.092	18	80.51	25.33	0.39	11.68		615	9.4	625
1751	271.821	50.123	5.445	391.077	957.128	0.089	16	83.07	21.58	0.2	11.79		481	8.2	489
1662	271.418	47.742	5.520	416.258	955.709	0.087	16	85.27	20.27	0.04	11.88		457	7.6	464
1588	267.160	44.716	5.520	444.428	940.715	0.085	15	87.24	18.99	0.02	11.89		415	7.4	422
1532	265.152	44.141	6.047	493.147	933.644	0.083	14	88.82	17.11	0	11.9		354	7.4	362
1457	262.741	41.522	6.047	524.251	925.154	0.081	13	91.08	16.10	-0.01	11.9		310	7.4	317

Table 7.32. Performance and Emission Results for Fuel Coded D35RSB50HP15

Speed (rpm)	Torque (Nm)	PB (kW)	mf (g/s)	Sfc (g/kWh)	bmep	ma (kg/s)	AFR	v (%)	b (%)	O_2 %	CO_2 %	CO ppm	NO ppm	NO_2 ppm	NO_x ppm
3094	16.392	4.271	1.72	1449.65	57.72	0.12	68	62.19	5.90	15.54	3.09	405	185	3.6	189
3040	32.874	9.444	1.77	674.65	115.75	0.12	66	62.73	12.68	15.3	3.23	397	211	6.5	218
3005	43.942	11.918	1.77	534.61	154.73	0.12	65	63.09	16.00	14.97	3.42	390	243	8.3	251
2899	77.175	20.494	1.97	345.25	271.75	0.11	58	64.21	24.77	13.76	4.1	362	366	12.3	378
2862	86.752	25.033	1.97	282.65	305.47	0.11	57	64.62	30.26	13.02	4.52	362	366	12.3	378
2695	130.012	35.877	2.61	262.12	457.80	0.11	42	66.56	32.63	11.36	5.46	266	697	17.6	715
2647	148.778	40.427	3.06	272.80	523.87	0.11	35	67.15	31.35	10.22	6.11	173	885	18.7	904
2614	154.332	42.054	3.25	278.56	543.43	0.11	33	67.56	30.70	9.85	6.32	152	950	18.5	968
2551	162.983	43.463	2.90	240.04	573.89	0.11	37	68.37	35.63	9.47	6.53	143	955	18.3	973
2492	176.100	45.634	3.25	256.31	620.08	0.10	32	69.16	33.37	8.78	6.92	134	971	17.8	989
2445	187.524	47.812	3.33	251.05	660.30	0.10	31	69.81	34.07	8.07	7.33	133	1003	16.7	1019
2408	195.544	48.900	3.32	244.73	688.54	0.10	31	70.33	34.95	7.59	7.6	139	1043	16.1	1059
2337	203.388	49.868	3.51	253.73	716.16	0.10	29	71.37	33.71	7.14	7.85	144	1076	16	1092
2293	216.861	52.121	3.45	238.60	763.61	0.10	29	72.04	35.84	6.3	8.33	164	1056	15.6	1072
2238	224.780	52.966	3.45	234.80	791.49	0.10	29	72.90	36.43	5.57	8.74	185	1042	15	1057
2207	232.322	53.534	3.42	230.28	818.05	0.10	29	73.39	37.14	5.06	9.03	274	1020	14.5	1034
2159	238.414	53.171	3.63	245.77	839.50	0.10	27	74.19	34.80	4.35	9.44	522	984	13.1	997
2096	243.331	53.279	3.71	250.36	856.81	0.10	26	75.27	34.16	3.97	9.65	781	961	12.3	974
2024	255.427	54.358	3.73	246.72	899.40	0.09	25	76.56	34.67	3.36	10	1624	937	11.1	948
1951	263.083	53.319	3.72	251.18	926.36	0.09	25	77.94	34.05	2.1	10.71	3610	882	10.7	893
1891	268.215	53.134	3.96	268.37	944.43	0.09	23	79.14	31.87	1.28	11.18		836	9.2	845
1824	271.049	52.221	3.96	273.06	954.41	0.09	23	80.54	31.32	1.28	11.18		808	8.7	817
1760	274.897	50.569	3.94	280.20	967.96	0.09	22	81.95	30.52	0.74	11.48		673	7.8	681
1640	273.957	47.710	4.46	336.33	964.65	0.08	19	84.80	25.43	0.28	11.74		499	7.1	506
1578	273.782	45.861	4.46	349.89	964.03	0.08	19	86.40	24.44	0.17	11.8		439	6.7	446
1541	273.957	44.441	4.46	361.07	964.65	0.08	18	87.40	23.69	0.11	11.84		395	6.5	402
1501	272.238	43.401	4.67	387.60	958.59	0.08	17	88.52	22.07	0.08	11.85		395	6.5	402